GEOTECHNICAL LABORATORY

TECHNICAL REPORT GL-92-10

IN SITU MATERIAL CHARACTERIZATION FOR PAVEMENT EVALUATION BY THE SPECTRAL-ANALYSIS-OF-SURFACE-WAVES (SASW) METHOD

by

Don R. Alexander

Geotechnical Laboratory

DEPARTMENT OF THE ARMY
Waterways Experiment Station, Corps of Engineers
3909 Halls Ferry Road, Vicksburg, Mississippi 39180-6199

July 1992
Final Report

Approved For Public Release; Distribution Is Unlimited

Prepared for DEPARTMENT OF THE ARMY
US Army Corps of Engineers
Washington, DC 20314-1000

REPORT DOCUMENTATION PAGE

Form Approved
OMB No. 0704-0188

1. AGENCY USE ONLY (Leave blank)	2. REPORT DATE	3. REPORT TYPE AND DATES COVERED
	July 1992	Final report

4. TITLE AND SUBTITLE
In Situ Material Characterization for Pavement Evaluation by the Spectral-Analysis-of-Surface-Waves (SASW) Method

5. FUNDING NUMBERS

6. AUTHOR(S)
Don R. Alexander

7. PERFORMING ORGANIZATION NAME(S) AND ADDRESS(ES)
USAE Waterways Experiment Station
Geotechnical Laboratory
3909 Halls Ferry Road
Vicksburg, MS 39180-6199

8. PERFORMING ORGANIZATION REPORT NUMBER
Technical Report
GL-92-10

9. SPONSORING/MONITORING AGENCY NAME(S) AND ADDRESS(ES)
US Army Corps of Engineers
20 Massachusetts Avenue, NW
Washington, DC 20314-1000

10. SPONSORING/MONITORING AGENCY REPORT NUMBER

11. SUPPLEMENTARY NOTES
Available from National Technical Information Service, 5285 Port Royal Road, Springfield, VA 22161

12a. DISTRIBUTION/AVAILABILITY STATEMENT
Approved for public release; distribution is unlimited.

12b. DISTRIBUTION CODE

13. ABSTRACT (Maximum 200 words)

Spectral-analysis-of-surface-waves (SASW) is a method of nondestructive testing for material characterization of pavement systems. SASW is based on the theory of stress waves propagating in elastic media with the key elements being the generation and measurement of Rayleigh waves. From these measurements, shear wave velocity and modulus profiles can be obtained for multilayered elastic systems.

SASW tests were conducted on six airfield pavement sites. Young's modulus profiles from SASW were compared with moduli backcalculated using falling weight deflectometer test results and with laboratory values.

Results indicate that SASW is a viable method for in situ characterization of pavement materials. Automation of testing and analyses techniques is needed for routine pavement evaluations. Research is needed to evaluate low strain effects on the moduli for surface, base, and subgrade materials and the effect of reflected waves on SASW measurements.

14. SUBJECT TERMS	15. NUMBER OF PAGES
See reverse.	156
	16. PRICE CODE

17. SECURITY CLASSIFICATION OF REPORT	18. SECURITY CLASSIFICATION OF THIS PAGE	19. SECURITY CLASSIFICATION OF ABSTRACT	20. LIMITATION OF ABSTRACT
Unclassified	Unclassified	Unclassified	

14. SUBJECT TERMS (Continued).

Backcalculation
Falling weight deflectometer
Nondestructive testing
Spectral-Analysis-of-Surface-Waves
Wave propagation
Young's modulus

PREFACE

This study was conducted by the Geotechnical Laboratory (GL), US Army Engineer Waterways Experiment Station (WES), Vicksburg, MS, as part of the work effort "Improved Nondestructive Testing Techniques in Pavement Evaluation" of the RDT&E Program AT40-PT-003. This study was conducted from August 1987 to December 1988.

This study was conducted under the general supervision of Dr. W. F. Marcuson III, Chief, GL; Mr. H. H. Ulery, Jr., former Chief, Pavement Systems Division (PSD); Dr. G. Hammitt II, Chief, PSD, and Mr. J. W. Hall, Jr., Chief, Engineering Testing and Evaluation Group, PSD. This report was prepared by Mr. D. R. Alexander under the direct supervision of Mr. R. W. Grau, Chief, Prototype Testing and Evaluation Unit, PSD. Drs. S. Nazarian, University of Texas at El Paso and D. R. Hiltunen, Penn State University, actively participated in the collection of surface wave data and provided technical support throughout the investigation.

At the time of publication of this report, Director of WES was Dr. Robert W. Whalin. Commander and Deputy Director was COL Leonard G. Hassell, EN.

TABLE OF CONTENTS

TABLE OF CONTENTS (concluded)

LIST OF FIGURES

LIST OF FIGURES (continued)

LIST OF FIGURES (continued)

LIST OF FIGURES (continued)

LIST OF FIGURES (continued)

LIST OF FIGURES (concluded)

LIST OF TABLES

LIST OF APPENDICES

In-Situ Material Characterization For Pavement Evaluation by the Spectral-Analysis-of-Surface-Waves (SASW) Method

I. INTRODUCTION

A. Background

In situ material characterization is necessary for the structural evaluation of existing pavement systems. In the past, the accepted method of evaluating pavements has been through destructive testing, where strength parameters are determined from field and laboratory evaluation of pavement layers. More recently, a growing acceptance of nondestructive testing (NDT) as a means of characterizing pavement materials has led to the development and widespread use of various NDT devices and pavement evaluation procedures. NDT offers the advantages of causing less interference to normal traffic operations and being less costly than destructive testing procedures.

In the late 1970's, the U. S. Army Engineer Waterways Experiment Station (WES) developed a methodology for evaluation of light aircraft pavements based upon multilayered elastic models and limiting stress/strain criteria (Bush, 1980). Modulus values can be determined using surface deflections obtained from a number of commercially available test devices, one of the most popular being the falling weight deflectometer (FWD). This procedure is currently being used extensively by the military for airfield pavement evaluation and is also being widely used by many Universities and engineering firms for pavement research and evaluation. However, with the layered elastic evaluation procedure, the pavement structure (layer thicknesses) must

be known and typically moduli can be backcalculated for only two or three layers. Therefore, it is evident that a fast, economical, and totally nondestructive method for determining in situ modulus profiles for pavement structures is needed.

SASW is a nondestructive method for measuring shear wave velocity and determining in situ elastic moduli of soil and pavement profiles as well as the thickness of each layer. SASW is based on the generation and detection of Rayleigh waves at strains below 0.001 percent where the elastic properties of the materials are independent of strain amplitude. The theory of elastic waves in layered media is utilized to reduce and analyze data collected in the field. Practical and theoretical aspects of SASW have been documented (Nazarian and Stokoe, 1985, 1986a). SASW has been under continuous development at the University of Texas since 1980 and at the Universities of Kentucky and Michigan since 1985. A review of the historical development by Nazarian (1984) revealed that the concepts of SASW are not new, however, civil engineering applications were limited prior to the appearance of modern spectral analyzers and theoretically based methods of determining the shear wave velocity profile from collected data (Nazarian, 1984). The use of SASW for nondestructive pavement evaluation is gaining in popularity and a number of case studies have been documented (Heisey, Stokoe, and Meyer 1982; Nazarian and Stokoe 1983; Nazarian, Stokoe, and Hudson 1983; Nazarian and Stokoe 1984; Drnevich, et al. 1985; Nazarian and Stokoe 1986; and Hiltunen 1988).

B. Purpose

The purpose of this study is to evaluate the applicability of SASW for material characterization of pavement systems in situ for the determination of load capacity and rehabilitation requirements.

C. Scope

The efficiency and practical feasibility of the SASW method were evaluated through a field testing program designed to include flexible, rigid, and composite (flexible over rigid) pavement structures. SASW field testing and data reduction techniques were utilized to obtain Young's modulus profiles for a total of six airfield pavement sites. For comparison, modulus values were backcalculated using the WES elastic layer method and FWD surface deflections. SASW moduli were also compared to laboratory resilient modulus and dynamic modulus values for the asphaltic concrete (AC) and Portland cement concrete (PCC) materials, respectively.

II. SPECTRAL-ANALYSIS-OF-SURFACE-WAVES (SASW) METHOD

A. *Wave Propagation*

For evaluation, most pavement sites can be approximated by a layered half-space since the depth of concern is usually not more than 20 ft. A pavement system can be modeled by a number of elastic, isotropic, homogeneous layers. Constant properties are assumed within each layer. If waves are assumed plane, the solution of wave equations reduces to a two-dimensional problem.

If an elastic half-space is disturbed by a vertical impact on the surface, body and surface waves will propagate in the medium. Body waves propagate radially outward in the medium and are composed of compression waves (P-waves) and shear waves (S-waves). Particle motion is parallel to the direction of propagation for P-waves and perpendicular to the direction of propagation for S-waves. Surface waves resulting from a vertical excitation are primarily Rayleigh waves (R-waves) which propagate away from the impact along a cylindrical wavefront near the surface with particle motion near the surface forming a retrograde ellipse. The amplitude of the wave decays exponentially with depth, such that at a depth of one wavelength, vertical and horizontal particle motion are only about 30 and 10 percent of surface values. It has been shown (Miller and Pursey, 1955) that approximately 67 percent of the input energy propagates in the form of R-waves while P- and S-waves carry about 26 and 7 percent of the energy, respectively. As the waves propagate, the increasing volume of medium encountered causes wave energy to dissipate or geometrical damping. While body waves are faster than surface waves,

they also attenuate much faster due to geometrical damping. Near the surface, body waves attenuate proportional to $1/r^2$ (where r is the distance from the source, while R-waves attenuate proportional to $1/\sqrt{r}$. Thus, in a relatively short distance from the source, most of the energy at the surface is R-wave energy. This, in addition to the fact that most of the energy from an impact goes into R-wave velocity, is beneficial to the SASW method.

The velocity of propagation of the different waves are related by Poisson's ratio. P-waves propagate faster than S-waves and the ratio of P- to S-wave velocity increases from 1.4 to infinity as the Poisson's ratio increases from 0.0 to 0.5. R-waves are the slowest with the ratio of R- to S-waves varying from 0.86 to 0.95 for Poisson's ratios of 0.0 and 0.5, respectively. The velocity of propagation is a direct indicator of the stiffness of a material and once the shear or compression wave velocity is known, the Young's modulus and shear modulus can be determined as:

$$G = \rho V_s^2 \qquad \text{(II-1)}$$

$$E = 2G(1 + \mu) = 2\rho V_s^2(1 + \mu) \qquad \text{(II-2)}$$

or

$$E = \rho V_p^2[(1 + \mu)(1 - 2\mu)/(1 - \mu)] \qquad \text{(II-3)}$$

where,

G = shear modulus,

E = Young's modulus,

ρ = mass density,

V_s = shear wave velocity,

μ = Poisson's ratio, and

V_p = compression wave velocity.

R-wave velocity will be constant and independent of frequency in a homogeneous, elastic half-space. For a case such as a pavement system, the stiffness of the layers varies with depth and the R-wave velocity will vary with frequency. Different frequencies will propagate at different velocities and an average velocity (phase velocity) for the material to a depth of 1- to 1-1/2 wavelengths will be measured. The variation of this phase velocity with wavelength (frequency) is called dispersion.

B. Frequency Domain Analysis

Analyses in the frequency domain are not new, however until recently, algorithms such as the Fourier transform required a prohibitive amount of computation time and were not efficient enough to be applied in the field. Development of microprocessors and the fast Fourier transform (FFT) have greatly extended the capability to measure and analyze dynamic systems in the frequency domain. The FFT and spectral analyses are now widely used in field and laboratory testing and are key components of SASW testing.

SASW measurements are made on two channels of data. A number of different measurements can be made once the signals have been Fourier transformed (transformed into the frequency domain). These measurements, spectral analyses, are basically statistical operations performed on the signals. This involves the correlation of the input or output with itself or the correlation of the input with the output, assuming that the object under test is a linear system.

Comparison of two signals is accomplished easily in the frequency domain. Mathematical operations can be performed more efficiently. For example, an integration in the time domain is a simple multiplication in the frequency domain. An important characteristic of most frequency domain measurements is that triggering does not have to be synchronized. This makes it possible to obtain enhanced records by averaging several signals. For repeatable signals, the average of several records will theoretically be free of random background noise. The spectral analyses functions of interest in SASW testing are described below.

Cross power spectrum. Signals from two channels obtained simultaneously can be compared utilizing the cross power spectrum, $G_{xy}(f)$, defined as:

$$G_{xy}(f) = S_x^*(f) * S_y(f) \qquad \text{(II-4)}$$

where,

$S_x^*(f)$ = the complex conjugate of the linear spectrum of the input,

$S_y(f)$ = linear spectrum of the output.

The linear spectrum is the Fourier transform of the signal recorded in the time domain. $G_{xy}(f)$ is a complex function and can be represented with real and imaginary components or with a magnitude and phase. The magnitude is a measure of the mutual power between the two signals. The phase is the relative phase between the signals at each frequency in the measurement bandwidth. Because the phase is relative, synchronized triggering is not necessary. The cross power spectrum is

the key measurement in SASW testing and is used to determine the travel times of surface waves at different frequencies.

Auto power spectrum. The auto power spectrum, G_{xx} is defined as:

$$G_{xx} = S_x(f) * S_x^*(f) \qquad \text{(II-5)}$$

where,

$S_x(f)$ = linear spectrum,

S_x^* = complex conjugate of the linear spectrum

The magnitude of the auto power spectrum is equal to the magnitude of the linear spectrum squared and is the energy at each frequency in the measurement bandwidth. Because the linear spectrum is multiplied by its complex conjugate, the auto power spectrum is a real valued function and does not contain any phase information, but can be used to identify dominant frequencies.

Coherence. The coherence function, $\gamma^2(f)$, is a real valued function with a value between zero and one corresponding to the ratio of the output power caused by the measured input to the total measured output defined as:

$$\gamma^2(f) = \frac{G_{yx}(f) * G_{yx}^*(f)}{G_{xx}(f) * G_{yy}(f)} \qquad \text{(II-6)}$$

where G_{yx}, G_{xx}, and G_{yy} are previously defined cross and auto power spectra averaged in the frequency domain over multiple input records. The coherence function should be used on averaged signals since it will always have a value of unity for one signal pair. A coherence value close to one indicates good correlation between the input and the output signals. A low coherence may indicate bad correlation, however, nonlinearity of the system and low frequency resolution can also result

in poor coherence. The coherence function is used in SASW testing to help identify frequencies providing accurate cross power spectrum phase values.

C. Overview

SASW is a nondestructive seismic method for determining in situ elastic moduli of pavement systems. To conduct SASW, two receivers are attached to the surface and a hammer is used to deliver a transient impact to the pavement. The impact generates energy over a range of frequencies. Wavelengths depend on the stiffness of the material and frequency of the wave. The energy of a surface wave decays rapidly with depth, therefore, different frequencies sample different depths.

The signal generated by the impact is recorded using a waveform analyzer and the time-domain record from each receiver is transformed into the frequency domain. This process is repeated several times and the results averaged to enhance the quality of the signal by eliminating the effects of random background noise.

Spectral analyses are then performed to obtain the cross power and coherence functions. The coherence value is used to monitor the quality of data during testing and to identify poor data during analysis. The cross power spectrum provides the relative phase shift at each frequency from which the travel time between the two receivers can be determined.

Because the frequencies that can be generated by a single source are limited, testing is performed at several spacings. Close spacings sample material near the surface and the source must generate high

frequencies. Larger spacings sample deeper layers and the source must generate more energy in the lower frequency ranges.

The first step in data reduction involves converting the field data into a dispersion curve. The dispersion curve is simply a plot of the surface wave velocity versus wavelength and can be developed from phase information of the cross power spectrum. The R-wave velocities determined in this manner are not actual velocities, but apparent (phase) velocities since the stiffness of layers near the surface will affect the measurement of velocities of underlying layers.

Finally, the shear wave velocity profile must be obtained from the dispersion curve. This process is called inversion and consists of determining the depth of each layer and the actual shear wave velocity of each layer from the apparent R-wave velocity versus wavelength information. Once the shear wave velocities are known, the shear and Young's modulus can be computed.

III. DATA COLLECTION

A. Test Sites

Test sites for this study were selected based on pavement structure and the availability of adequate data to verify pavement conditions at the time of SASW testing. The six airfield pavement sites listed in Table 1 represent a wide range of pavement types, thicknesses, and subgrade conditions. These sites were selected in conjunction with a separate study that was being conducted by WES to evaluate various NDT devices and, for reference purposes, site numbers in Table 1 correspond to the previously reported values (Bentsen, Bush, and Harrison 1988). During that study, a test pit was excavated within each site at a reference point location for structure verification, in-place strength measurements, and sampling of materials for laboratory testing. Field and laboratory test results, extracted from the previous report, for each of the six sites included in this study are summarized in Tables 2-6. Table 2 is a summary of test pit data including layer thicknesses and in-place density, water content, and strength measurements. In-place strengths are reported in terms of the California bearing ratio (CBR) for flexible pavement layers and the modulus of subgrade reaction, k, (from a plate bearing test) for rigid pavement layers. Base and subgrade material classifications are presented in Table 3. Laboratory resilient moduli for the AC layers determined using procedures described in ASTM D 4123-82 (ASTM 1988) are shown in Table 4 for temperatures of 77- and 104-degrees fahrenheit. Flexural strengths determined using ASTM C-78-84 (ASTM 1986) and Young's modulus values from ASTM C-215-85 (ASTM 1988) for the PCC

TABLE 1. GENERAL SITE DESCRIPTION

Site	Airport/Airfield	Pavement Thickness in.	Type	Physical Location
3	NAS Pensacola, FL	10.0	PCC	North end of taxiway parallel to runway 1-19
4	NAS Pensacola, FL	5.5	AC	North end of taxiway parallel to runway 1-19
8	Birmingham ANG/ Birmingham Municipal, AL	7.0 7.0	AC PCC	Southwest end of ANG aircraft apron
10	Birmingham ANG/ Birmingham Municipal, AL	2.0 7.0	AC PCC	Taxiway E between runway 18-36 and holding apron
11	Sheppard AFB Wichita Falls, TX	21.0	PCC	Alert apron at North end of airbase
12	Sheppard AFB Wichita Falls, TX	7.0	AC	Access taxiway North of control tower between taxiway E and school apron

TABLE 2. TEST PIT DATA (THICKNESS, DENSITY, WATER CONTENT, CBR, AND K)

Site	Pavement Thick. in.	Pavement Type	Nuclear Density Dry pcf	Nuclear Density Wet pcf	Nuclear Water Content %	Drive Cylinder Density Dry pcf	Drive Cylinder Density Wet pcf	Oven Dry Water Content %	Depth in.	CBR %	k pci
3	10.0	PCC	---	---	----	---	---	----	----	---	---
	4.0	Base	115	128	13.0	---	---	9.5	10.0	---	303
	----	Subgrade	104	123	18.4	---	---	15.5	14.0	---	---
4	5.5	AC	---	---	----	---	---	----	----	---	---
	13.5	Base	128	138	11.2	---	---	8.2	5.5	88	---
			125	135	10.1	---	---	6.4	12.0	100	---
	----	Subgrade	108	126	18.3	---	---	14.5	19.0	16	---
8	6.5	AC	---	---	----	---	---	----	----	---	---
	7.0	PCC	---	---	----	---	---	----	----	---	---
	----	Subgrade	115	137	19.3	---	---	18.6	13.5	---	27
10	2.0	AC	---	---	----	---	---	----	----	---	---
	7.0	PCC	---	---	----	---	---	----	----	---	---
	14.0	Base	111	131	13.8	---	---	17.9	9.0	---	192
	----	Subgrade	---	---	----	---	---	----	----	---	---
11	21.0	PCC	---	---	----	---	---	----	----	---	---
	6.0	Base	134	142	7.1	---	---	6.1	21.0	---	82
12	7.0	AC	---	---	----	---	---	----	----	---	---
	20.0	Base	143	147	3.8	---	---	3.1	7.0	117	---
	----	Subgrade	---	---	----	109	127	15.7	27.0	13	---
			---	---	----	96	---	21.6	41.0	4.3	---

TABLE 3. SOIL CLASSIFICATION TEST RESULTS

Site	Layer	Atterberg Limits LL	PL	PI	Specific Gravity	Percent Passing #4 Sieve	Classification
3	BASE	NP	NP	NP	2.65	80	GRAVELY SILTY SAND (SP-SM)
	SUBGRADE	NP	NP	NP	2.64	100	SILTY SAND (SP-SM)
4	BASE	19	13	6	2.67	82	GRAVELY SILTY SAND (SM-SC)
	SUBGRADE	NP	NP	NP	2.65	100	SILTY SAND (SP-SM)
8	SUBGRADE	30	14	16	2.72	88	GRAVELY SANDY CLAY (CL)
10	BASE	33	15	18	2.69	--SAMPLE CONTAINED ASPHALT--NO TESTS--	
	SUBGRADE	38	15	23	2.74	94	SANDY CLAY (CL)
11	BASE	17	10	7	2.69	64	GRAVELY SILTY SAND (SP-SM)
	SUBGRADE	23	11	12	2.69	98	CLAYEY SAND (SC)
12	BASE	15	10	5	2.71	53	SANDY SILTY GRAVEL (GP-GM)
	SUBGRADE	35	22	13	2.68	100	SANDY CLAY (CL)

TABLE 4. LABORATORY RESILIENT MODULUS OF AC SURFACE LAYERS

Site	Lift	Sample Thickness in.	Average Instantaneous Resilient Modulus, psi	
			77 Deg F	104 Deg F
4	1	2.50	1,568,500	619,759
	2	2.54	1,348,381	349,607
8	1	2.68	903,572	400,887
	2	2.74	596,460	257,620
10	1	2.02	804,228	356,960
12	1	2.17	669,266	648,946
	2	1.70	1,230,766	757,317
	3	2.84	1,177,419	1,181,251

TABLE 5. LABORATORY TEST RESULTS, PCC LAYERS

Site No.	Dynamic Modulus psi	Flexural Strength psi
3	5,556,000	905
8	5,487,000	820
10	6,794,000	745
11	5,363,000	510

TABLE 6. CONDITION SURVEY RESULTS

Site	PCI	Rating	Prevalent Distresses
3	82	Very Good	Low-severity patching (large and small) Low-severity joint and corner spalls
4	97	Excellent	None
8	64	Good	Low-severity block cracking
10	68	Good	Low-severity longitudinal and transverse cracking Medium-severity joint reflection cracking
11	68	Good	High-severity joint seal damage Low- and medium-severity small patches
12	76	Very Good	Low-severity longitudinal and transverse cracking

layers are presented in Table 5. Results of a condition survey conducted to determine the pavement condition index (PCI) for each site are summarized in Table 6. The PCI is a numerical indicator based on a scale of 0 to 100 and is determined by measuring pavement surface distress that reflects the surface condition of the pavement.

B. SASW Testing Equipment

SASW test equipment used during this investigation included recording devices for monitoring, recording, and performing spectral analysis on waveforms, sources for generating waveforms, receivers for measuring waveforms, and a power supply.

A Hewlett Packard (HP) Model 3562A Dynamic Signal Analyzer equipped with an HP Model 9153A combined 10 megabyte hard disk and 3-1/4 in. floppy disk drive was used in this study for collecting and storing SASW data records. The HP 3562A is a versatile 2-channel device with a sampling rate of up to 100 kHz per channel. Spectral analyses functions such as the FFT, cross power spectrum, auto power spectrum, and coherence can be performed immediately, thereby allowing the frequency domain functions to be viewed in the field.

Impact excitation was used throughout this study. The impact sources were an array of hammers including a 4 oz. ball peen, 8 oz. ball peen, 40 oz. sledge, and 8 lb. sledge.

Both velocity transducers and accelerometers were used in this study. All receivers were vertically oriented. Geosource Model PC-3 velocity transducers were used for low frequency measurements (below 1000 Hz). PCB Piezotronics, Inc. Model 308B02 accelerometers (resonant frequency: 32 kHz; Sensitivity: 1000 mV/g), powered by a PCB Model

483A 12 channel power supply, were used for high frequency measurements associated with pavement surface layers. Coupling between the pavement surface and receivers was accomplished using a No. 2 plastilina sculpting clay.

The power supply used throughout this study was a Honda Model EM2200X portable, gasoline generator with a maximum power of 2.2 kva. An Omega Engineering, Inc., Omegascope infrared temperature gun was used for determining the surface temperature of asphalt surface layers at the time of testing.

C. SASW Testing Procedures

SASW tests were conducted at one location within each test site corresponding to the reference point location referred to previously. The common receivers midpoint (CRMP) geometry test procedure shown schematically in Figure 1 was used for all SASW testing with the centerline located at the reference point. Distances of 0.25-, 0.5-, 1.0-, 2.0-, 4.0-, and 8.0-ft. were marked off on either side of the imaginary centerline corresponding to spacings of 0.5-, 1.0-, 2.0-, 4.0-, 8.0-, and 16.0-ft. which were typically used. Data were collected for additional spacings only when deemed necessary based on visual observations of the data records during testing.

It should be noted in Figure 1 that two tests are indicated for each spacing with the source on opposite sides of the imaginary centerline. These are termed forward and reverse profiles and can be averaged to minimize the effect of any internal phase shift between receivers.

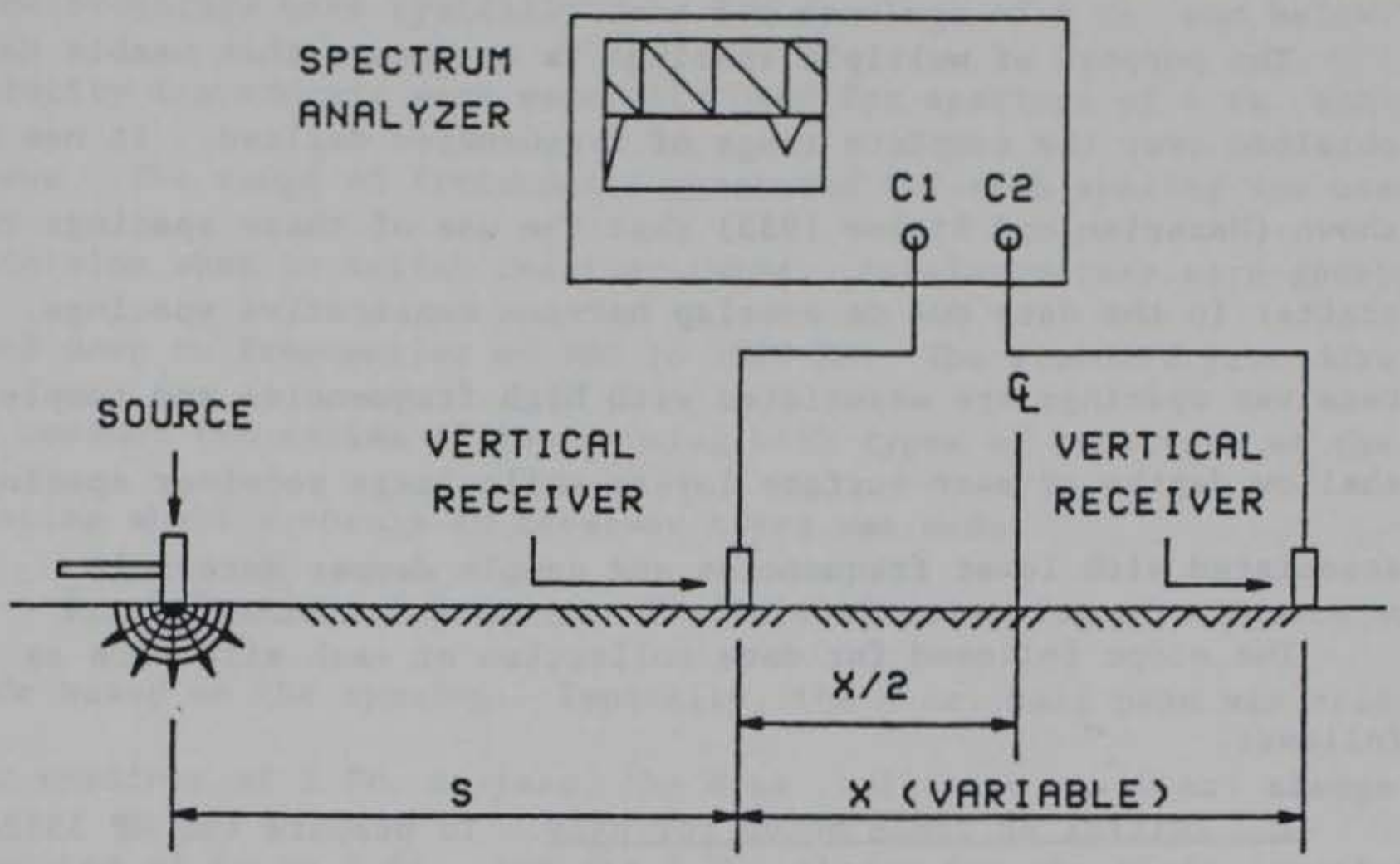

(A) GENERAL CONFIGURATION OF SASW TESTS

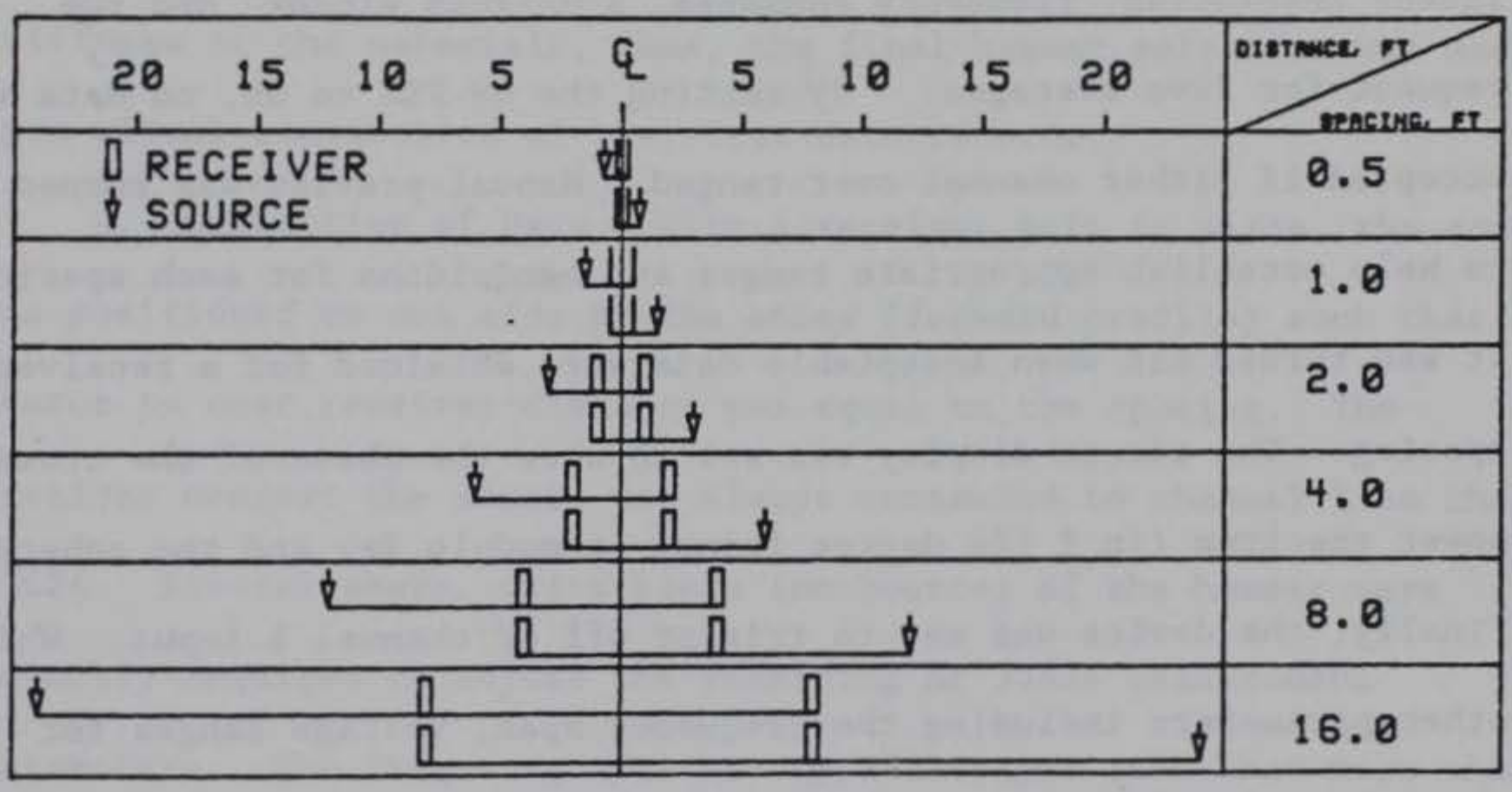

(B) COMMON RECEIVERS MIDPOINT GEOMETRY

Figure 1. Schematic of SASW test arrangement (after Nazarian, 1984)

The purpose of multiple spacings is to insure that usable data are obtained over the complete range of frequencies desired. It has been shown (Nazarian and Stokoe 1983) that the use of these spacings reduces scatter in the data due to overlap between consecutive spacings. Close receiver spacings are associated with high frequencies and sample shallow depths or near surface layers while large receiver spacings are associated with lower frequencies and sample deeper materials.

The steps followed for data collection at each site were as follows:

1. Initial HP 3562A Setup for SASW. To prepare the HP 3562A for SASW testing, the following measurement parameters were specified: linear resolution, frequency response, a uniform window, and the request for five averages. By setting the OV REJ to ON, no data were accepted if either channel over-ranged. Manual preview was turned ON to help establish appropriate ranges and bandwidths for each spacing. It was turned off when acceptable data were obtained for a receiver spacing. The screen display was set to show the phase of the cross power spectrum (in ± 180 degree format or modulo 2π) and the coherence. Finally, the device was set to trigger off of channel 1 input. While other parameters including the frequency span, voltage ranges for channels 1 and 2, the trigger level, and the trigger delay, were adjusted during testing depending on the particular spacing and source, this completes the initial setup of the analyzer.

2. Receiver Selection. A combination of accelerometers and velocity transducers were used for testing the six pavement sites.

Accelerometers were typically used for spacings of 4 ft. and below. Velocity transducers were generally used for spacings of 4 ft. and above. The range of frequencies generated for each spacing was used to determine when to switch receiver types. Accelerometers were generally used down to frequencies of 500 to 1000 Hz. The standard procedure was to conduct two series of tests using both types of receivers at the spacing where a change in receiver types was made.

3. Selection of Sources. The initial selection of a source was made based on the spacing. Typically, the 4 oz. ball peen was selected for spacings of 2 ft. or less, the 8 oz. ball peen or 40 oz. sledge for spacings of 4- to 8-ft., and the 8 lb. sledge for the 16 ft. spacing. The actual frequencies required for each spacing are dependent on the stiffness of the materials, thus, the final hammer selection was made upon visual examination of the first data records.

4. Collection of Data. With a receiver pair in place, the source was positioned on one side or the other (forward profile) such that the source to near receiver distance was equal to the spacing. The receiver nearest the source was always connected to channel 1 on the HP 3562A. Several sharp, crisp blows (no bounce) of the hammer were normally required to adjust the remaining HP 3562A measurement parameters. The frequency span was typically set such that more than three-fourths of the frequency range contained high quality (high coherence) data. The voltage ranges were set as low as possible without overloading to obtain the best resolution in the analog to digital conversion. With the manual preview function, time signals could be viewed after the first impact to determine if further

adjustments were necessary. After the frequency span and voltage ranges were established, the trigger level was set to trigger about halfway up the first major pulse on channel 1. A pre-trigger delay was then set for channels 1 and 2 to insure that the initial portion of the signal was obtained. The pre-trigger delay was set at approximately 10 percent of the total time record. These parameters generally had to be set for each receiver spacing.

After all the measurement parameters were set, the manual preview was turned off and signals from five impacts collected. The phase and coherence records were saved on disk. The file naming convention used was a three digit numerical value for each pair of records preceded by a "P" or "C" for phase and coherence. Then, without relocating the receivers, the same test was performed with the source on the opposite side of the receivers (reverse profile) with the receiver cables switched on the HP 3562A. Pertinent testing information was recorded on specially designed SASW data forms.

Steps 3 through 5 were repeated for each receiver spacing. SASW field data obtained following these procedures are presented in Appendices A-F (located immediately following the main text) for Sites 3, 4, 8, 10, 11, and 12 respectively.

IV. ANALYSIS OF DATA

SASW data reduction was accomplished in two phases. First, the field data for each site was converted to a dispersion curve. The second phase then consisted of determining the shear wave velocity profile by inverting the dispersion curve.

A. Determination of Dispersion Curve

The phase of the cross power spectrum and coherence records obtained from spectral analyses were both used during the construction of dispersion curves. While the actual dispersion curve was computed from the phase information, the coherence record was used to help identify frequency ranges containing "good" data. Nazarian and Stokoe (1986) showed that frequencies having a coherence value greater than 0.90 provide useful data. While this criterion was not rigidly followed, the coherence was used extensively to evaluate the quality of data. The phase of the cross power spectrum, with "poor" data ranges removed was used to calculate the dispersion curve.

For a particular frequency, f, a phase difference of 360 degrees is associated with a travel time between receivers of one period (1/f). Knowing the phase for a particular frequency (ϕ), the travel time, t, can be computed as:

$$t = \frac{\phi}{360\ (f)} \qquad \text{(IV-1)}$$

The phase velocity for a given frequency can then be obtained as

$$V_{ph} = \frac{X}{t} \qquad \text{(IV-2)}$$

where X is the distance between receivers and the corresponding

wavelength is:

$$L_R = \frac{V_{ph}}{f} \qquad \text{(IV-3)}$$

Repeating this procedure for all frequencies yields the dispersion curve for the given receiver spacing and source location. This curve is then filtered to remove all wavelengths greater than twice the receiver spacing. These wavelengths are too long for a given receiver spacing and may not have traveled a sufficient distance to adequately sample a depth proportional to the wavelength. The procedure is repeated for all spacings and source locations and the data combined to construct the total dispersion curve to represent the site.

The computer program SASW, containing data analysis routines presented by Hiltunen (1988), was used to reduce the field data collected during this study and construct the dispersion curves. The computer program SASW requires the existence of a pre-established data file identifying data records to be included in the dispersion curve and filtering information for the removal of bad data. Data files created for each site, containing the following information for all spacings and source locations, are included in Appendices A-F:

Line 1: Name of data file containing phase information

Line 2: Cutoff frequency (the maximum frequency for which usable data are available for a particular record, determined by visual examination of phase and coherence records)

Line 3: Number of poor data ranges to be removed before constructing dispersion curve (determined by visual

examination of phase and coherence records)

Lines 4_1 through 4_N (N = number of poor data ranges): Range containing poor data that are to be removed from phase information (for each range of poor data, the starting frequency, ending frequency, and number of phase wraps occurring prior to the ending frequency must be specified).

Line 5: Receiver spacing, ft.

The computer program SASW uses the above information and performs the following steps to construct the dispersion curve for a site:

a. Converts raw phase data from ± 180 degree format to a continuous format and eliminates frequencies containing poor quality data,

b. Redigitizes unwrapped phase vs. frequency data,

c. Generates dispersion curve data from converted phase data,

d. Run dispersion curve data through wavelength/receiver spacing filter to remove all wavelengths greater than twice the spacing,

e. Generates an average dispersion curve,

f. Compacts the dispersion curve data (reduces files to a more manageable size by averaging consecutive data points when the frequencies are within two percent of each other and the velocities are within four percent of each other).

Final dispersion curves are shown in Figures 2-7 for sites 3, 4, 8, 10, 11, and 12 respectively. The transition between the high velocity portion of the dispersion curve, corresponding to the surface

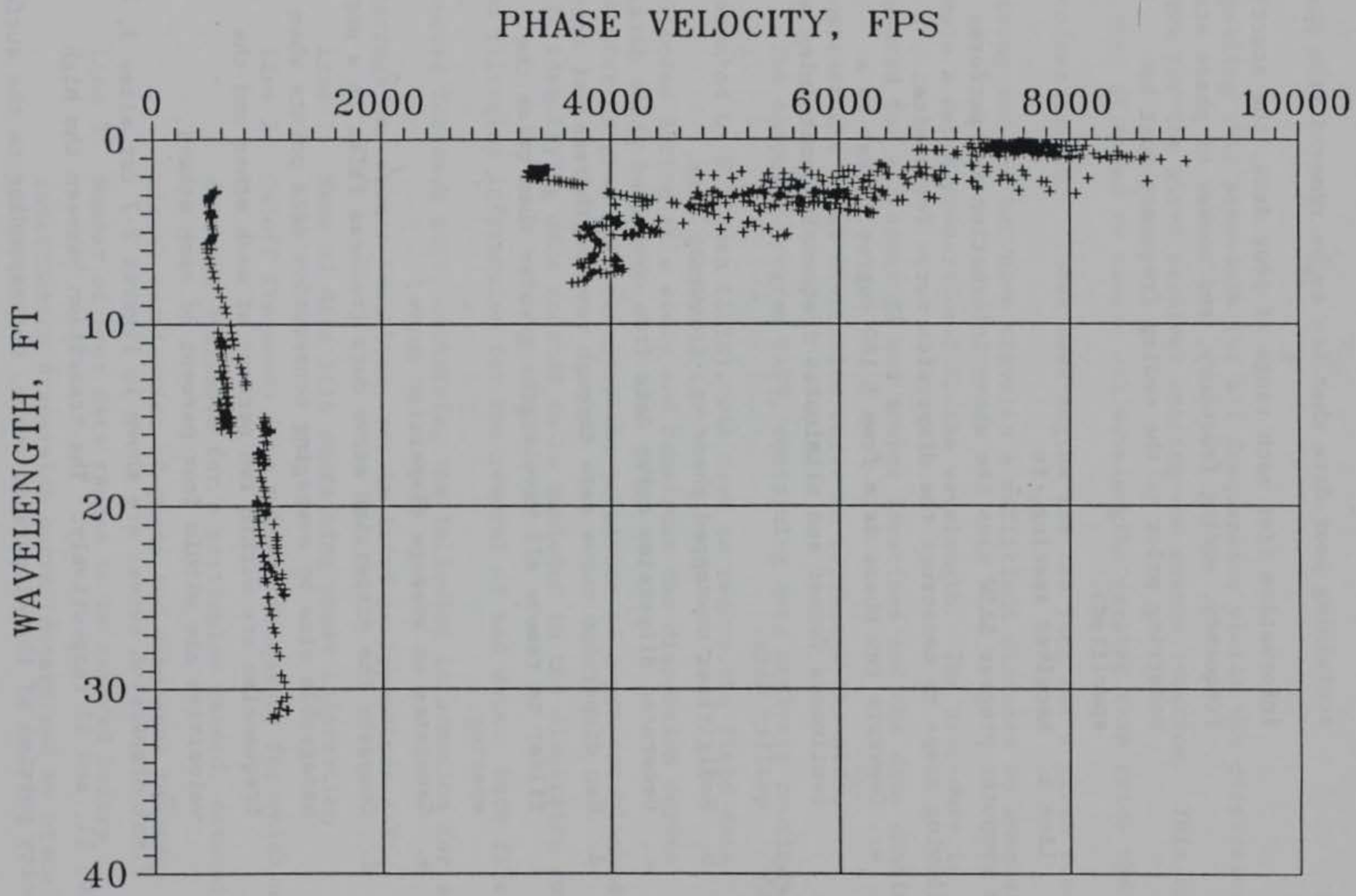

Figure 2. Experimental dispersion curve for site 3 (10" PCC/4" base/silty sand)

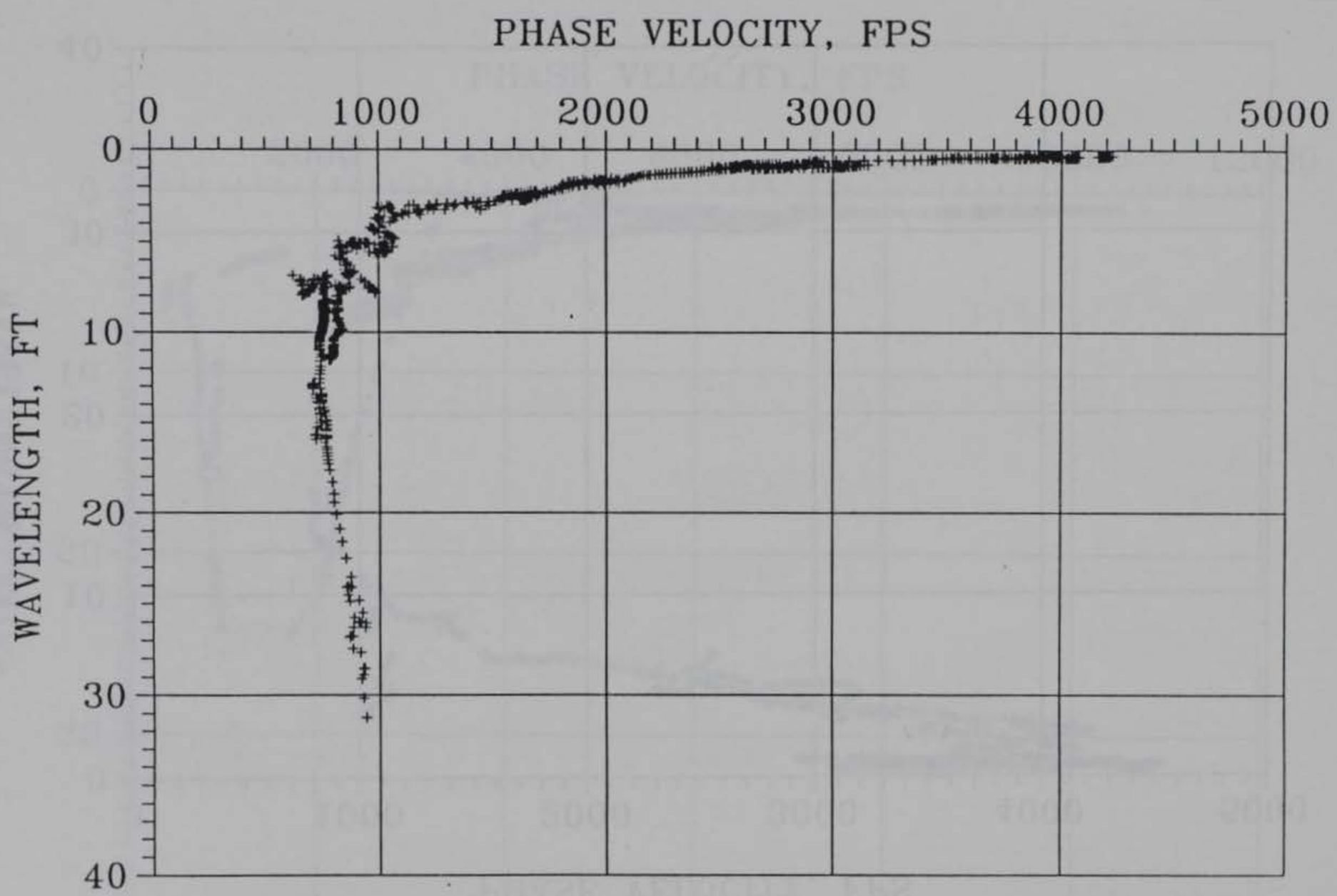

Figure 3. Experimental dispersion curve for site 4 (5.5" AC/13.5" base/silty sand)

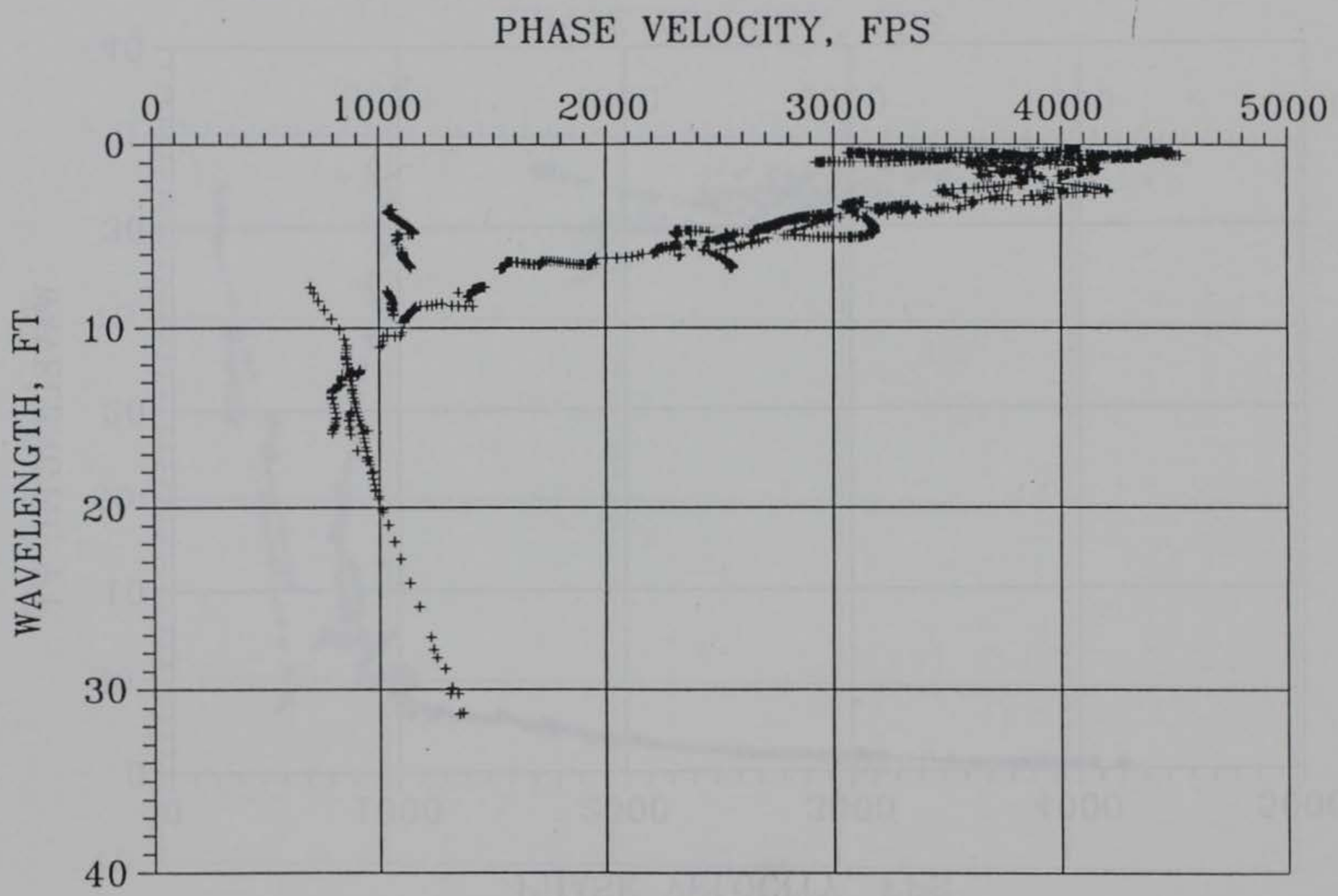

Figure 4. Experimental dispersion curve for site 8 (6.5" AC/7" PCC/sandy clay)

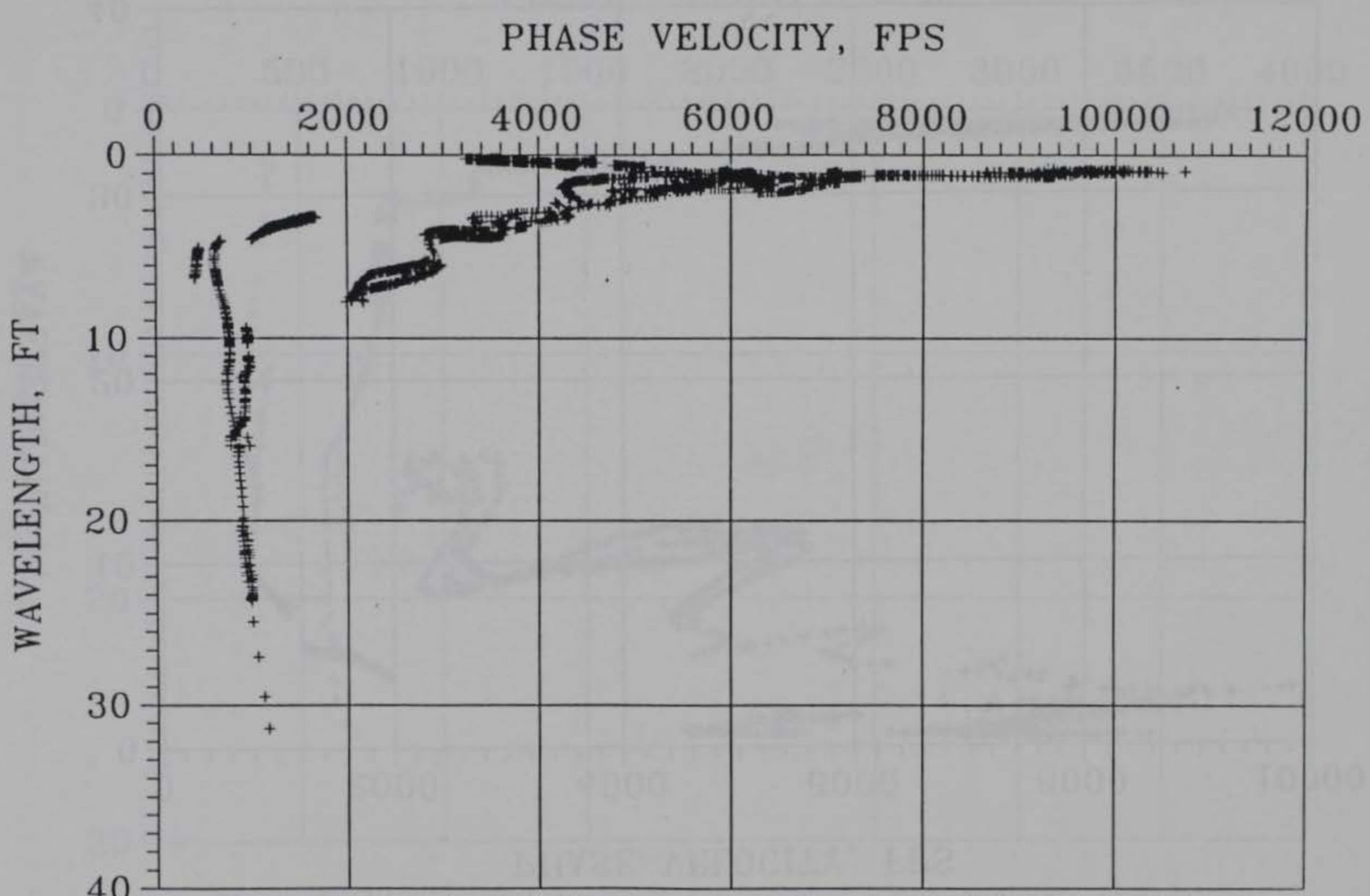

Figure 5. Experimental dispersion curve for site 10 (2" AC/7" PCC/14" base/sandy clay)

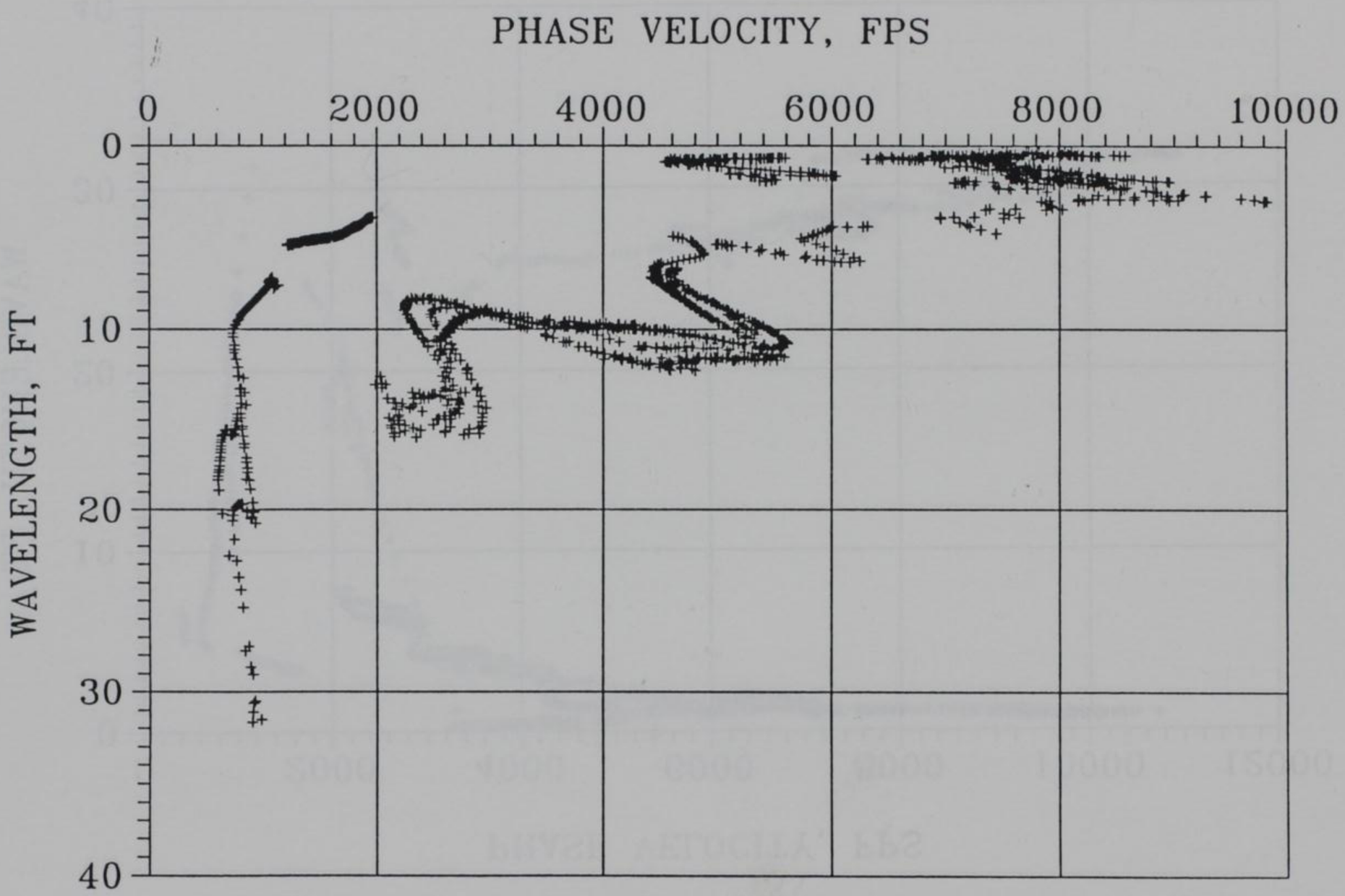

Figure 6. Experimental dispersion curve for site 11 (21" PCC/6" base/clayey sand)

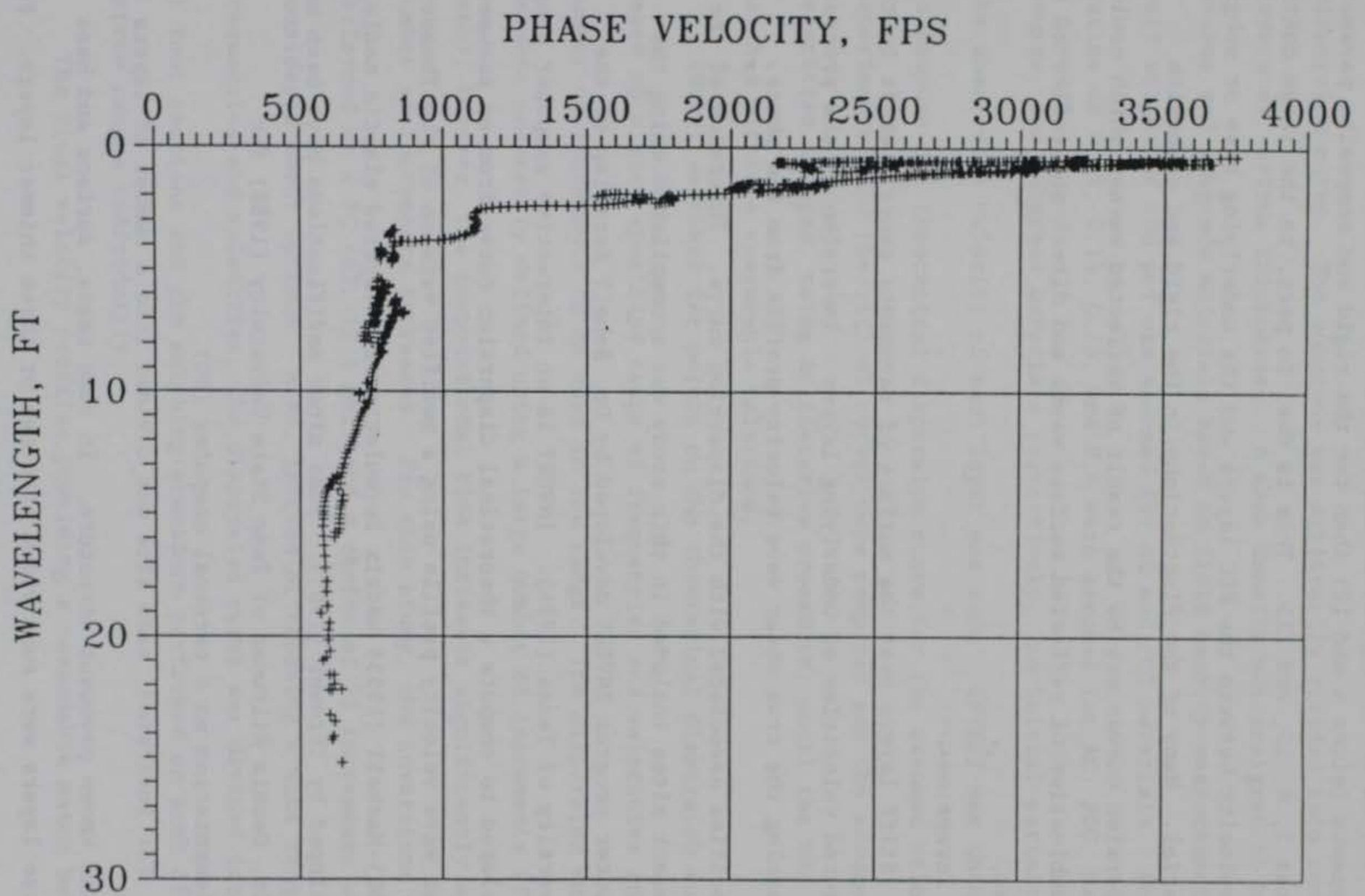

Figure 7. Experimental dispersion curve for site 12 (7" AC/20" base/sandy clay)

layer and the lower velocity portion of the curve, corresponding to the subgrade is much smoother and more continuous for the flexible pavements (sites 4 and 12) than for the rigid and composite pavements (sites 3, 8, 10, and 11). This is due, in part, to the large contrast in velocity between the PCC layers and the underlying base or subgrade material. Many of the fluctuations in the rigid and composite dispersion curves may be the result of reflected waves, which could be a combination of reflected surface waves and direct and reflected body waves.

B. Inversion

Stiff layers near the surface of pavements cause a shift in the measured velocities of underlying layers. Inversion is the process of obtaining the true shear wave velocity profile from the phase velocities associated with the dispersion curve. Inversion of the six pavement sites included in this study was accomplished using the computer program INVERT developed by Dr. Soheil Nazarian of the University of Texas (1984). INVERT is an interactive computer program developed to compute a theoretical dispersion curve from an assumed shear wave velocity profile using a modified version of the Thomson (1950)-Haskell (1953) matrix formulation for layered elastic media, as developed by Thrower (1965). Some minor modifications have been made by Dr. Dennis Hiltunen of Penn State University (1988) for implementation on a personal computer (PC).

For inversion, each site was divided into a number of layers based on the known pavement structure. In some cases, surface and base course layers were subdivided into two or three thinner layers. For

each site, a semi-infinite layer was located at a depth of approximately one-third of the maximum wavelength found in the dispersion curve. The subgrade was arbitrarily divided into several layers of various thicknesses. A mass density was assigned to base course and subgrade materials based on field density measurements. A unit weight of 150 pcf was assumed for AC and PCC materials. Poisson's ratios of 0.35, 0.15, 0.35, and 0.4 were assumed for AC, PCC, base course, and subgrade materials respectively. An initial estimate of the shear wave velocity of each layer was made. INVERT was then used to compute the theoretical dispersion curve for the assumed velocities. Experimental and theoretical curves were compared and the assumed velocities changed, using an iterative procedure, until the two curves matched within a reasonable tolerance.

INVERT searches for points on the theoretical dispersion curve based on a user specified range of frequencies and velocities and number of increments to be used in the range. The dispersion curve can be more accurately defined using a large number of increments (finer mesh), however, the computational time increases significantly as the number of increments increases. For this study, the inversions were performed on a PC (AT, 12.5 MHz) and a choice of 21 increments was considered about optimum. Also, instead of choosing a wide range of frequencies and velocities, the dispersion curve was divided into three or four sections and the matching procedure performed on each of the narrow ranges individually.

The final velocity profiles providing a reasonable match between

theoretical and experimental curves were assumed to be the true shear wave velocity with depth. A comparison of the measured and theoretical dispersion curves for sites 3, 4, 8, 10, 11, and 12 are shown in Figures 8-13 respectively. The Young's modulus was then computed for each layer using equation II-2.

The final velocity profiles and computed layer moduli are summarized in Tables 7-12 for the six sites. During inversion of the rigid pavements (sites 3 and 11), it was observed that the theoretical dispersion curve was not very sensitive to the velocity of the base course layers and the reported moduli may be in error. This was due to the large contrast in velocity between the PCC layer and the underlying base course and the fact that the base course layer was relatively thin.

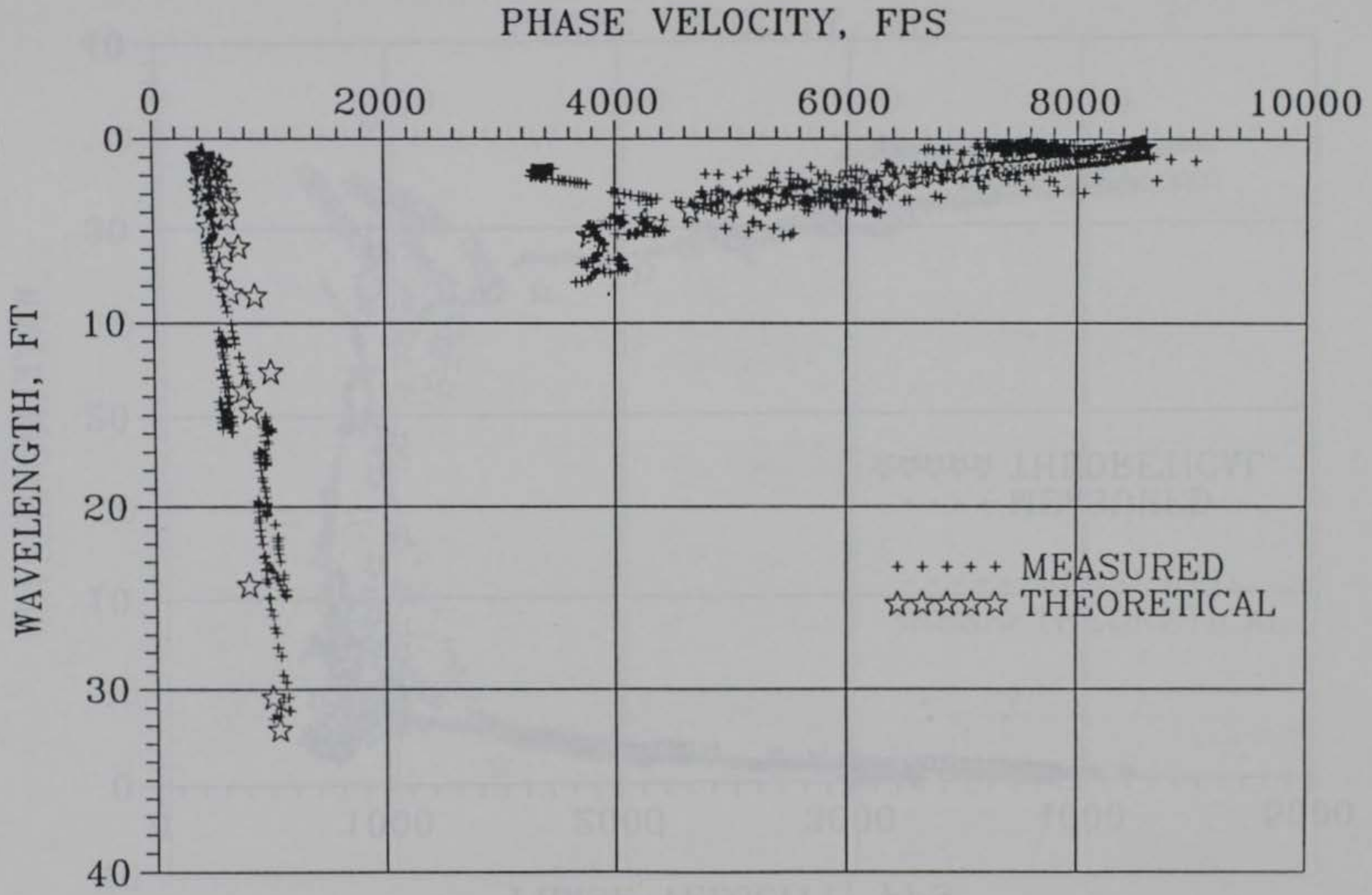

Figure 8. Comparison of measured and theoretical dispersion curves (after inversion) for site 3 (10" PCC/4" base/silty sand)

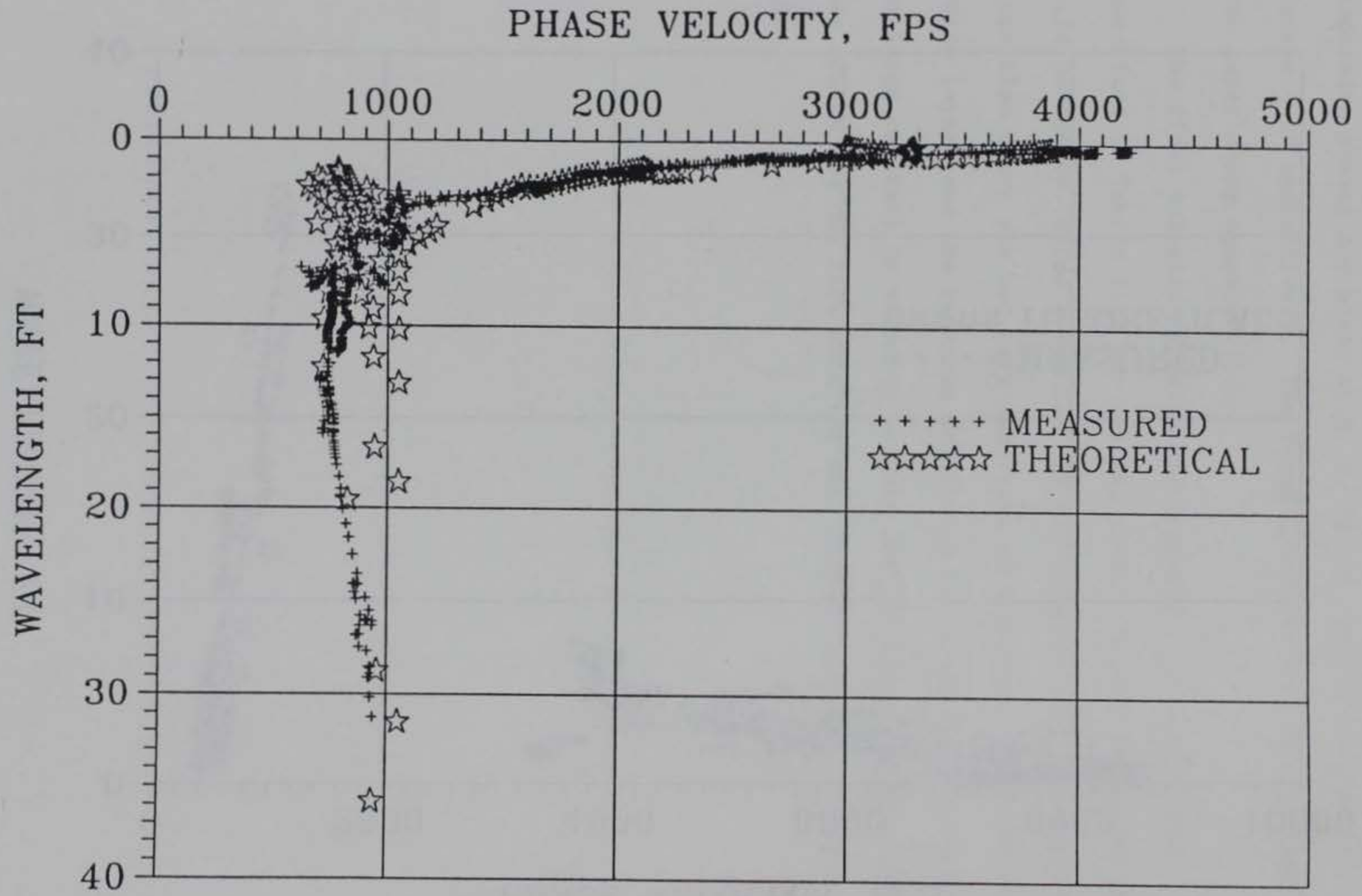

Figure 9. Comparison of measured and theoretical dispersion curves (after inversion) for site 4 (5.5" AC/13.5" base/silty sand)

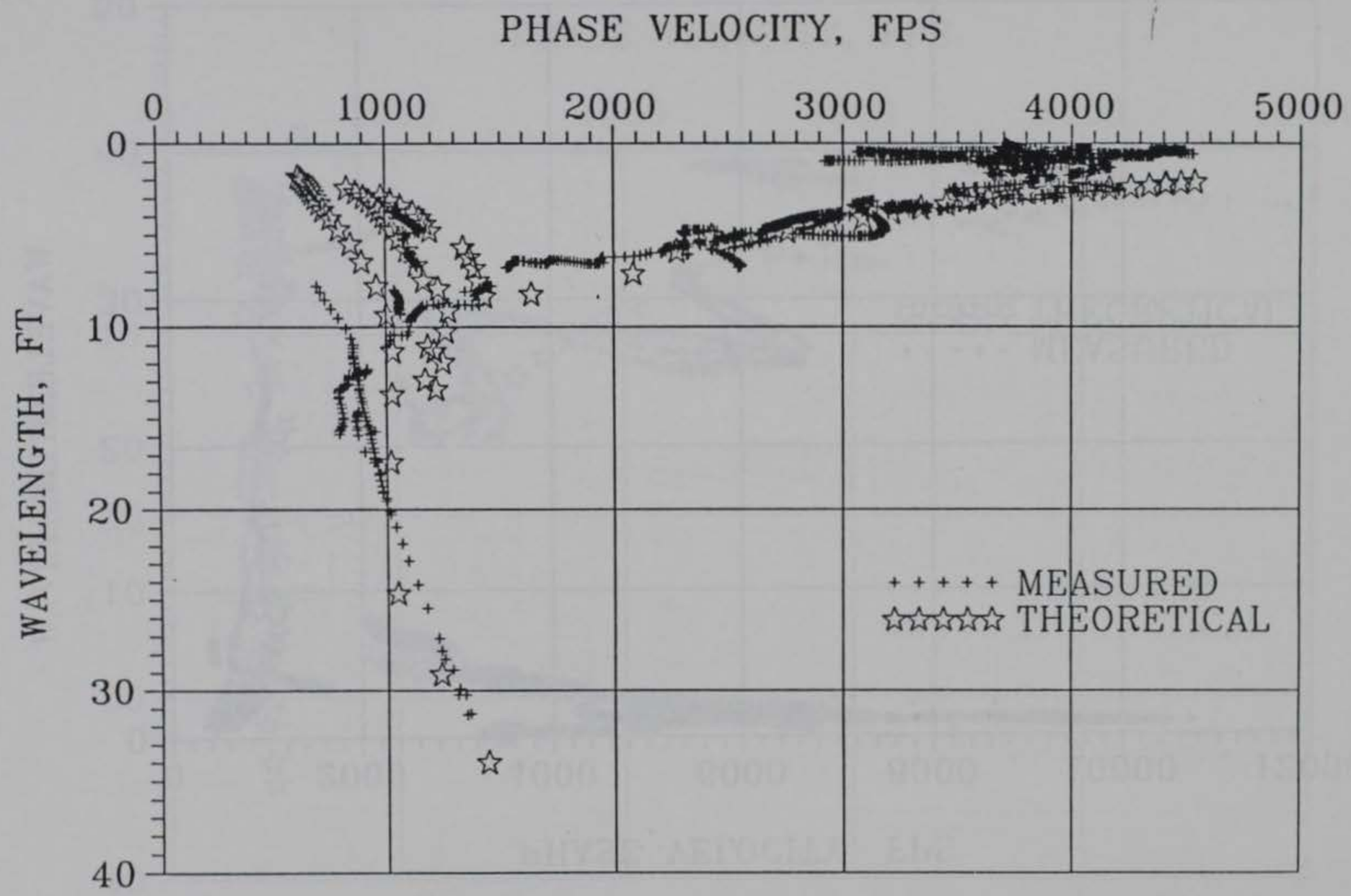

Figure 10. Comparison of measured and theoretical dispersion curves (after inversion) for site 8 (6.5" AC/7" PCC/sandy clay)

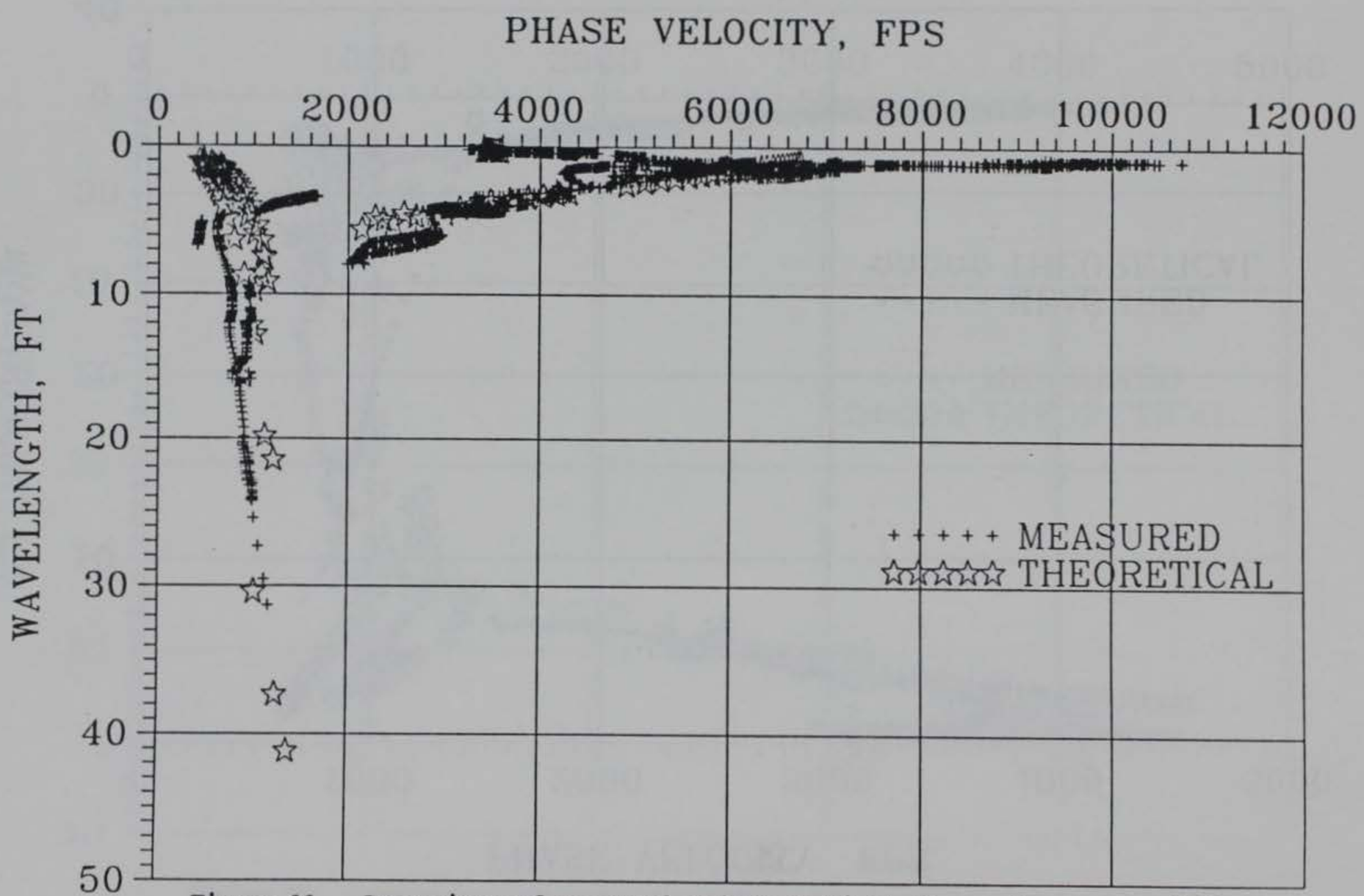

Figure 11. Comparison of measured and theoretical dispersion curves (after inversion) for site 10 (2" AC/7" PCC/14" base/sandy clay)

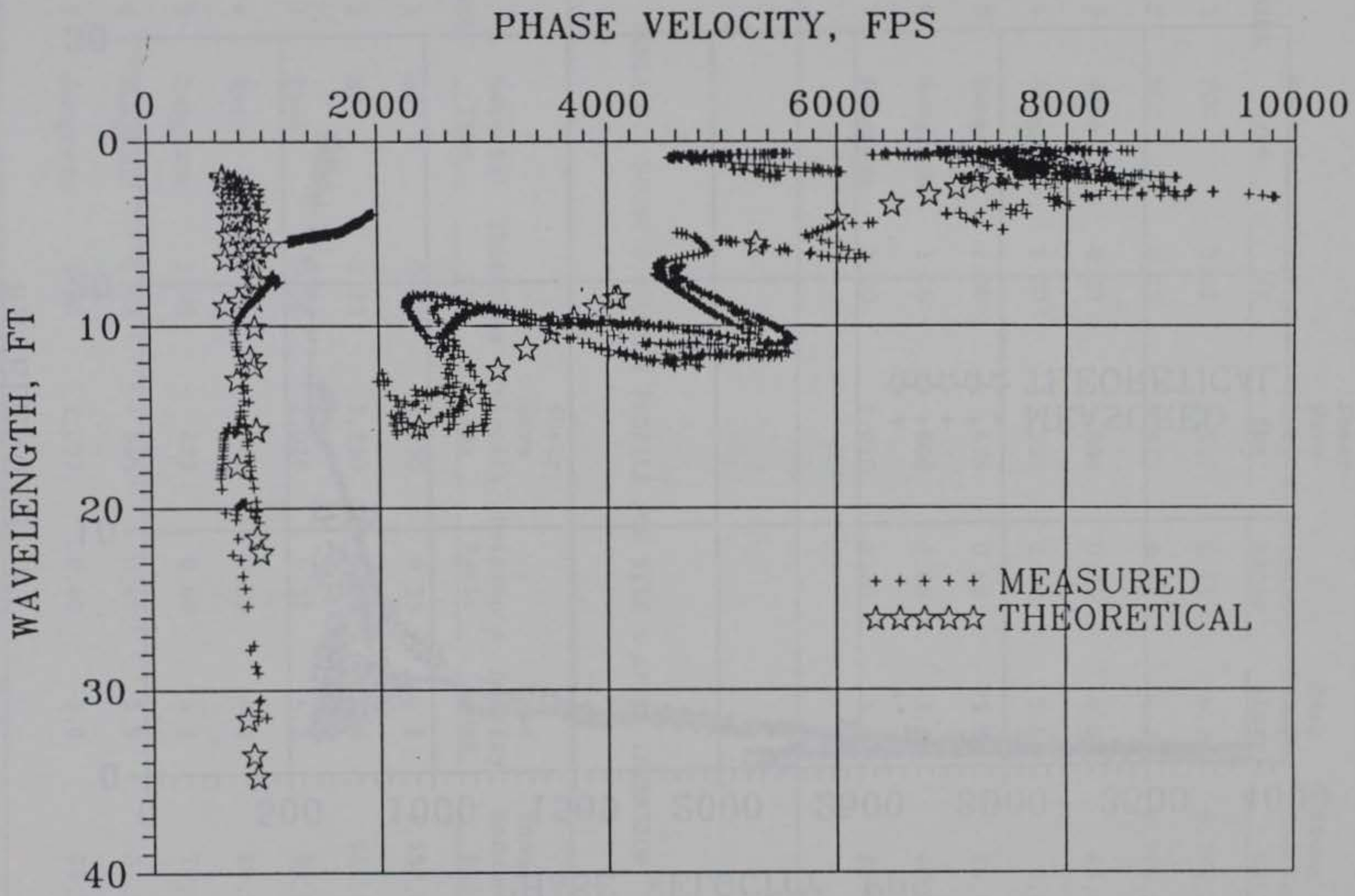

Figure 12. Comparison of measured and theoretical dispersion curves (after inversion) for site 11 (21" PCC/6" base/clayey sand)

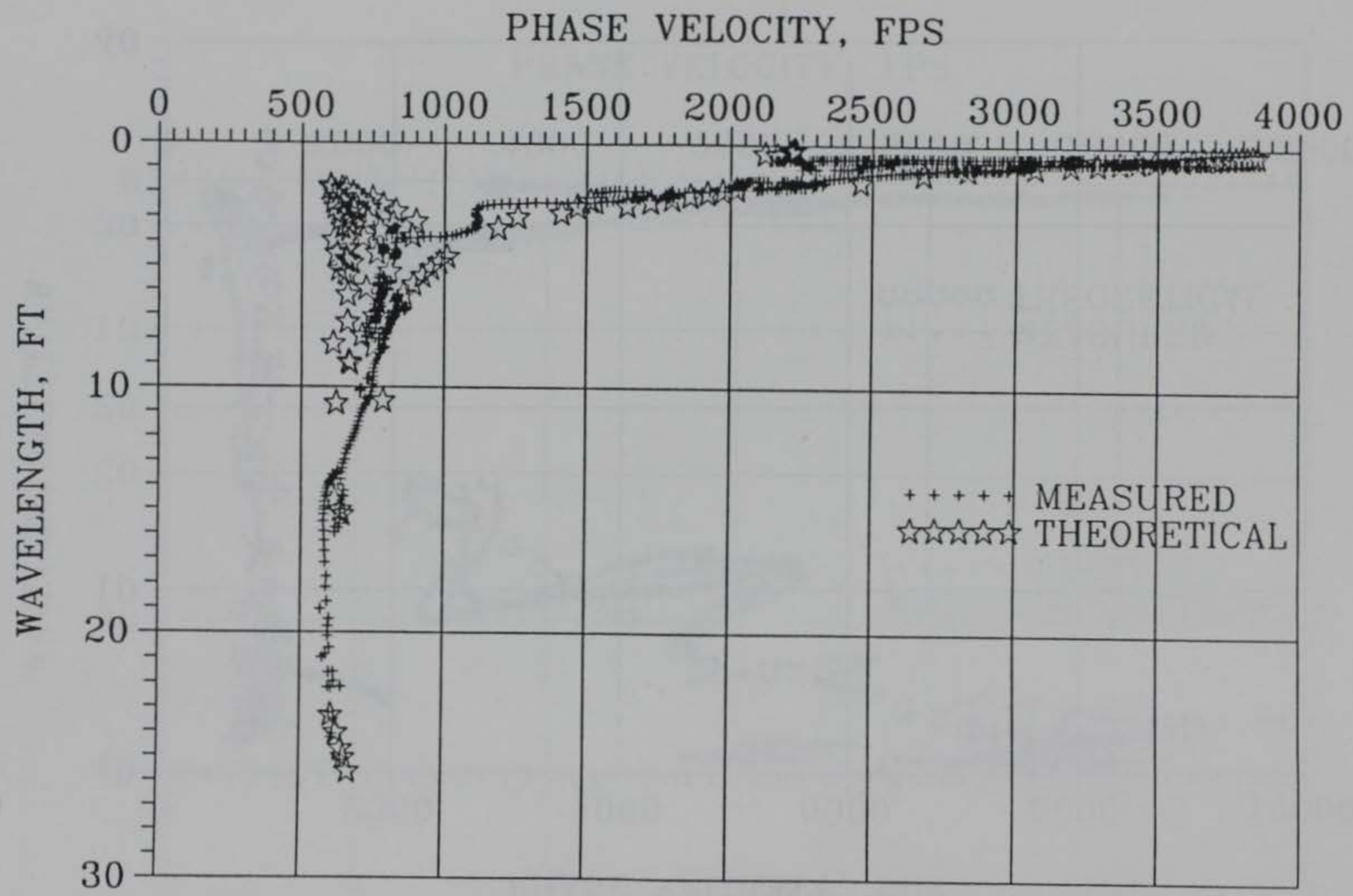

Figure 13. Comparison of measured and theoretical dispersion curves (after inversion) for site 12 (7" AC/20" base/sandy clay)

TABLE 7. YOUNG'S MODULUS PROFILE FOR SITE 3 AFTER INVERSION

Layer	Material Type	Thickness ft	Shear Wave Velocity fps	Poisson's Ratio	Mass Density slugs	Young's Modulus psi
1	PCC	0.42	9,517	0.15	4.7	6,799,286
2	PCC	0.42	9,517	0.15	4.7	6,799,286
3	Base	0.33	804	0.35	4.0	48,481
4	Subgrade	2.00	357	0.40	3.8	9,417
5	Subgrade	2.00	474	0.40	3.8	16,601
6	Subgrade	3.00	800	0.40	3.8	47,289
7	Subgrade	1.00	1,050	0.40	3.8	81,463

TABLE 8. YOUNG'S MODULUS PROFILE FOR SITE 4 AFTER INVERSION

Layer	Material Type	Thickness ft	Shear Wave Velocity fps	Poisson's Ratio	Mass Density slugs	Young's Modulus psi
1	AC	0.23	4,250	0.35	4.6	1,557,891
2	AC	0.23	3,250	0.35	4.6	911,016
3	Base	0.56	1,026	0.35	4.2	82,898
4	Base	0.56	941	0.35	4.2	69,732
5	Subgrade	2.00	429	0.40	3.9	13,956
6	Subgrade	1.00	645	0.40	3.9	31,549
7	Subgrade	1.00	1,037	0.40	3.9	81,549

TABLE 9. YOUNG'S MODULUS PROFILE FOR SITE 8 AFTER INVERSION

Layer	Material Type	Thickness ft	Shear Wave Velocity fps	Poisson's Ratio	Mass Density slugs	Young's Modulus psi
1	AC	0.27	3,960	0.35	4.7	1,381,941
2	AC	0.27	3,960	0.35	4.7	1,381,941
3	PCC	0.58	6,840	0.15	4.7	3,512,169
4	Subgrade	1.00	428	0.40	4.2	14,960
5	Subgrade	2.00	720	0.40	4.2	42,336
6	Subgrade	2.00	1,000	0.40	4.2	81,667
7	Subgrade	2.00	1,100	0.40	4.2	98,817
8	Subgrade	1.00	1,200	0.40	4.2	117,600

TABLE 10. YOUNG'S MODULUS PROFILE FOR SITE 10 AFTER INVERSION

Layer	Material Type	Thickness ft	Shear Wave Velocity fps	Poisson's Ratio	Mass Density slugs	Young's Modulus psi
1	AC	0.17	3,600	0.35	4.7	1,142,100
2	PCC	0.58	9,300	0.15	4.7	6,492,756
3	Base	0.59	988	0.35	4.1	75,041
4	Base	0.59	988	0.35	4.1	75,041
5	Subgrade	1.50	424	0.40	4.2	14,682
6	Subgrade	2.00	697	0.40	4.2	39,674
7	Subgrade	2.00	955	0.40	4.2	74,482
8	Subgrade	2.00	1,082	0.40	4.2	95,609
9	Subgrade	1.00	1,200	0.40	4.2	117,600

TABLE 11. YOUNG'S MODULUS PROFILE FOR SITE 11 AFTER INVERSION

Layer	Material Type	Thickness ft	Shear Wave Velocity fps	Poisson's Ratio	Mass Density slugs	Young's Modulus psi
1	PCC	0.88	8,727	0.15	4.7	5,717,329
2	PCC	0.88	8,622	0.15	4.7	5,580,579
3	Base	0.50	810	0.35	4.4	54,128
4	Subgrade	2.00	404	0.40	3.9	12,377
5	Subgrade	3.00	364	0.40	3.9	10,048
6	Subgrade	2.00	408	0.40	3.9	12,624
7	Subgrade	1.00	900	0.40	3.9	61,425

TABLE 12. YOUNG'S MODULUS PROFILE FOR SITE 12 AFTER INVERSION

Layer	Material Type	Thickness ft	Shear Wave Velocity fps	Poisson's Ratio	Mass Density slugs	Young's Modulus psi
1	AC	0.20	4,367	0.35	4.6	1,644,847
2	AC	0.20	2,939	0.35	4.6	745,003
3	AC	0.20	2,221	0.35	4.6	425,458
4	Base	0.84	747	0.35	4.6	48,128
5	BAse	0.84	651	0.35	4.6	36,553
6	Subgrade	3.00	559	0.40	3.9	23,696
7	Subgrade	3.00	501	0.40	3.9	19,034
8	Subgrade	1.00	650	0.40	3.9	32,040

V. ELASTIC LAYER METHODOLOGY

A. Procedure

A study conducted at WES (Bush 1980) has shown that the deflection basin produced by applying a load to the surface of a pavement with an NDT device can be used to derive the Young's modulus of pavement layers. A computer optimization routine was developed to determine a set of modulus values that provide the best fit between a measured deflection basin and a computed deflection basin when given an initial estimate of the elastic modulus values and a limiting range of moduli.

Initially, a set of modulus values is assumed and the theoretical deflection is computed at offsets corresponding to the measured deflections. Subsequently, each modulus is varied individually, and a new set of deflections is computed for each variation. A simplified description of the iterative process for adjusting the modulus values and matching the deflection basins is shown in Figure 14. This illustration is for one deflection and one layer. For multiple deflections and layers, the solution is obtained by developing a set of equations that define the slope and intercept for each deflection and each unknown layer modulus as follows:

$$\text{Log (Deflection}_j\text{)} = A_{ji} + S_{ji}(\text{Log } E_i)$$

where

A = intercept,

S = slope,

j = 1, 2, ... ND [ND = number of deflections], and

i = 1, 2, ... NL [NL = number of layers with unknown moduli]

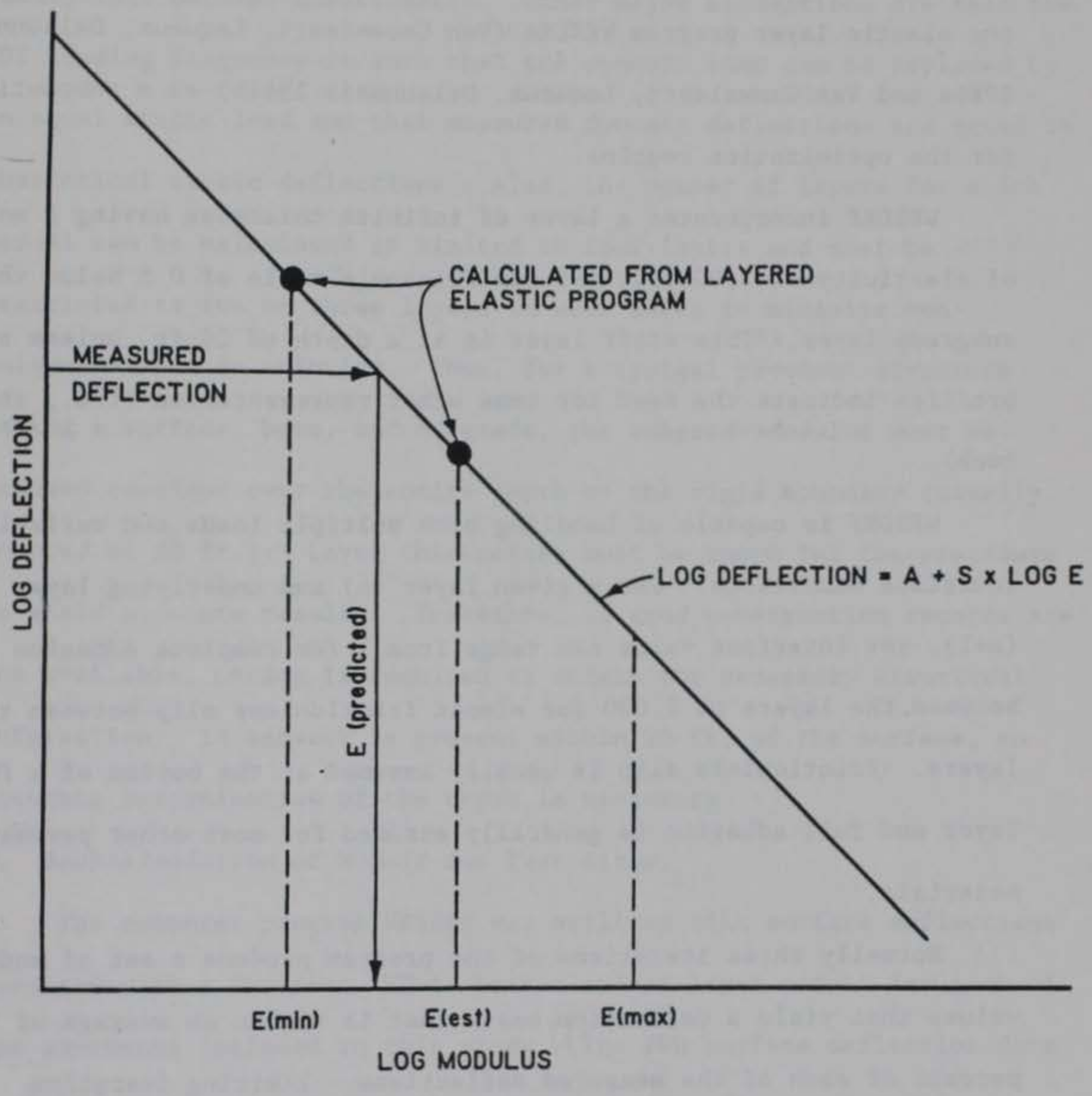

Figure 14. Simplified description of how deflection basins are matched in WESDEF (one deflection and one layer)

B. WESDEF

The modulus backcalculation computer program WESDEF was developed (Van Cauwelaert, Alexander, White, and Barker 1988) by incorporating the elastic layer program WESLEA (Van Cauwelaert, Lequeux, Delaunnois 1986a and Van Cauwelaert, Lequeux, Delaunnois 1986b) as a subroutine for the optimization routine.

WESDEF incorporates a layer of infinite thickness having a modulus of elasticity of 1,000,000 psi and Poisson's ratio of 0.5 below the subgrade layer. This stiff layer is at a depth of 20 ft. unless soil profiles indicate the need for some other representation (i.e., shallow rock).

WESDEF is capable of handling both multiple loads and variable interface conditions. For a given layer (n) and underlying layer (n+1), the interface value can range from 1 for complete adhesion between the layers to 1,000 for almost frictionless slip between the layers. Frictionless slip is usually assumed at the bottom of a PCC layer and full adhesion is generally assumed for most other pavement materials.

Normally three iterations of the program produce a set of modulus values that yield a deflection basin that is within an average of 3 percent of each of the measured deflections. Limiting iteration criteria require that the absolute sum of the percent differences between computed and measured deflections or the predicted change in modulus values be less than 10 percent.

C. Limitations of Elastic Layer Deflection Based Procedure

Limitations of the elastic layer approach include the assumptions

of elastic, homogenous layers extending horizontally to infinity. For the case of badly cracked pavements, the validity of these basic assumptions becomes questionable. Other major assumptions are that the NDT loading frequency is such that the dynamic load can be replaced by an equal static load and that measured dynamic deflections are equal to theoretical static deflections. Also, the number of layers for which moduli can be calculated is limited to four layers and must be restricted to two or three layers in most cases to minimize non-uniqueness of the solution. Thus, for a typical pavement structure having a surface, base, and subgrade, the subgrade modulus must be assumed constant over the entire depth to the rigid boundary (usually located at 20 ft.). Layer thicknesses must be known for the procedure to yield accurate results. Therefore, if good construction records are not available, coring is required to obtain the necessary structural information. If bedrock is present within 20 ft. of the surface, an accurate determination of the depth is necessary.

D. Backcalculation of Moduli for Test Sites

The computer program WESDEF was utilized with surface deflections measured with a Dynatest FWD to backcalculate layer moduli for each of the pavements included in this study. The FWD surface deflection data in Table 13, extracted from the previous report discussed earlier (Bentsen, Bush, and Harrison), were collected within each test site on the reference point location.

The Dynatest Model 8003 FWD is a trailer-mounted, impulse load device that can produce a load between 1,500 and 24,000 lb. The

TABLE 13. FWD REFERENCE POINT TEST DATA

Site	Date Tested	Force lbs	Deflection, mils For offset from center of load, in. 0	12	24	36	48	60	72	Mean Pavement Temperature Deg Fahrenheit
3	08-08-87	25344	8.6	7.9	7.3	6.2	5.4	4.3	3.5	102.7
4	08-08-87	24534	38.9	22.2	11.6	7.0	4.8	3.6	2.8	105.3
8	08-12-87	25265	21.0	10.6	8.1	5.4	3.3	2.2	1.5	112.0
10	08-12-87	25360	11.7	10.3	8.6	6.7	5.0	3.5	2.7	96.6
11	08-17-87	25805	3.1	2.9	2.8	2.7	2.6	2.2	2.2	102.1
12	08-18-88	24518	49.6	29.4	14.9	8.2	5.5	4.2	3.8	105.3

single-pulse transient load is generated by a weight dropping on rubber pads which transmit the force to the pavement through an 11.8-in.-diameter dense rubber plate cushioned with a thin rubber pad. Deflections are determined using seven geophones that are typically placed 1-ft. apart from the center of the load, but the outer six can be varied from 12 to 95 in. away from the plate. The falling weight system is controlled by a Hewlett-Packard Inter Personal Computer (IPC) and can produce up to eight loadings selected from any combination of four adjustable drop heights in a 1-2 minute period. Load and deflection data are recorded on paper for each loading and can be automatically saved to a magnetic disk.

The modulus values predicted by WESDEF for sites 3, 4, 8, 10, 11, and 12 are shown on the computer outputs in Figures 15-20. For each site, an attempt was made to compute modulus values for all layers and this was successfully done for sites 4, 8, and 12. WESDEF was unable to predict realistic values for the base course layers beneath the rigid pavements (sites 3 and 11) and a composite modulus was obtained for the combined base and subgrade layers. WESDEF was unable to predict realistic modulus values for all four layers at site 10 and a modulus value of 230,000 psi was assigned for the thin AC surface layer based on the mean pavement temperature at the time of testing and Figure 21.

**********WESDEF OUTPUT SUMMARY**********

NUMBER OF ITERATIONS PERFORMED: 2

DEFLECTIONS COMPUTED FOR FINAL MODULUS VALUES
****

POSITION	SENSOR OFFSET IN.	MEASURED DEFLECTION MILS	COMPUTED DEFLECTION MILS	DIFFERENCE	% DIFF.
1	3.0	8.6	8.7	-0.1	-0.9
2	12.0	7.9	8.1	-0.2	-2.1
3	24.0	7.3	7.2	0.1	2.0
4	36.0	6.2	6.2	0.0	0.4
5	48.0	5.4	5.2	0.2	3.4
6	60.0	4.3	4.3	0.0	-0.9
7	72.0	3.5	3.6	-0.1	-1.6
		ABSOLUTE SUM:		0.7	11.3
		ARITHMETIC SUM:			0.3
		AVERAGE:		0.1	1.6

FINAL MODULUS VALUES
****

LAYER NO.	MATERIAL TYPE	MODULUS PSI	POISSON'S RATIO	THICK. IN.	INTERFACE VALUE
1	PCC	8242664.	0.15	10.00	1000.
2	SUBGRADE	19264.	0.40	230.00	1.
3	RIGID BOUNDARY	1000000.	0.50	1.00	1.
4	RIGID BOUNDARY	1000000.	0.50	1.00	1.
5	RIGID BOUNDARY	1000000.	0.50	SEMI-INF	

ABSOLUTE SUM OF % DIFF. NOT WITHIN TOLERANCE
CHANGE IN MODULUS VALUES WITHIN TOLERANCE

Figure 15. WESDEF output summary for site 3 (10" PCC/4" base/silty sand)

**********WESDEF OUTPUT SUMMARY**********

NUMBER OF ITERATIONS PERFORMED: 3

DEFLECTIONS COMPUTED FOR FINAL MODULUS VALUES
****

POSITION	SENSOR OFFSET IN.	MEASURED DEFLECTION MILS	COMPUTED DEFLECTION MILS	DIFFERENCE	% DIFF.
1	3.0	38.9	39.6	-0.7	-1.8
2	12.0	22.2	21.8	0.4	1.8
3	24.0	11.6	11.7	-0.1	-0.8
4	36.0	7.0	7.3	-0.3	-4.8
5	48.0	4.8	5.0	-0.2	-4.1
6	60.0	3.6	3.6	0.0	1.0
7	72.0	2.8	2.6	0.2	7.0
			ABSOLUTE SUM:	2.0	21.4
			ARITHMETIC SUM:		-1.8
			AVERAGE:	0.3	3.1

FINAL MODULUS VALUES
****

LAYER NO.	MATERIAL TYPE	MODULUS PSI	POISSON'S RATIO	THICK. IN.	INTERFACE VALUE
1	AC	206491.	0.35	5.50	1.
2	BASE OR SUBBASE	35844.	0.35	13.50	1.
3	SUBGRADE	20491.	0.40	221.00	1.
4	RIGID BOUNDARY	1000000.	0.50	1.00	1.
5	RIGID BOUNDARY	1000000.	0.50	SEMI-INF	

REACHED MAX NO OF ITERATIONS
ABSOLUTE SUM OF % DIFF. NOT WITHIN TOLERANCE
CHANGE IN MODULUS VALUES WITHIN TOLERANCE

Figure 16. WESDEF output summary for site 4 (5.5" AC/13.5" base/silty sand)

**********WESDEF OUTPUT SUMMARY**********

NUMBER OF ITERATIONS PERFORMED: 3

DEFLECTIONS COMPUTED FOR FINAL MODULUS VALUES
****

POSITION	SENSOR OFFSET IN.	MEASURED DEFLECTION MILS	COMPUTED DEFLECTION MILS	DIFFERENCE	% DIFF.
1	3.0	21.0	21.8	-0.8	-4.0
2	12.0	10.6	10.7	-0.1	-1.2
3	24.0	8.1	7.5	0.6	7.3
4	36.0	5.4	5.0	0.4	7.0
5	48.0	3.3	3.4	-0.1	-2.1
6	60.0	2.2	2.3	-0.1	-5.5
7	72.0	1.5	1.7	-0.2	-11.4
			ABSOLUTE SUM:	2.3	38.5
			ARITHMETIC SUM:		-10.0
			AVERAGE:	0.3	5.5

FINAL MODULUS VALUES
****

LAYER NO.	MATERIAL TYPE	MODULUS PSI	POISSON'S RATIO	THICK. IN.	INTERFACE VALUE
1	AC	114603.	0.35	6.50	1.
2	PCC	942662.	0.15	7.00	1000.
3	SUBGRADE	34479.	0.40	226.50	1.
4	RIGID BOUNDARY	1000000.	0.50	1.00	1.
5	RIGID BOUNDARY	1000000.	0.50	SEMI-INF	

REACHED MAX NO OF ITERATIONS
ABSOLUTE SUM OF % DIFF. NOT WITHIN TOLERANCE
CHANGE IN MODULUS VALUES NOT WITHIN TOLERANCE

Figure 17. WESDEF output summary for site 8 (6.5" AC/7" PCC/sandy clay)

**********WESDEF OUTPUT SUMMARY**********

NUMBER OF ITERATIONS PERFORMED: 3

DEFLECTIONS COMPUTED FOR FINAL MODULUS VALUES

POSITION	SENSOR OFFSET IN.	MEASURED DEFLECTION MILS	COMPUTED DEFLECTION MILS	DIFFERENCE	% DIFF.
1	3.0	11.7	12.8	-1.1	-9.2
2	12.0	10.3	10.3	0.0	-0.1
3	24.0	8.6	8.4	0.2	2.7
4	36.0	6.7	6.5	0.2	2.9
5	48.0	5.0	4.9	0.1	1.9
6	60.0	3.5	3.6	-0.1	-2.9
7	72.0	2.7	2.7	0.0	-1.5
			ABSOLUTE SUM:	1.8	21.2
			ARITHMETIC SUM:		-6.1
			AVERAGE:	0.3	3.0

FINAL MODULUS VALUES

LAYER NO.	MATERIAL TYPE	MODULUS PSI	POISSON'S RATIO	THICK. IN.	INTERFACE VALUE
1	AC	230000.	0.35	2.00	1.
2	PCC	6928886.	0.15	7.00	1000.
3	BASE OR SUBBASE	17183.	0.35	14.00	1.
4	SUBGRADE	27372.	0.40	217.00	1.
5	RIGID BOUNDARY	1000000.	0.50	SEMI-INF	

REACHED MAX NO OF ITERATIONS
ABSOLUTE SUM OF % DIFF. NOT WITHIN TOLERANCE
CHANGE IN MODULUS VALUES NOT WITHIN TOLERANCE

Figure 18. WESDEF output summary for site 10 (2" AC/7" PCC/14" base/sandy clay)

**********WESDEF OUTPUT SUMMARY**********

NUMBER OF ITERATIONS PERFORMED: 1

DEFLECTIONS COMPUTED FOR FINAL MODULUS VALUES
****

POSITION	SENSOR OFFSET IN.	MEASURED DEFLECTION MILS	COMPUTED DEFLECTION MILS	DIFFERENCE	% DIFF.
1	3.0	3.1	3.2	-0.1	-3.8
2	12.0	2.9	3.0	-0.1	-4.6
3	24.0	2.8	2.9	-0.1	-3.8
4	36.0	2.7	2.8	-0.1	-2.4
5	48.0	2.6	2.6	0.0	-0.3
6	60.0	2.2	2.4	-0.2	-11.0
7	72.0	2.2	2.3	-0.1	-3.4
		ABSOLUTE SUM:		0.7	29.3
		ARITHMETIC SUM:			-29.3
		AVERAGE:		0.1	4.2

FINAL MODULUS VALUES
****

LAYER NO.	MATERIAL TYPE	MODULUS PSI	POISSON'S RATIO	THICK. IN.	INTERFACE VALUE
1	PCC	12498614.	0.15	21.00	1000.
2	SUBGRADE	15837.	0.40	219.00	1.
3	RIGID BOUNDARY	1000000.	0.50	1.00	1.
4	RIGID BOUNDARY	1000000.	0.50	1.00	1.
5	RIGID BOUNDARY	1000000.	0.50	SEMI-INF	

ABSOLUTE SUM OF % DIFF. NOT WITHIN TOLERANCE
CHANGE IN MODULUS VALUES WITHIN TOLERANCE

Figure 19. WESDEF output summary for site 11 (21" PCC/6" base/clayey sand)

**********WESDEF OUTPUT SUMMARY**********

NUMBER OF ITERATIONS PERFORMED: 3

DEFLECTIONS COMPUTED FOR FINAL MODULUS VALUES
****

POSITION	SENSOR OFFSET IN.	MEASURED DEFLECTION MILS	COMPUTED DEFLECTION MILS	DIFFERENCE	% DIFF.
1	3.0	49.6	51.4	-1.8	-3.6
2	12.0	29.4	28.0	1.4	4.9
3	24.0	14.9	14.6	0.3	2.2
4	36.0	8.2	8.9	-0.7	-8.0
5	48.0	5.5	6.0	-0.5	-8.9
6	60.0	4.2	4.3	-0.1	-2.4
7	72.0	3.8	3.2	0.6	15.9
			ABSOLUTE SUM:	5.4	45.8
			ARITHMETIC SUM:		0.0
			AVERAGE:	0.8	6.5

FINAL MODULUS VALUES
****

LAYER NO.	MATERIAL TYPE	MODULUS PSI	POISSON'S RATIO	THICK. IN.	INTERFACE VALUE
1	AC	126030.	0.35	7.00	1.
2	BASE OR SUBBASE	20839.	0.35	20.00	1.
3	SUBGRADE	16872.	0.40	213.00	1.
4	RIGID BOUNDARY	1000000.	0.50	1.00	1.
5	RIGID BOUNDARY	1000000.	0.50	SEMI-INF	

REACHED MAX NO OF ITERATIONS
ABSOLUTE SUM OF % DIFF. NOT WITHIN TOLERANCE
CHANGE IN MODULUS VALUES WITHIN TOLERANCE

Figure 20. WESDEF output summary for site 12 (7" AC/20" base/sandy clay)

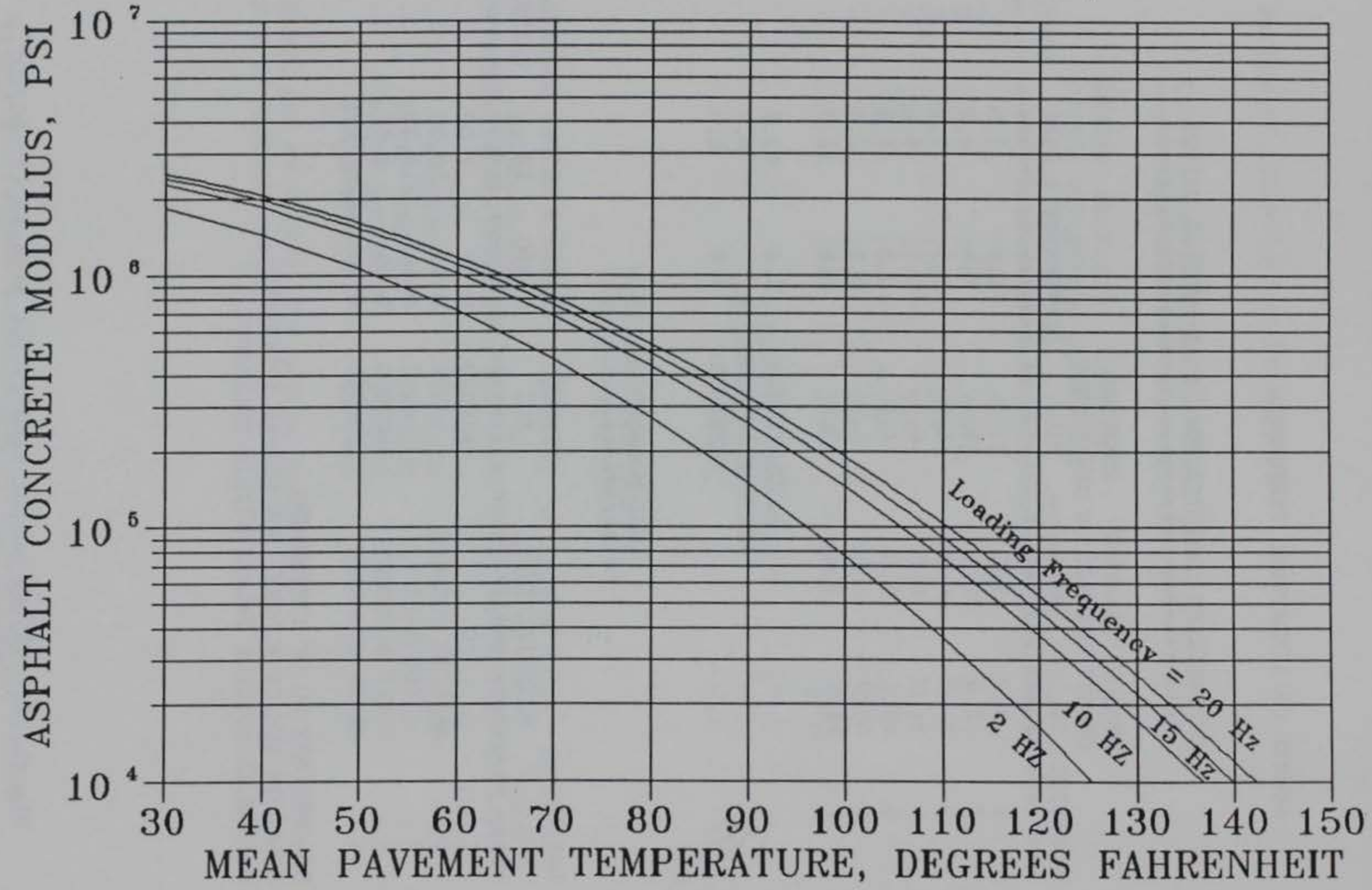

Figure 21. Prediction of AC modulus for bituminous layers

VI. SUMMARY AND DISCUSSION

A. Summary

Applicability of SASW to pavement testing has been demonstrated through field testing and material characterization of six airfield pavement sites. SASW is a relatively new procedure based on the generation and detection of surface waves. Using the theory of elastic waves in layered media, data are reduced and analyzed (computer programs SASW and INVERT) to determine a continuous Young's modulus profile with depth for a pavement structure as well as the thickness of each layer. SASW testing is performed at strains below 0.001 percent and the elastic properties of the materials tested can be assumed independent of strain amplitude. The average time required for field data collection was 51 minutes per test. Reduction and analysis of SASW data required 1 to 1-1/2 days per site using a PC (AT). Analysis time could be reduced significantly by performing the inversions on a mainframe computer or a faster PC (386 machine). It should also be noted that the layering for inversion was based on actual pavement thicknesses and no attempt was being made to determine layer thicknesses. If the thicknesses would not have been available, computational time requirements would have made it necessary to use a faster computer to obtain results similar to those presented. The shear wave velocity profiles presented herein could be further refined by subdividing the layers and continuing the inversion process.

Fluctuations in the SASW field data records due to reflected waves presented some difficulty in the interpretation of data for the construction of dispersion curves for the sites with PCC layers. The

effects of these fluctuations could be seen in the dispersion curve, making it difficult to perform the inversion process which requires visual matching of the experimental and theoretical data. The effect of reflected waves on SASW testing has been addressed by Sheu, Stokoe, and Roesset (1988). Another problem encountered with rigid pavements was the relative insensitivity of the inversion process to the velocity of a thin base course layer beneath a PCC layer.

For comparison with SASW, the WES elastic layer NDT methodology has also been presented. The WES procedure utilizes surface deflection measurements from a loading device, such as the FWD, and elastic layer theory to determine a set of modulus values that provides the best fit between the measured and computed deflections. Data analyses are accomplished using an optimization routine (WESDEF) that performs the iterative basin matching process. With this procedure, modulus values could not be computed for thin base course layers located directly beneath PCC layers.

SASW and WESDEF Young's modulus profiles for sites 3, 4, 8, 10, 11, and 12 are presented graphically in Figures 22-27 and in tabular form in Table 14. Laboratory derived moduli for the AC and PCC layers are included in Table 14.

B. Comparison of Moduli for Different Material Types

Soil (subgrade, base, and subbase). Hardin and Drnevich (1972) have suggested that the main factors affecting moduli measured in the laboratory are state of stress, void ratio, and strain amplitude. For in situ tests using SASW, strain amplitude will have essentially no

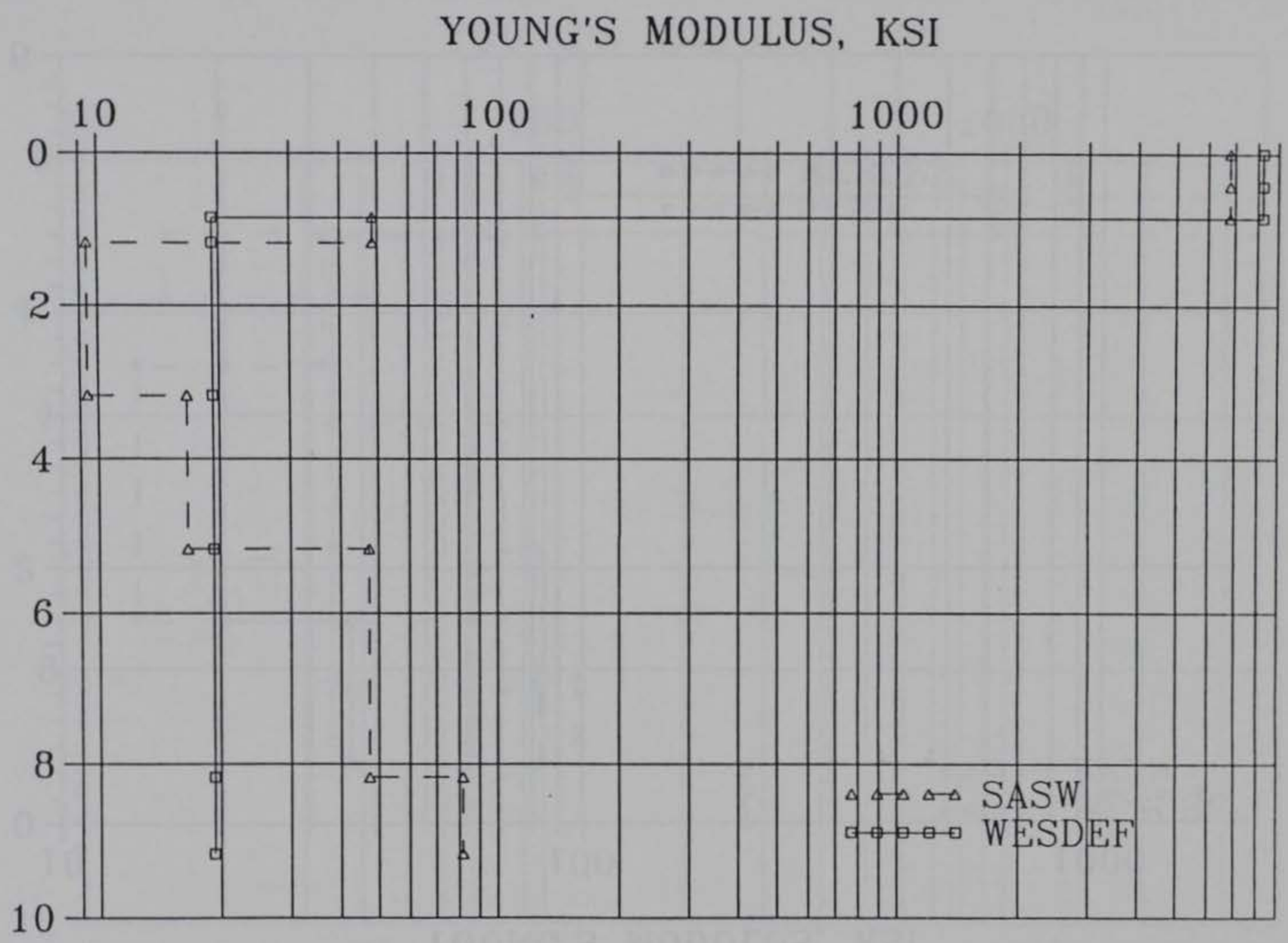

Figure 22. SASW and WESDEF Young's modulus profiles for site 3 (10" PCC/4" base/silty sand)

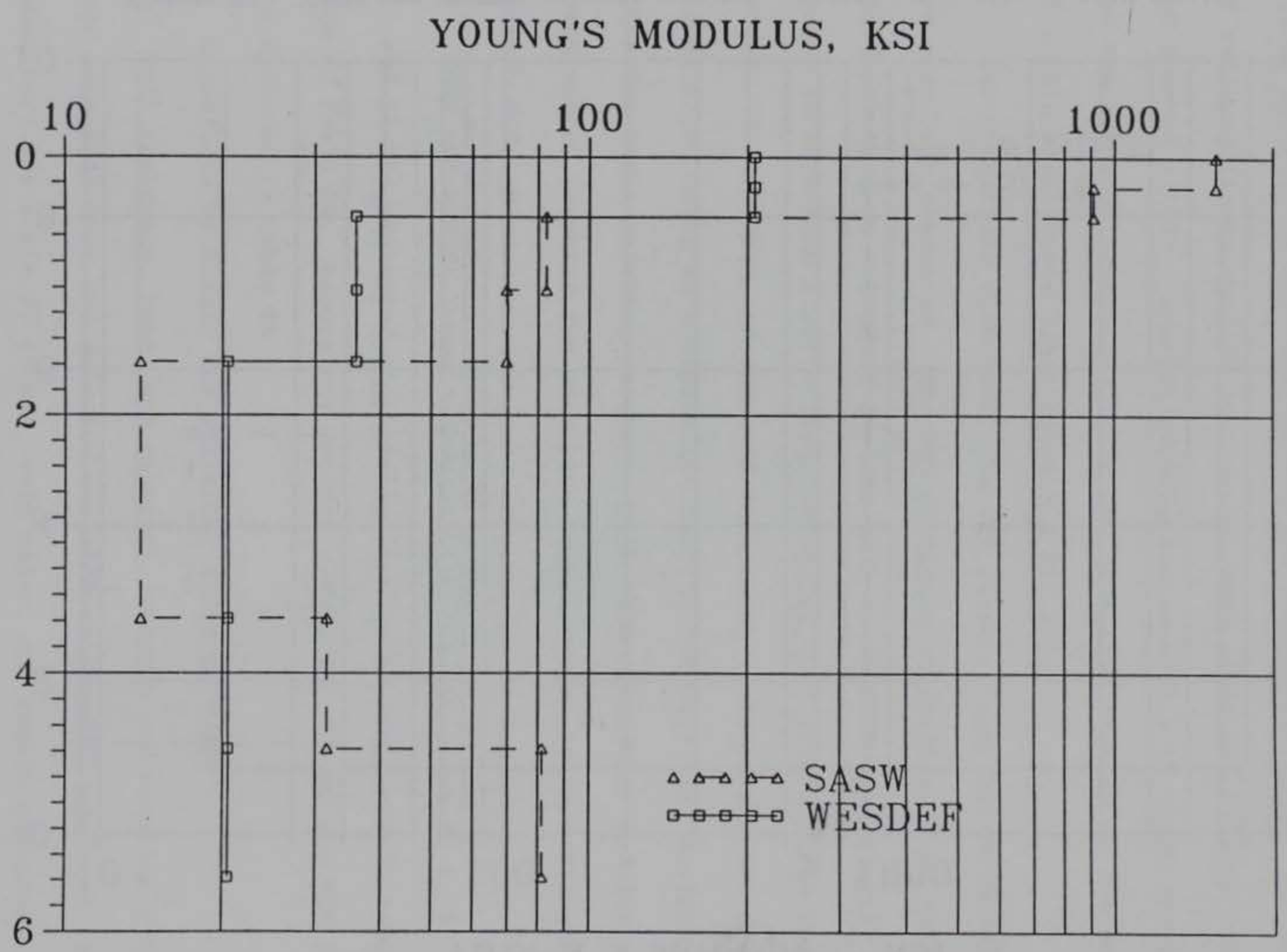

Figure 23. SASW and WESDEF Young's modulus profiles for site 4 (5.5" AC/13.5" base/silty sand)

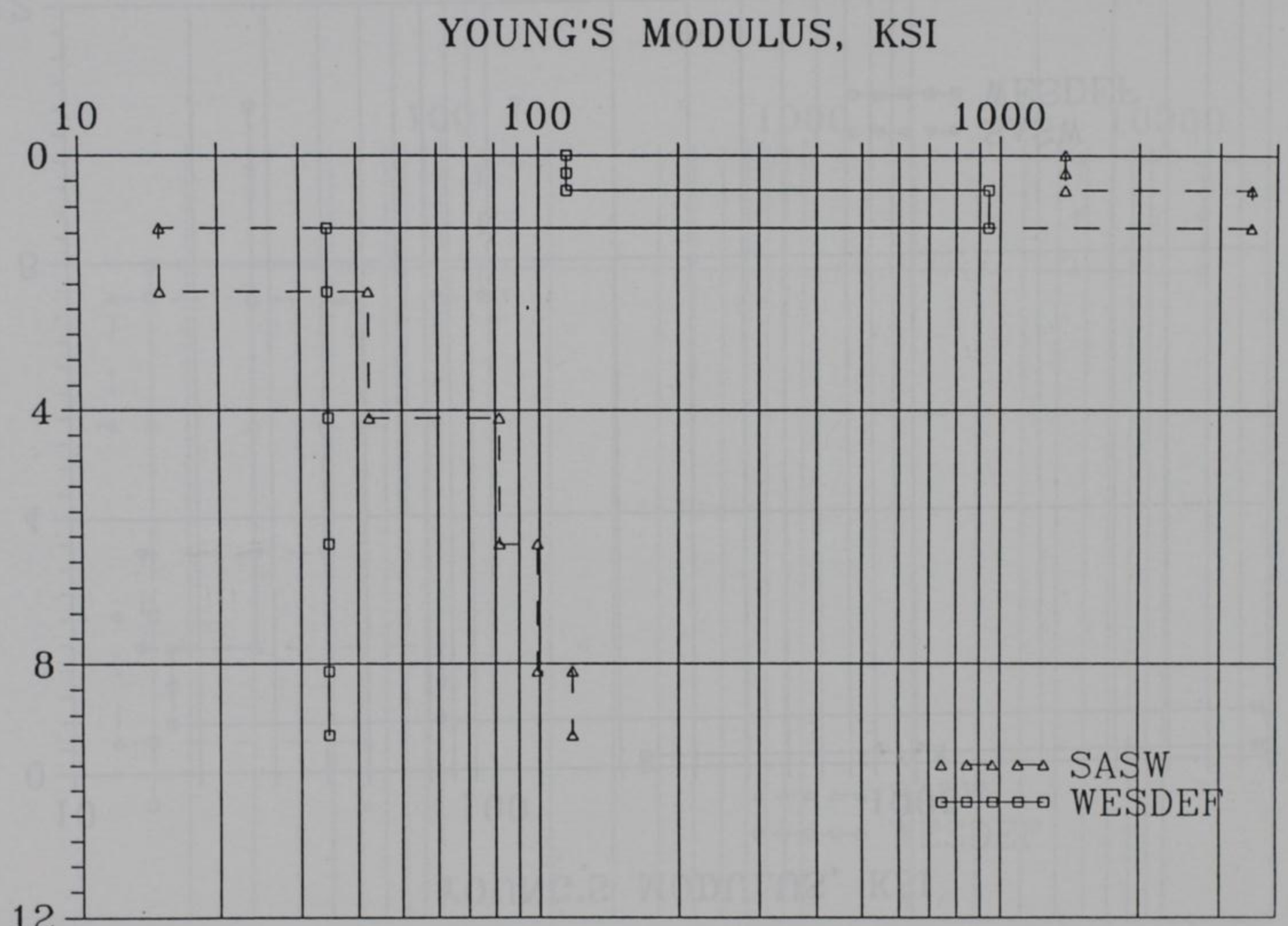

Figure 24. SASW and WESDEF Young's modulus profiles for site 8 (6.5" AC/7" PCC/sandy clay)

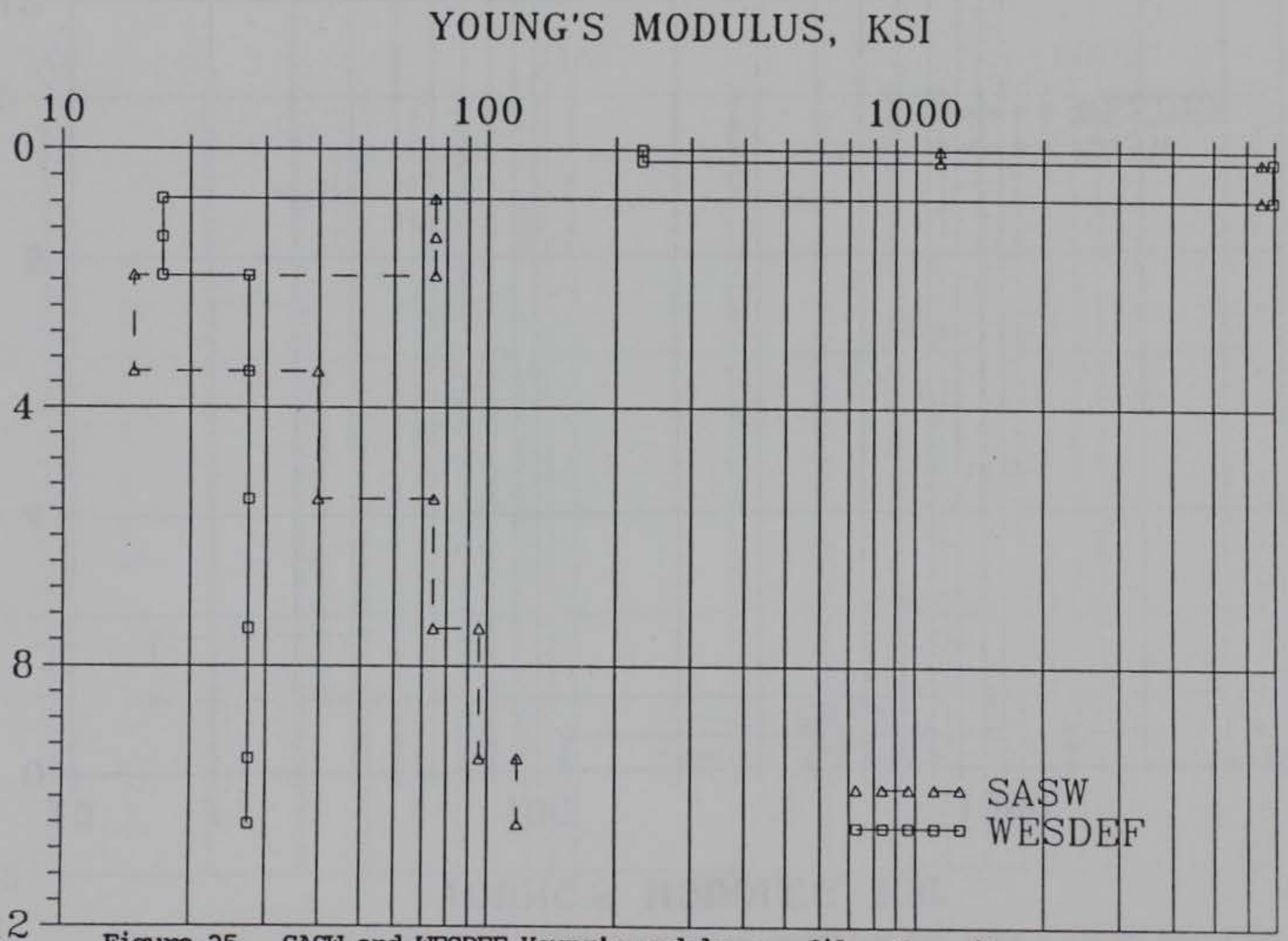

Figure 25. SASW and WESDEF Young's modulus profiles for site 10 (2" AC/7" PCC/14" base/sandy clay)

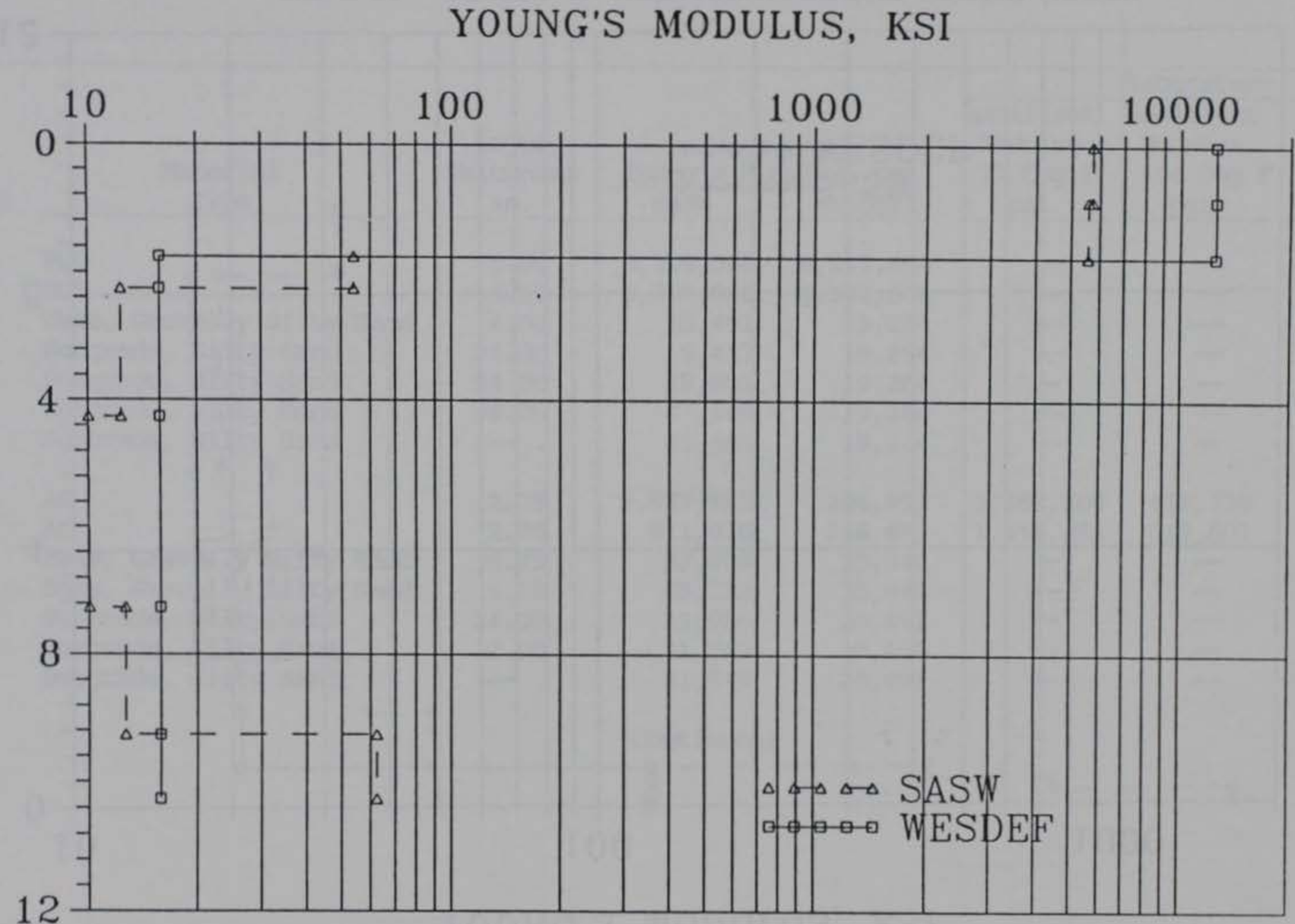

Figure 26. SASW and WESDEF Young's modulus profiles for site 11 (21" PCC/6" base/clayey sand)

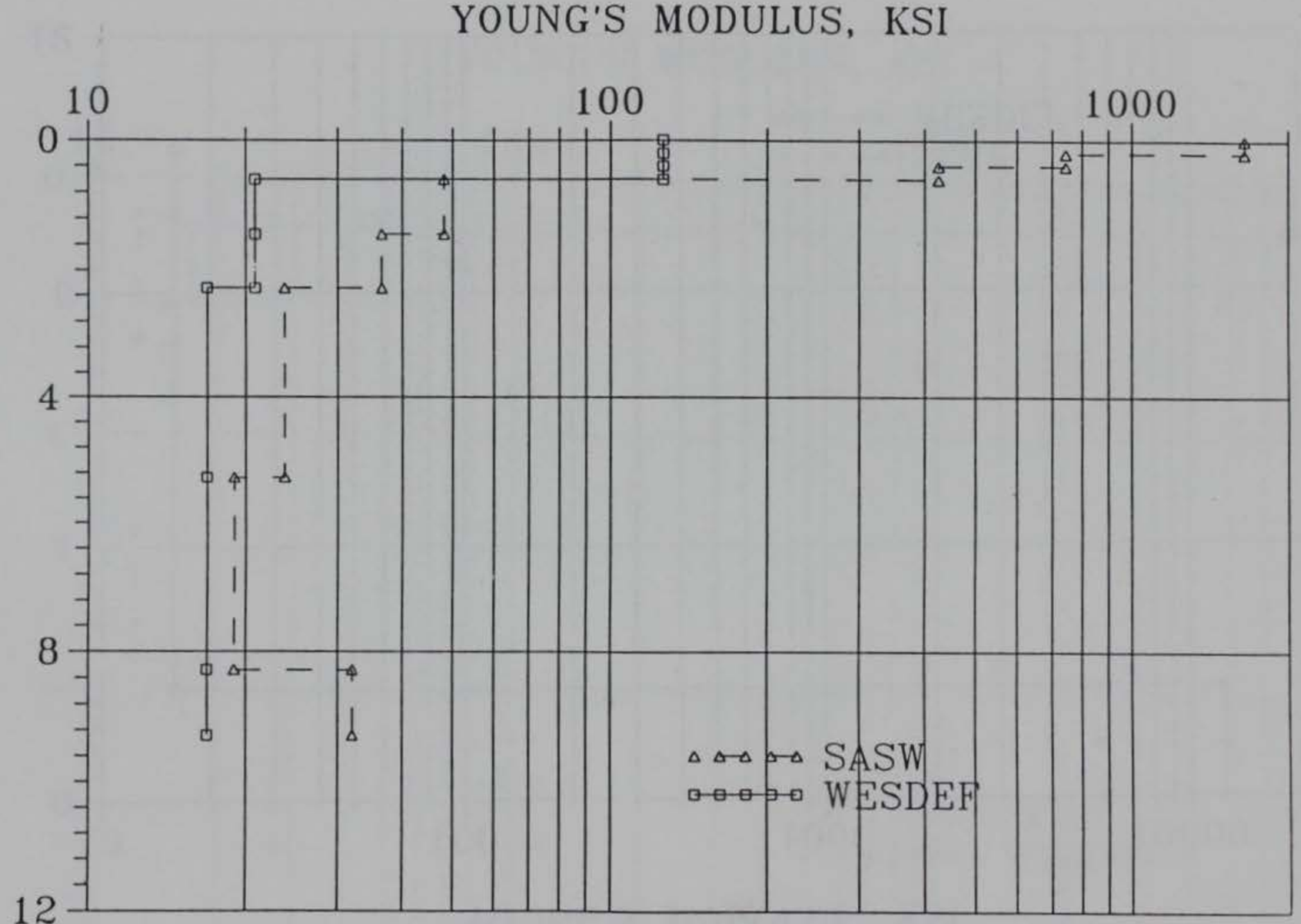

Figure 27. SASW and WESDEF Young's modulus profiles for site 12 (7" AC/20" base/sandy clay)

TABLE 14. SUMMARY OF FIELD AND LABORATORY MODULUS VALUES

Site	Material Type	Layer Thickness in.	Young's Modulus, psi		Laboratory		
			SASW	WESDEF	Resilient Modulus 77 Deg F psi	Resilient Modulus 104 Deg F psi	Dynamic Young's Modulus psi
3	PCC	5.00	6,799,000	8,242,664	--	--	5,556,000
	PCC	5.00	6,799,000	8,242,664	--	--	5,556,000
	Base, Gravelly Silty Sand	4.00	48,481	19,264	--	--	--
	Subgrade, Silty Sand	24.00	9,417	19,264	--	--	--
	Subgrade, Silty Sand	24.00	16,601	19,264	--	--	--
	Subgrade, Silty Sand	36.00	47,289	19,264	--	--	--
	Subgrade, Silty Sand	--	81,463	19,264	--	--	--
4	AC	2.75	1,557,891	206,491	1,568,500	619,759	--
	AC	2.75	911,016	206,491	1,348,381	349,607	--
	Base, Gravelly Silty Sand	6.75	82,898	35,844	--	--	--
	Base, Gravelly Silty Sand	6.75	69,732	35,844	--	--	--
	Subgrade, Silty Sand	24.00	13,956	20,491	--	--	--
	Subgrade, Silty Sand	12.00	31,549	20,491	--	--	--
	Subgrade, Silty Sand	--	81,549	20,491	--	--	--

(Continued)

TABLE 14. (Continued)

Site	Material Type	Layer Thickness in.	Young's Modulus, psi		Laboratory		
			SASW	WESDEF	Resilient Modulus 77 Deg F psi	Resilient Modulus 104 Deg F psi	Dynamic Young's Modulus psi
8	AC	3.25	1,381,941	114,603	903,572	400,887	--
	AC	3.25	1,381,941	114,603	596,460	257,620	--
	PCC	7.00	3,512,169	942,662	--	--	5,487,000
	Subgrade, Gravelly Sandy Clay	12.00	14,960	34,479	--	--	--
	Subgrade, Gravelly Sandy Clay	24.00	42,336	34,479	--	--	--
	Subgrade, Gravelly Sandy Clay	24.00	81,667	34,479	--	--	--
	Subgrade, Gravelly Sandy Clay	24.00	98,817	34,479	--	--	--
	Subgrade, Gravelly Sandy Clay	--	117,600	34,479	--	--	--
10	AC	2.00	1,142,100	230,000	804,228	356,960	--
	PCC	7.00	6,492,756	6,928,886	--	--	6,794,000
	Base	7.00	75,041	17,183	--	--	--
	Base	7.00	75,041	17,183	--	--	--
	Subgrade, Sandy Clay	18.00	14,682	27,372	--	--	--
	Subgrade, Sandy Clay	24.00	39,674	27,372	--	--	--
	Subgrade, Sandy Clay	24.00	74,482	27,372	--	--	--
	Subgrade, Sandy Clay	24.00	95,609	27,372	--	--	--
	Subgrade, Sandy Clay	--	117,600	27,372	--	--	--

(Continued)

TABLE 14. (Concluded)

Site	Material Type	Layer Thickness in.	Young's Modulus, psi		Laboratory		
			SASW	WESDEF	Resilient Modulus 77 Deg F psi	Resilient Modulus 104 Deg F psi	Dynamic Young's Modulus psi
11	PCC	10.50	5,717,329	12,498,614	--	--	5,363,000
	PCC	10.50	5,580,579	12,498,614	--	--	5,363,000
	Base, Gravelly Silty Sand	6.00	54,128	15,837	--	--	--
	Subgrade, Clayey Sand	24.00	12,377	15,837	--	--	--
	Subgrade, Clayey Sand	36.00	10,048	15,837	--	--	--
	Subgrade, Clayey Sand	24.00	12,624	15,837	--	--	--
	Subgrade, Clayey Sand	--	61,425	15,837	--	--	--
12	AC	2.33	1,644,847	126,030	669,266	648,946	--
	AC	2.33	745,003	126,030	1,230,766	757,317	--
	AC	2.33	425,458	126,030	1,177,419	1,181,251	--
	Base, Sandy Silty Gravel	10.00	48,128	20,839	--	--	--
	Base, Sandy Silty Gravel	10.00	36,553	20,839	--	--	--
	Subgrade, Sandy Clay	36.00	23,696	16,872	--	--	--
	Subgrade, Sandy Clay	36.00	19,034	16,872	--	--	--
	Subgrade, Sandy Clay	--	32,040	16,872	--	--	--

effect on the in situ tests because the measurements are performed at very low strains. Numerous studies have shown that shear moduli are nearly constant up to a shearing strain of 0.01 percent with only a slight decrease in the strain range from 0.001 to 0.01 percent. The modulus determined in this constant range is referred to as the low-amplitude, initial tangent, or maximum modulus. As the strain increases above 0.01 percent, moduli decrease significantly and are normally determined in the laboratory or are estimated from empirical correlations.

To illustrate the variation in Young's modulus with normal strain, Nazarian and Stokoe (1986) presented the resonant column data in Figures 28 and 29 for a stiff clay. A constant modulus is observed below strain levels of 0.001 in Figure 28 and the low-amplitude modulus increases with increasing confining pressure. In Figure 29, the normalized modulus is also constant below 0.001 percent and is equal to the maximum modulus. When normalized, all of the modulus-strain curves are nearly independent of confining pressure and if a such a curve is available for a material, the moduli at higher strains can be determined once the maximum modulus has been measured (i.e., small strain in situ measurements such as SASW).

For the type and magnitude of loading applied by the FWD, the strain levels are not known and the modulus values from WESDEF may not be the maximum values. Therefore, direct comparisons between SASW and WESDEF values for the soil materials will be questionable without laboratory test results to verify behavior. Of more importance here will be the relative stiffnesses indicated by each procedure.

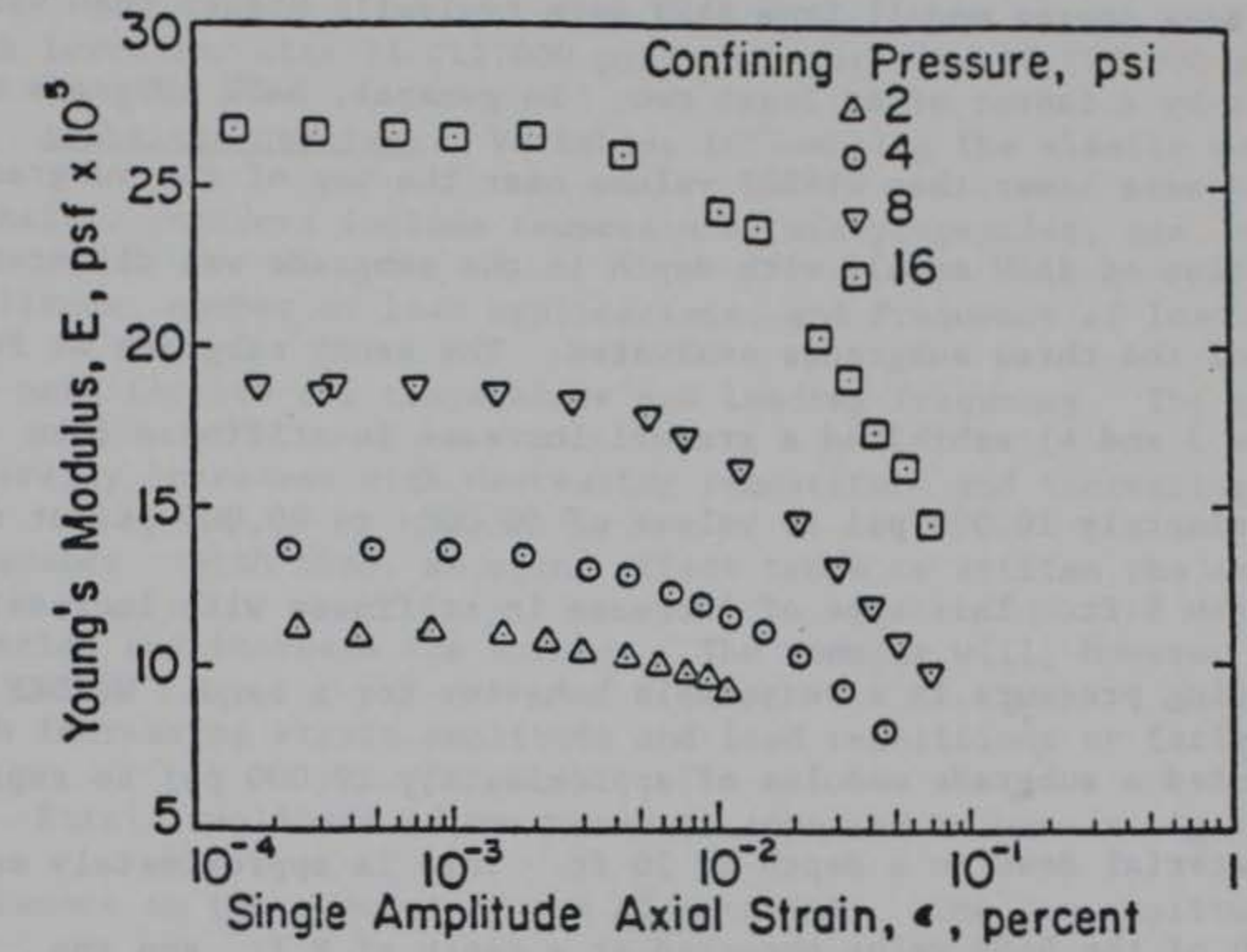

Figure 28. Variation of Young's modulus with strain amplitude at different confining pressures of an unsaturated clay subgrade (from Nazarian and Stokoe, 1986a)

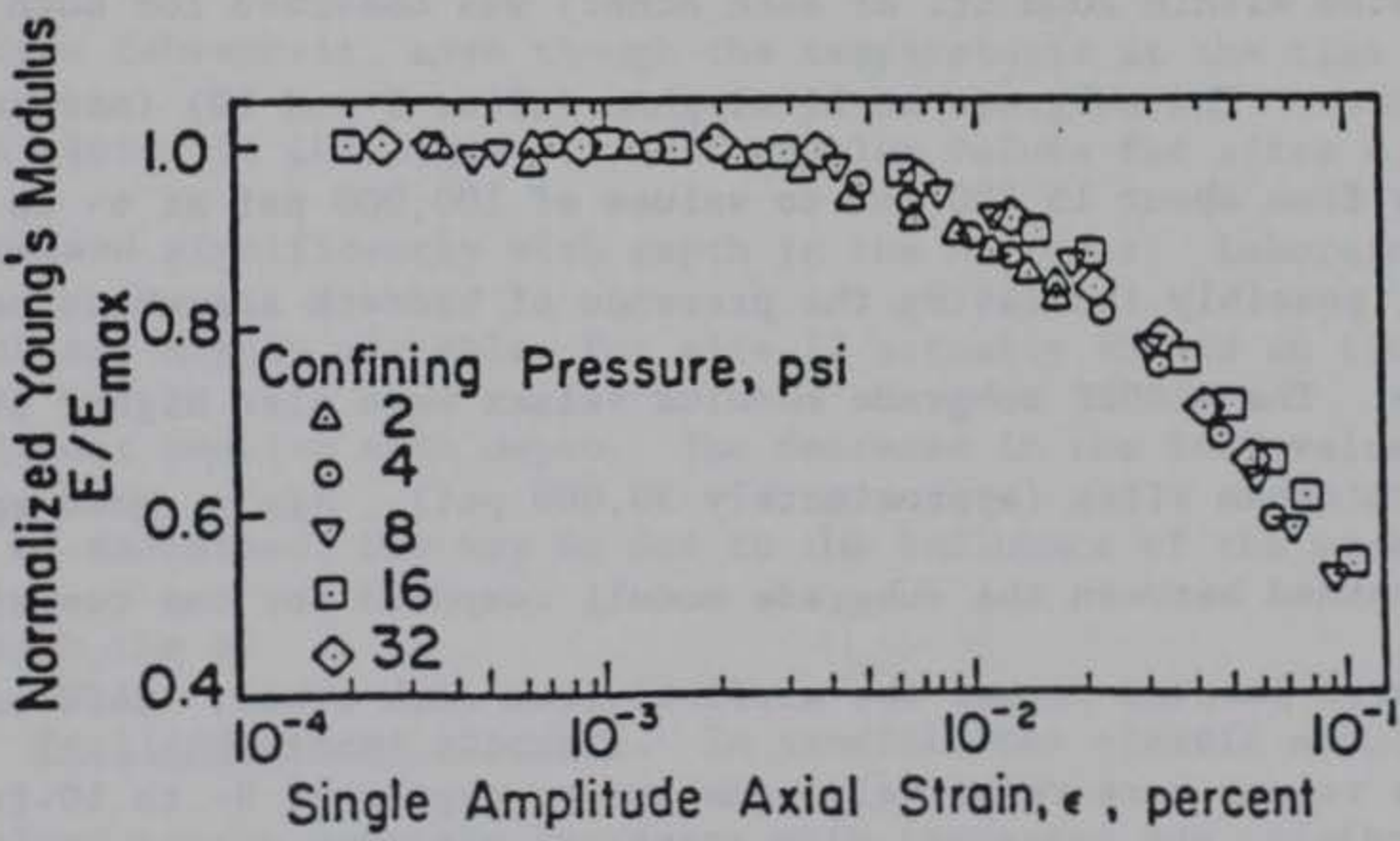

Figure 29. Variation of normalized Young's modulus with strain amplitude of an unsaturated clay subgrade (from Nazarian and Stokoe, 1986b)

Base course moduli from SASW were typically higher than WESDEF values by a factor of at least two. In general, SASW subgrade modulus values were lower than WESDEF values near the top of the subgrade. Variation of SASW moduli with depth in the subgrade was different for each of the three subgrades evaluated. The sandy subgrade at Pensacola (sites 3 and 4) exhibited a gradual increase in stiffness from approximately 10,000 psi to values of 50,000- to 80,000-psi at depths of 6- to 8-ft. This type of increase in stiffness with increasing confining pressure is a reasonable behavior for a sand. WESDEF predicted a subgrade modulus of approximately 20,000 psi to represent the material down to a depth of 20 ft. This is approximately one fourth of the SASW value observed at a depth of 8 ft. and the difference may be due to the strain amplitude of measurement. Close agreement between the subgrade modulus values obtained for sites 3 and 4 (located within 2000 ft. of each other) was observed for both procedures. The subgrade at Birmingham (sites 8 and 10) increased sharply from about 15,000 psi to values of 100,000 psi at 6- to 8-ft. depths, possibly indicating the presence of bedrock somewhere near the surface. The WESDEF subgrade modulus values were also higher at the two Birmingham sites (approximately 30,000 psi). Again, good agreement was obtained between the subgrade moduli computed for the two sites which were located across the airfield from each other. SASW subgrade modulus values were relatively constant to depths of 8- to 10-ft. in the sandy clay material at Wichita Falls (sites 11 and 12). WESDEF modulus values were approximately the same for the two sites, located across the airfield from each other. SASW subgrade modulus values were

much lower for site 11 (12,000 psi) than for site 12 (20,000 psi).

Asphaltic concrete. Variables influencing the elastic modulus of asphaltic concrete include temperature, mix properties, age, strain amplitude, number of load applications, and frequency of loading. The two main factors are temperature and loading frequency. The modulus generally increases with decreasing temperature and increasing frequency. With time, an aging affect tends to stiffen the asphaltic material and increase the modulus. The modulus will, however, decrease with increasing strain amplitude and load repetitions or fatigue.

Strain amplitude of measurements appeared to have a significant influence on the modulus of the AC materials. The low amplitude SASW modulus values were consistently higher than the WESDEF values (ranging from three to ten times the WESDEF values). The SASW values seemed to agree more closely with the resilient modulus values determined at 77 degrees fahrenheit, even though the temperatures at the time of testing were closer to 104 degrees. SASW modulus values for sites 4 and 12 decreased significantly with depth in the AC layer. Laboratory values, which are highly variable, for site 12 actually showed an increase in resilient modulus with depth. The decrease in the SASW values could not be explained, but may be due to the influence of the weaker layer beneath the AC.

Portland cement concrete. In general, the elastic modulus of Portland cement concrete increases with increased age, rising rapidly during the first few months and continuing for up to three years. Two major factors affecting the modulus are the water-cement ratio and the

type of aggregate. High cement factor and low water-cement ratio lead to higher elastic moduli. A higher modulus can be expected for concrete made with stiffer aggregate. Many mixing and curing variables affect the strength of concrete and generally will influence the modulus in a similar manner, but to a lesser extent.

PCC moduli from SASW appeared more reasonable than WESDEF values in several cases. WESDEF predicted values over 8,000,000 psi for sites 3 and 11, which would normally be considered unrealistically high. SASW modulus values agreed better with laboratory values than did WESDEF values. SASW values were within 25 percent of laboratory values for three out of four sites and correlation of the two appears promising.

VII. CONCLUSIONS

The major conclusions resulting from this research are as follows:

1) SASW is a viable method for in situ material characterization of pavement systems. In situ Young's modulus profiles can be obtained for flexible, rigid, and composite pavement structures. The ability to identify layering within a pavement structure and the change in stiffness within layers has many applications in pavement design and evaluation including the development of better models for predicting soil behavior for use with elastic layer or more advanced finite element routines.

2) SASW data reduction can be accomplished on a personal computer (PC) to the extent of identifying relative material stiffnesses which would be an immediate benefit to the current elastic layer deflection-based procedure. Determination of pavement layer thicknesses or a more refined inversion process will require a mainframe computer or a fast PC (386 machine).

3) PCC modulus values from SASW appeared reasonable for the four rigid and composite pavements tested, while WESDEF predicted unrealistically high values for two of the sites. SASW values were typically within 25 percent of laboratory dynamic moduli and the existence of a correlation between the two appears promising.

4) AC moduli determined from low strain amplitude SASW measurements were three to ten times higher than the values predicted by WESDEF. Laboratory resilient modulus values

determined at 77 degrees fahrenheit agreed more closely with SASW moduli than did 104 degree values, which should be closer to the actual pavement temperatures measured when the SASW tests were conducted.

5) The effect of low strain amplitude was evident in the magnitude of SASW base and subgrade moduli. SASW moduli were, in some cases, typically two to four times higher than WESDEF base course and subgrade values.

6) Low amplitude (maximum) modulus values may have application for pavement design based on laboratory test results. The ability to translate between laboratory and field conditions using SASW appears promising.

7) SASW testing and data reduction techniques are somewhat time consuming, but could be automated to greatly increase the efficiency.

VIII. RECOMMENDATIONS

This study has shown that SASW can provide certain enhancements to the current deflection-based elastic layer procedure and may have important applications for laboratory-based pavement design. However, several areas requiring further research have been identified. Based on the results of this study, the following recommendations are offered:

1) Evaluate methods for automating data collection and reduction techniques to improve the efficiency of SASW for routine pavement evaluation.
2) Evaluate low strain effects on SASW soil moduli by comparing measured values to laboratory resilient moduli.
3) Evaluate methods for minimizing the effects of reflected waves on SASW test results.
4) Conduct SASW field tests on pavements with bedrock at a known depth to evaluate the ability of SASW to determine its presence and approximate depth.
5) Pursue the development of a correlation between SASW PCC moduli and the laboratory dynamic modulus.
6) Further investigate the effects of low strain measurements on AC materials.

REFERENCES

1. Bush, A. J., III, "Nondestructive Testing for Light Aircraft Pavements, Phase II," FAA report FAA-RD-80-9-II, Department of Transportation, Federal Aviation Administration, Washington, D. C., 1980.

2. Nazarian, S. and Stokoe, K. H. II (1985), "In Situ Determination of Elastic Moduli of Pavement Systems by Spectral-Analysis-of-Surface-Waves Method (Practical Aspects)," Research Report 368-1F, Center of Transportation Research, The University of Texas at Austin, August, 159 pp.

3. Nazarian, S., Stokoe, K. H. II (1986a), "In Situ Determination of Elastic Moduli of Pavement Systems by Spectral-Analysis-of-Surface-Waves Method (Theoretical Aspects)," Research Report No. 437-2, Center for Transportation Research, The University of Texas at Austin, November, 114 pp.

4. Nazarian, S. (1984), "In Situ Determination of Elastic Moduli of Soil Deposits and Pavement Systems by Spectral-Analysis-of-Surface-Waves Method," Ph.D. Dissertation, The University of Texas at Austin, 453 pp.

5. Heisey, J. S., Stokoe, K. H. II, and Meyer, A. H. (1982), "Moduli of Pavement Systems From Spectral Analysis of Surface Waves," Research Record No. 852, Transportation Research Board, pp. 22-31.

6. Nazarian, S. and Stokoe, K. H. II (1983), "Evaluation of Moduli and Thicknesses of Pavement Systems by Spectral-Analysis-of-Surface-Waves Method," Research Report No. 256-4, Center for

Transportation Research, The University of Texas at Austin, December, 123 pp.

7. Nazarian, S., Stokoe, K. H. II, and Hudson, W. R. (1983), "Use of Spectral Analysis of Surface Waves Method for Determination of Moduli and Thicknesses of Pavement Systems," Research Record No. 930, Transportation Research Board, Washington, D. C., pp. 38-45.

8. Nazarian, S. and Stokoe, K. H. II (1984), "Nondestructive Testing of Pavements Using Surface Waves," Research Record No. 993, Transportation Research Board, pp. 67-79.

9. Drnevich, V. P., Kim, S. I., Alexander, D. R., and Kohn, S. D. (1985), "Spectral Analysis of Surface Waves in Pavement Systems with Random Noise Excitation," Expanded Abstracts with Biographies, 55th Annual International Society of Exploration Geophysicists Meeting, Washington, D. C., October 6-10, pp. 143-145.

10. Nazarian, S. and Stokoe, K. H. II (1986b), "Use of Surface Waves in Pavement Evaluation," Research Record No. 1070, Transportation Research Board, Washington, D. C., pp. 132-144.

11. Hiltunen, D. R. (1988), "Experimental Evaluation of Variables Affecting the Testing of Pavements by the Spectral-Analysis-of-Surface-Waves Method," Technical Report GL-88-12, Department of the Army, Waterways Experiment Station, Corps of Engineers, Vicksburg, Mississippi, 303 pp.

12. Miller, G. F. and Pursey, H. (1955), "On the Partition of Energy Between Elastic Waves in a Semi-Infinite Solid," Proceedings of

the Royal Society, A, Vol. 233, pp. 55-69.

13. Bentsen, R. A., Bush, A. J., III, and Harrison, J. A., "Evaluation of Nondestructive Test Equipment for Airfield Pavements, Phase I, Description of Tests and Data Collected," draft Technical Report, Department of the Army, Waterways Experiment Station, Corps of Engineers, Vicksburg, Mississippi 39180-0631, June 1988.

14. American Society for Testing and Materials, "Standard Test Method for Indirect Tension Test for Resilient Modulus of Bituminous Mixtures," Designation: D 4123-82, Annual Book of ASTM Standards, Vol. 4.03, Philadelphia, Pennsylvania, 1988.

15. American Society for Testing and Materials, "Standard Test Method for Flexural Strength of Concrete (Using Simple Beam with Third-Point Loading)," Designation: C 78-84, Annual Book of ASTM Standards, Vol. 4.02, Philadelphia, Pennsylvania, 1986.

16. American Society for Testing and Materials, "Standard Test Method for Fundamental Transverse, Longitudinal, and Torsional Frequencies of Concrete Specimens," Designation: C 215-85, Annual Book of ASTM Standards, Vol. 4.02, Philadelphia, Pennsylvania, 1988.

17. Thomson, W. T. (1950), "Transmission of Elastic Waves Through a Stratified Soil Medium," Journal of Applied Physics, Vol. 21, No. 2, February, pp. 89-93.

18. Haskell, N. A. (1953), "The Dispersion of Surface Waves on Multilayered Media," Bulletin of the Seismological Society of America, Vol. 43, No. 1, January, pp. 17-34.

19. Thrower, E. N. (1965), "The Computation of the Dispersion of Elastic Waves in Layered Media," Journal of Sound and Vibration, Academic Press, London, England, Vol. 2, No. 3, July, pp. 210-226.

20. Van Cauwelaert, F. J., Alexander, D. R., White, T. D., and Barker, W. R., "Multilayer Elastic Program for Backcalculating Layer Moduli in Pavement Evaluation," draft paper submitted to ASTM for publication in STP, 1988.

21. Van Cauwelaert, Lequeux, Delaunnois, "Computer Programs for the Determination of Stresses and Displacements in Four Layered Systems," WES Research Contract DAJA45-86-M-0483, 1986a.

22. Van Cauwelaert, Lequeux, Delaunnois, "Stresses and Displacements in Four Layered Systems with Fixed Bottom," Cerisis asbl., Mons, Belgium, 1986b.

23. Sheu, Jiun-Chyuan, Stokoe, K. H. , II, and Roesset, Jose M. (1988), "Effect of Reflected Waves on SASW Testing of Pavements," Paper No. 875077 presented at the 67th Annual Meeting of the Transportation Research Board (January 11-14, 1988), Center for Transportation Research, The University of Texas at Austin, Austin, Texas.

24. Hardin, B. O. and Drnevich, V. P. (1972), "Shear Modulus and Damping in Soils: Measurement and Parameter Effects," Journal of the Soil Mechanics and Foundations Division, ASCE, Vol. 98, No. SM6, June, pp. 603-624.

APPENDICES

APPENDIX A: SASW TEST DATA AND RESULTS FOR SITE 3

FIELD DATA SHEET FOR SASW TESTS (HP 3562A/9153A)

TEST SITE: Site 3, Pensacola NAS START TIME: 1731 TEMP, F: 105°

TEST DATE: 8-7-87 ENDING TIME: 1859 TEMP, F: 99°

Source Type	Near Receiver Type	Near Receiver ID	Far Receiver Type	Far Receiver ID	Receiver Spacing (ft)	SNR Distance (ft)	Profile (F=Fwd., R=Rev.)	No. of Ave.	Freq. BW (Hz)	Site File No.	Data File Names
4 oz Ball Peen	Accel.	PCB 308B02 SN19926	Accel.	PCB 308B02 SN19927	0.5	0.5	F*	5	KHz 100	120	P120 C120
"	"	"	"	"	0.5	0.5	R	5	100	121	P121 C121
"	"	"	"	"	1.0	1.0	R	5	50	122	P122 C122
"	"	"	"	"	1.0	1.0	F	5	50	123	P123 C123
8 oz. Ball Peen	"	"	"	"	2.0	2.0	F	5	25	124	P124 C124
"	"	"	"	"	2.0	2.0	R	5	25	125	P125 C125
"	"	"	"	"	4.0	4.0	R	5	3.125	126	P126 C126
"	"	"	"	"	4.0	4.0	F	5	3.125	127	P127 C127
40 oz Sledge	Vel.	Geo-Source PC-3	Vel.	Geo-Source PC-3	4.0	4.0	R	5	1	128	P128 C128
"	"	"	"	"	4.0	4.0	F	5	1	129	P129 C129
8 lb Sledge	"	"	"	"	8.0	8.0	F	5	Hz 250	130	P130 C130
"	"	"	"	"	8.0	8.0	R	5	250	131	P131 C131
"	"	"	"	"	16.0	16.0	R	5	250	132	P132 C132
"	"	"	"	"	16.0	16.0	F	5	250	133	P133 C133

* Source on South Side

Figure A1. SASW field data form for Site 3

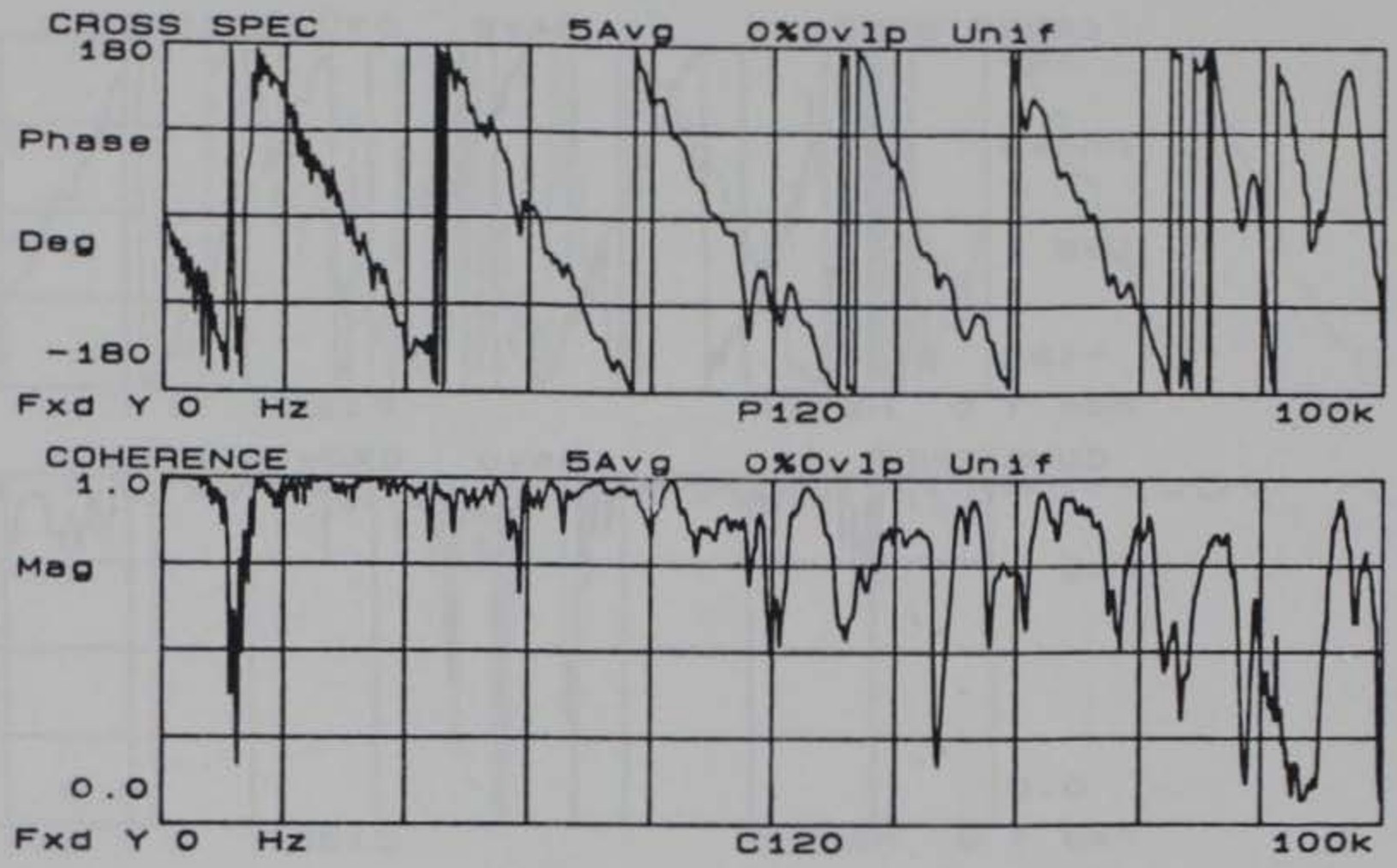

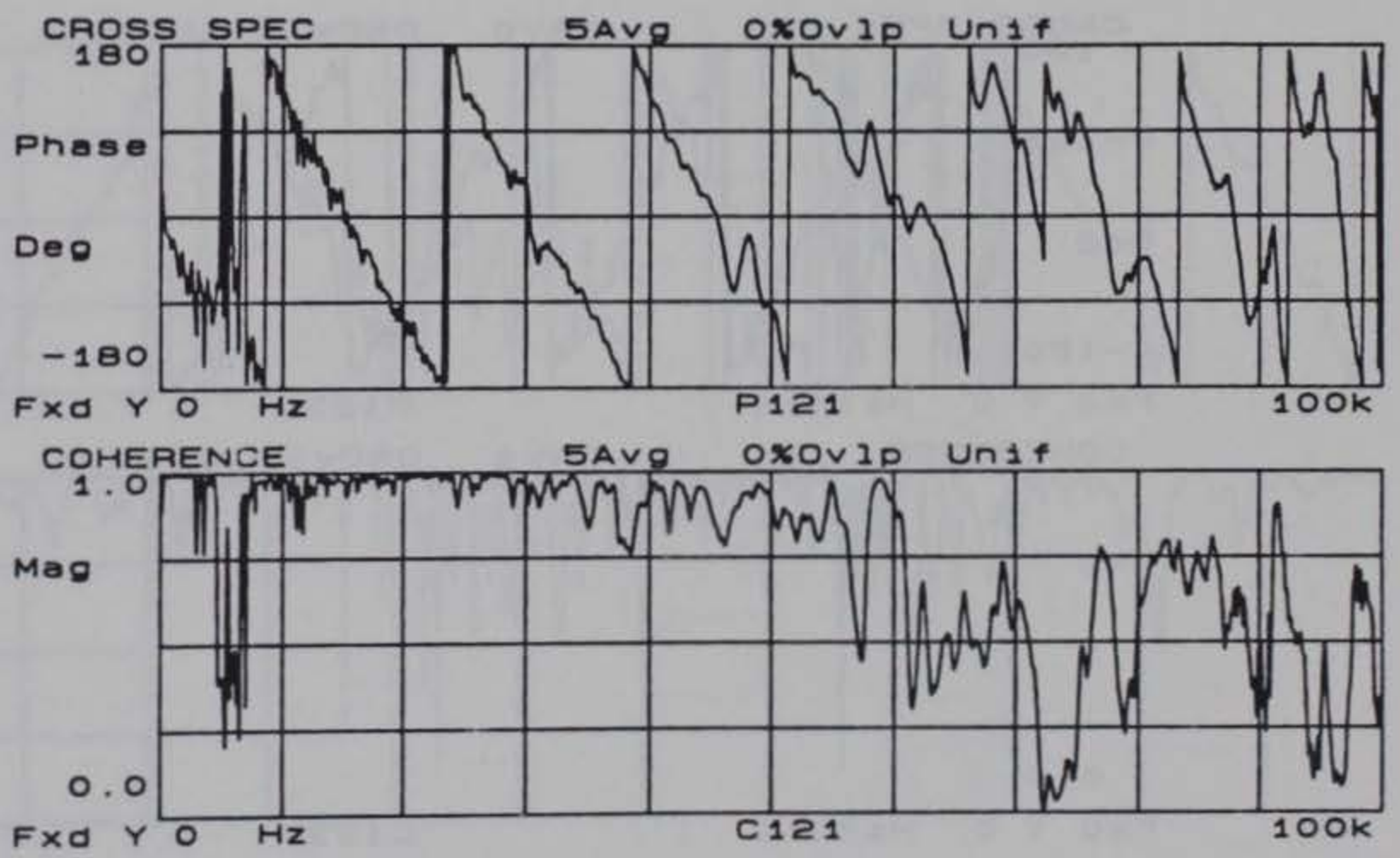

Figure A2. Phase and coherence records for 0.5 ft. receiver spacing at Site 3

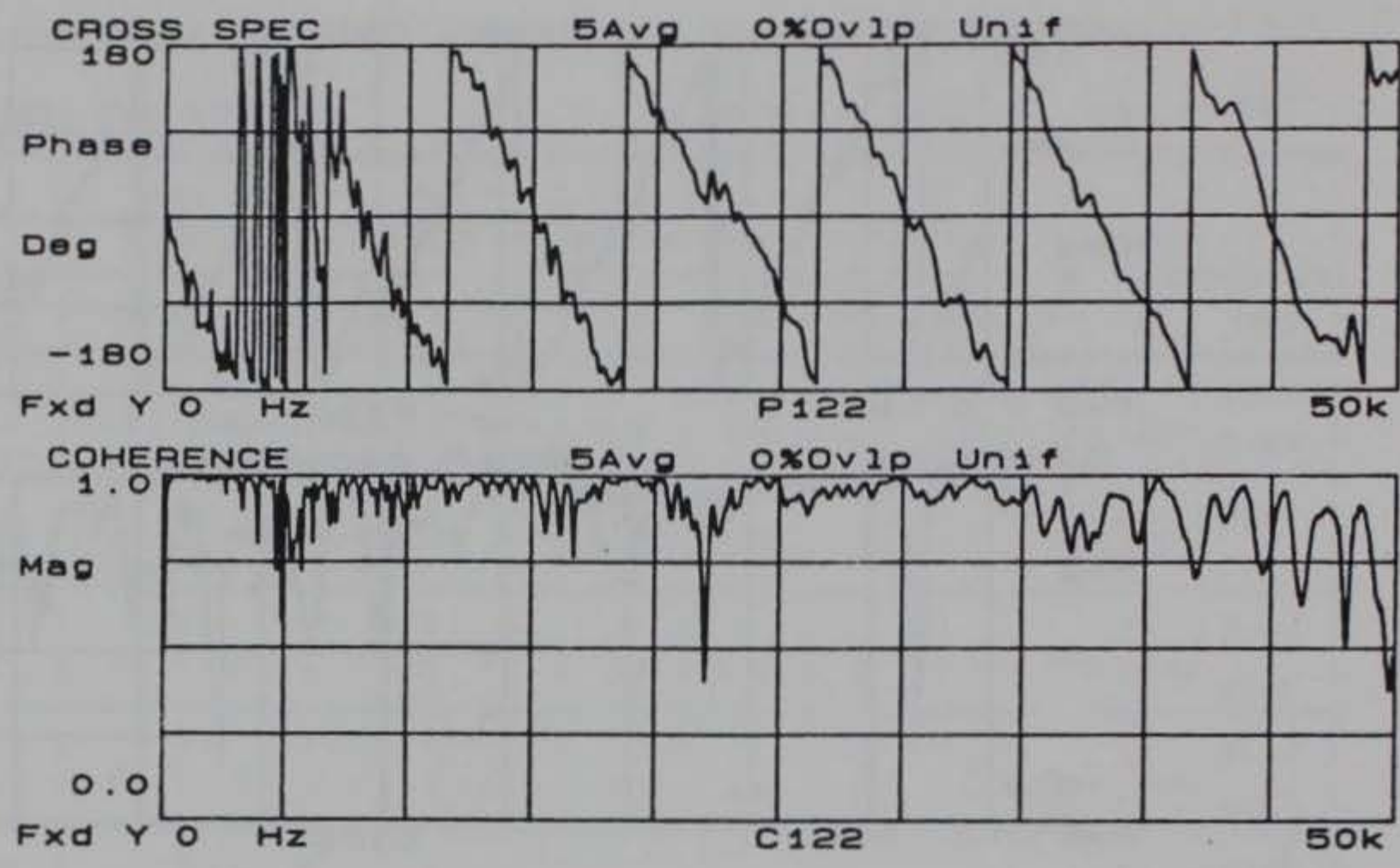

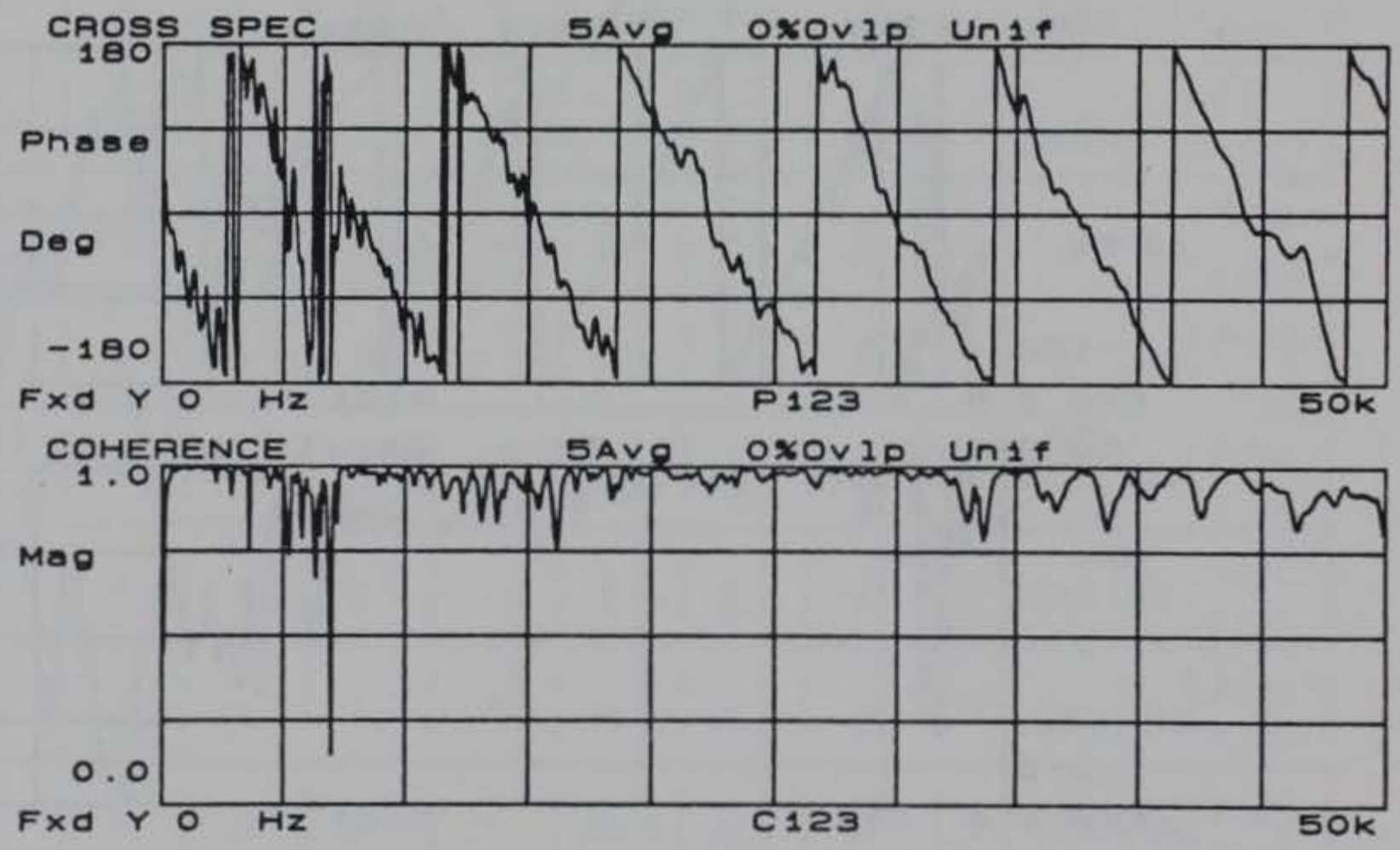

Figure A3. Phase and coherence records for 1.0 ft. receiver spacing at Site 3

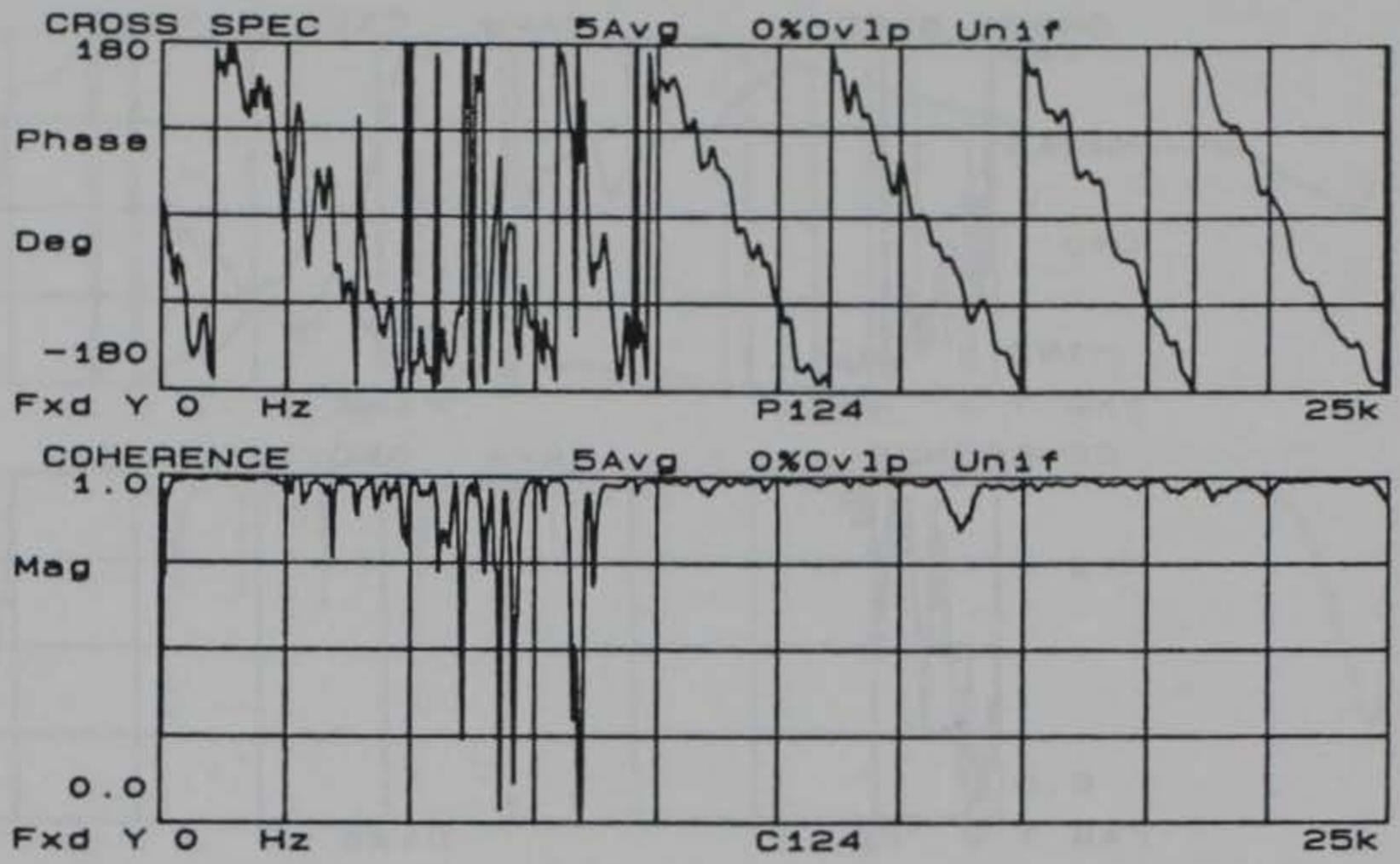

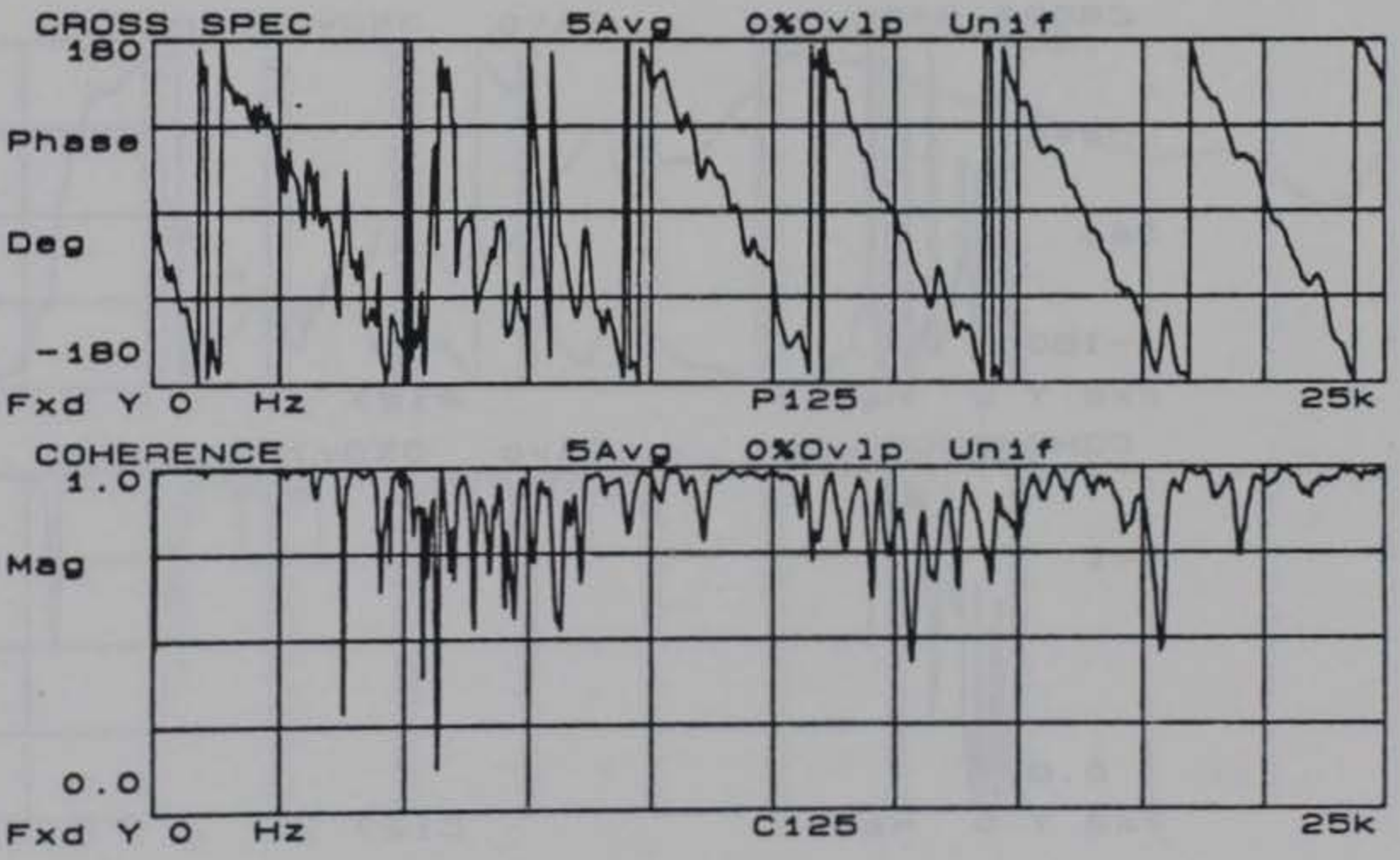

Figure A4. Phase and coherence records for 2.0 ft. receiver spacing at Site 3

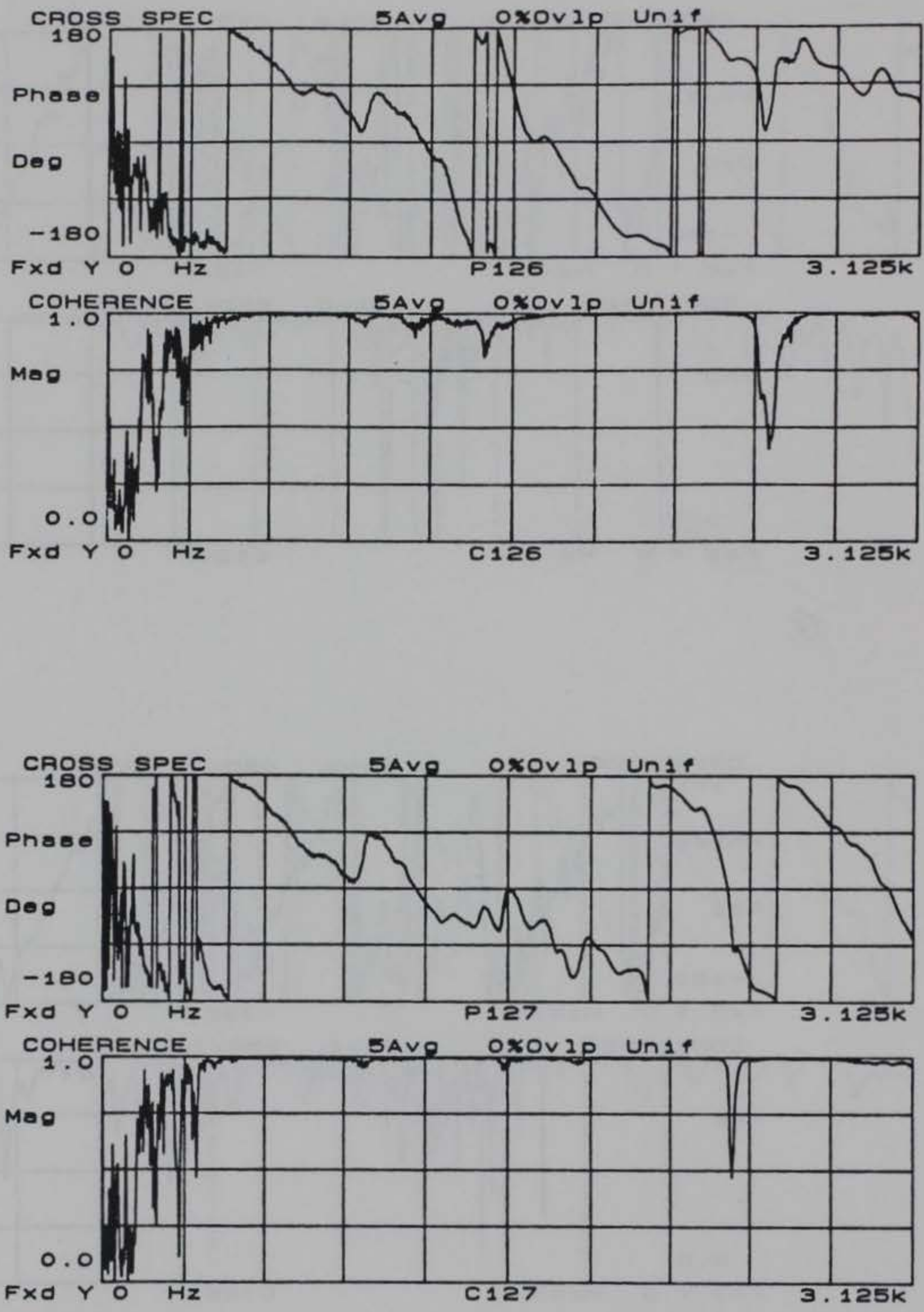

Figure A5. Phase and coherence records for 4.0 ft. receiver spacing at Site 3 (accelerometer data)

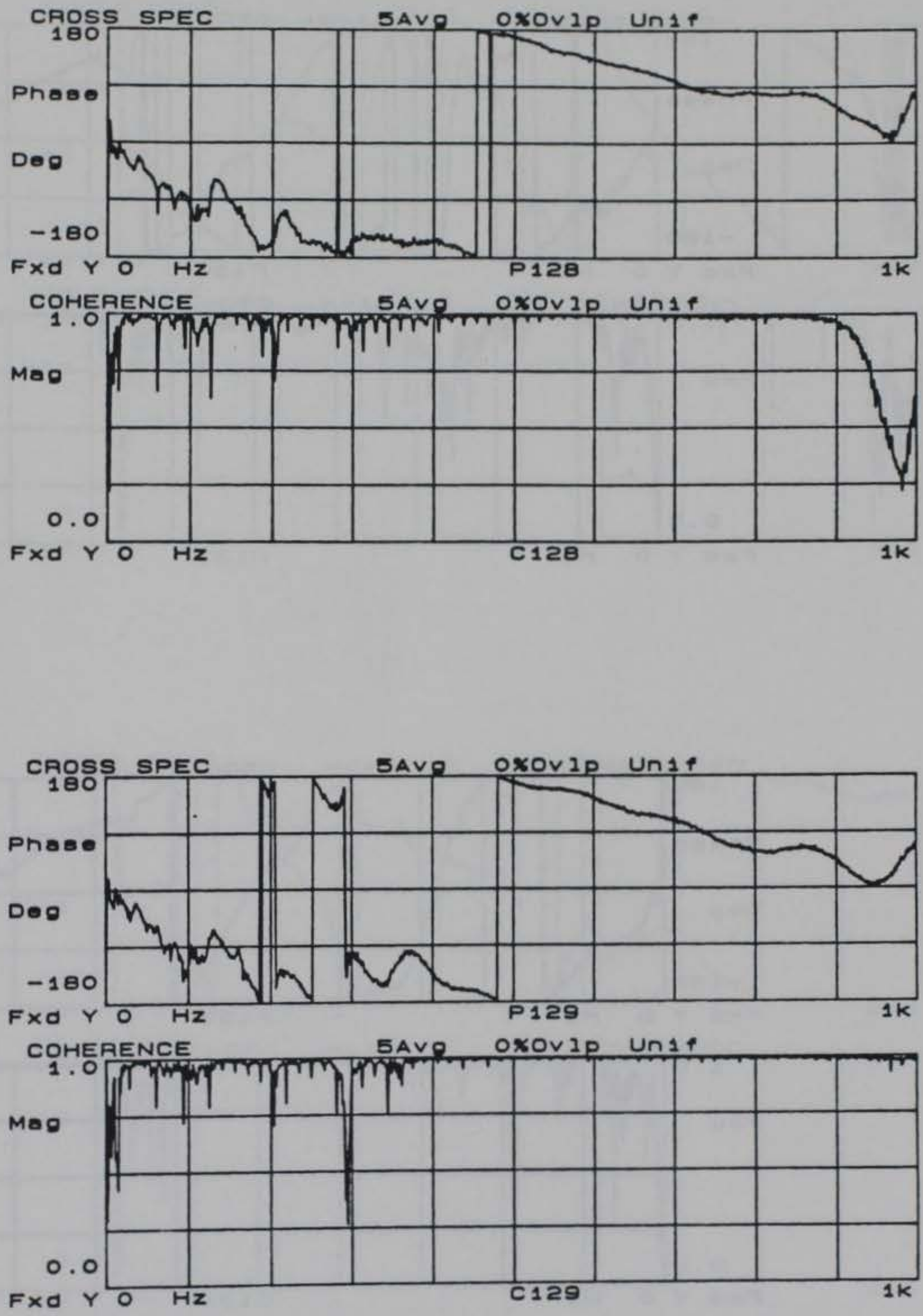

Figure A6. Phase and coherence records for 4.0 ft. receiver spacing at Site 3 (velocity transducer data)

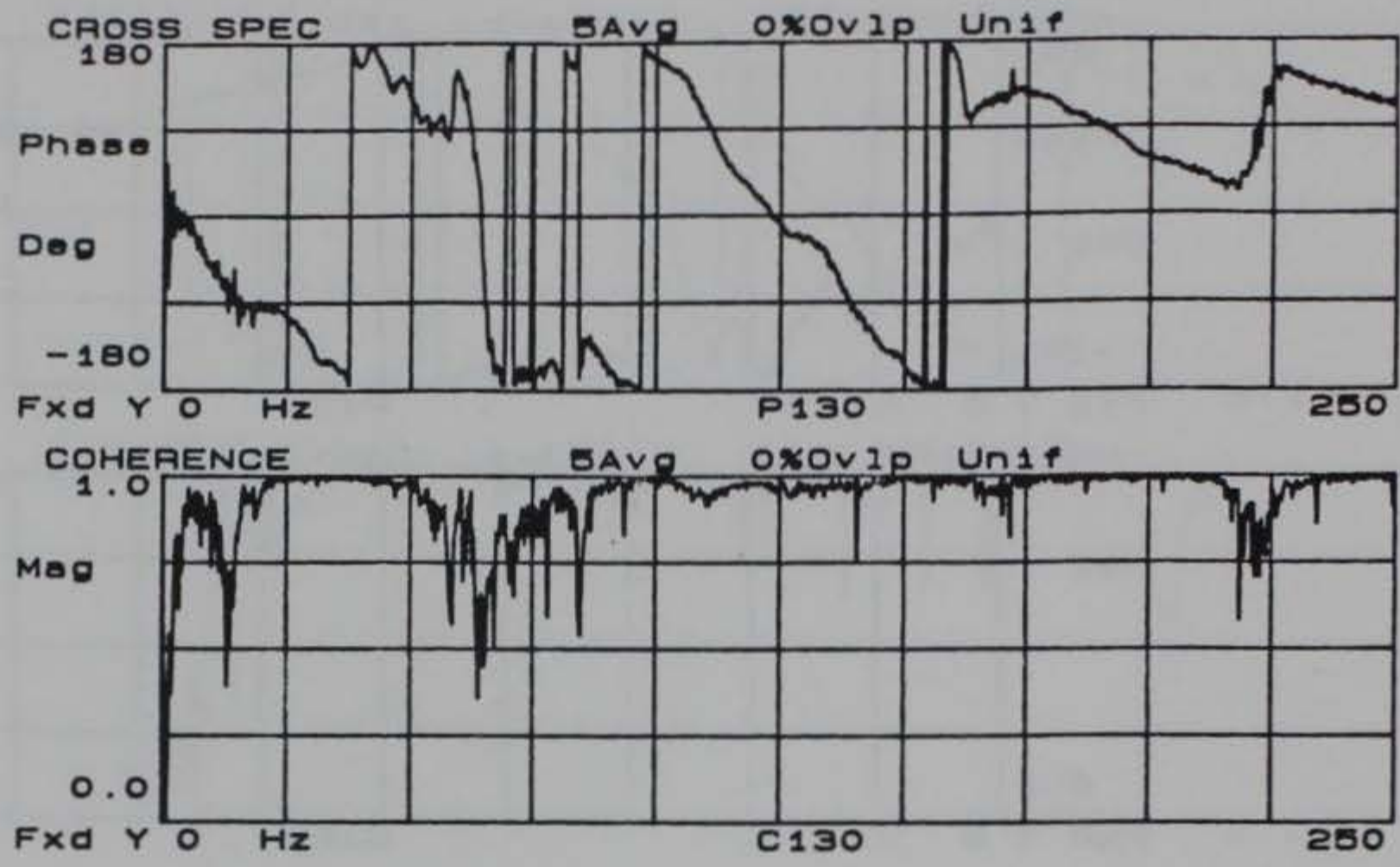

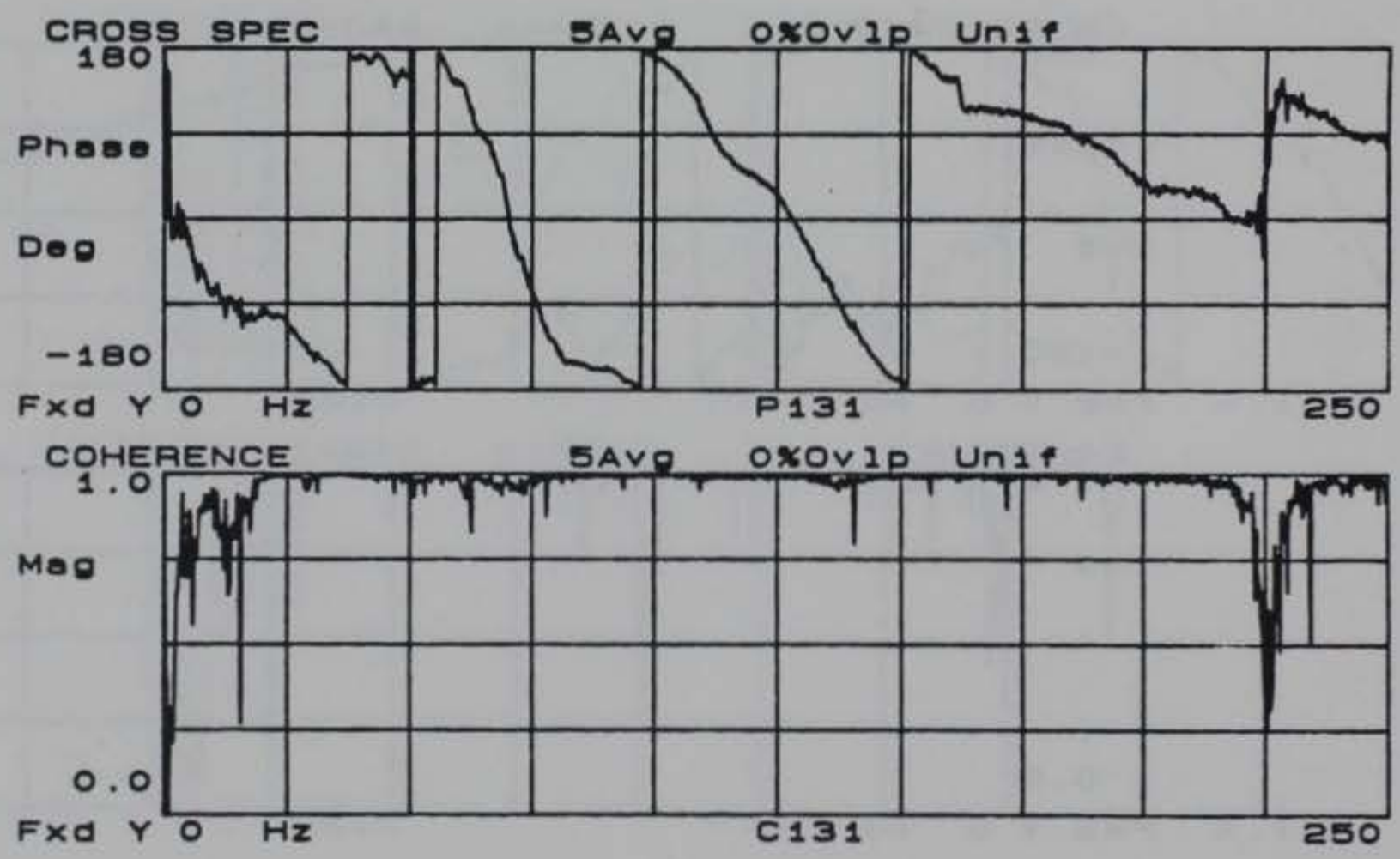

Figure A7. Phase and coherence records for 8.0 ft. receiver spacing at Site 3

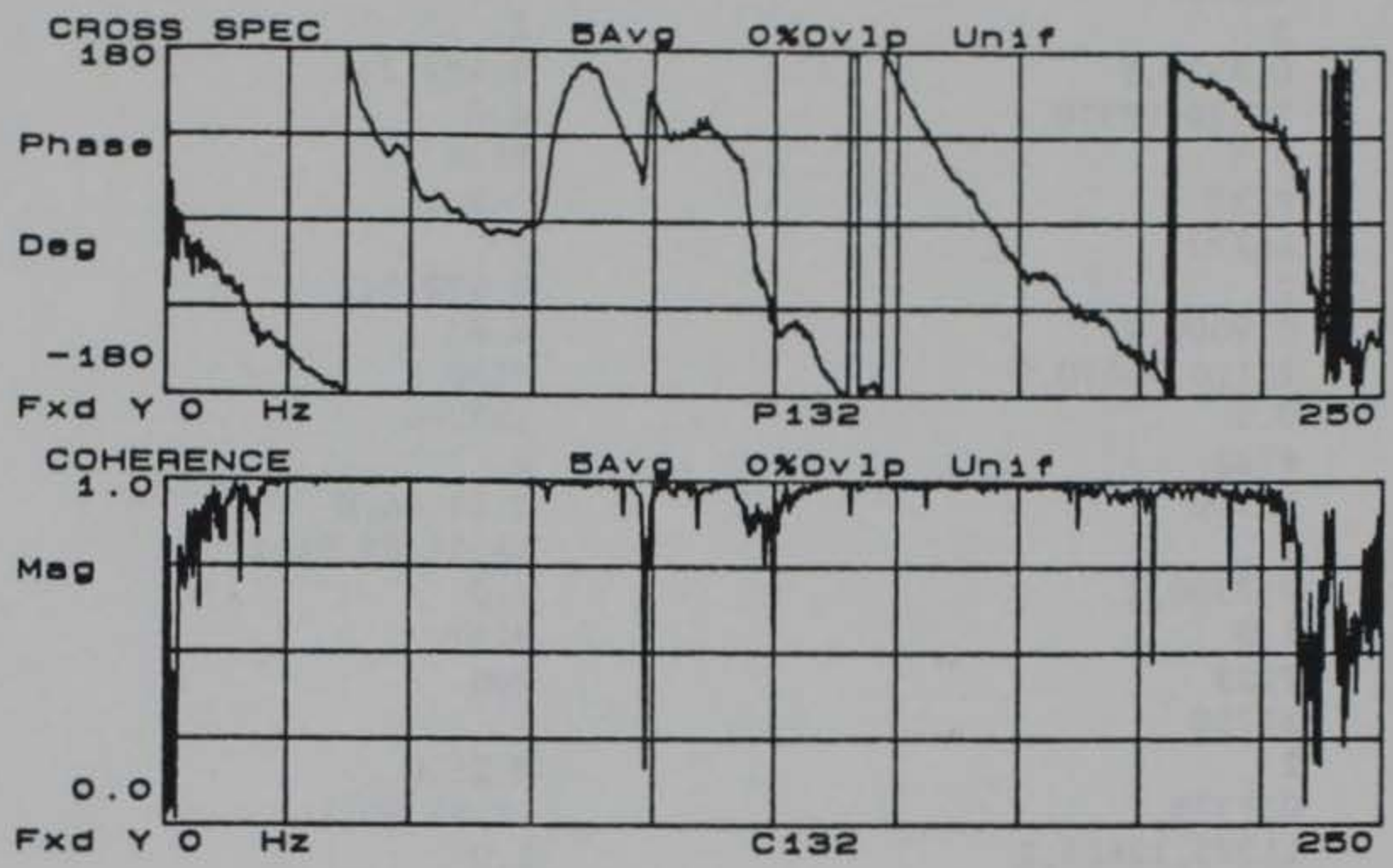

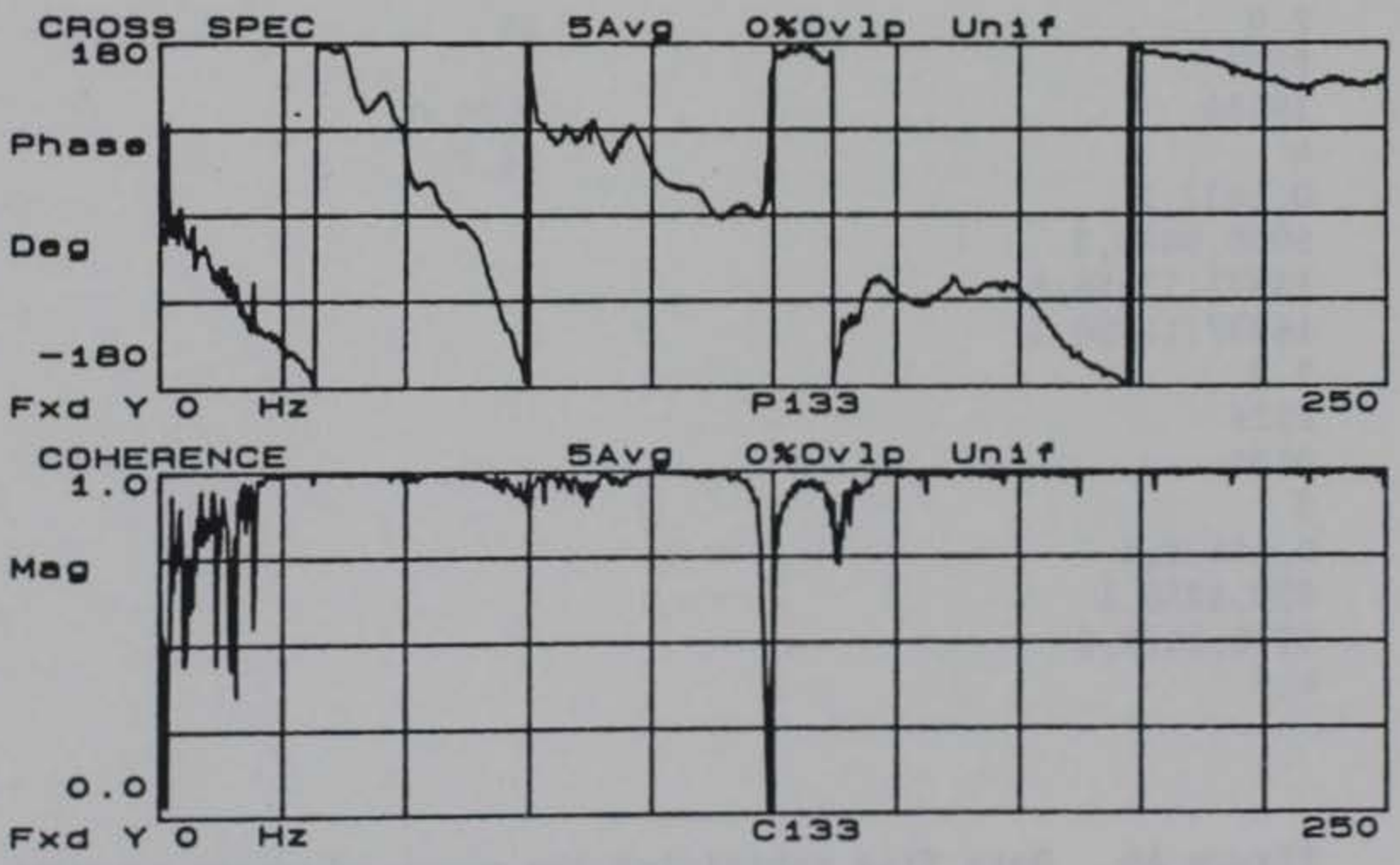

Figure A8. Phase and coherence records for 16.0 ft. receiver spacing at Site 3

```
P120
46370
2
0,8120,1
22120,23370,2
0.5
P121
44870
2
0,9000,1
23120,23870,2
0.5
P122
30500
1
0,7500,1
1.0
P123
31750
2
0,7375,1
11375,12625,2
1.0
P124
21000
2
0,1125,1
3625,10000,3
2.0
P125
19656
4
0,1437,1
5000,9875,3
13375,13656,4
16937,17250,5
2.0
P126
2125
3
0,464.8,1
950,1250,1
1375,1520,2
4.0
P127
2250
1
0,492.2,1
4.0
P128
742.5
1
0,472.5,1
4.0
P130
153.44
2
0,23.44,0
56.56,85.94,1
8.0
P131
200
2
0,25,0
47.81,60,1
8.0
P132
64.69
1
0,25,0
16.0
P133
64
1
0,25,0
16.0
```

Figure A9. Data file containing the names of phase records, cutoff frequencies, poor data ranges, and receiver spacings used by the computer program SASW in constructing the dispersion curve for Site 3

APPENDIX B: SASW TEST DATA AND RESULTS FOR SITE 4

FIELD DATA SHEET FOR SASW TESTS (HP 3562A/9153A)

TEST SITE: Site 4, Pensacola NAS START TIME: 1923 TEMP, F: 103°

TEST DATE: 8-7-87 ENDING TIME: 1948 TEMP, F: 101°

Source	Near Receiver		Far Receiver		Receiver Spacing	SNR Distance	Profile (F=Fwd., R=Rev.)	No. of Ave.	Freq. BW	Site File No.	Data File Names
Type	Type	ID	Type	ID	(ft)	(ft)			(Hz)		
4 oz. Ball Peen	Accel.	PCB 308B02 SN 19926	Accel.	PCB 308B02 SN 19927	0.5	0.5	F*	5	KHz 25	140	P140 C140
"	"	"	"	"	0.5	0.5	R	5	25	141	P141 C141
"	"	"	"	"	1.0	1.0	R	5	12.5	142	P142 C142
"	"	"	"	"	1.0	1.0	F	5	12.5	143	P143 C143
"	"	"	"	"	2.0	2.0	F	5	6.25	144	P144 C144
"	"	"	"	"	2.0	2.0	R	5	6.25	145	P145 C145
40 oz. Sledge	"	"	"	"	4.0	4.0	R	5	2	146	P146 C146
"	"	"	"	"	4.0	4.0	F	5	2	147	P147 C147
"	Vel.	Geo-Source PC-3	Vel.	Geo-Source PC-3	4.0	4.0	F	5	Hz 625	148	P148 C148
"	"	"	"	"	4.0	4.0	R	5	625	149	P149 C149
8 lb Sledge	"	"	"	"	8.0	8.0	R	5	312.5	150	P150 C150
"	"	"	"	"	8.0	8.0	F	5	312.5	151	P151 C151
"	"	"	"	"	16.0	16.0	F	5	160	152	P152 C152
"	"	"	"	"	16.0	16.0	R	5	160	153	P153 C153

* Source on South Side

Figure B1. SASW field data form for Site 4

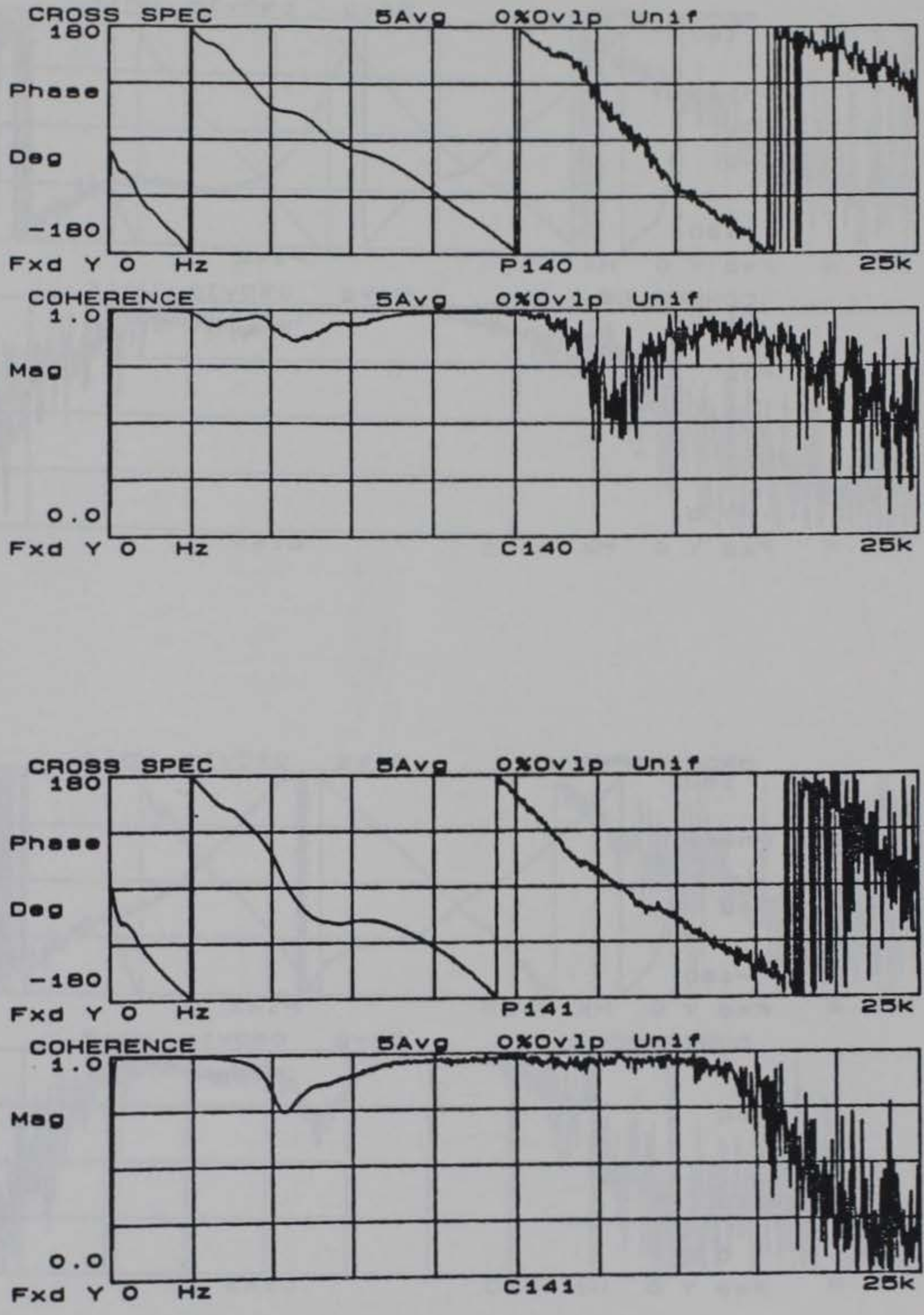

Figure B2. Phase and coherence records for 0.5 ft. receiver spacing at Site 4

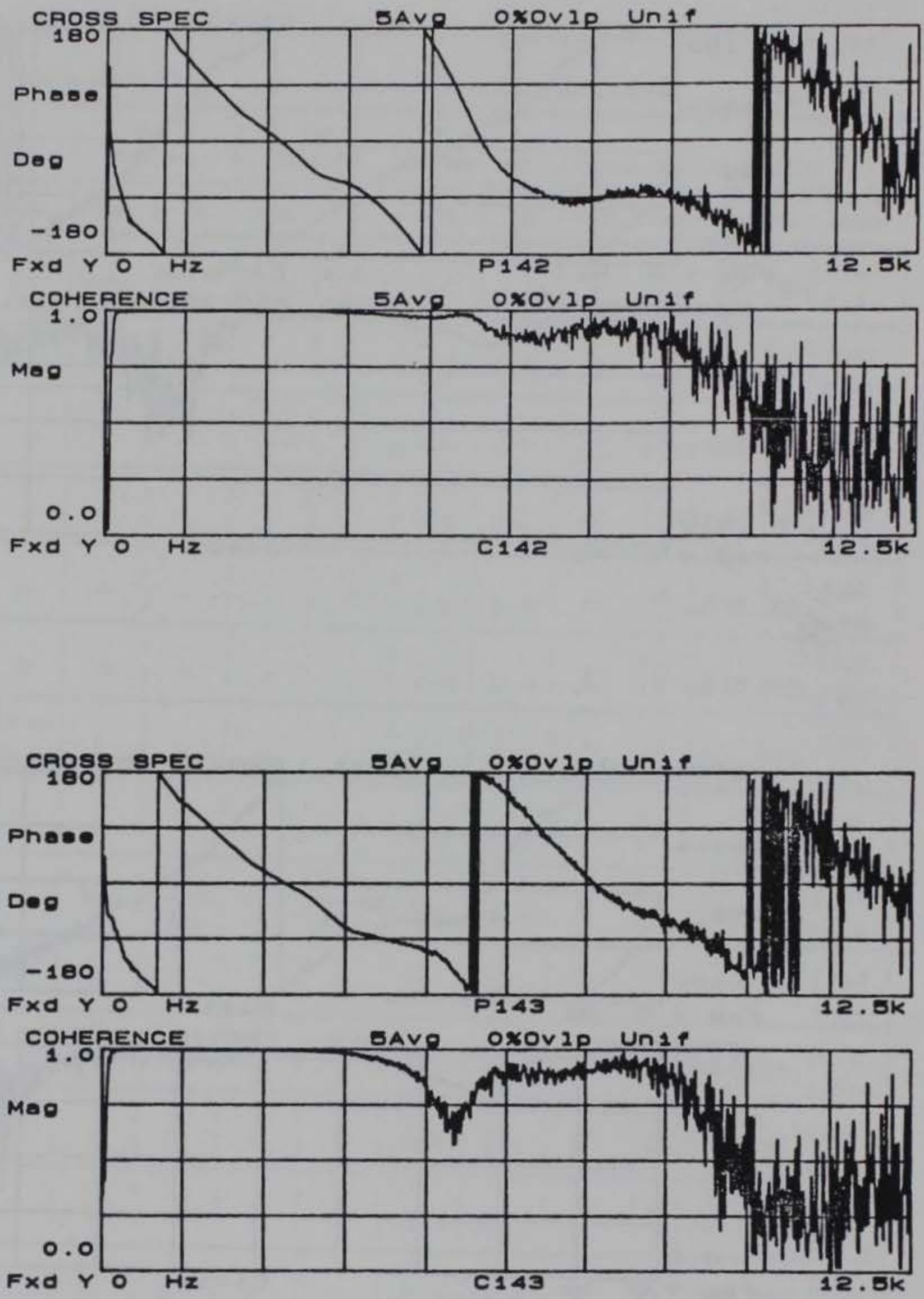

Figure B3. Phase and coherence records for 1.0 ft. receiver spacing at Site 4

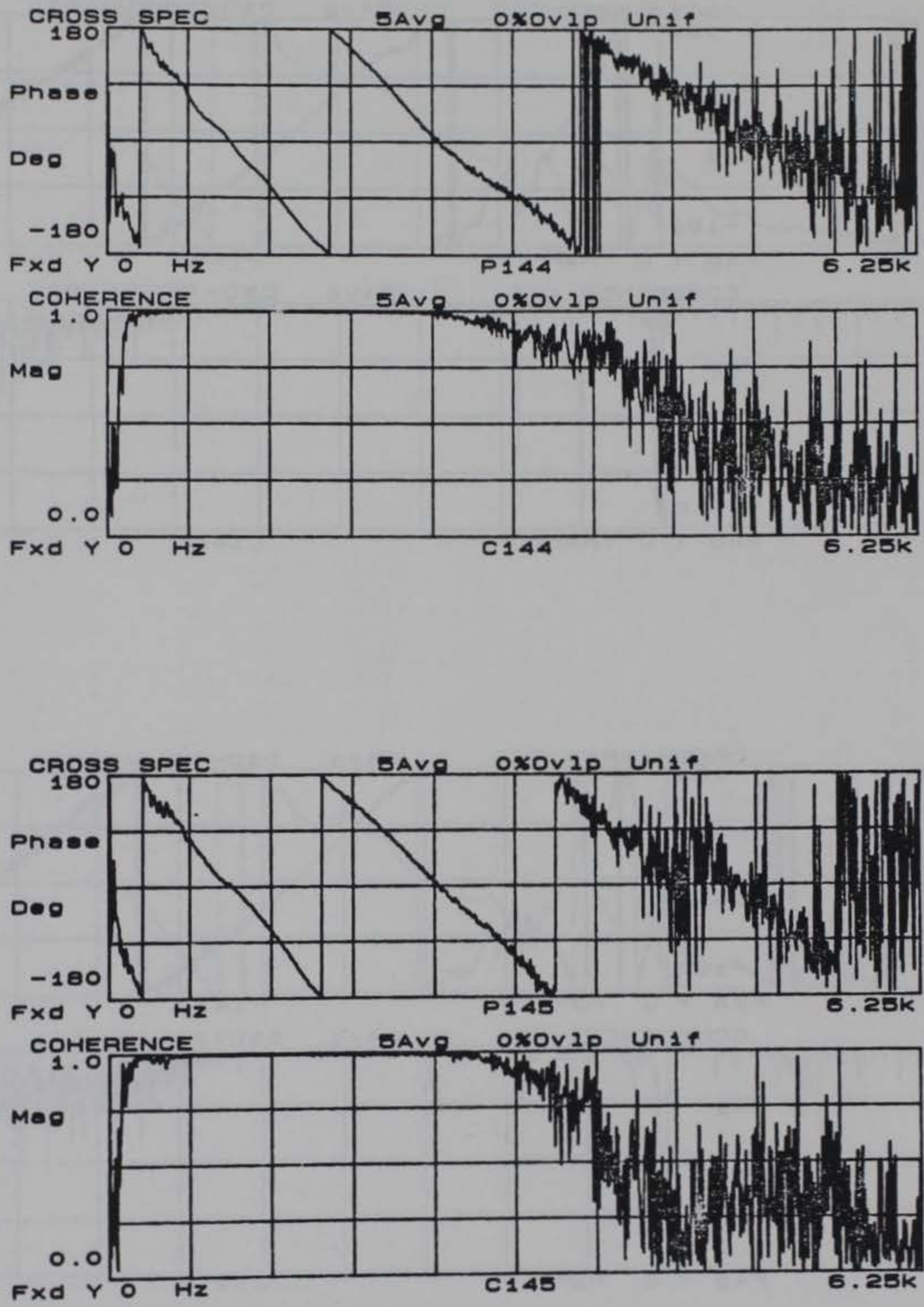

Figure B4. Phase and coherence records for 2.0 ft. receiver spacing at Site 4

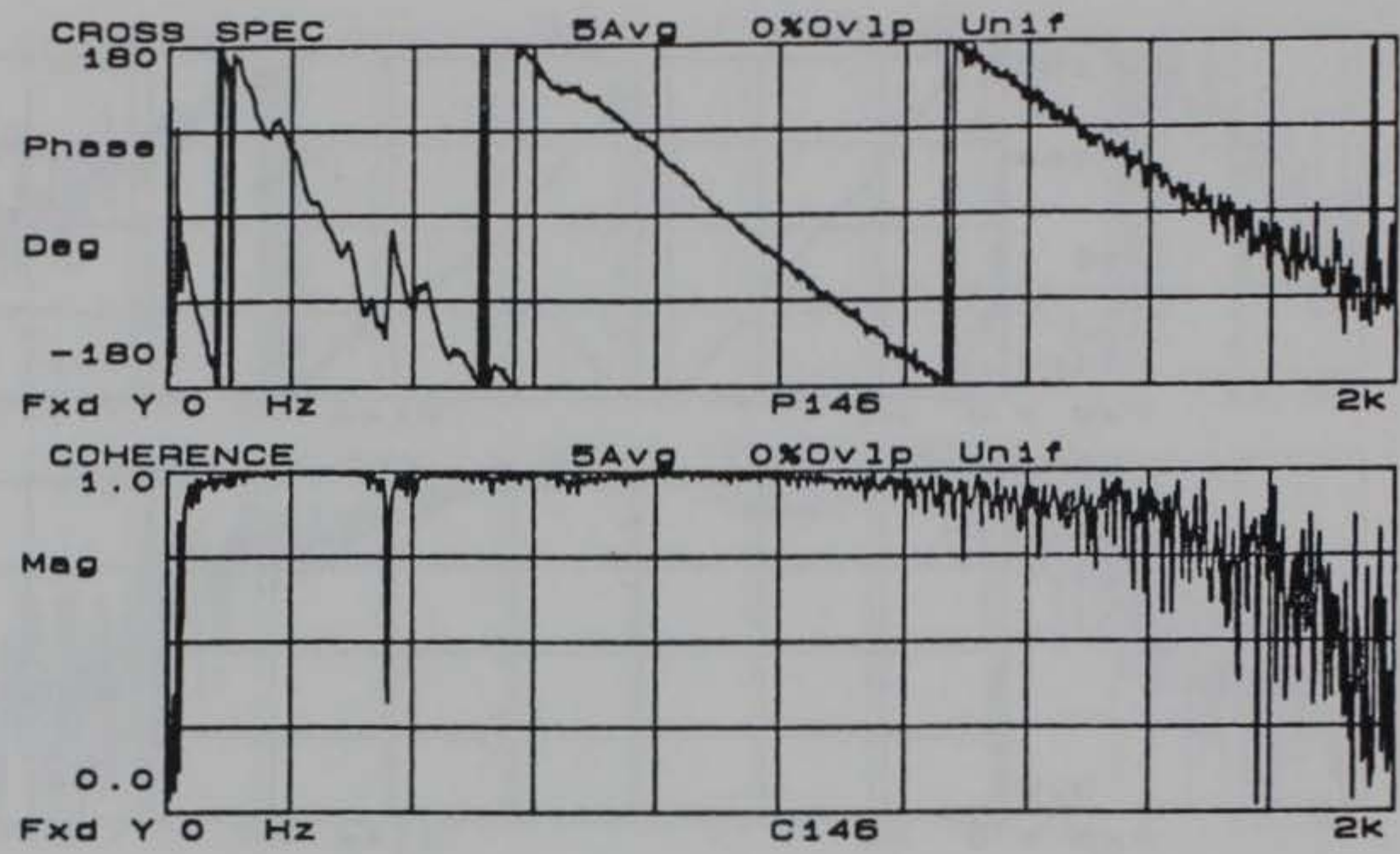

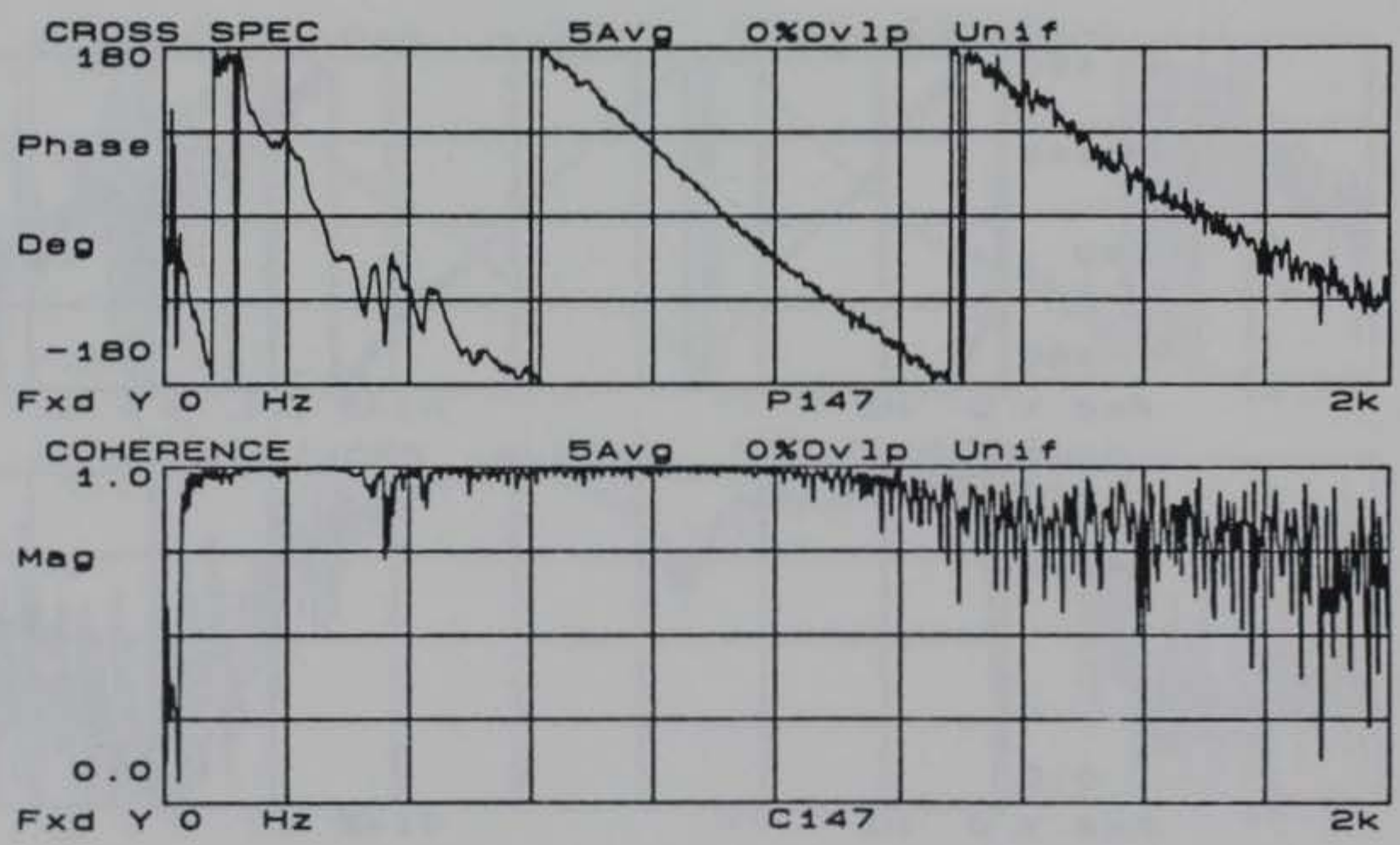

Figure B5. Phase and coherence records for 4.0 ft. receiver spacing at Site 4 (accelerometer data)

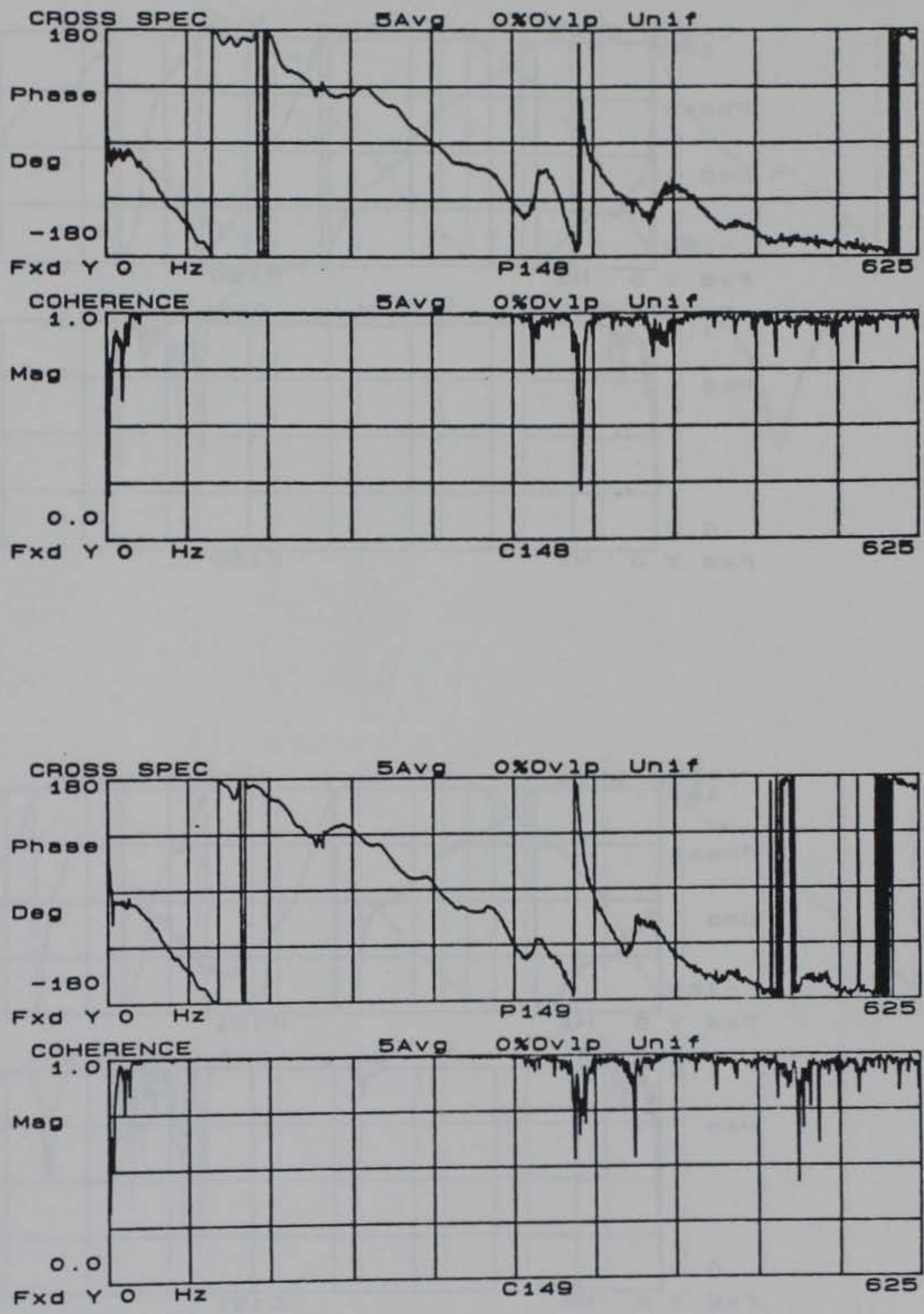

Figure B6. Phase and coherence records for 4.0 ft. receiver spacing at Site 4 (velocity transducer data)

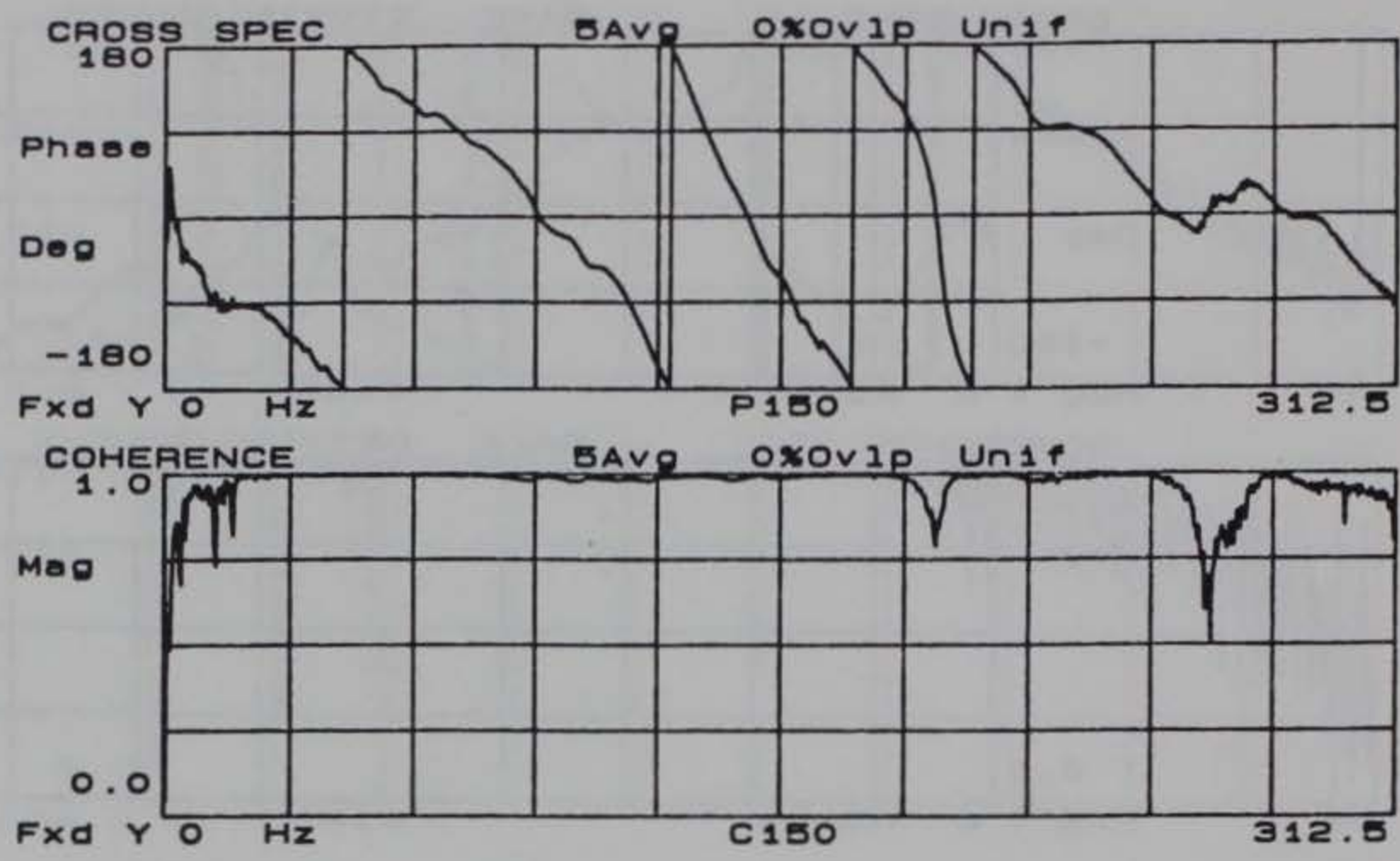

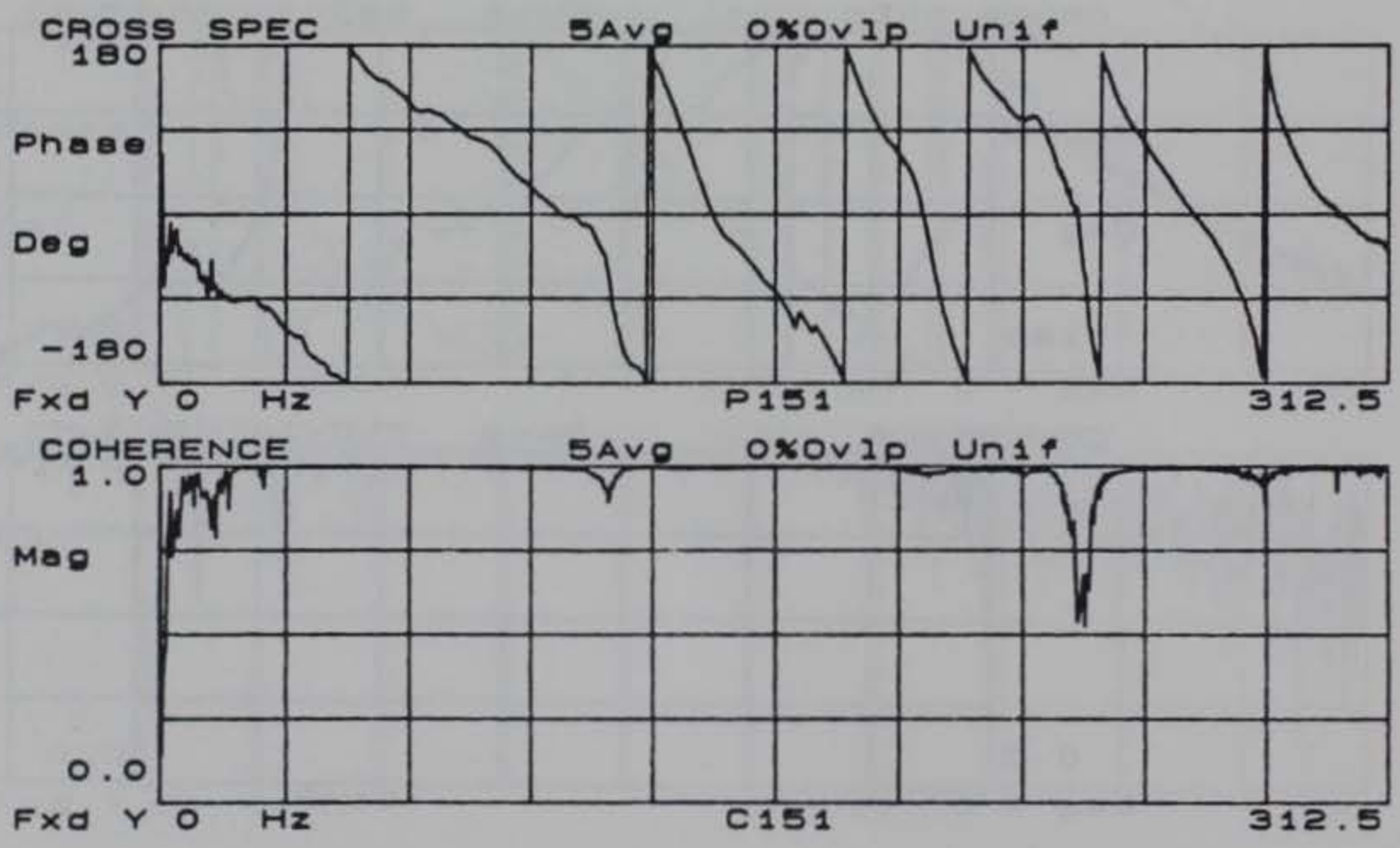

Figure B7. Phase and coherence records for 8.0 ft. receiver spacing at Site 4

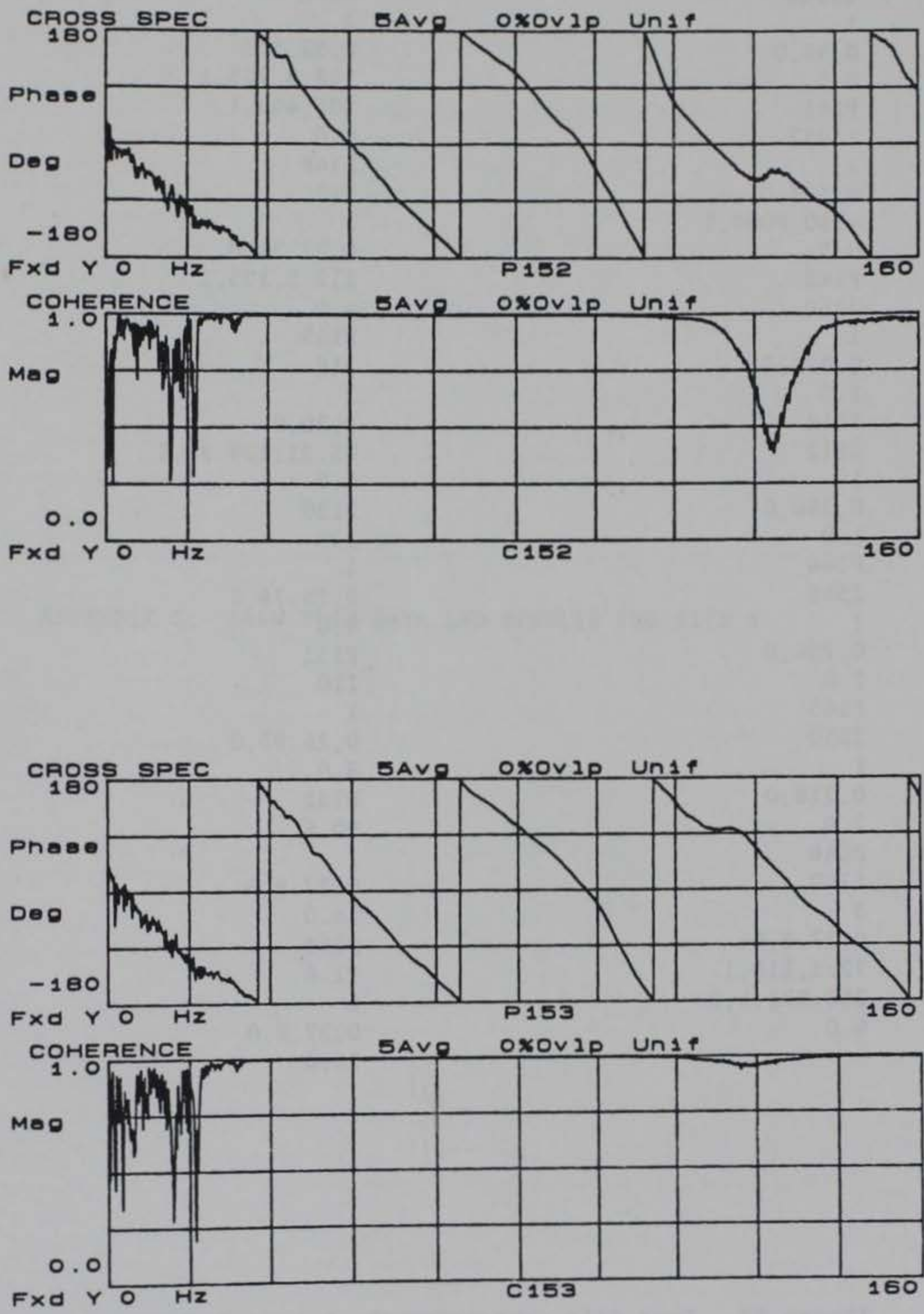

Figure B8. Phase and coherence records for 16.0 ft. receiver spacing at Site 4

```
P140
13300
1
0,94,0
0.5
P141
13937
2
0,531,0
4750,8000,1
0.5
P142
3250
1
0,375,0
1.0
P143
3812
1
0,344,0
1.0
P144
2546
1
0,234,0
2.0
P145
2850
1
0,218,0
2.0
P146
1240
3
0,27.5,0
72.5,110,1
350,572.5,2
4.0
P147
1275
3
0,52.5,0
112.5,125,1
305,445,1
4.0
P148
267
2
0,27.34,0
112.5,125,1
4.0
P149
310
2
0,30,0
95.31,109.37,1
4.0
P150
113
1
0,25.78,0
8.0
P151
110
1
0,26.95,0
8.0
P152
90.6
1
0,27.8,0
16.0
P153
91.6
1
0,27.8,0
16.0
```

Figure B9. Data file containing the names of phase records, cutoff frequencies, poor data ranges, and receiver spacings used by the computer program SASW in constructing the dispersion curve for Site 4

APPENDIX C: SASW TEST DATA AND RESULTS FOR SITE 8

FIELD DATA SHEET FOR SASW TESTS (HP 3562A/9153A)

TEST SITE: Site 8, Birmingham START TIME: 1011 TEMP, F: 101°

TEST DATE: 8-12-87 ENDING TIME: 1115 TEMP, F: 113°

Source Type	Near Receiver Type	Near Receiver ID	Far Receiver Type	Far Receiver ID	Receiver Spacing (ft)	SNR Distance (ft)	Profile (F=Fwd., R=Rev.)	No. of Ave.	Freq. BW (Hz)	Site File No.	Data File Names
4 oz Ball Peen	Accel.	PCB 308B02 SN 19926	Accel.	PCB 308B02 SN 19927	0.5	0.5	F*	5	KHz 20	320	P320 C320
"	"	"	"	"	0.5	0.5	R	5	20	321	P321 C321
"	"	"	"	"	1.0	1.0	R	5	12.5	322	P322 C322
"	"	"	"	"	1.0	1.0	F	5	12.5	323	P323 C323
"	"	"	"	"	2.0	2.0	F	5	10	324	P324 C324
"	"	"	"	"	2.0	2.0	R	5	10	325	P325 C325
40 oz Sledge	"	"	"	"	4.0	4.0	R	5	4	326	P326 C326
"	"	"	"	"	4.0	4.0	F	5	4	327	P327 C327
8 lb. Sledge	Vel.	Geo-source PC-3	Vel.	Geo-source PC-3	4.0	4.0	F	5	1	328	P328 C328
"	"	"	"	"	4.0	4.0	R	5	1	329	P329 C329
"	"	"	"	"	8.0	8.0	R	5	Hz 500	330	P330 C330
"	"	"	"	"	8.0	8.0	F	5	500	331	P331 C331
"	"	"	"	"	16.0	16.0	F	5	250	332	P332 C332
"	"	"	"	"	16.0	16.0	R	5	250	333	P333 C333
"	"	"	"	"	16.0	16.0	F	5	100	334	P334 C334
"	"	"	"	"	16.0	16.0	R	5	100	335	P335 C335

* Source on West Side

Figure C1. SASW field data form for Site 8

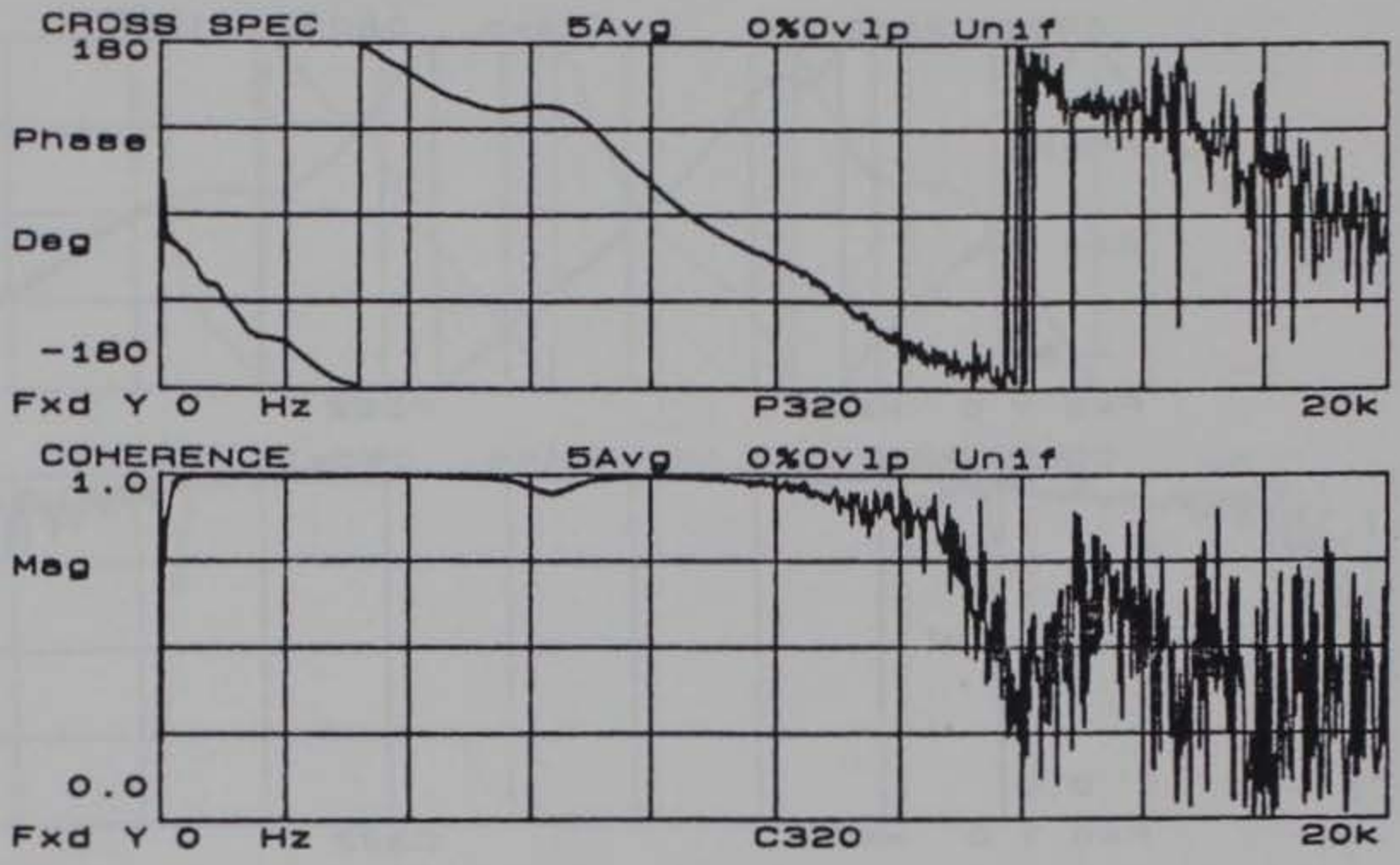

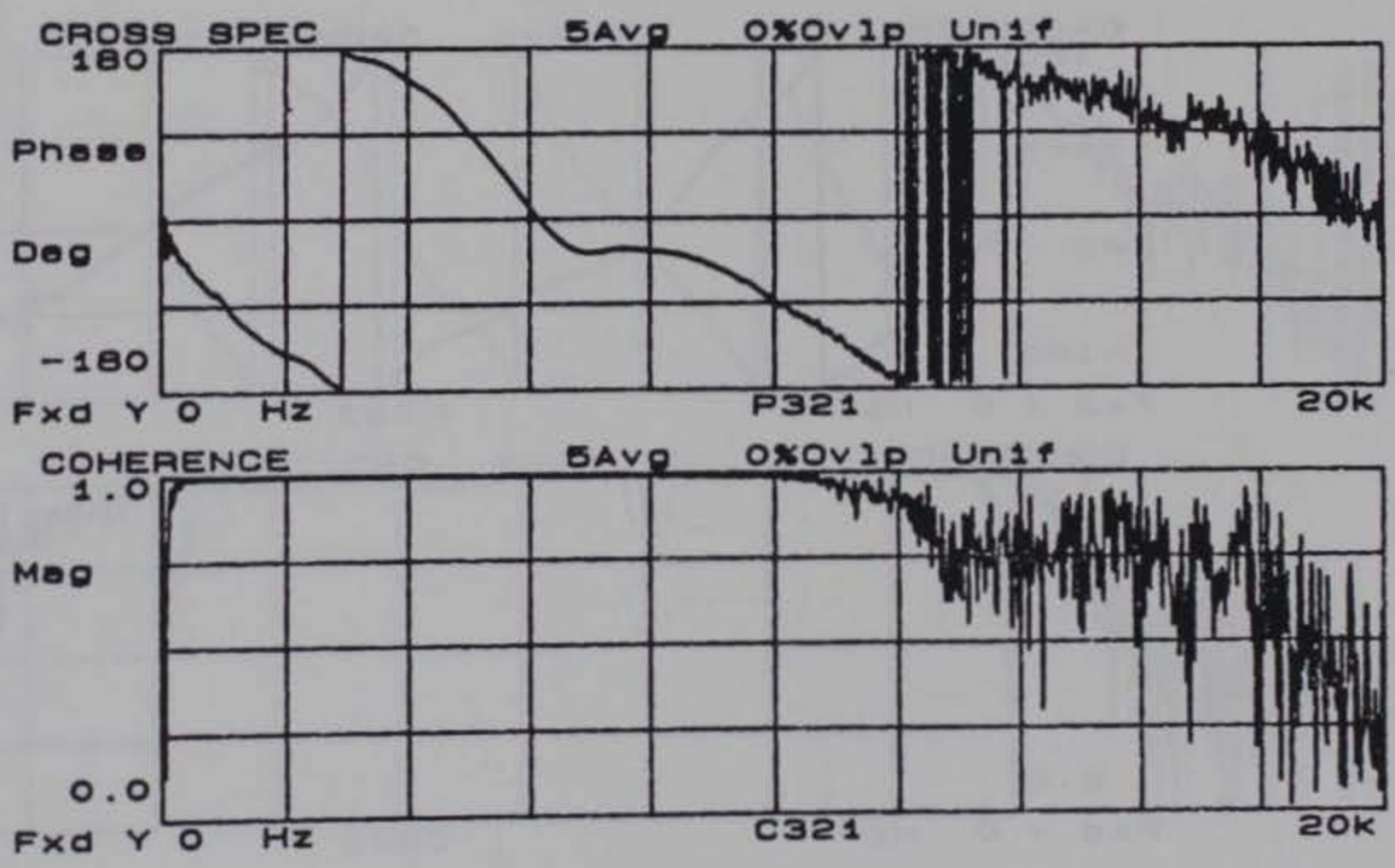

Figure C2. Phase and coherence records for 0.5 ft. receiver spacing at Site 8

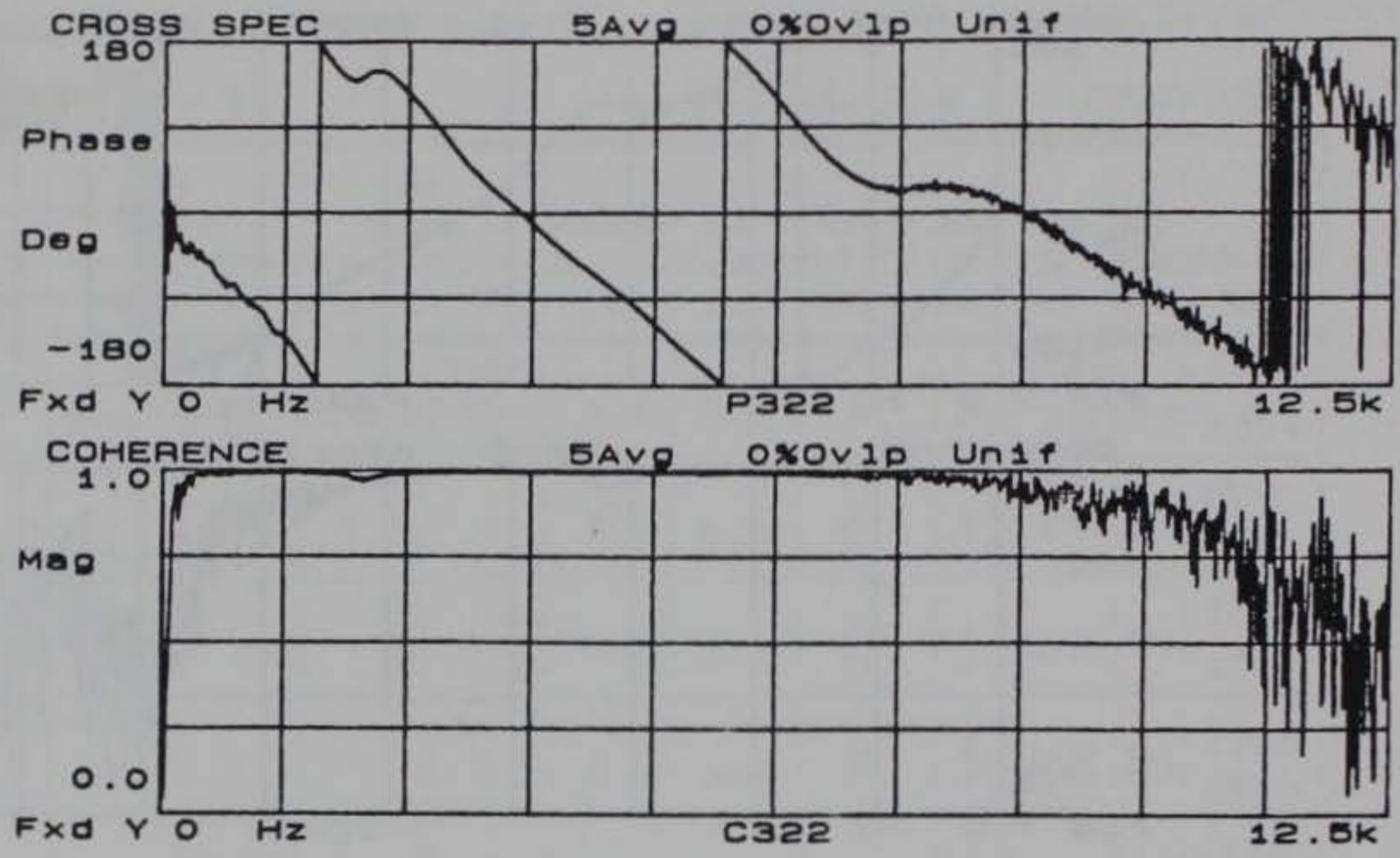

Figure C3. Phase and coherence records for 1.0 ft. receiver spacing at Site 8

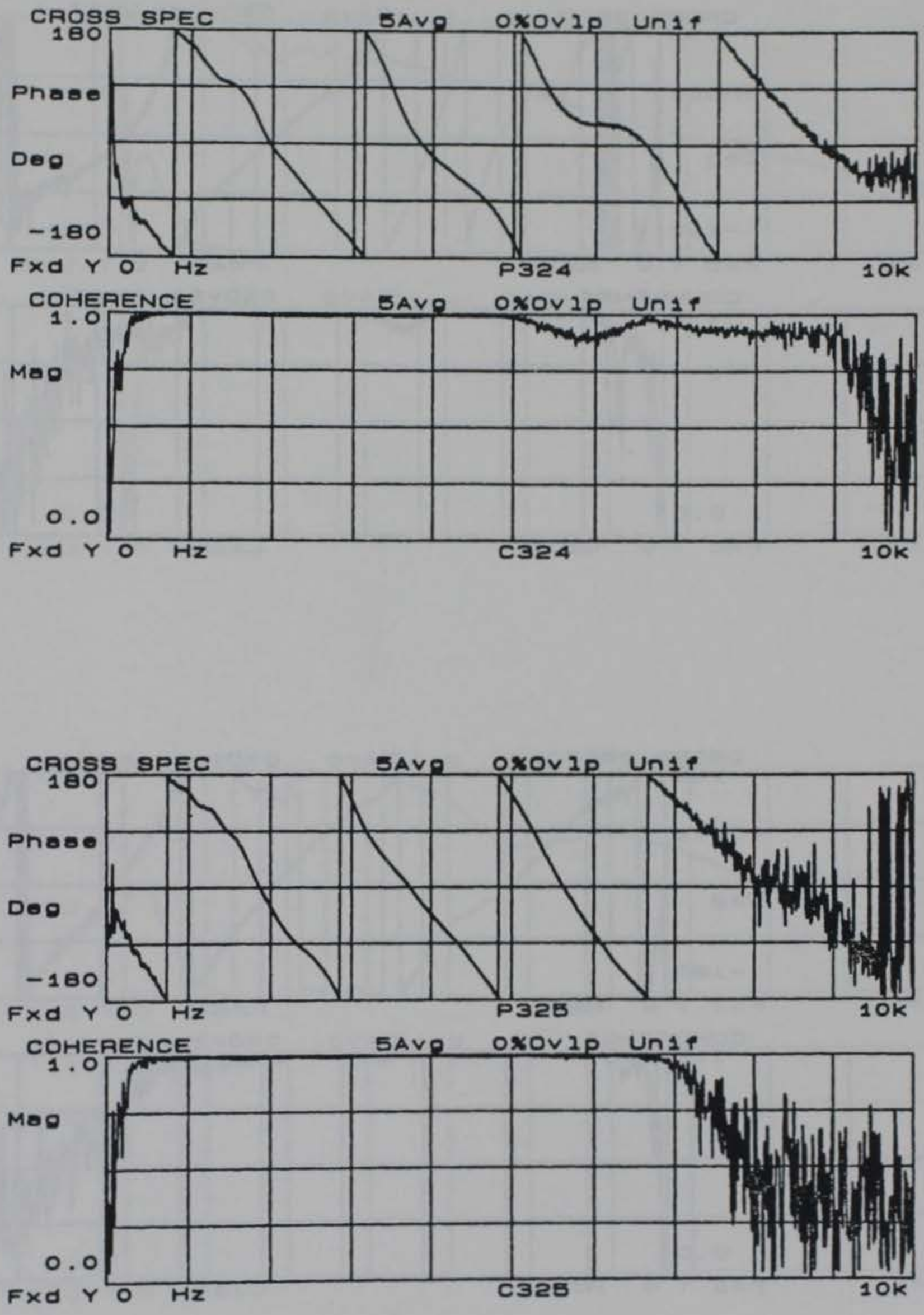

Figure C4. Phase and coherence records for 2.0 ft. receiver spacing at Site 8

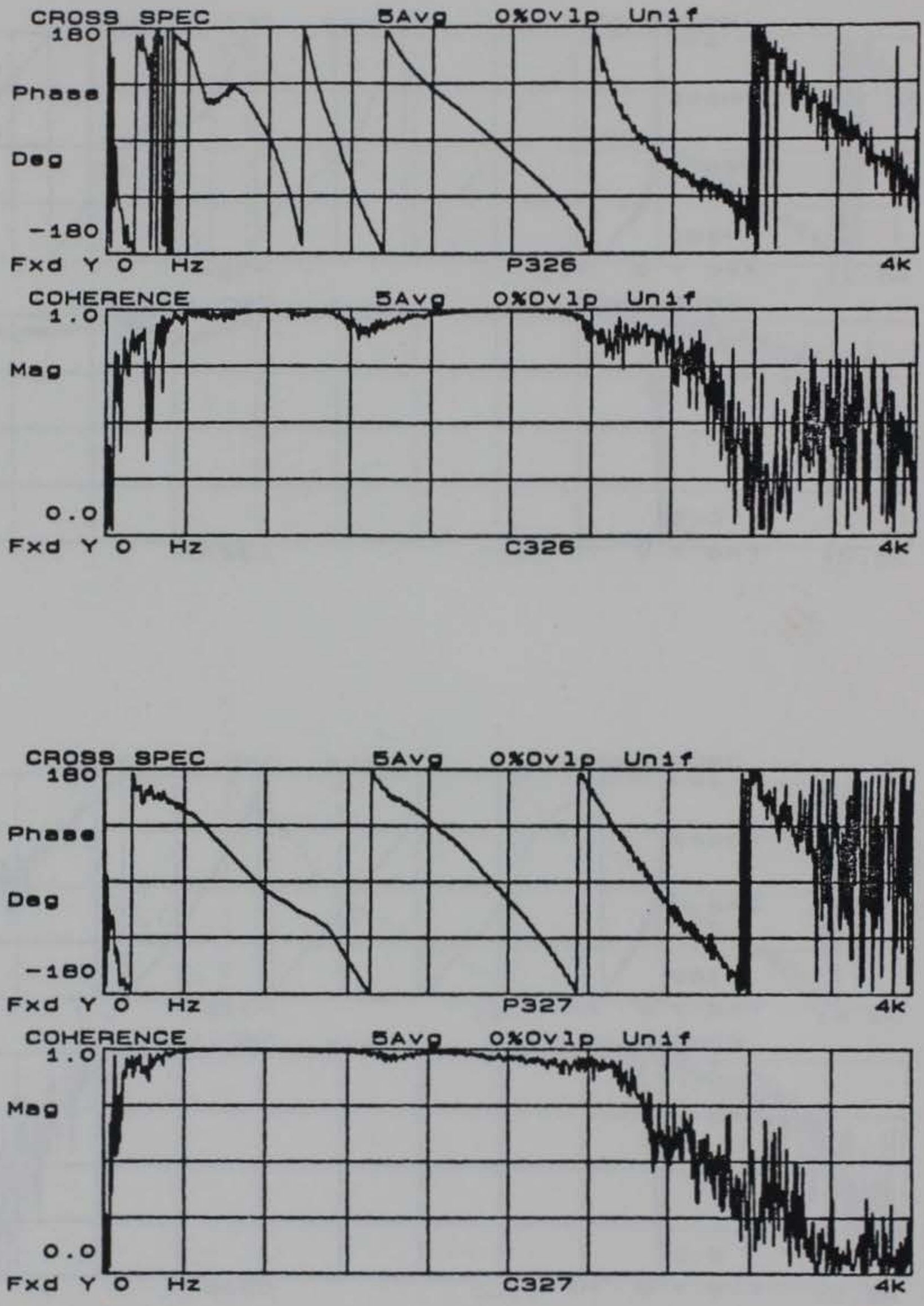

Figure C5. Phase and coherence records for 4.0 ft. receiver spacing at Site 8 (accelerometer data)

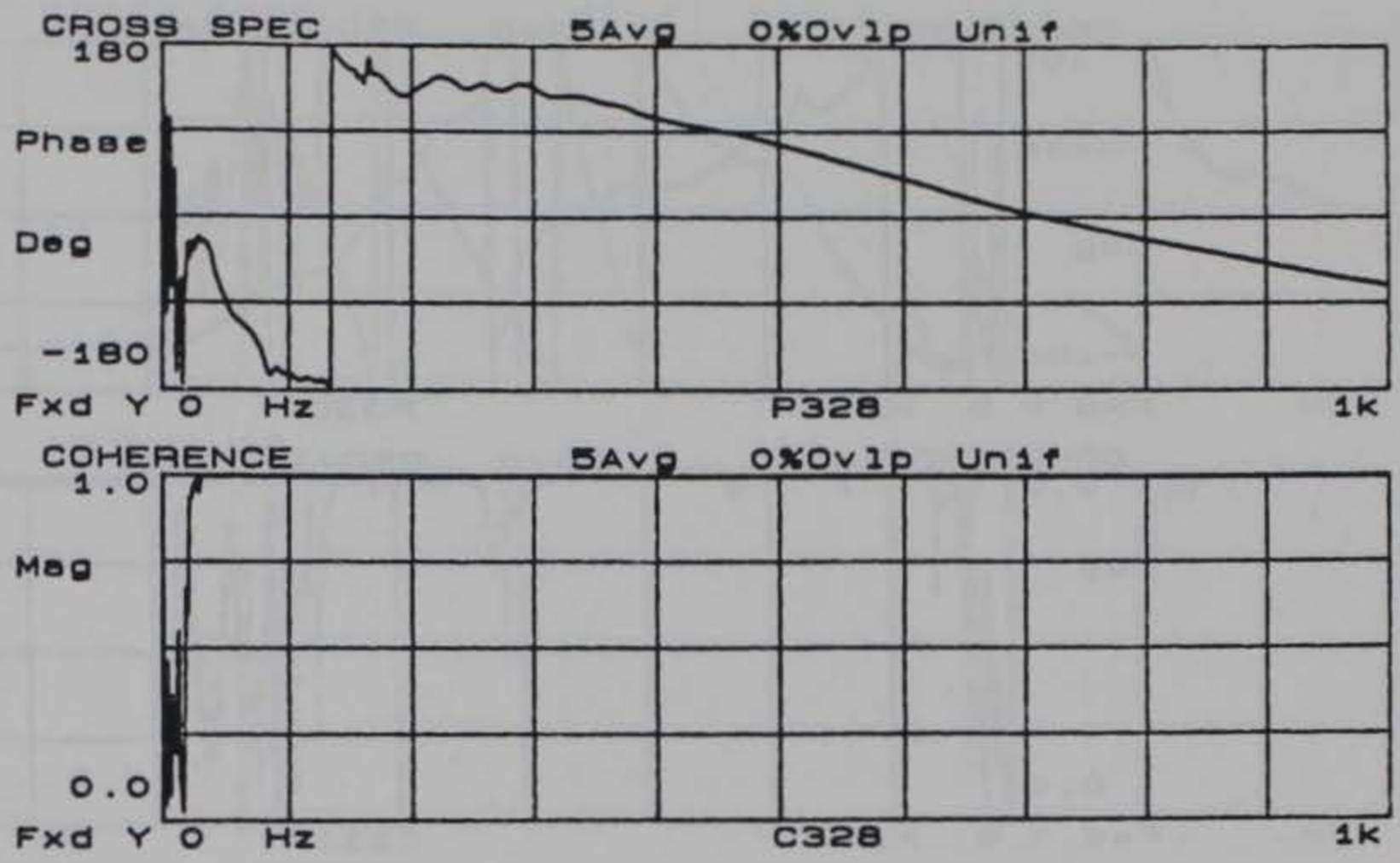

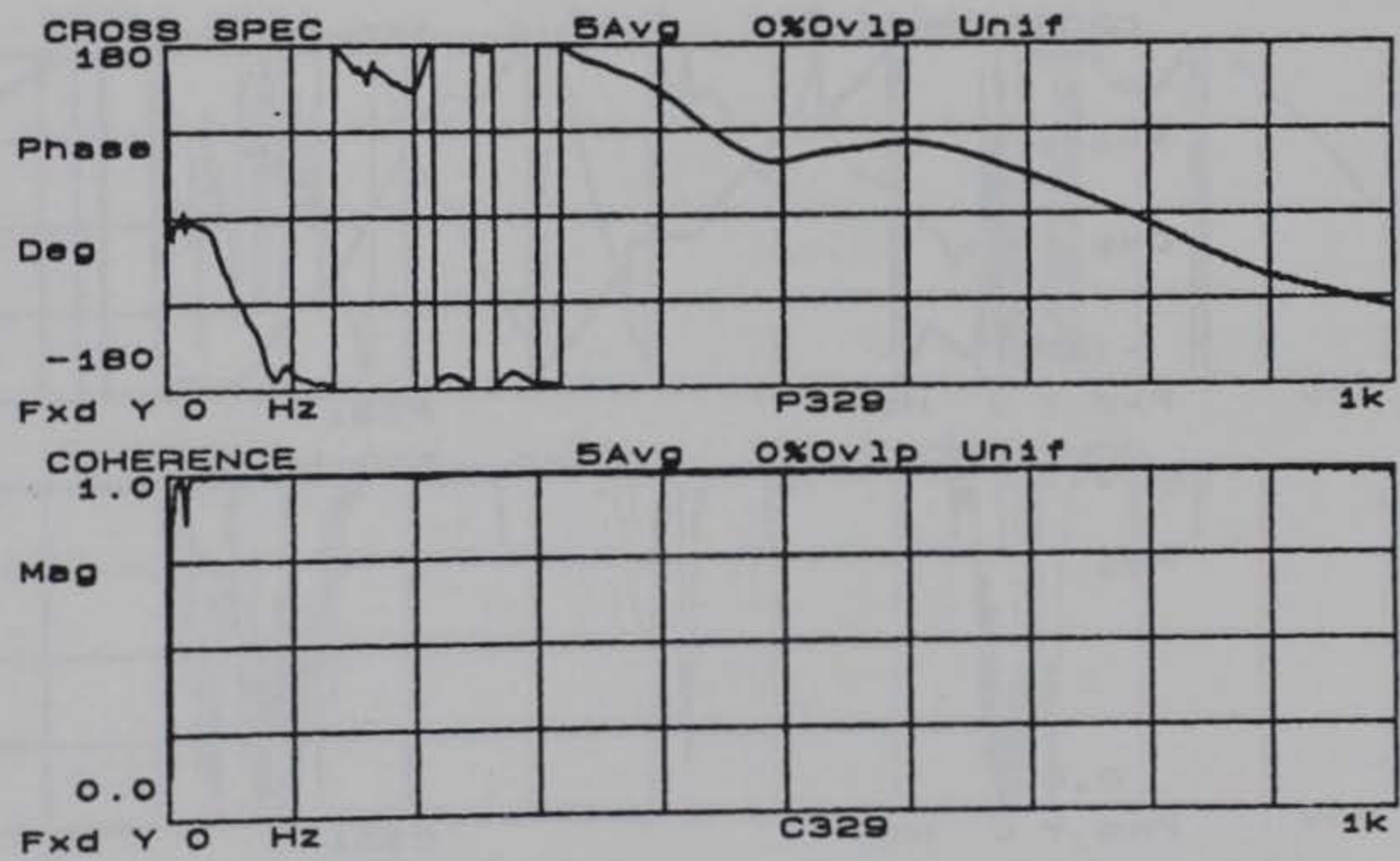

Figure C6. Phase and coherence records for 4.0 ft. receiver spacing at Site 8 (velocity transducer data)

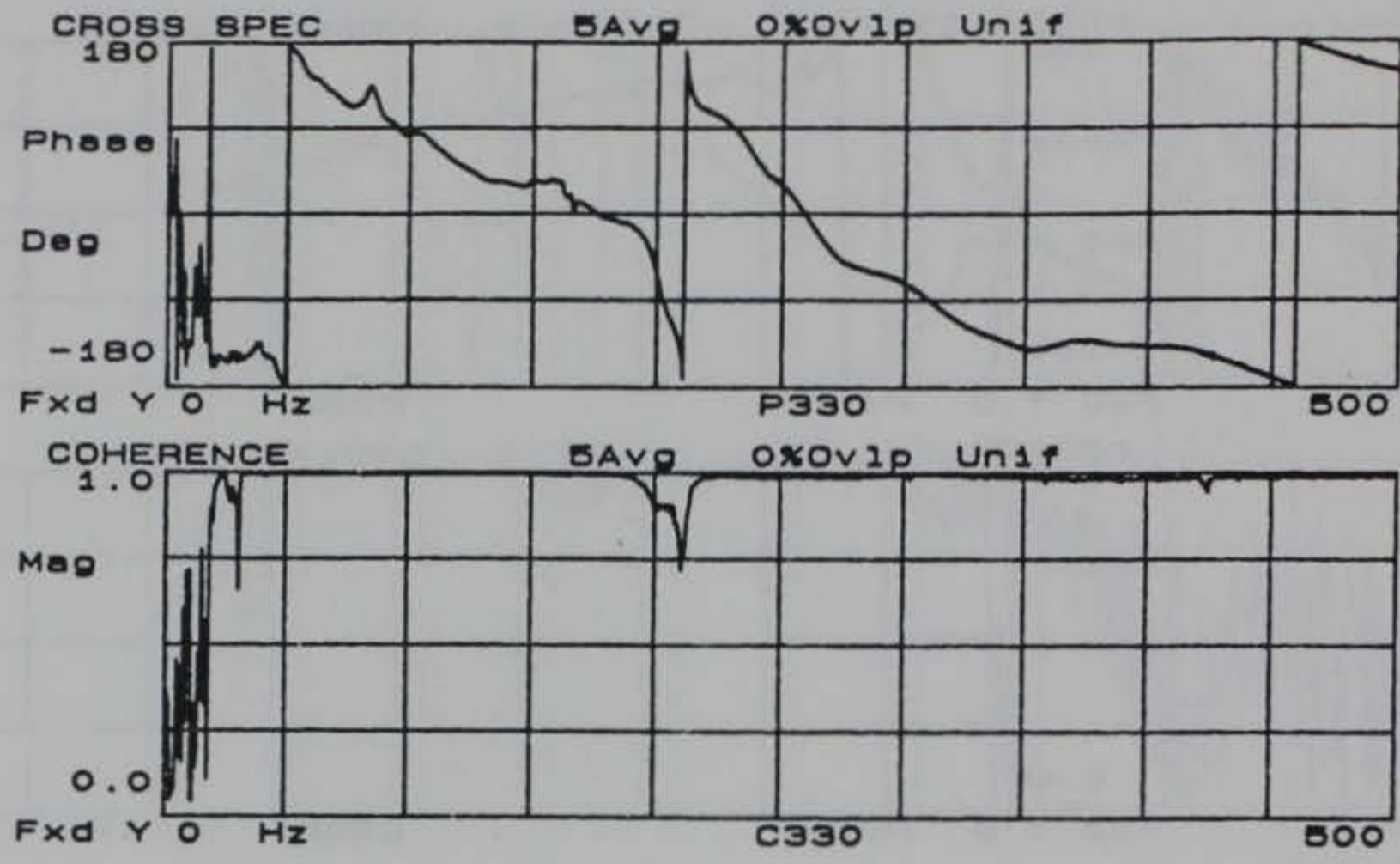

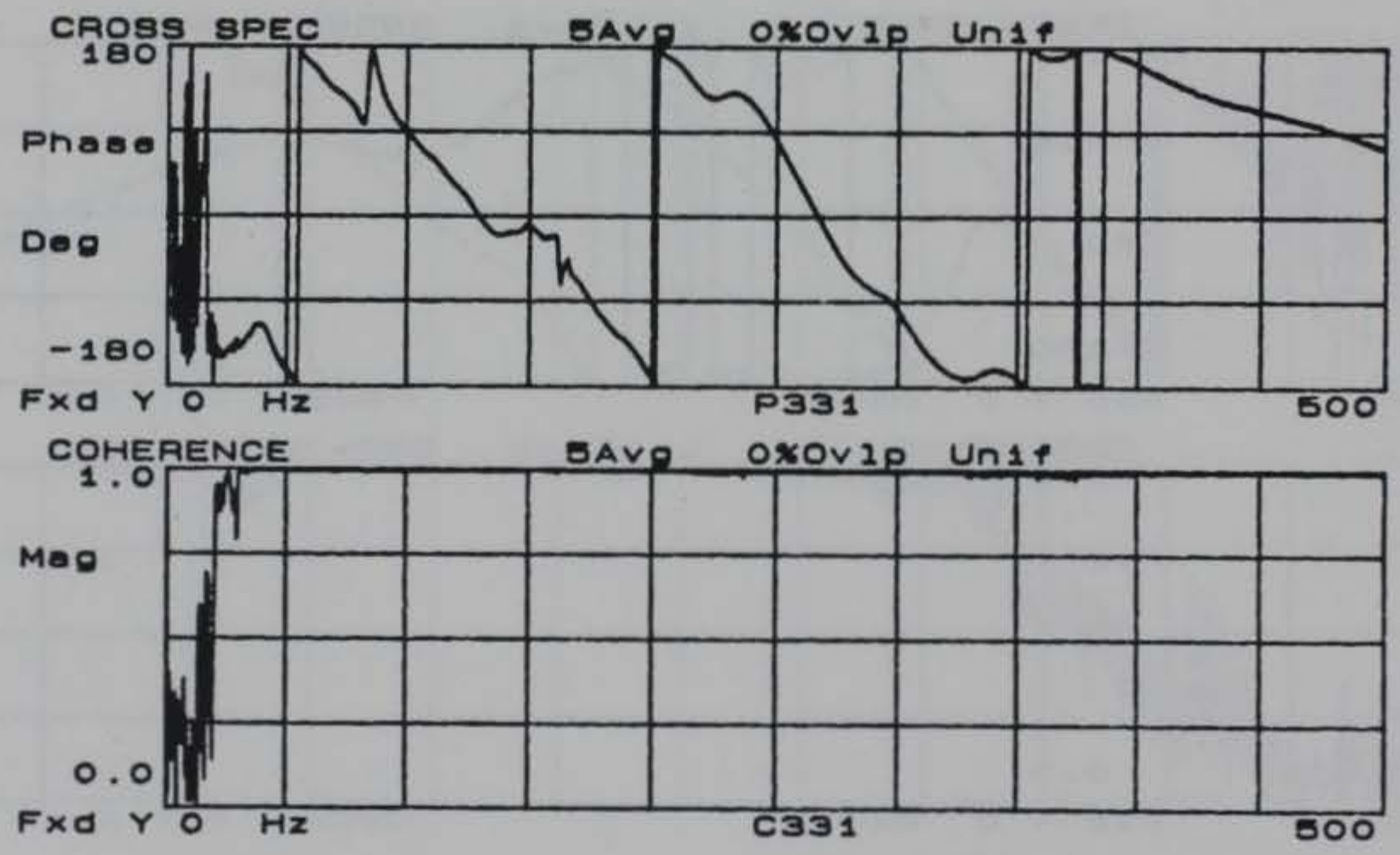

Figure C7. Phase and coherence records for 8.0 ft. receiver spacing at Site 8

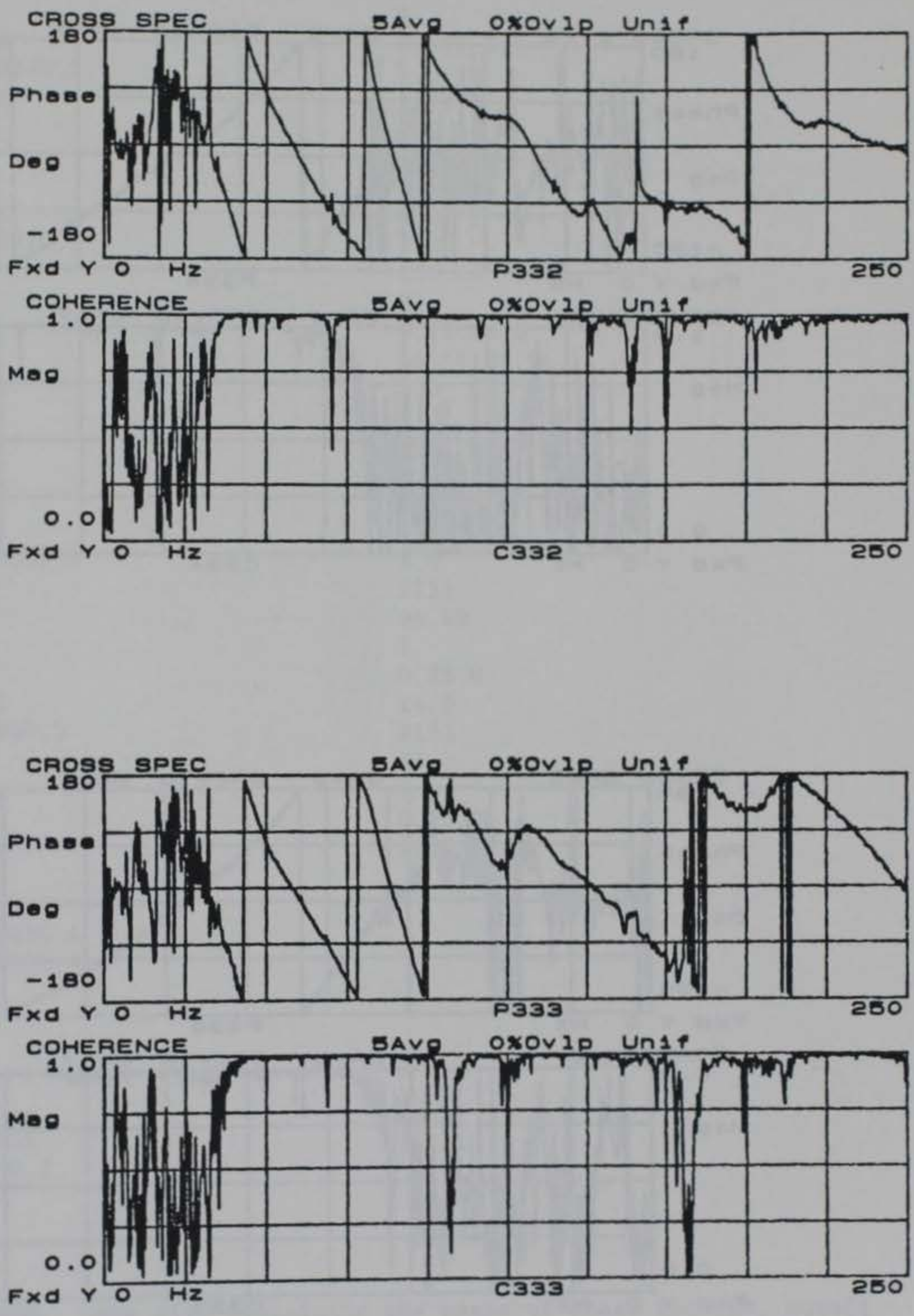

Figure C8. Phase and coherence records for 16.0 ft. receiver spacing at Site 8 (250 Hz bandwidth)

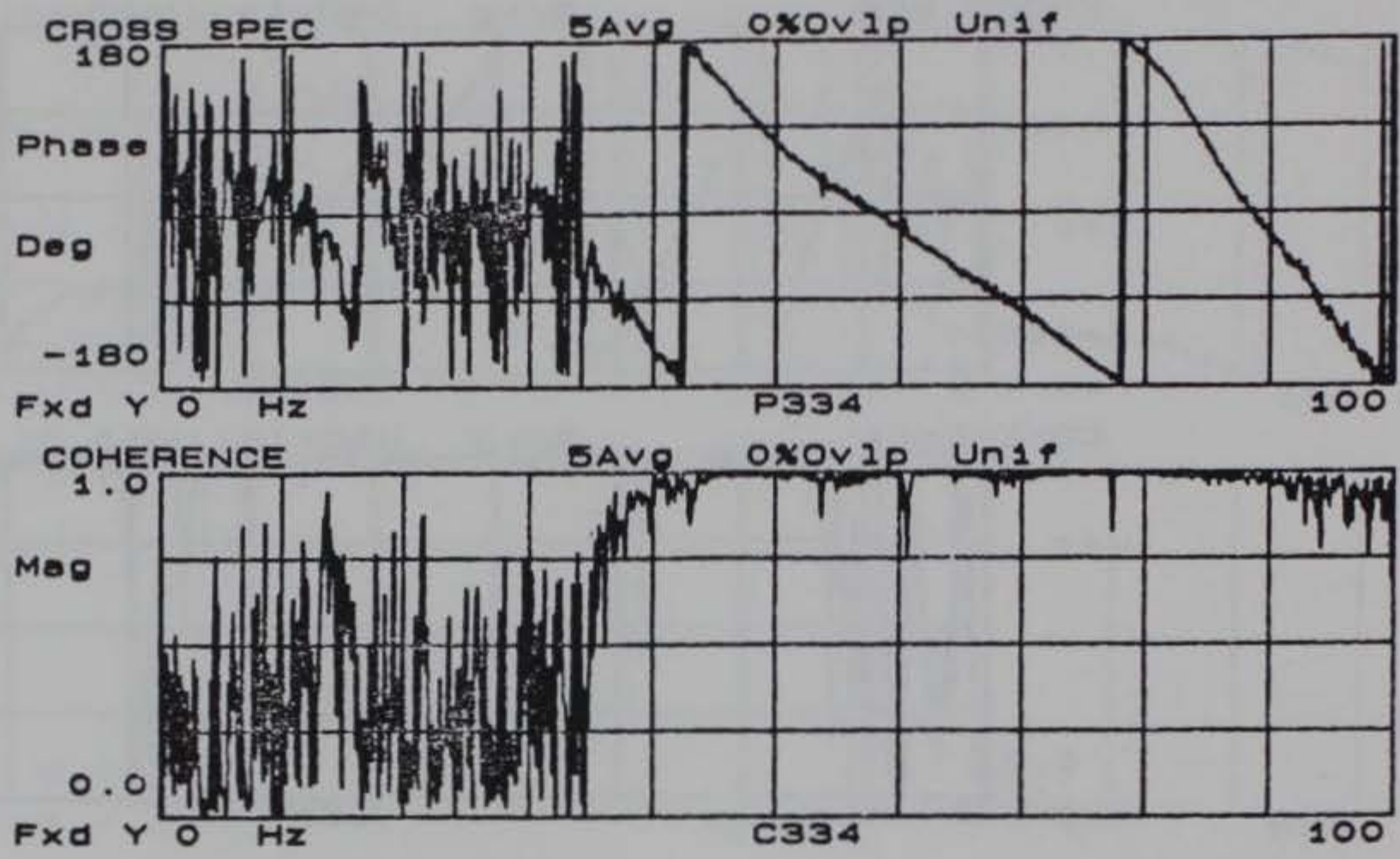

Figure C9. Phase and coherence records for 16.0 ft. receiver spacing at Site 8 (100 Hz bandwidth)

```
P120
46370
2
0,8120,1
22120,23370,2
0.5
P121
44870
2
0,9000,1
23120,23870,2
0.5
P122
30500
1
0,7500,1
1.0
P123
31750
2
0,7375,1
11375,12625,2
1.0
P124
21000
2
0,1125,1
3625,10000,3
2.0
P125
19656
4
0,1437,1
5000,9875,3
13375,13656,4
16937,17250,5
2.0
P126
2125
3
0,464.8,1
950,1250,1
1375,1520,2
4.0
P127
2250
1
0,492.2,1
4.0
P128
742.5
1
0,472.5,1
4.0
P130
153.44
2
0,23.44,0
56.56,85.94,1
8.0
P131
200
2
0,25,0
47.81,60,1
8.0
P132
64.69
1
0,25,0
16.0
P133
64
1
0,25,0
16.0
```

Figure C10. Data file containing the names of phase records, cutoff frequencies, poor data ranges, and receiver spacings used by the computer program SASW in constructing the dispersion curve for Site 8

APPENDIX D: SASW TEST DATA AND RESULTS FOR SITE 10

FIELD DATA SHEET FOR SASW TESTS (HP 3562A/9153A)

TEST SITE: Site 10, Birmingham START TIME: 1531 TEMP, F: 117°

TEST DATE: 8-12-87 ENDING TIME: 1616 TEMP, F: 109°

Source Type	Near Receiver Type	Near Receiver ID	Far Receiver Type	Far Receiver ID	Receiver Spacing (ft)	SNR Distance (ft)	Profile (F=Fwd., R=Rev.)	No. of Ave.	Freq. BW (Hz)	Site File No.	Data File Names
4 oz. Ball Peen	Accel.	PCB 308B02 SN19926	Accel.	PCB 308B02 SN19927	0.5	0.5	F*	5	KHz 12.5	360	P360 C360
"	"	"	"	"	0.5	0.5	R	5	12.5	361	P361 C361
"	"	"	"	"	0.25	0.25	F	5	20	362	P362 C362
"	"	"	"	"	0.25	0.25	R	5	20	363	P363 C363
"	"	"	"	"	1.0	1.0	R	5	12.5	364	P364 C364
"	"	"	"	"	1.0	1.0	F	5	12.5	365	P365 C365
"	"	"	"	"	2.0	2.0	F	5	12.5	366	P366 C366
"	"	"	"	"	2.0	2.0	R	5	12.5	367	P367 C367
40 oz. Sledge	"	"	"	"	4.0	4.0	R	5	10	368	P368 C368
"	"	"	"	"	4.0	4.0	F	5	10	369	P369 C369
"	Vel.	Geo-Source PC-3	Vel.	Geo-Source PC-3	4.0	4.0	F	5	1	370	P370 C370
"	"	"	"	"	4.0	4.0	R	5	1	371	P371 C371
8 lb. Sledge	"	"	"	"	16.0	16.0	F	5	Hz 100	372	P372 C372
"	"	"	"	"	16.0	16.0	R	5	100	373	P373 C373
"	"	"	"	"	8.0	8.0	R	5	500	374	P374 C374
"	"	"	"	"	8.0	8.0	F	5	500	375	P375 C375

* Source on East Side

Figure D1. SASW field data form for Site 10

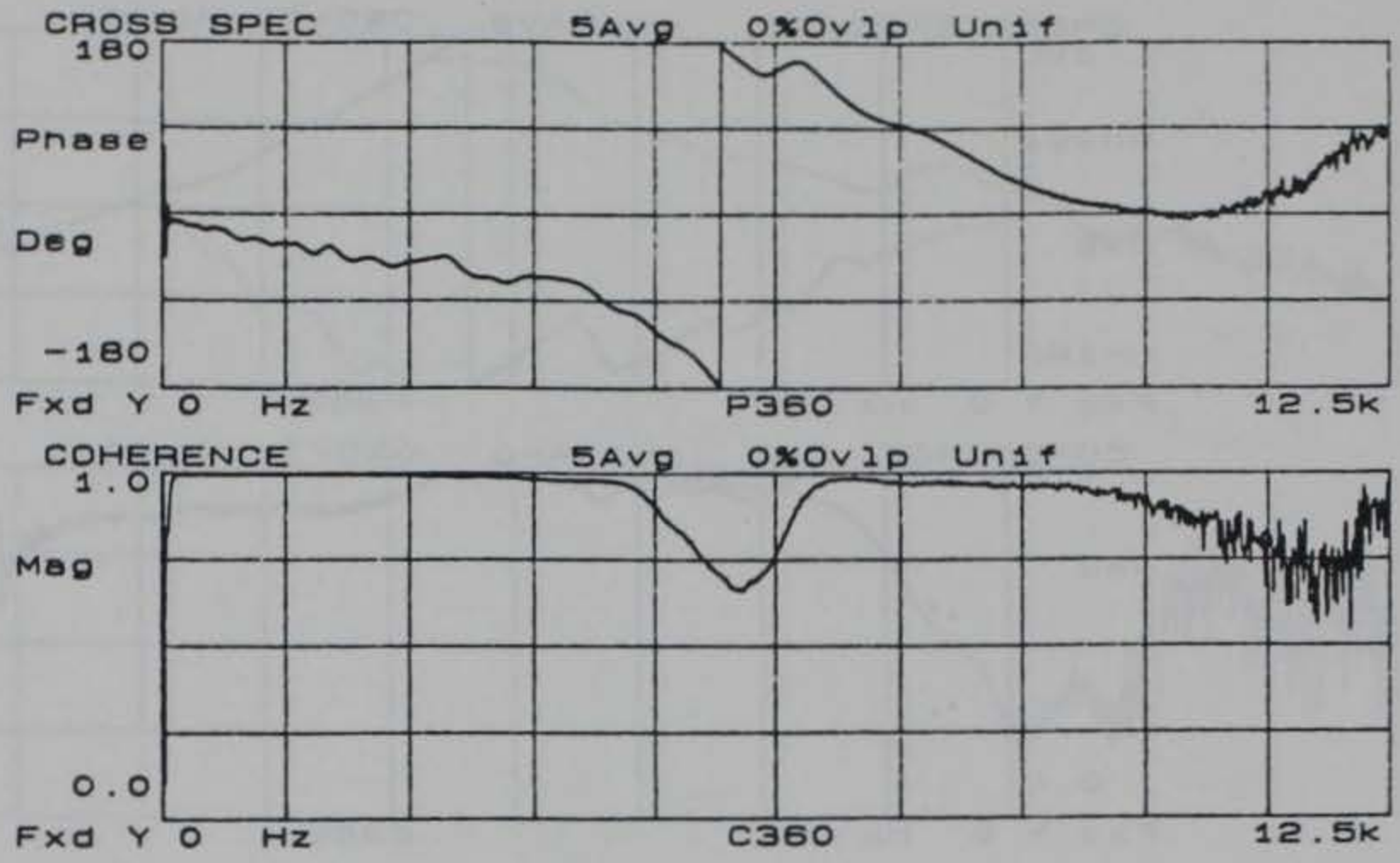

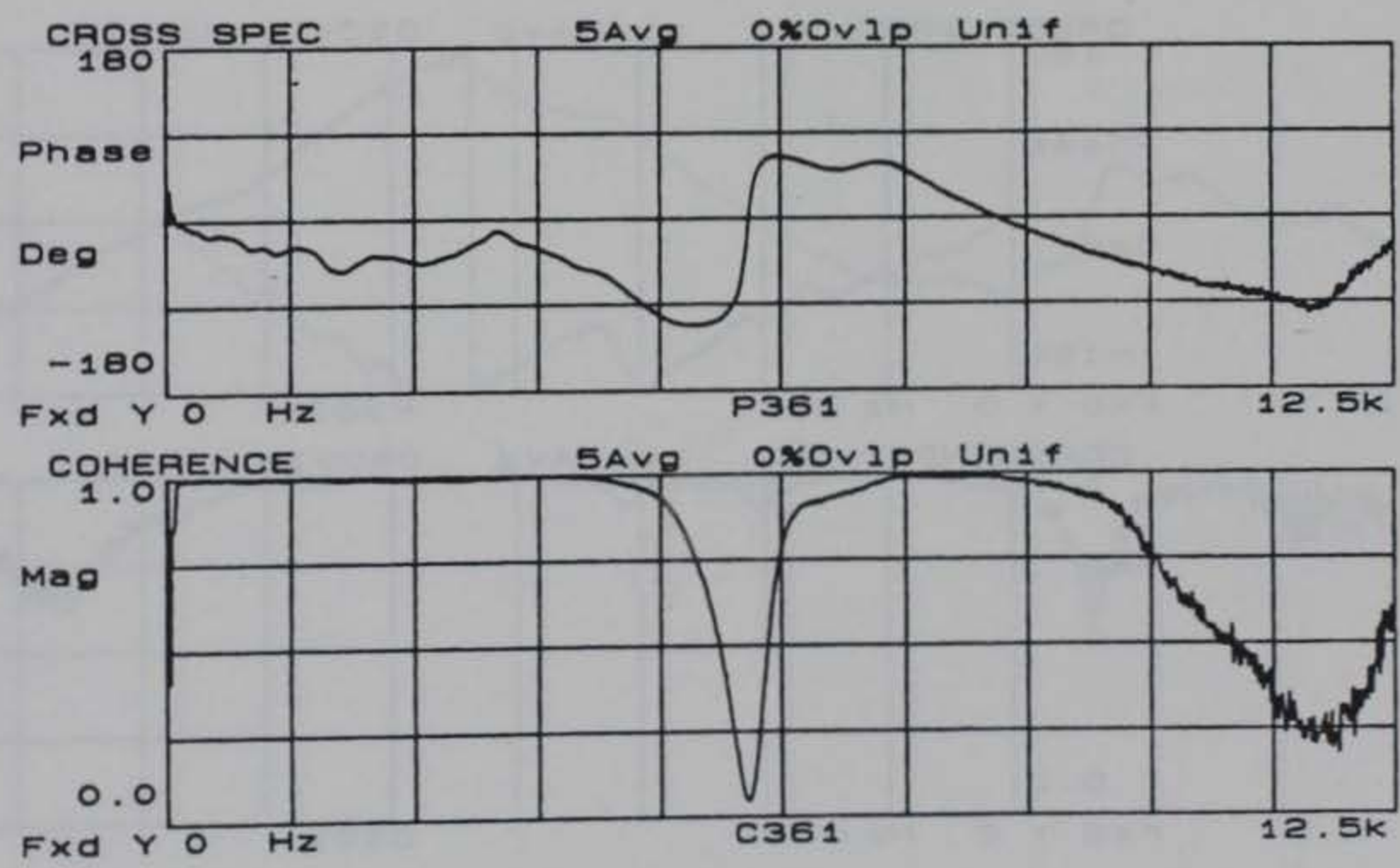

Figure D2. Phase and coherence records for 0.5 ft. receiver spacing at Site 10

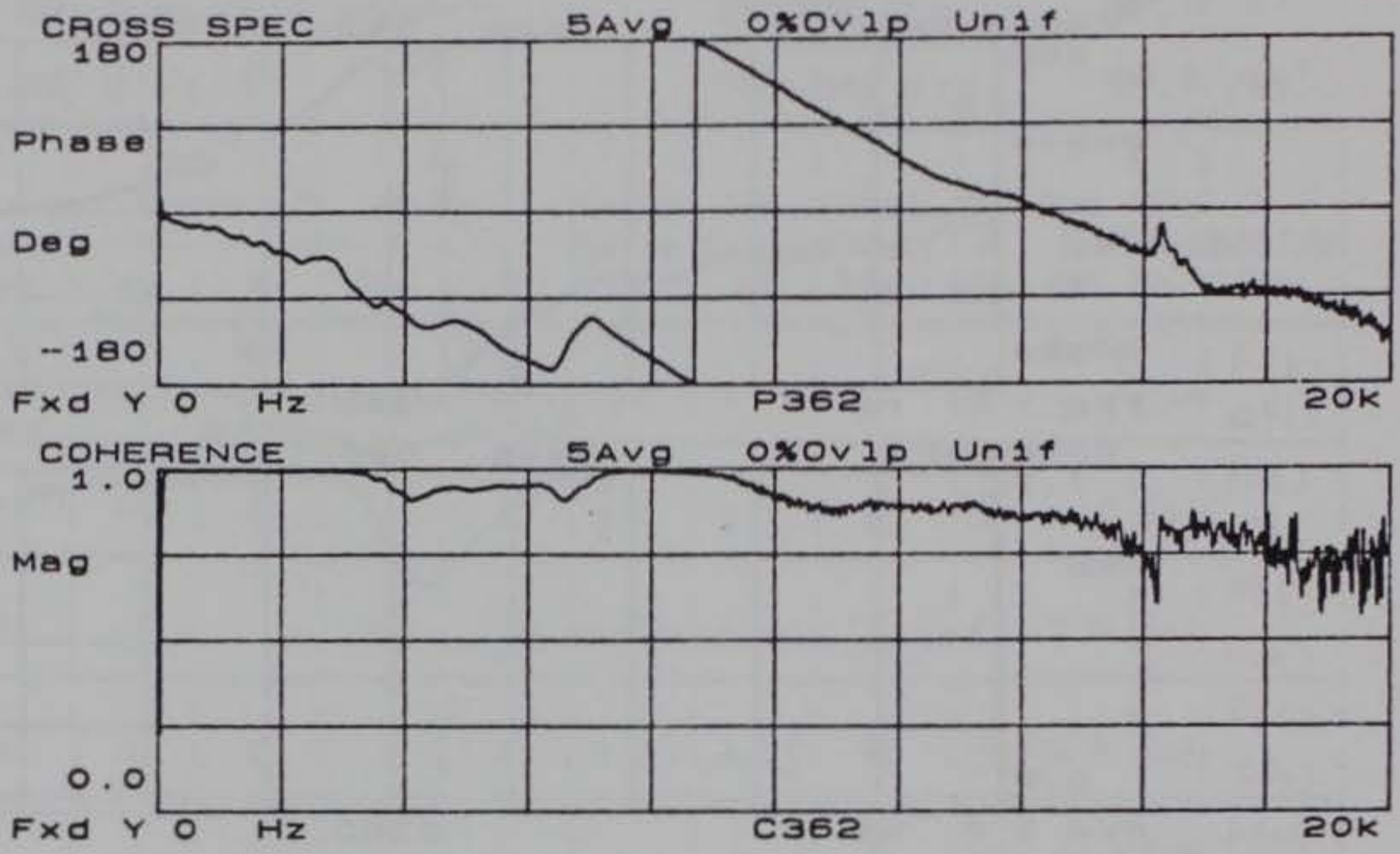

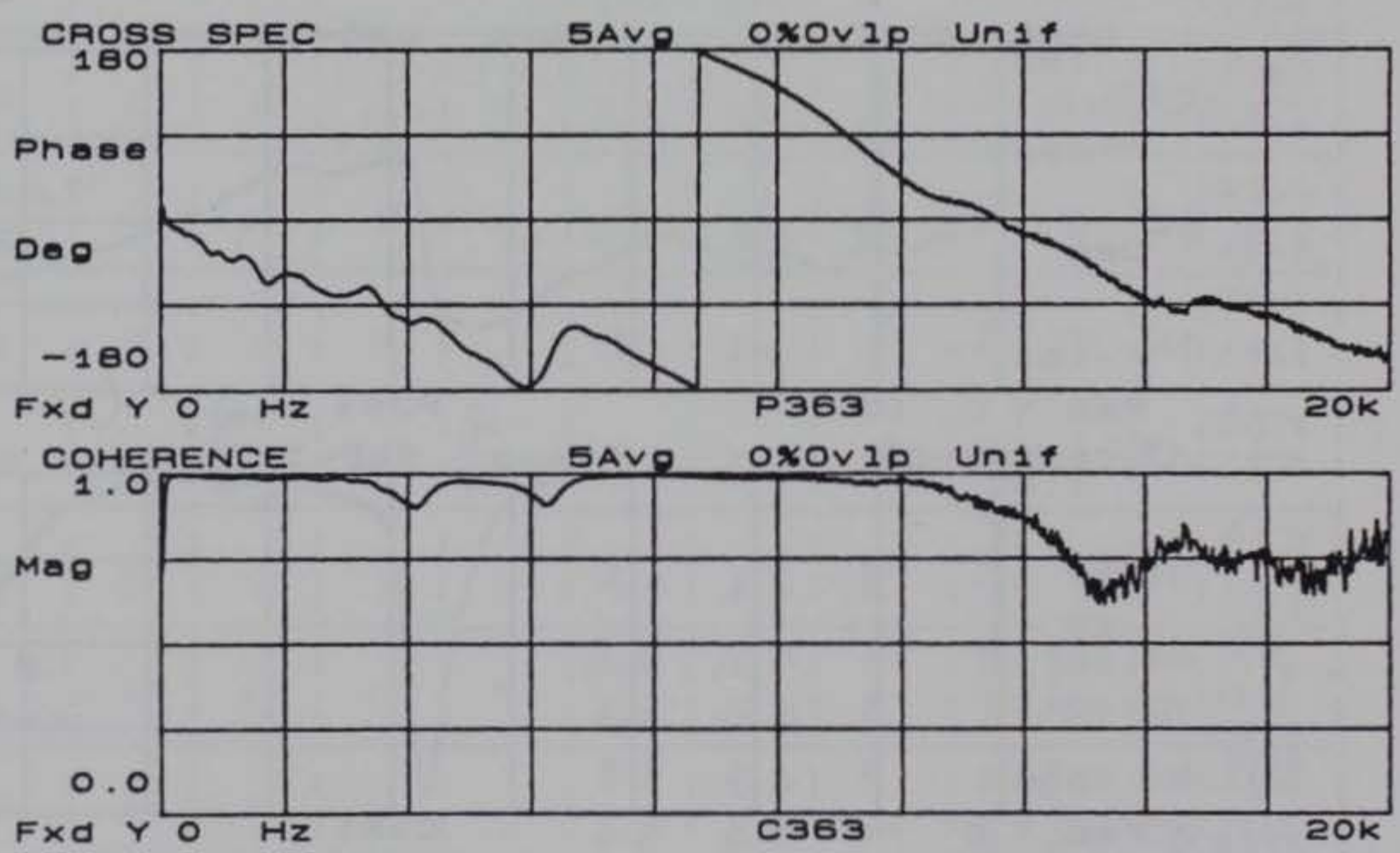

Figure D3. Phase and coherence records for 0.25 ft. receiver spacing at Site 10

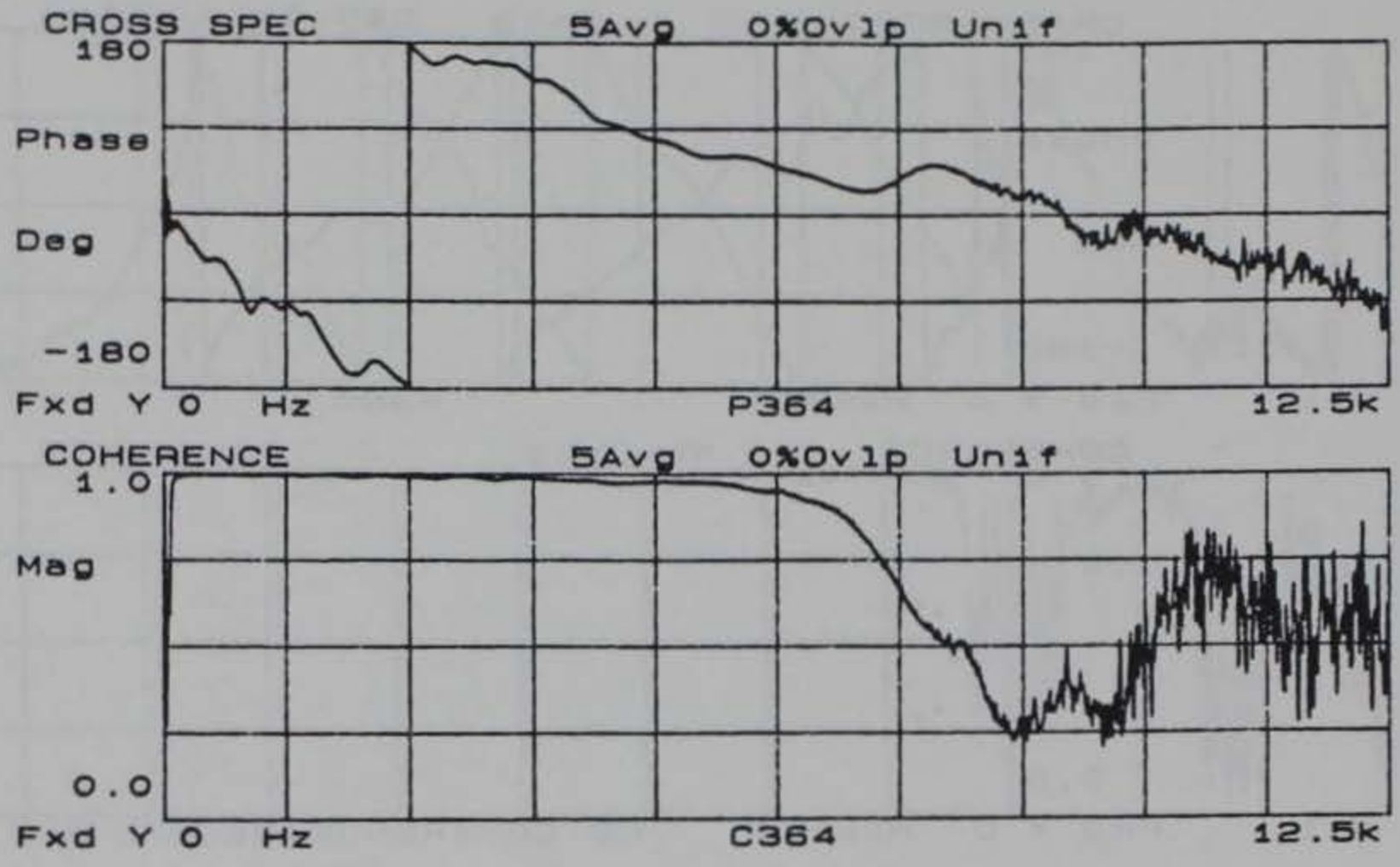

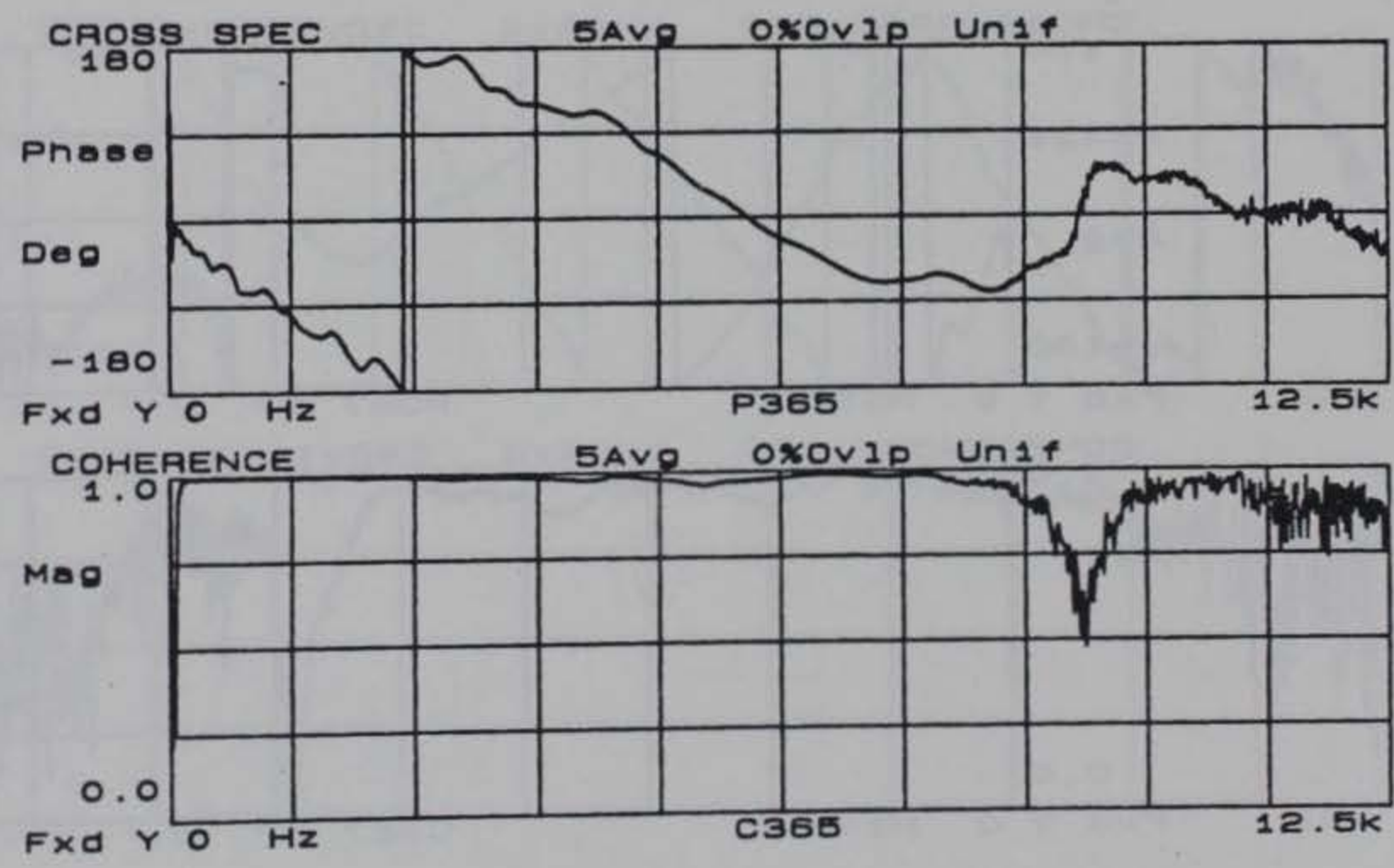

Figure D4. Phase and coherence records for 1.0 ft. receiver spacing at Site 10

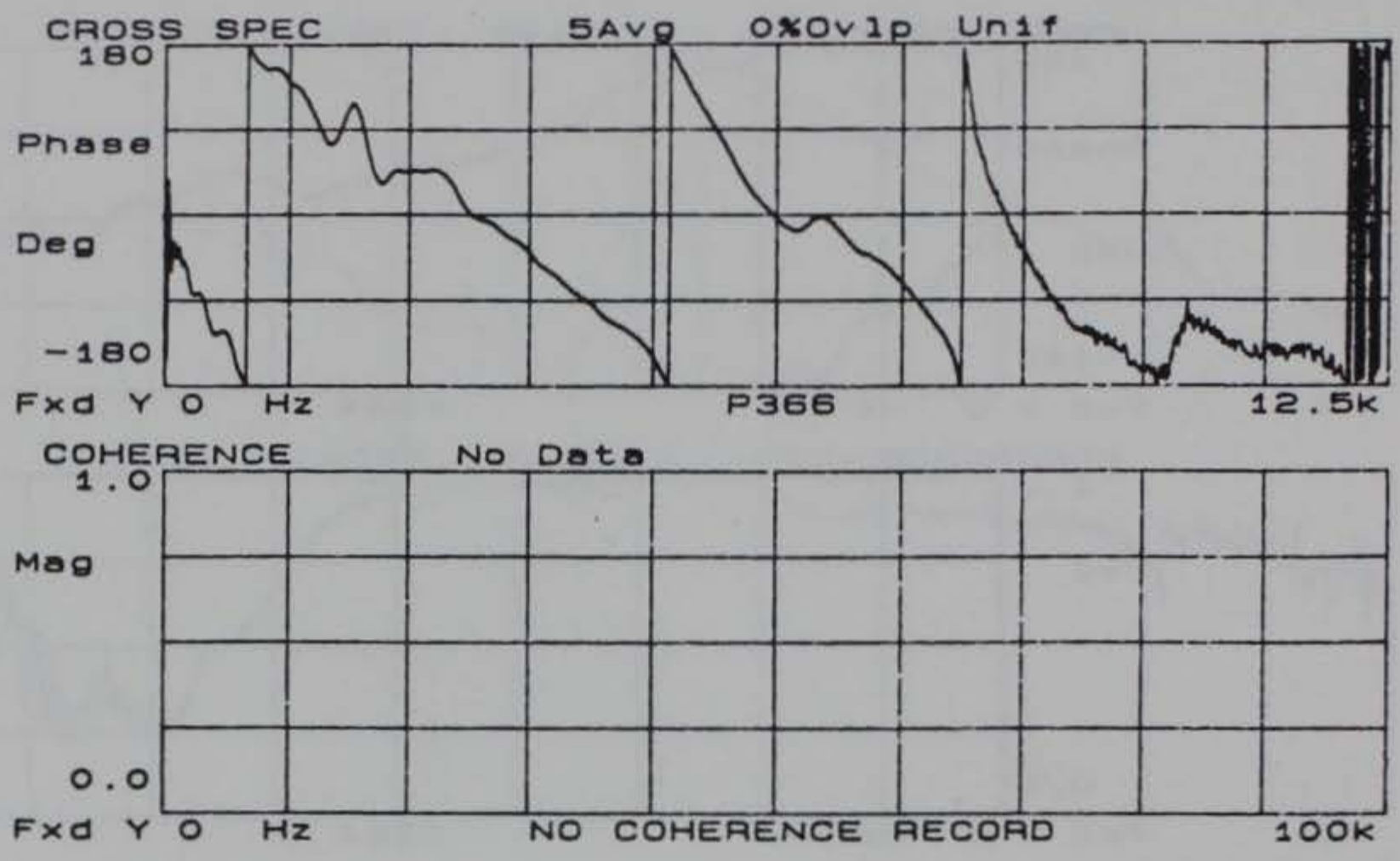

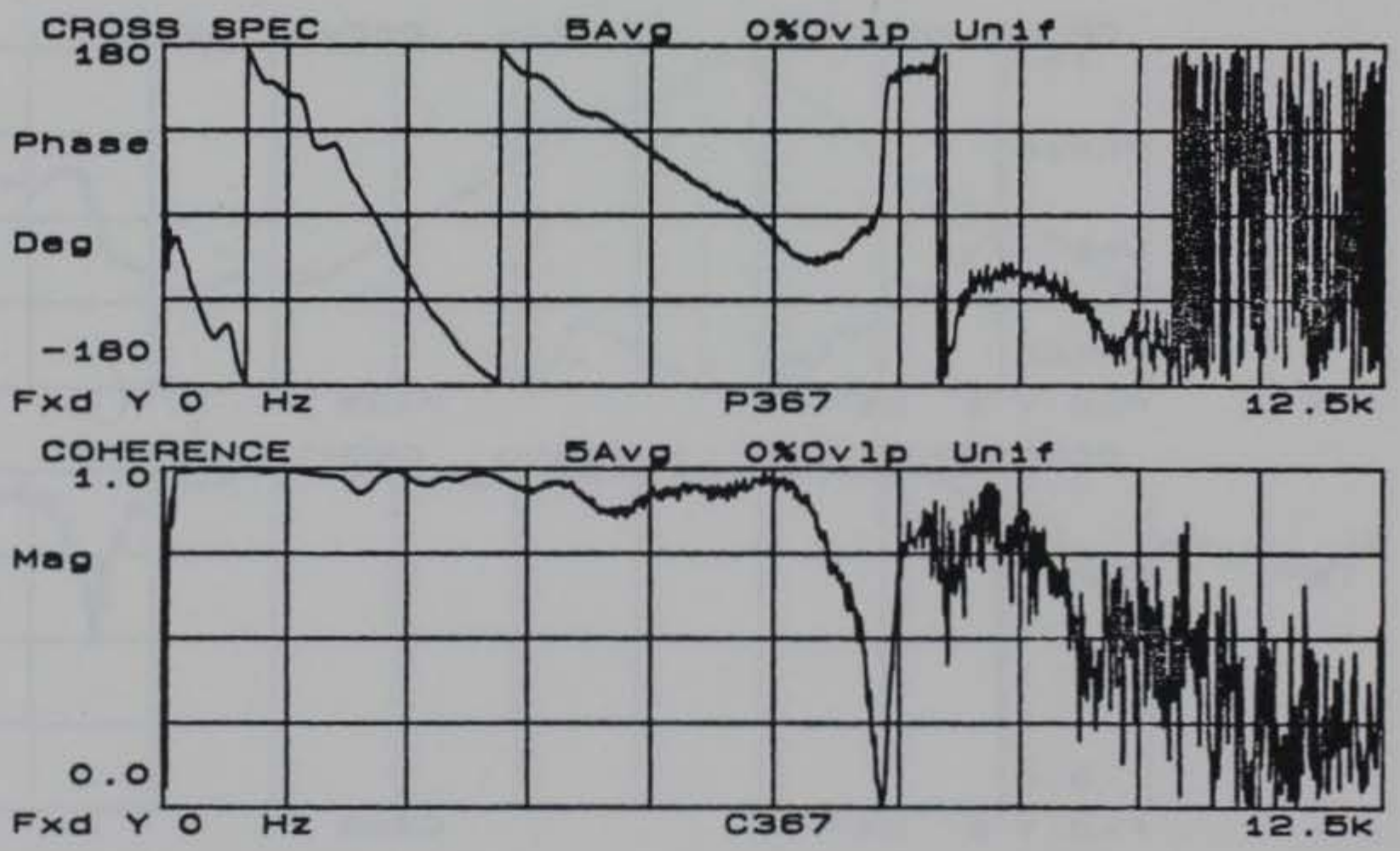

Figure D5. Phase and coherence records for 2.0 ft. receiver spacing at Site 10

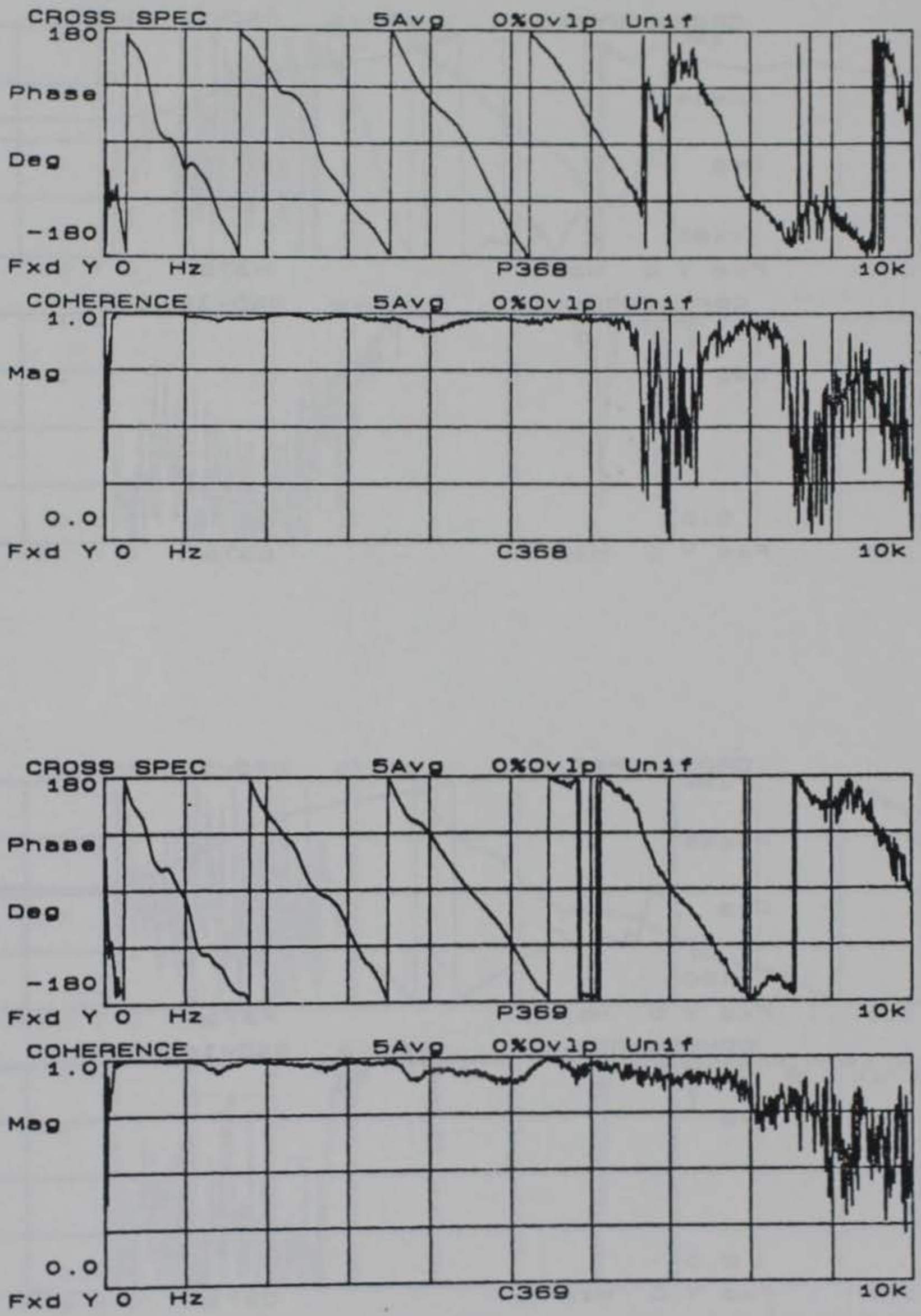

Figure D6. Phase and coherence records for 4.0 ft. receiver spacing at Site 10 (accelerometer data)

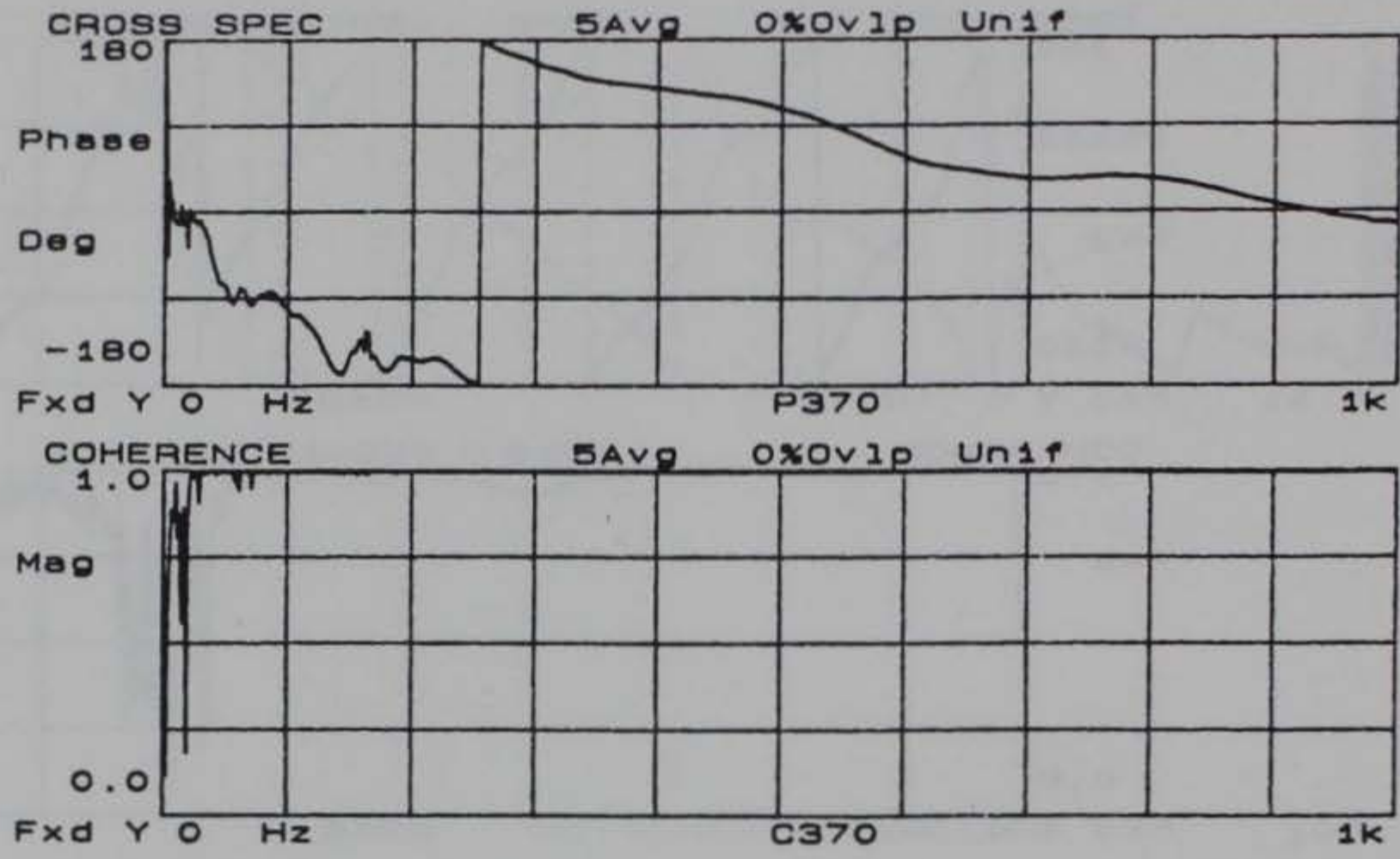

Figure D7. Phase and coherence records for 4.0 ft. receiver spacing at Site 10 (velocity transducer data)

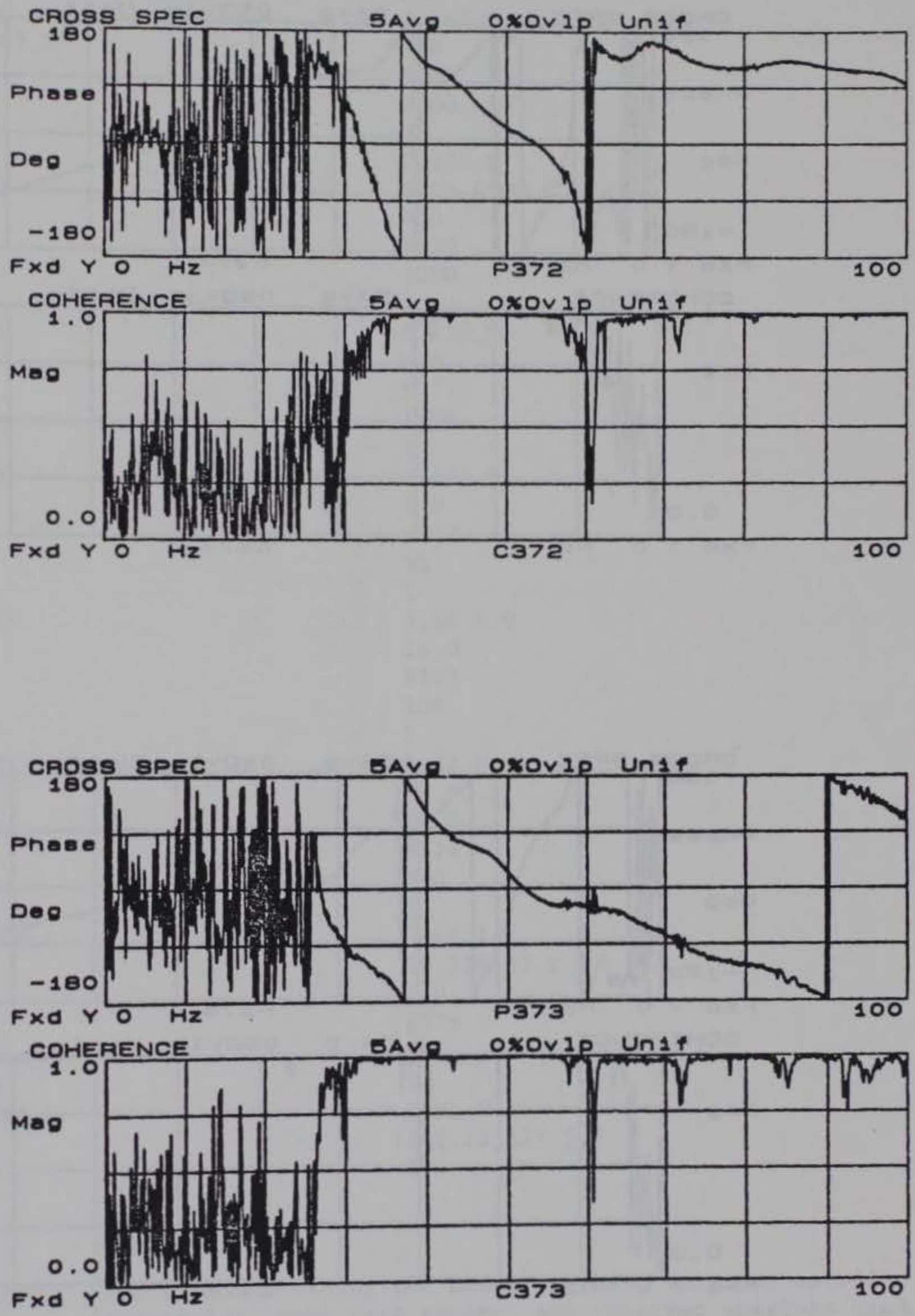

Figure D8. Phase and coherence records for 16.0 ft. receiver spacing at Site 10

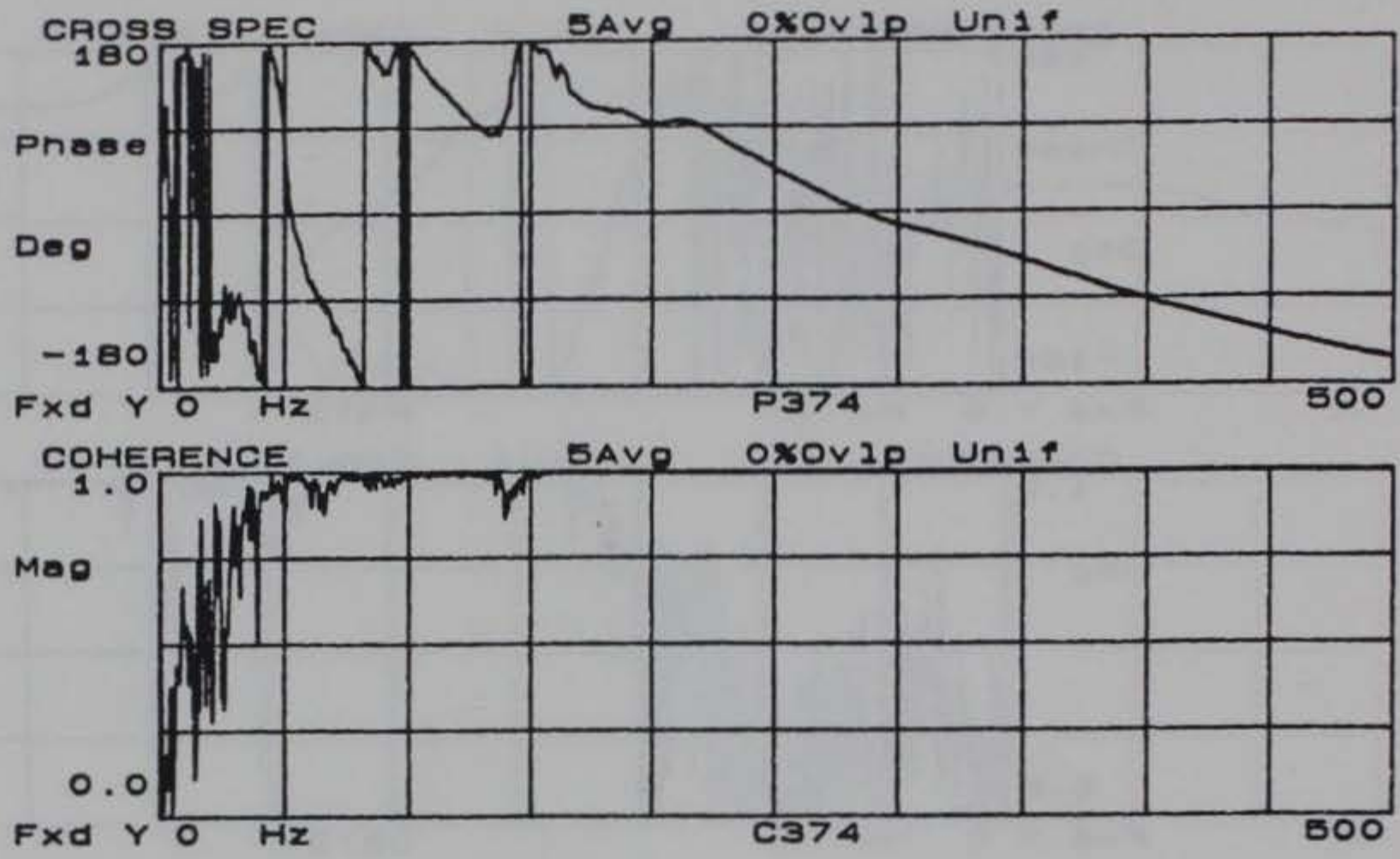

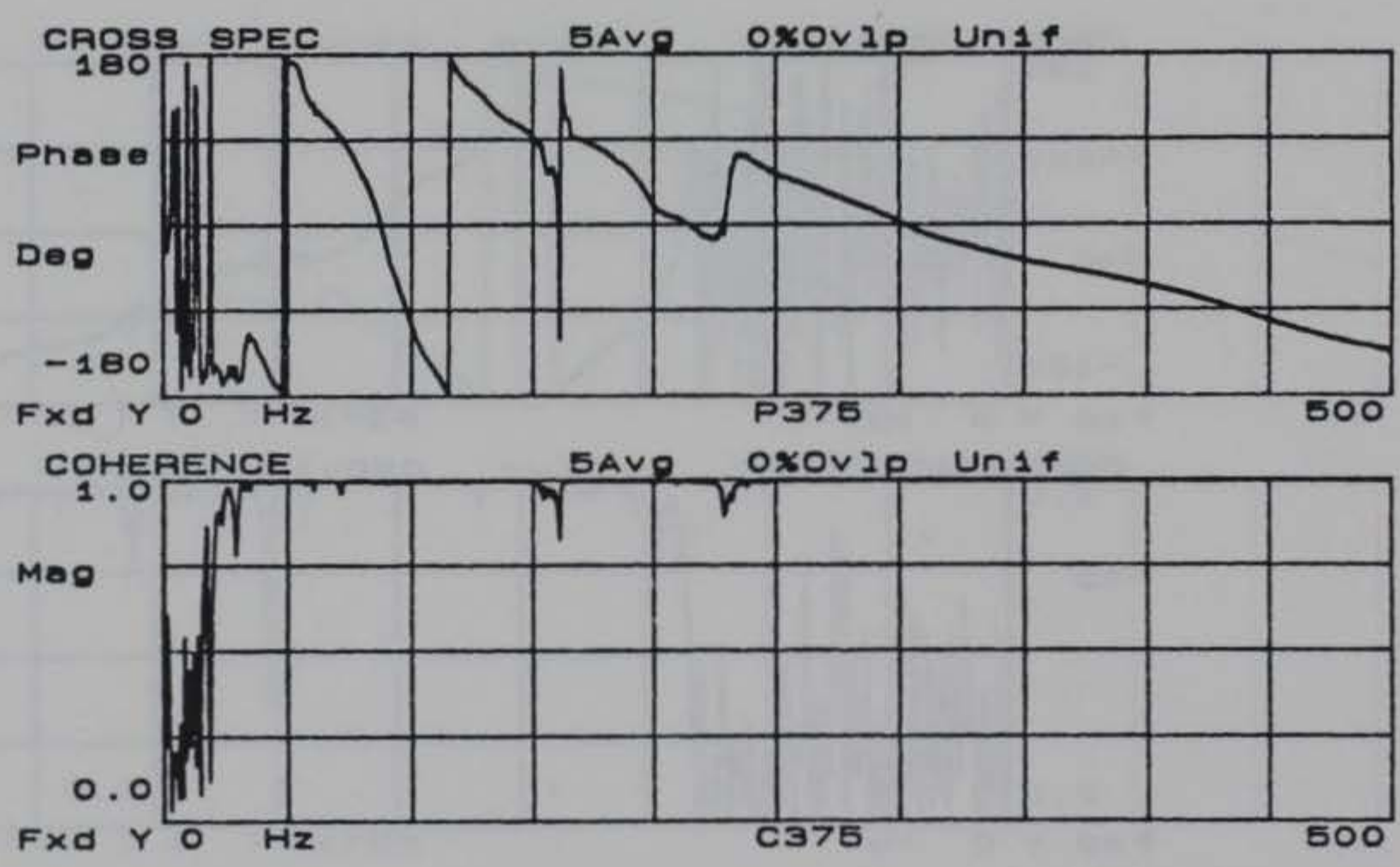

Figure D9. Phase and coherence records for 8.0 ft. receiver spacing at Site 10

```
P360
8984
2
0,4328,0
6094,7187,1
0.5
P361
11500
1
0,7406,1
0.5
P362
15800
1
0,7000,0
0.25
P363
20000
1
0,7000,0
0.25
P364
12500
1
0,2250,0
1.0
P365
7000
1
0,2125,0
1.0
P366
6344
2
0,703,0
1656,3109,1
2.0
P367
6344
2
0,734,0
1406,1766,1
2.0
P368
6400
1
0,187,0
4.0
P369
7700
2
0,225,0
5300,6300,4
4.0
P370
1000
1
0,230,0
4.0
P371
1000
1
0,205,0
4.0
P372
55
1
0,36.5,0
16.0
P373
100
2
0,32,0
88,92,2
16.0
P374
500
2
0,60,1
90,216.25,2
8.0
P375
500
2
0,35,0
148.75,237.5,2
8.0
```

Figure D10. Data file containing the names of phase records, cutoff frequencies, poor data ranges, and receiver spacings used by the computer program SASW in constructing the dispersion curve for Site 10

APPENDIX E: SASW TEST DATA AND RESULTS FOR SITE 11

FIELD DATA SHEET FOR SASW TESTS (HP 3562A/9153A)

TEST SITE: Site 11, Sheppard AFB START TIME: 1033 TEMP, F:

TEST DATE: 8-16-87 ENDING TIME: 1127 TEMP, F:

Source Type	Near Receiver Type	Near Receiver ID	Far Receiver Type	Far Receiver ID	Receiver Spacing (ft)	SNR Distance (ft)	Profile (F=Fwd., R=Rev.)	No. of Ave.	Freq. BW (Hz)	Site File No.	Data File Names
4oz Ball Peen	Accel.	PCB 308B02 SN 19926	Accel.	PCB 308B02 SN 19927	0.5	0.5	F*	5	50 kHz	A20	P420 C420
〃	〃	〃	〃	〃	0.5	0.5	R	5	50	A21	P421 C421
〃	〃	〃	〃	〃	1.0	1.0	R	5	25	A22	P422 C422
〃	〃	〃	〃	〃	1.0	1.0	F	5	25	A23	P423 C423
8 oz Ball Peen	〃	〃	〃	〃	2.0	2.0	F	5	25	A24	P424 C424
〃	〃	〃	〃	〃	2.0	2.0	R	5	25	A25	P425 C425
〃	〃	〃	〃	〃	4.0	4.0	F	5	10	A26	P426 C426
〃	〃	〃	〃	〃	4.0	4.0	R	5	10	A27	P427 C427
8 lb Sledge	〃	〃	〃	〃	8.0	8.0	R	5	2.5	A28	P428 C428
〃	〃	〃	〃	〃	8.0	8.0	F	5	2.5	A29	P429 C429
〃	Vel.	Geo-Source PC-3	Vel.	Geo-Source PC-3	8.0	8.0	F	5	1	A30	P430 C430
〃	〃	〃	〃	〃	8.0	8.0	R	5	1	A31	P431 C431
〃	〃	〃	〃	〃	16.0	16.0	R	5	HZ 500	A32	P432 C432
〃	〃	〃	〃	〃	16.0	16.0	F	5	500	A33	P433 C433
〃	〃	〃	〃	〃	16.0	16.0	F	5	250	A34	P434 C434

* Source on North Side

Figure E1. SASW field data form for Site 11

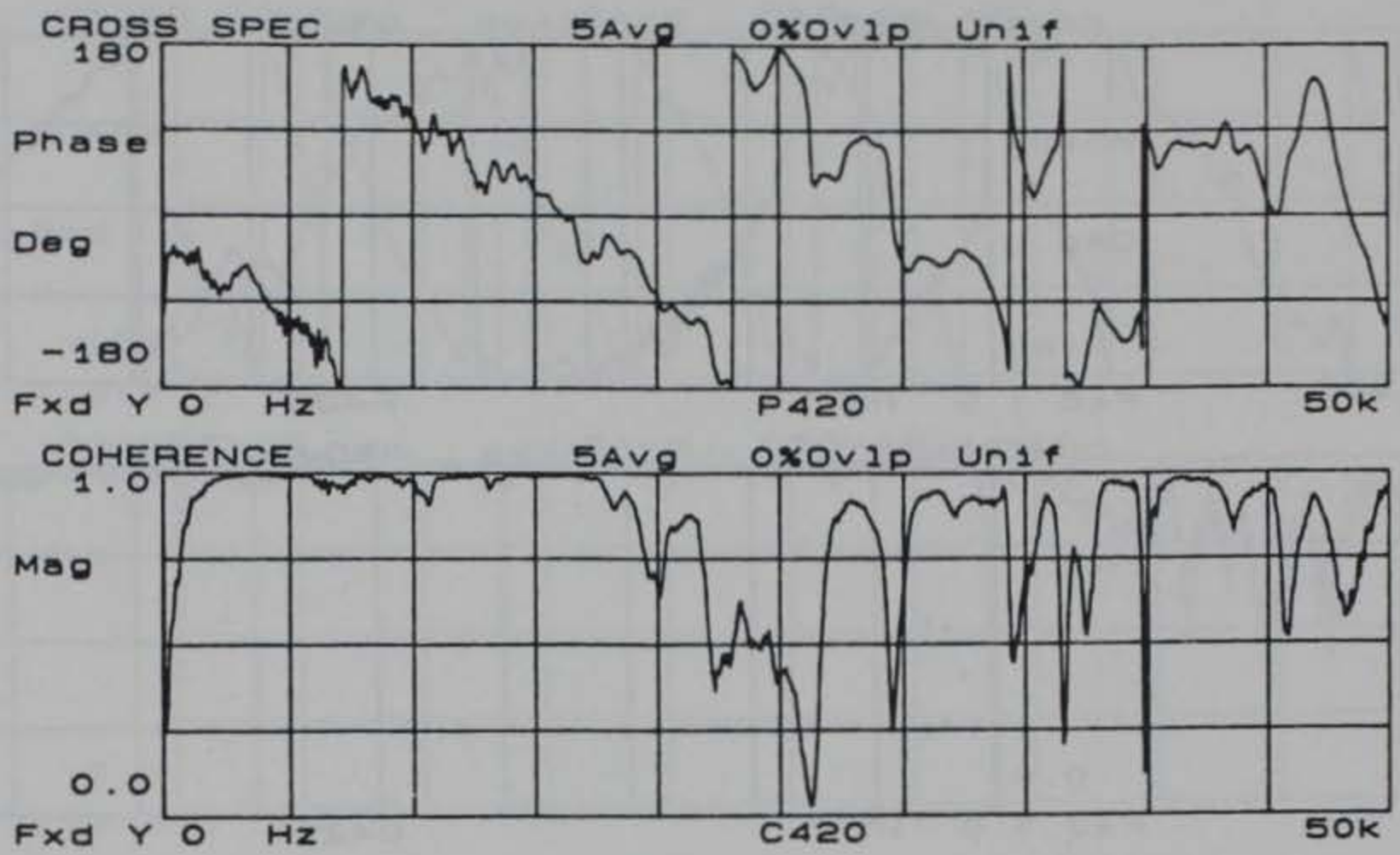

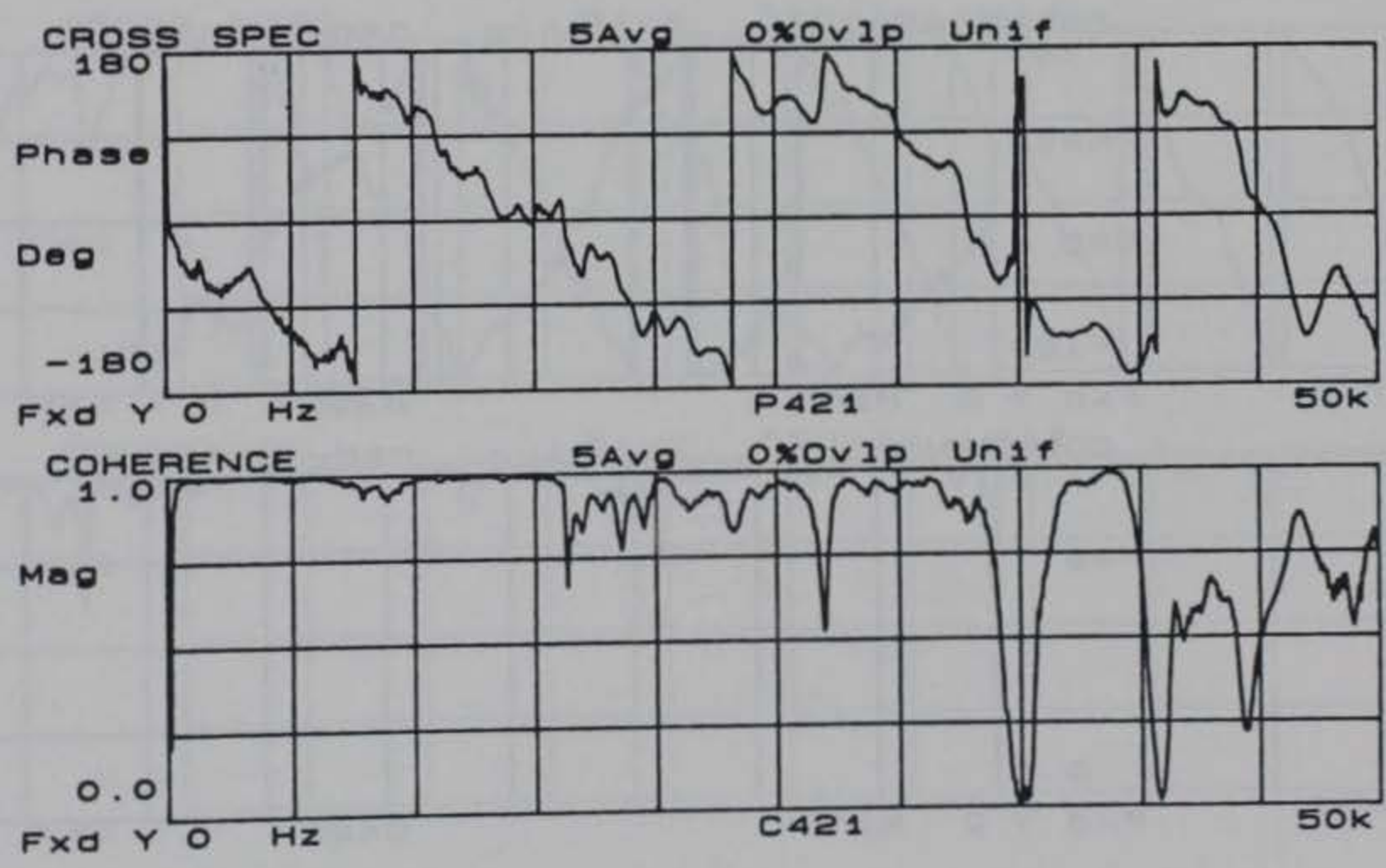

Figure E2. Phase and coherence records for 0.5 ft. receiver spacing at Site 11

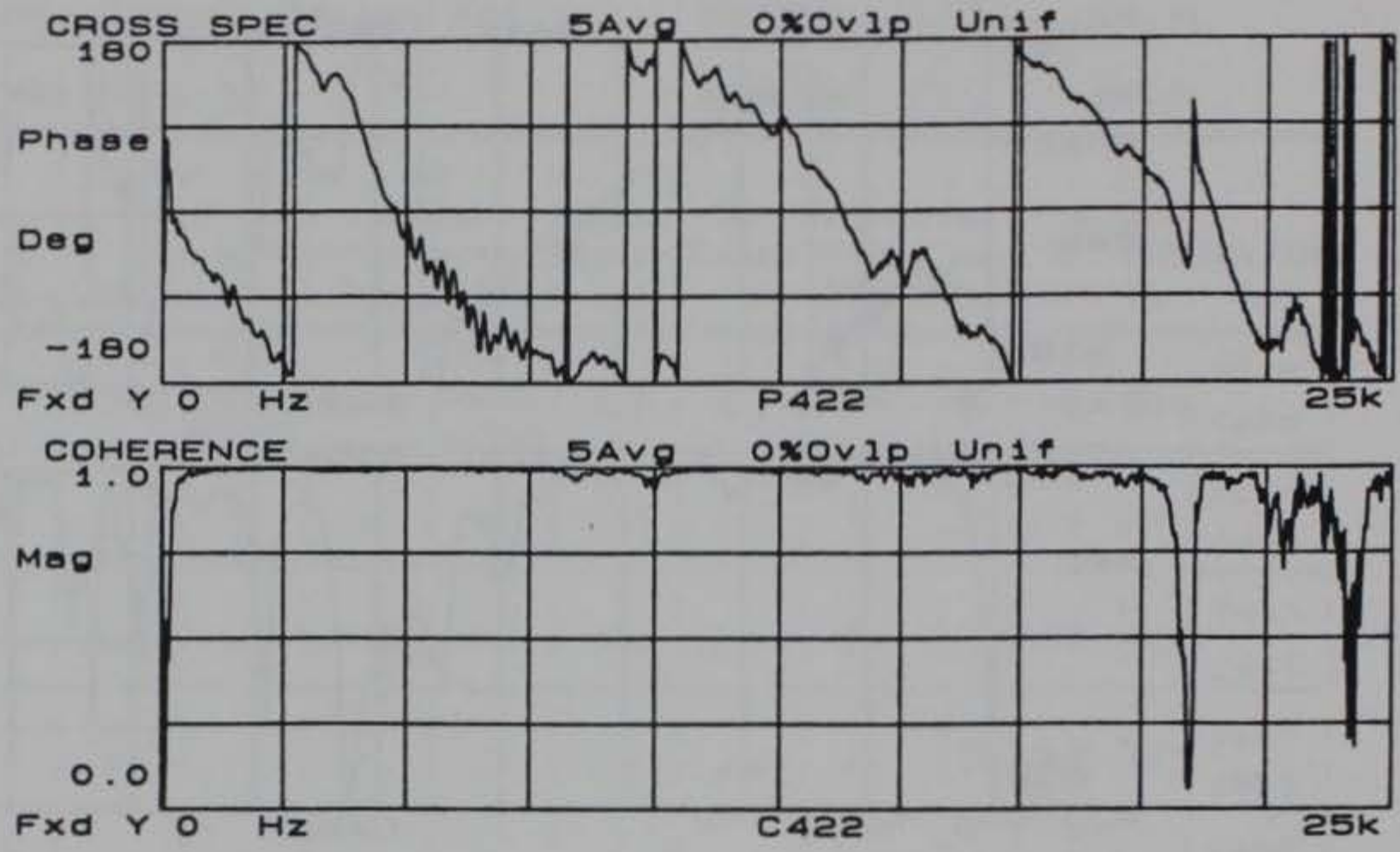

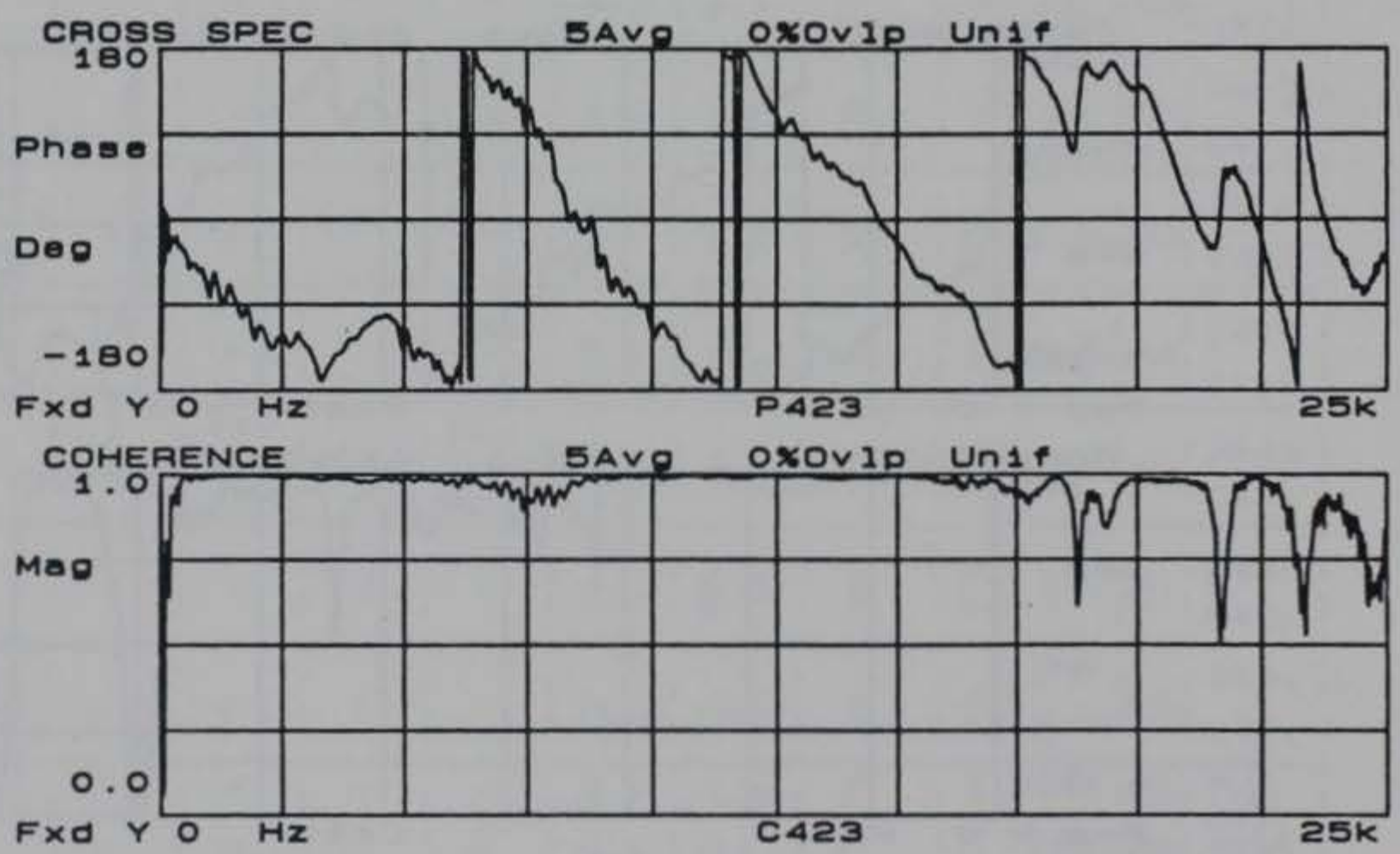

Figure E3. Phase and coherence records for 1.0 ft. receiver spacing at Site 11

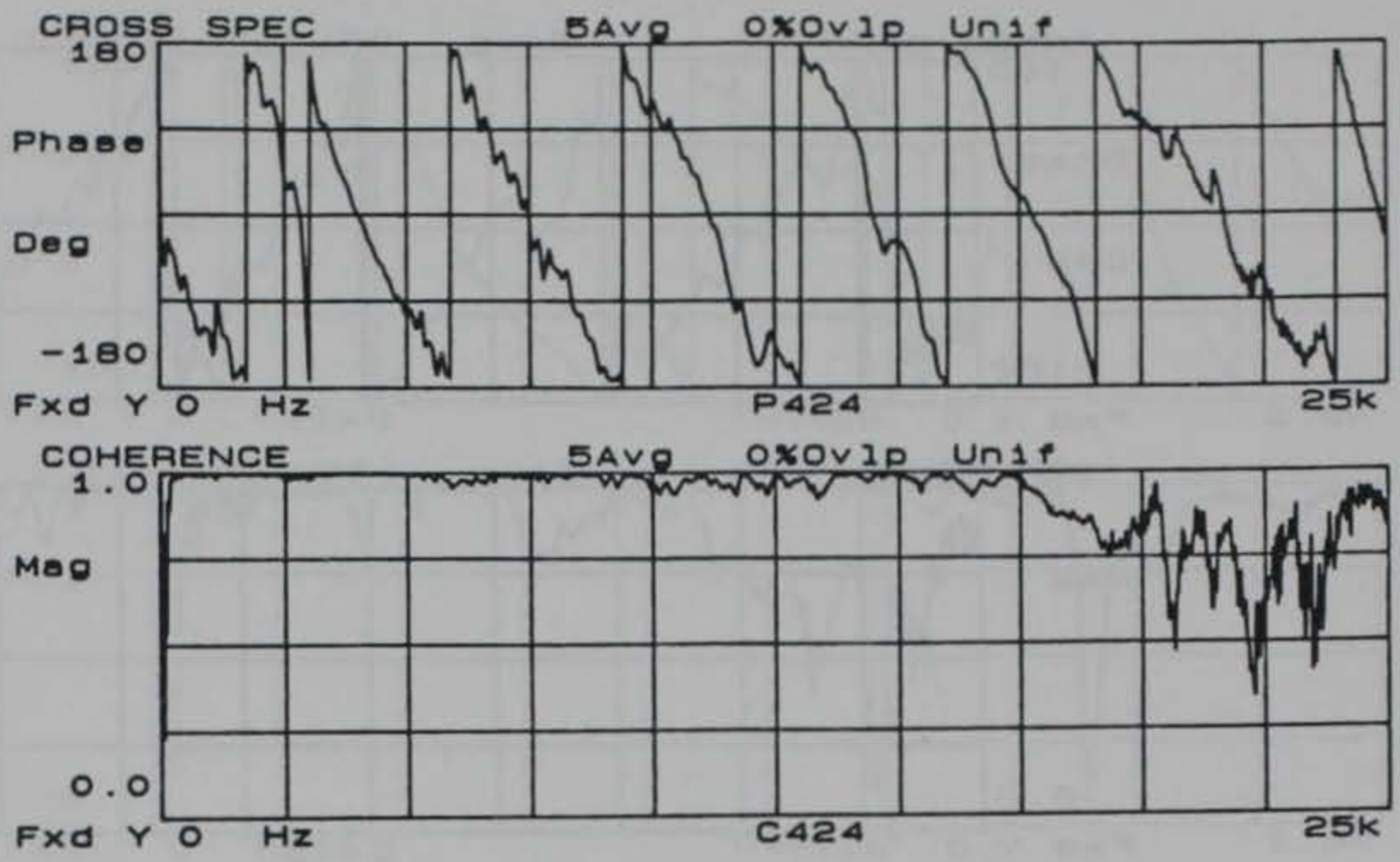

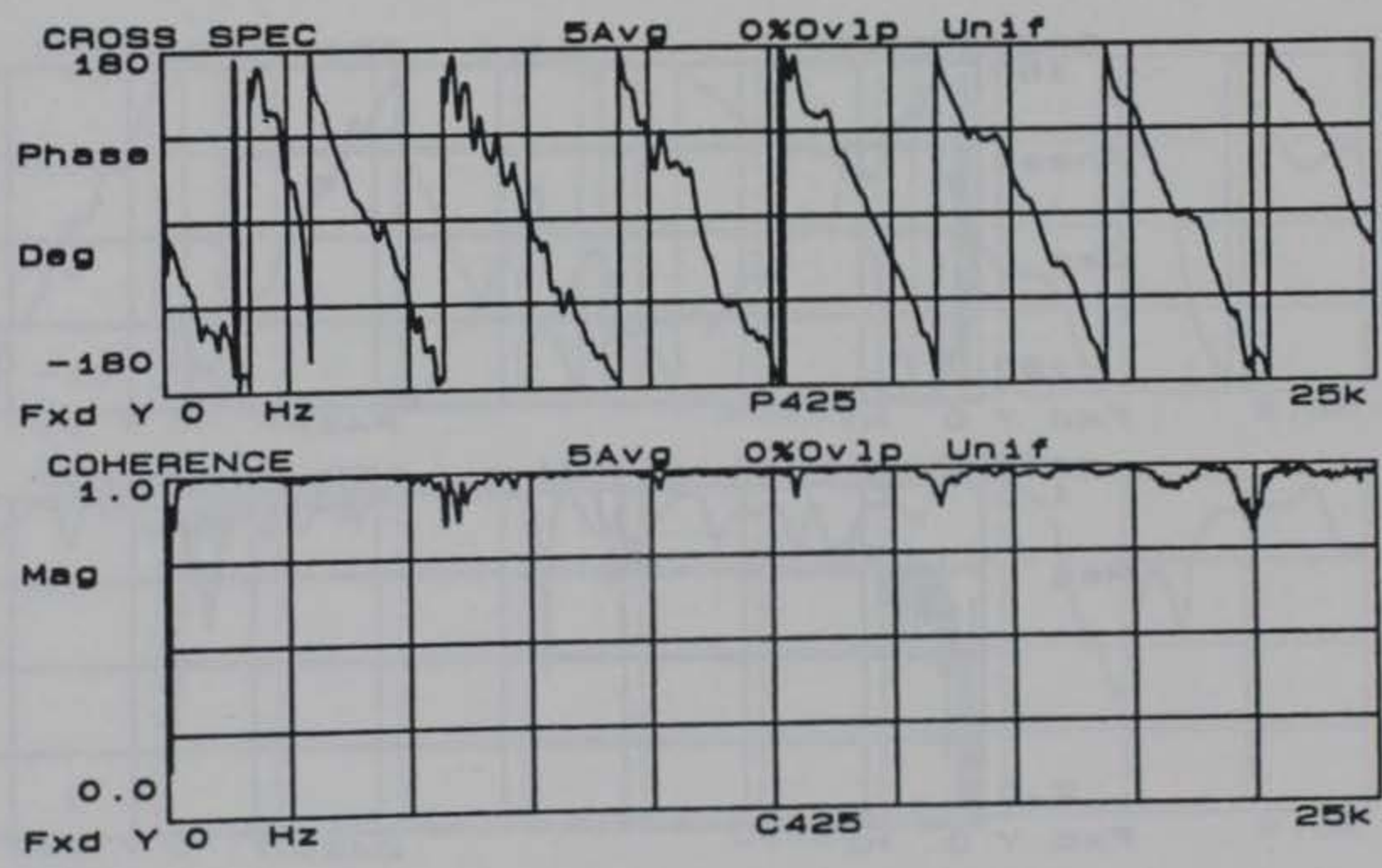

Figure E4. Phase and coherence records for 2.0 ft. receiver spacing at Site 11

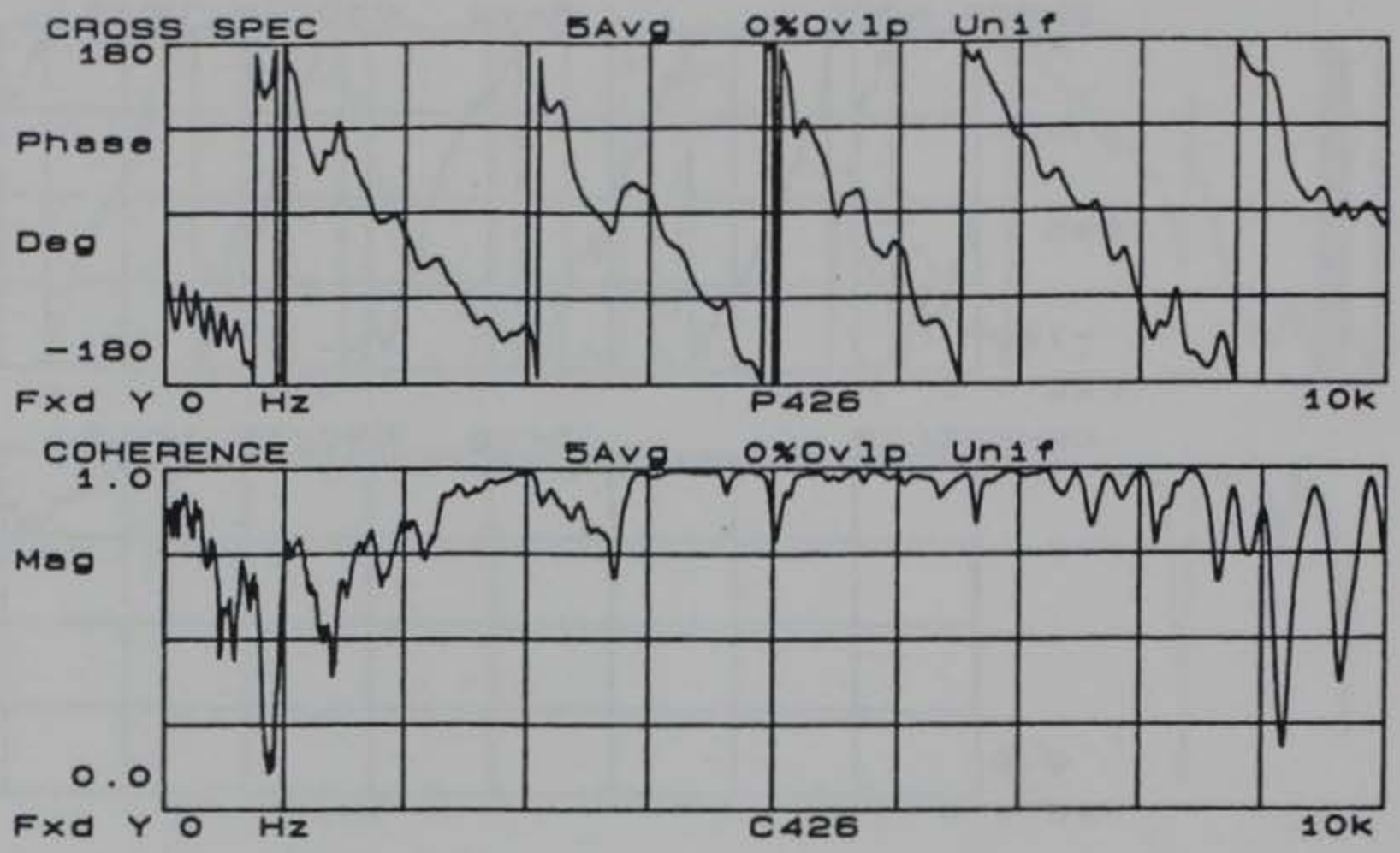

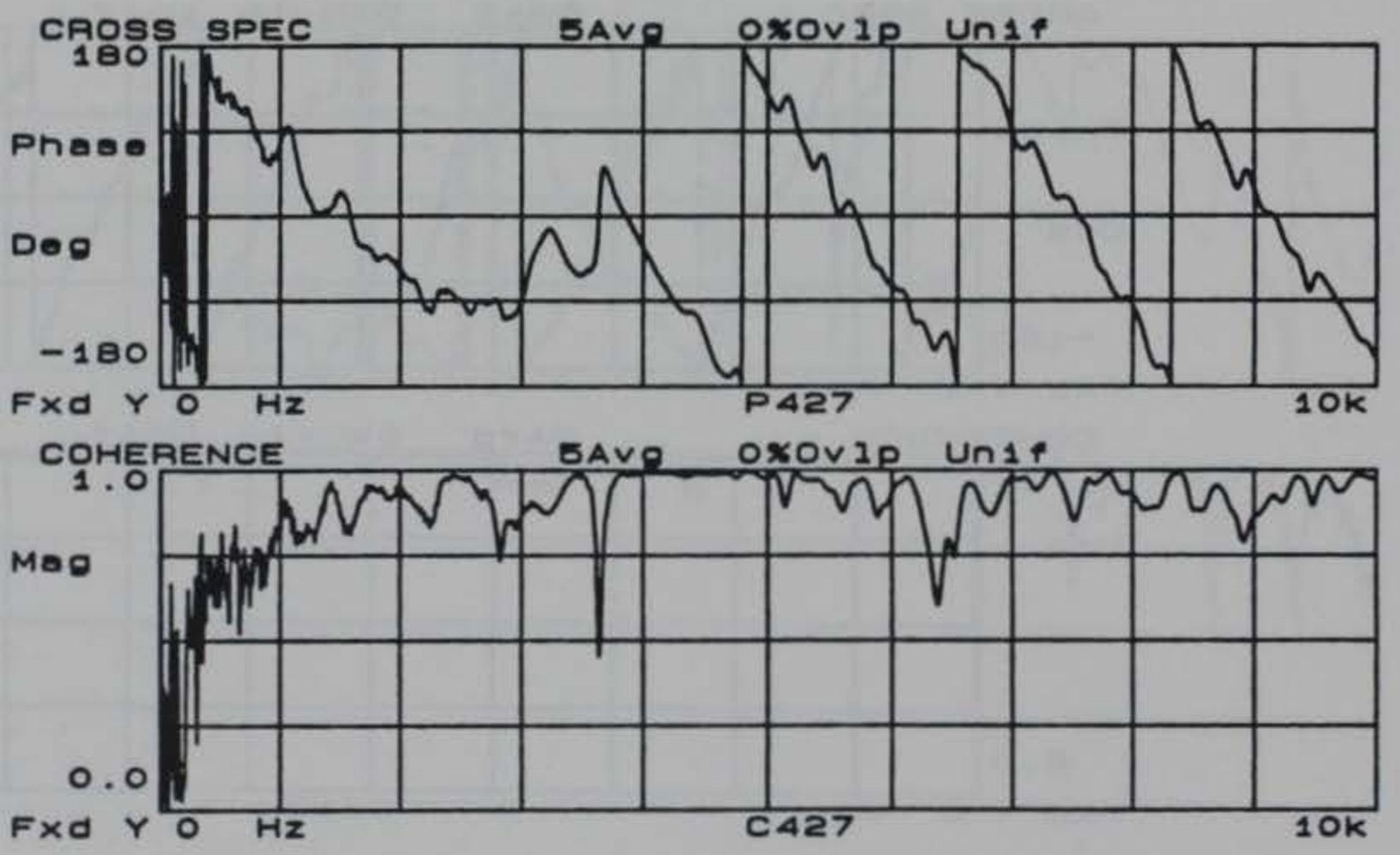

Figure E5. Phase and coherence records for 4.0 ft. receiver spacing at Site 11

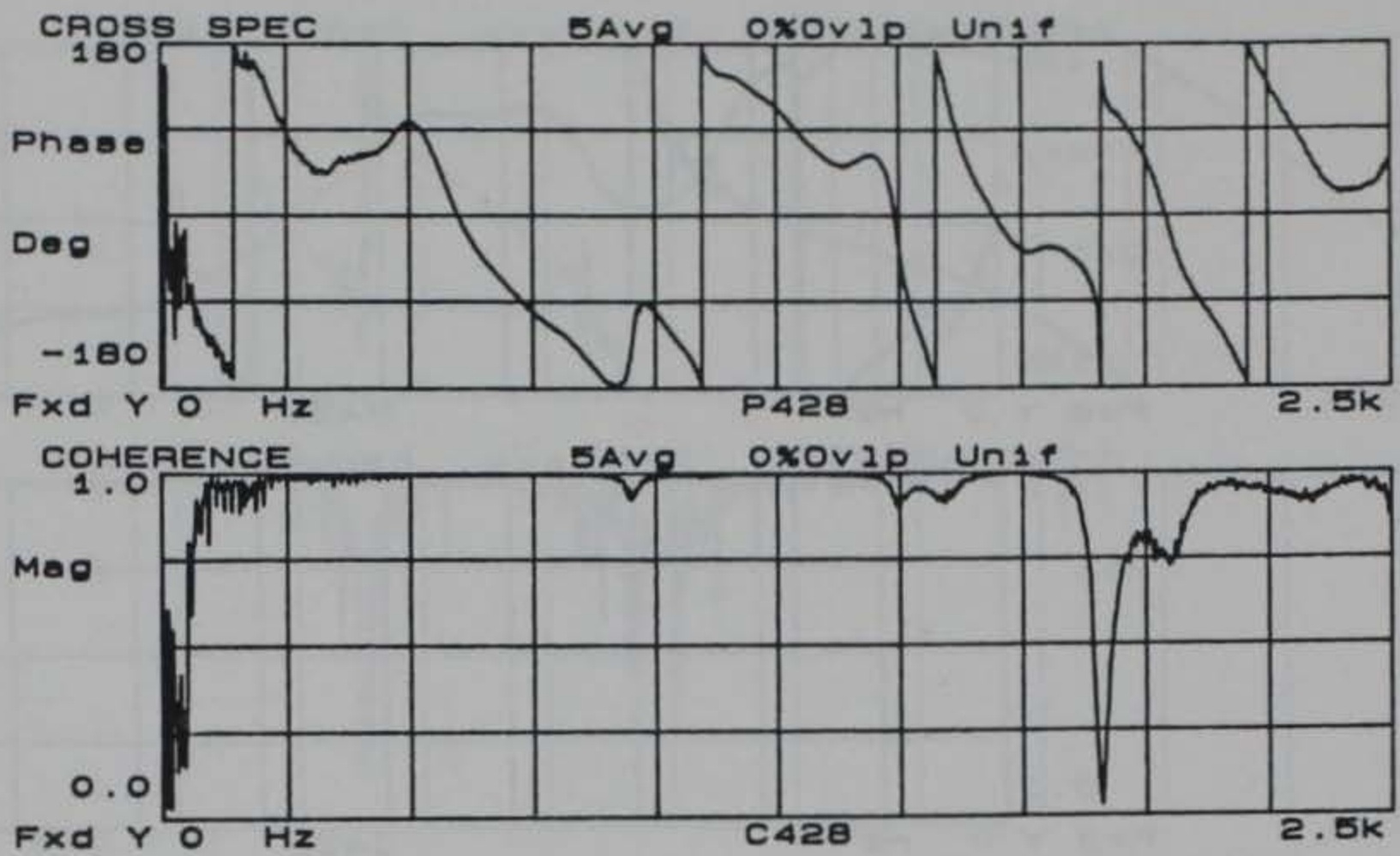

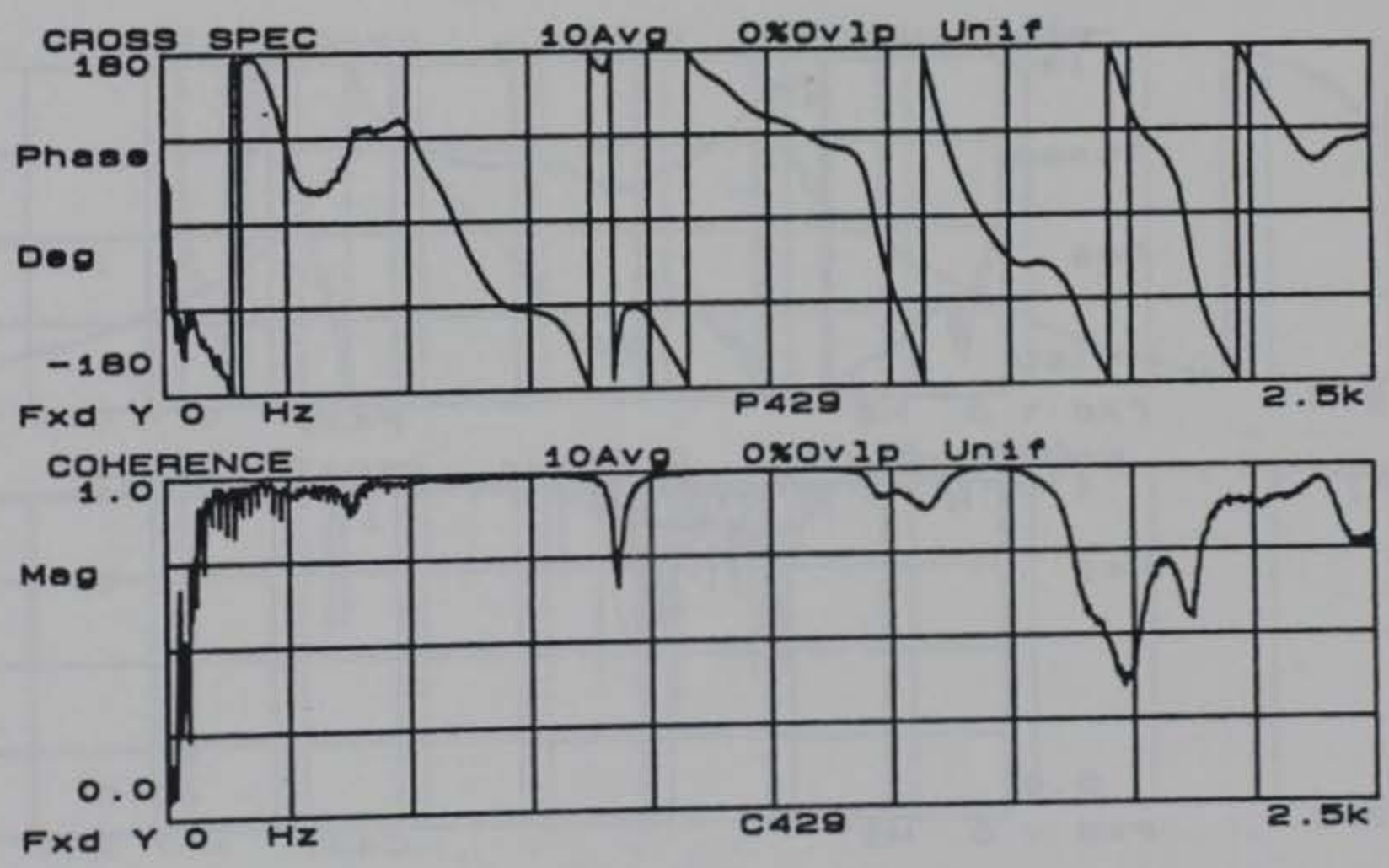

Figure E6. Phase and coherence records for 8.0 ft. receiver spacing at Site 11 (accelerometer data)

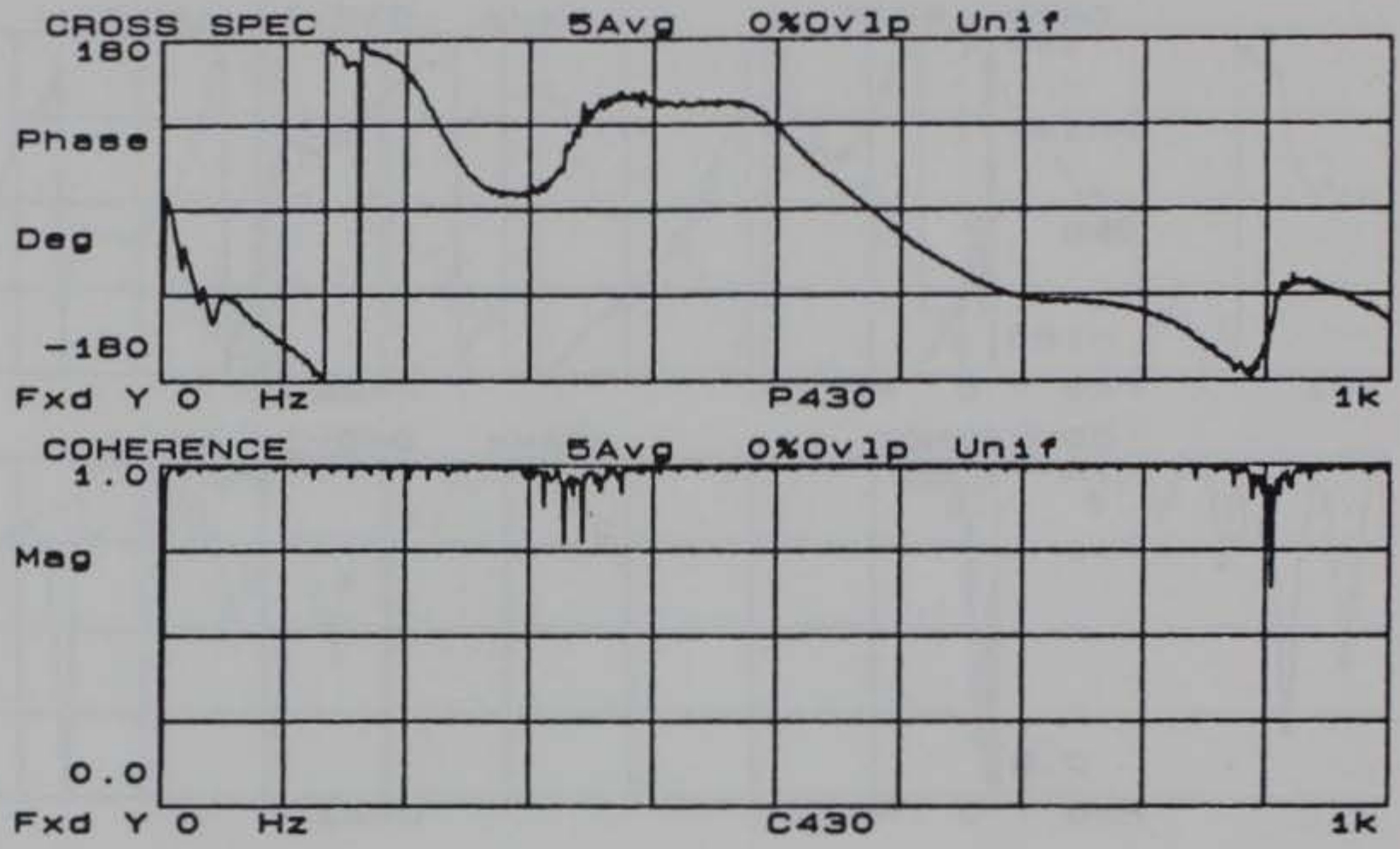

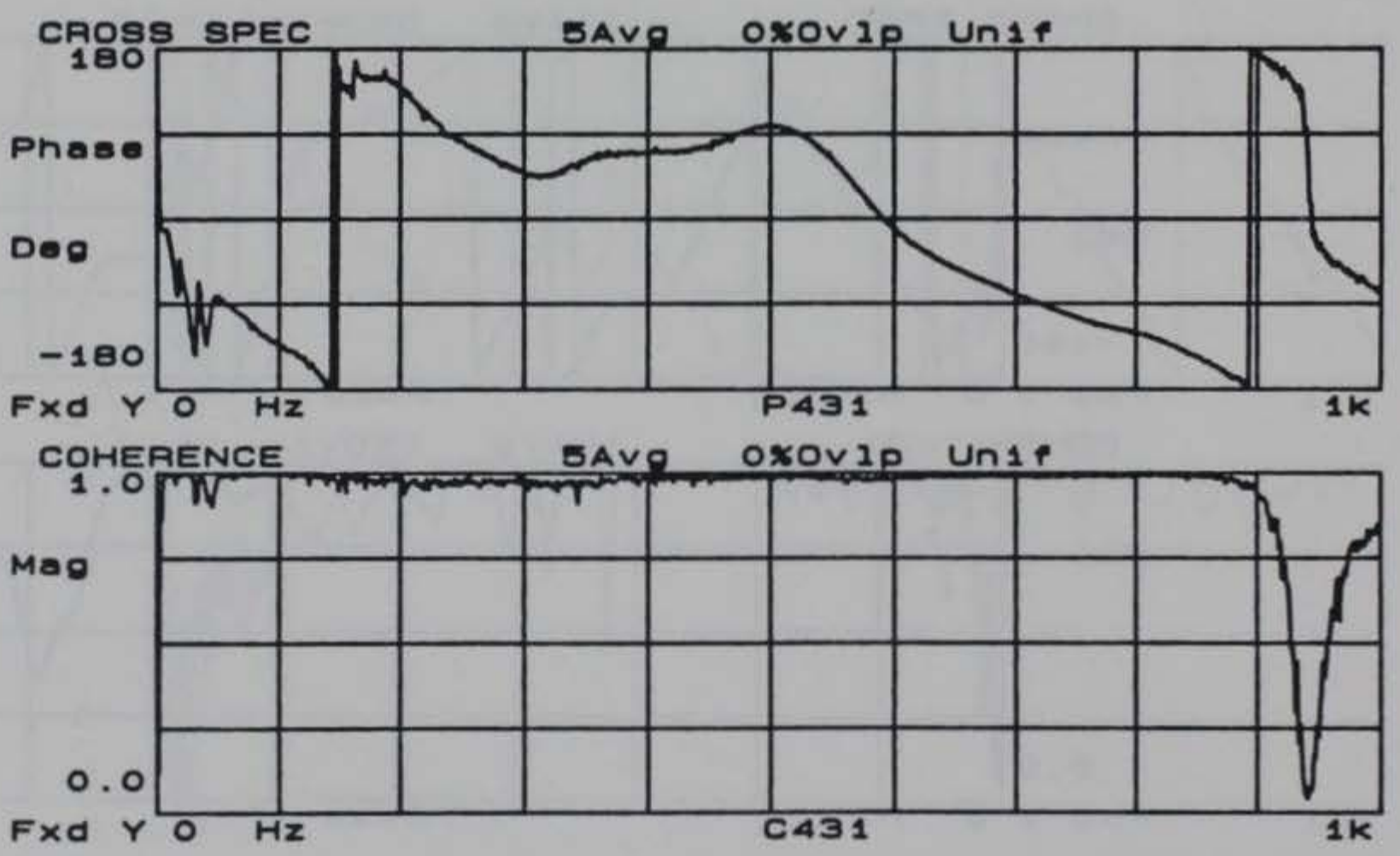

Figure E7. Phase and coherence records for 8.0 ft. receiver spacing at Site 11 (velocity transducer data)

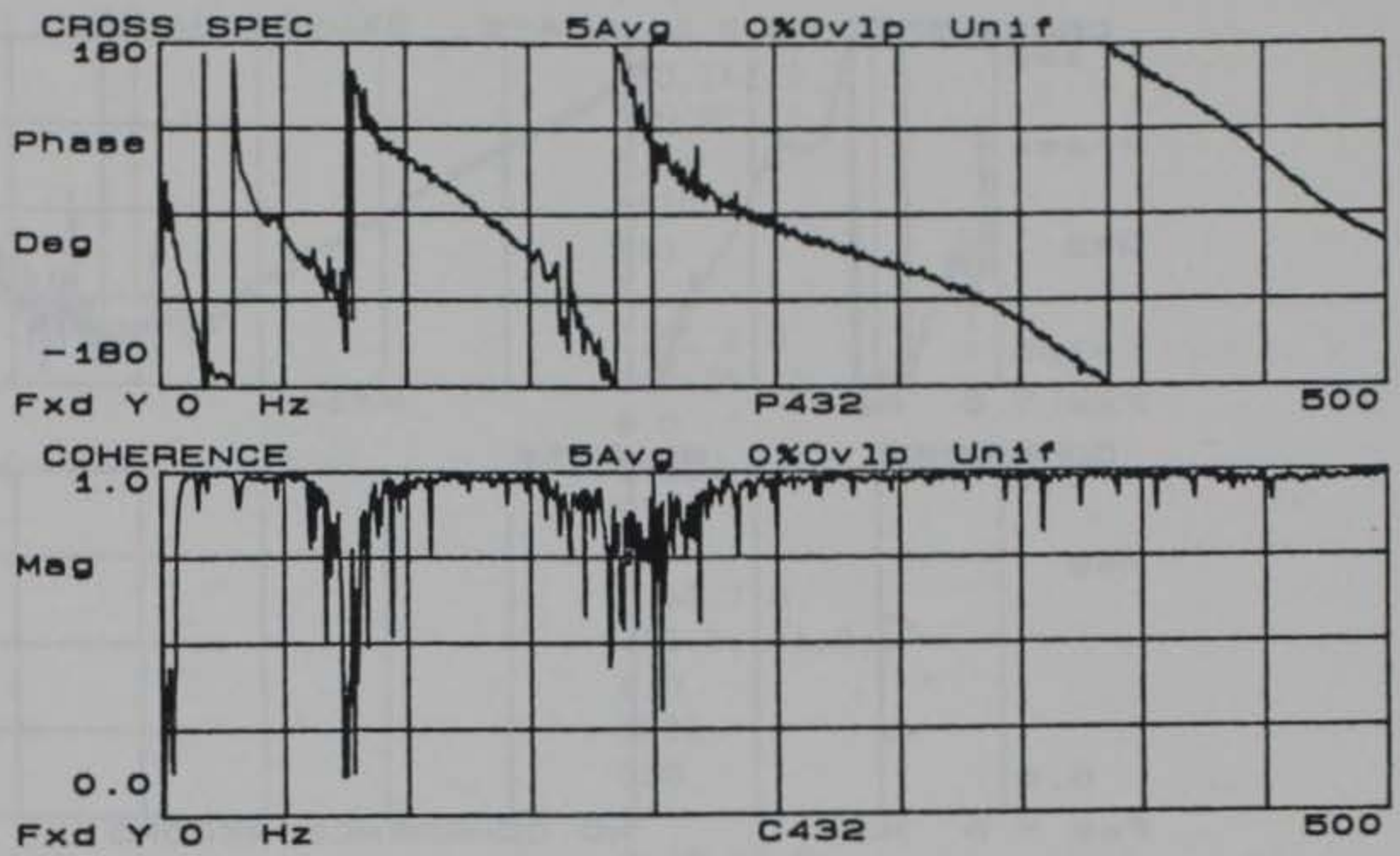

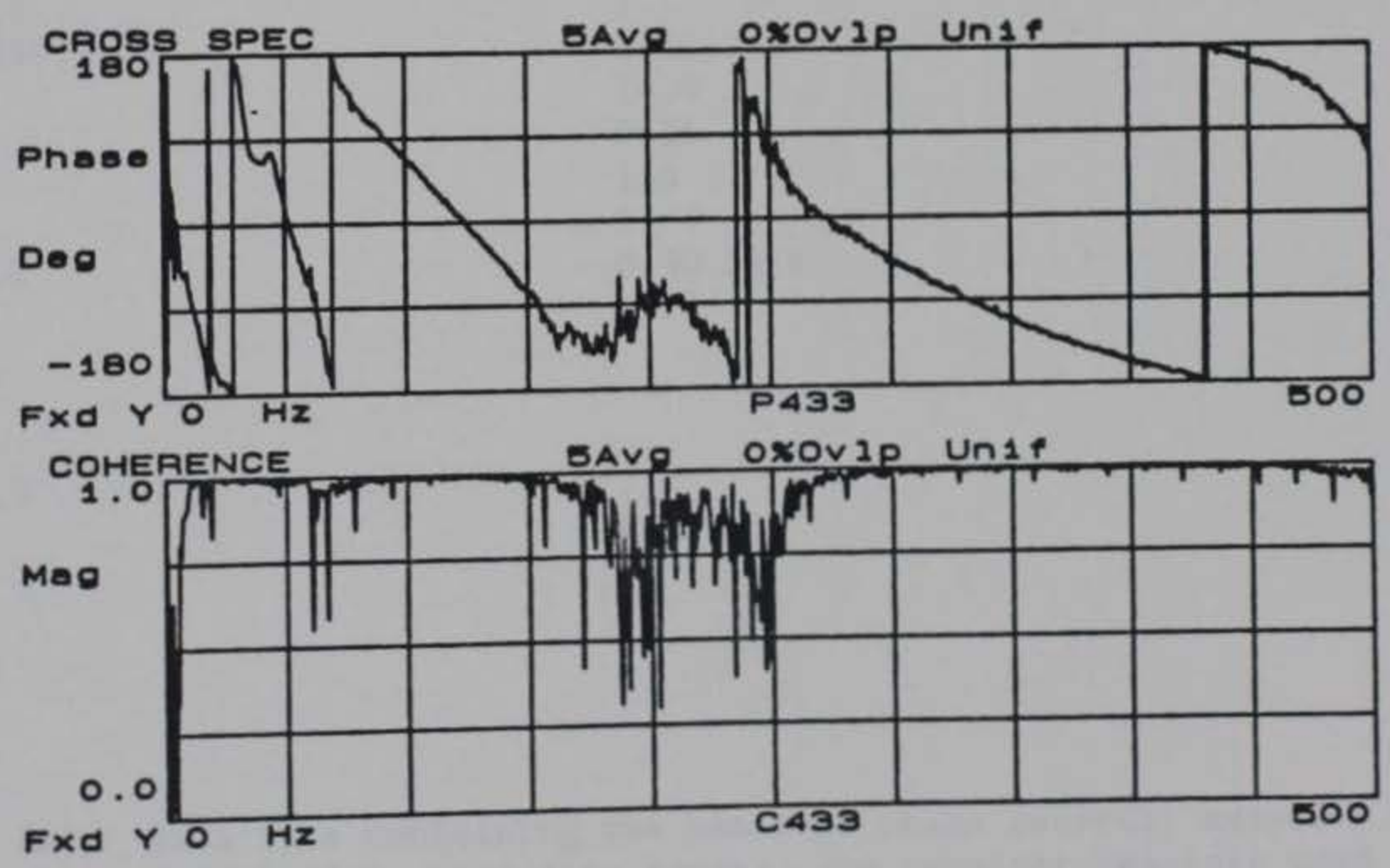

Figure E8. Phase and coherence records for 16.0 ft. receiver spacing at Site 11 (500 Hz bandwidth)

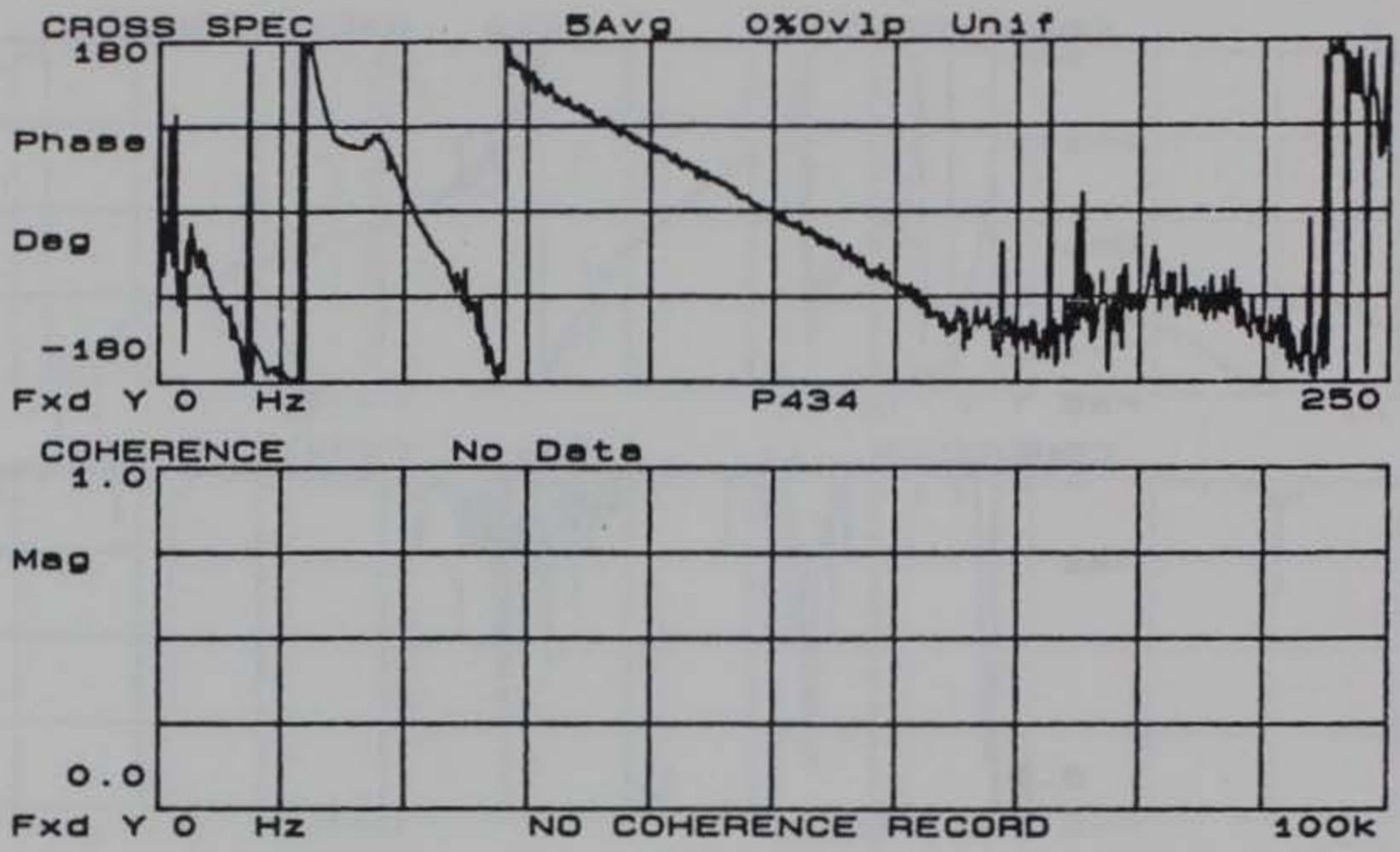

Figure E9. Phase and coherence records for 16.0 ft. receiver spacing at Site 11 (250 Hz bandwidth)

```
P420
17000
1
0,8000,1
0.5
P421
24000
1
0,8100,1
0.5
P422
8000
1
0,1500,0
1.0
P424
11000
1
0,3212,1
2.0
P425
11000
1
0,3187,1
2.0
P426
7500
2
0,1537,1
4913,5250,3
4.0
P427
9000
1
0,3687,2
4.0
P428
1378
1
0,53.1,0
8.0
P429
1428
3
0,46.9,0
150,162.5,1
700,925,1
8.0
P430
883
2
0,51.2,0
160,165,1
8.0
P431
936
2
0,48.7,0
142.5,151.2,1
8.0
P432
500
3
0,19.37,0
58.75,86.25,2
150,225,3
16.0
P433
150
1
0,20,0
16.0
P434
150
1
0,30.31,1
16.0
```

Figure E10. Data file containing the names of phase records, cutoff frequencies, poor data ranges, and receiver spacings used by the computer program SASW in constructing the dispersion curve for Site 11

APPENDIX F: SASW TEST DATA AND RESULTS FOR SITE 12

FIELD DATA SHEET FOR SASW TESTS (HP 3562A/9153A)

TEST SITE: Site 12, Sheppard AFB START TIME: 1248 TEMP, F: 103°**

TEST DATE: 8-18-87 ENDING TIME: 1317 TEMP, F: 106°

Source Type	Near Receiver Type	Near Receiver ID	Far Receiver Type	Far Receiver ID	Receiver Spacing (ft)	SNR Distance (ft)	Profile (F=Fwd., R=Rev.)	No. of Ave.	Freq. BW (Hz)	Site File No.	Data File Names
4 oz Ball Peen	Accel.	PCB 308B02 SN 19926	Accel.	PCB 308B02 SN 19927	0.5	0.5	F*	5	kHz 20	480	P480 C480
"	"	"	"	"	0.5	0.5	R	5	20	481	P481 C481
"	"	"	"	"	1.0	1.0	R	5	10	482	P482 C482
"	"	"	"	"	1.0	1.0	F	5	10	483	P483 C483
8 oz Ball Peen	"	"	"	"	2.0	2.0	R	5	6.25	484	P484 C484
"	"	"	"	"	2.0	2.0	F	5	6.25	485	P485 C485
40 oz Sledge	Vel.	Geo-Source PC3	Vel.	Geo-Source PC3	4.0	4.0	F	5	Hz 500	486	P486 C486
"	"	"	"	"	4.0	4.0	R	5	500	487	P487 C487
8 lb Sledge	"	"	"	"	8.0	8.0	R	5	500	488	P488 C488
"	"	"	"	"	8.0	8.0	F	5	500	489	P489 C484
"	"	"	"	"	16.0	16.0	F	5	500	490	P490 C490
"	"	"	"	"	16.0	16.0	R	5	500	491	P491 C491

* Source on North Side

** Mean Pavement Temperature obtained by averaging the temperatures measured at the center and 1 in. from the top and bottom of AC.

Figure F1. SASW field data form for Site 12

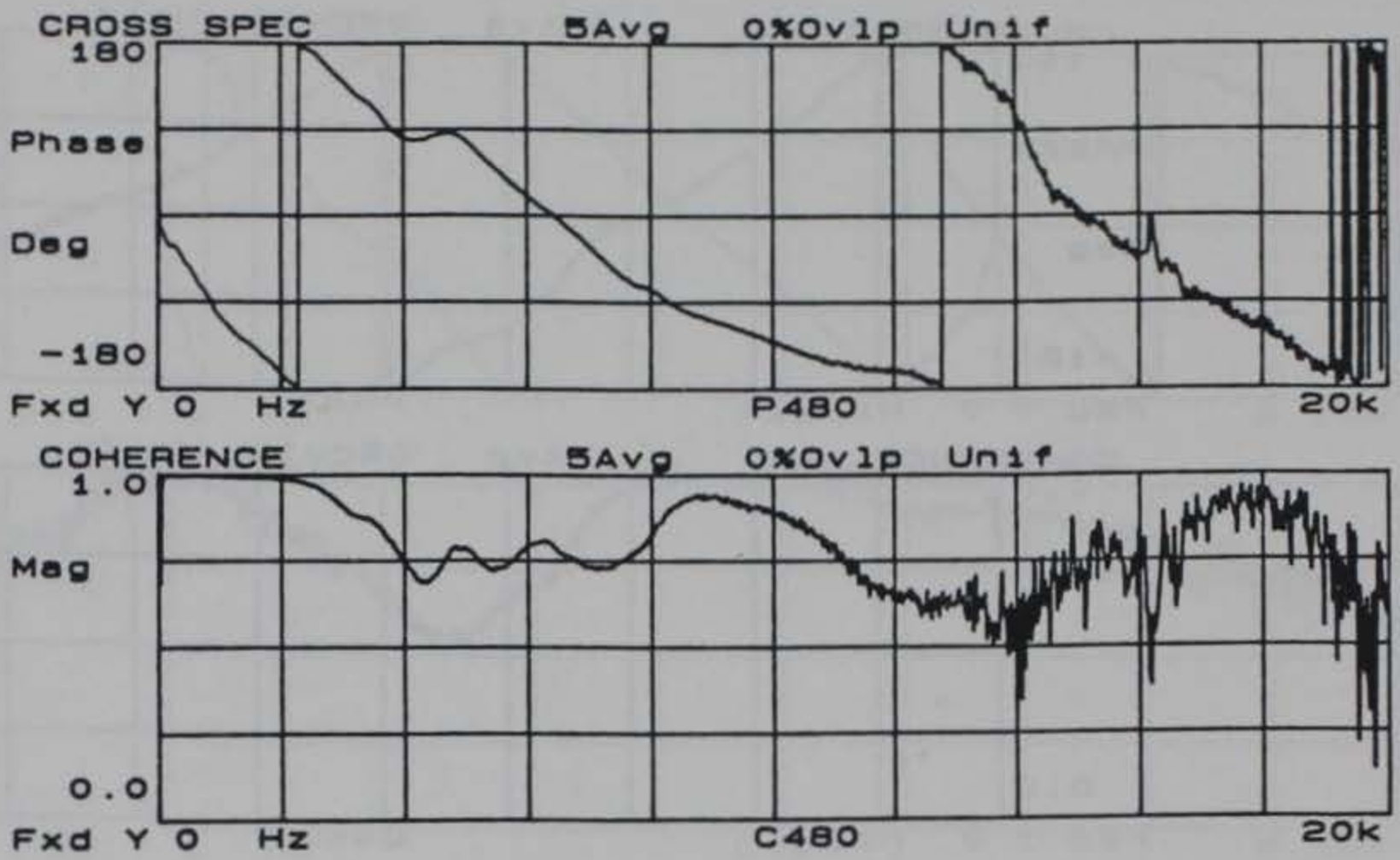

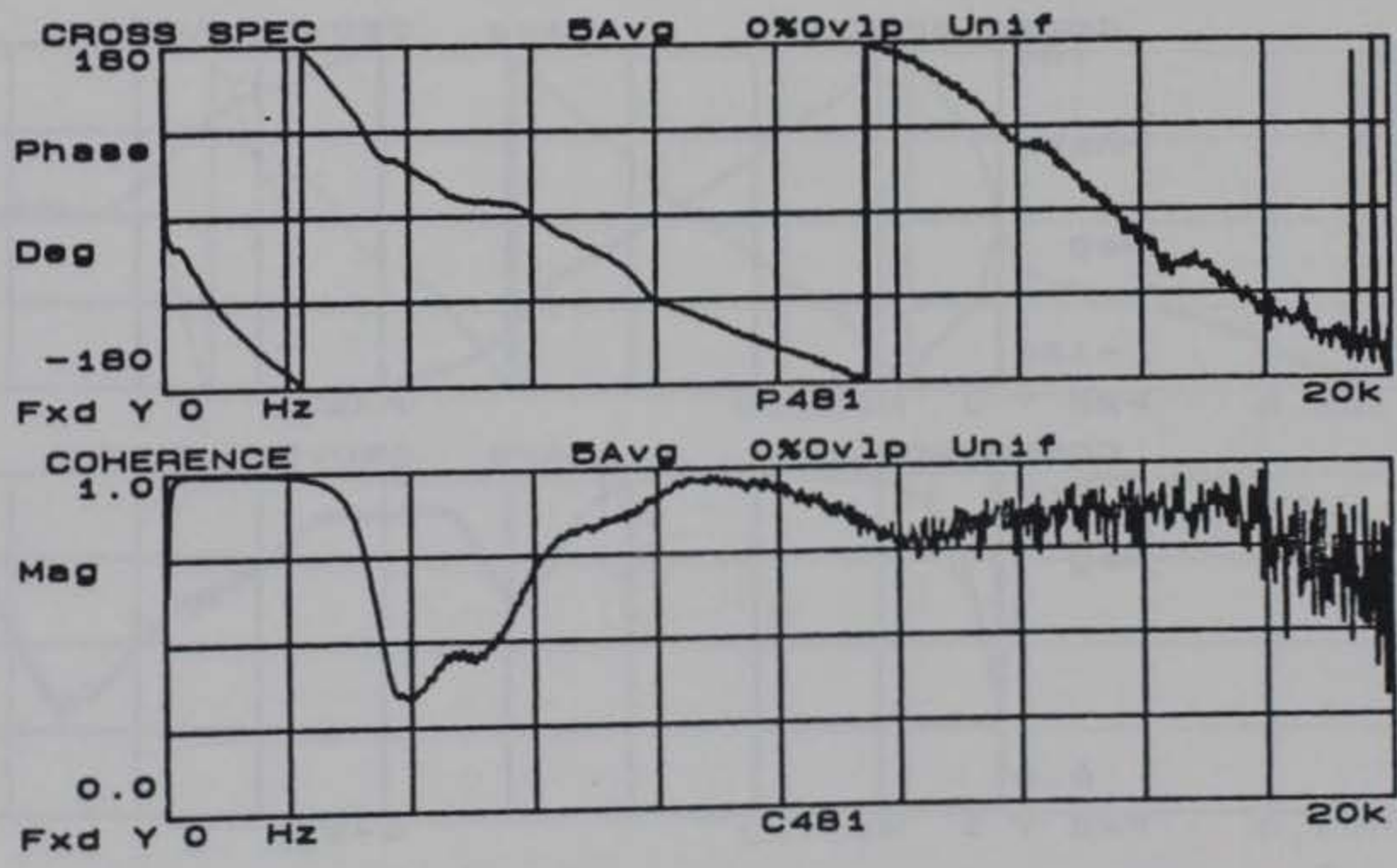

Figure F2. Phase and coherence records for 0.5 ft. receiver spacing at Site 12

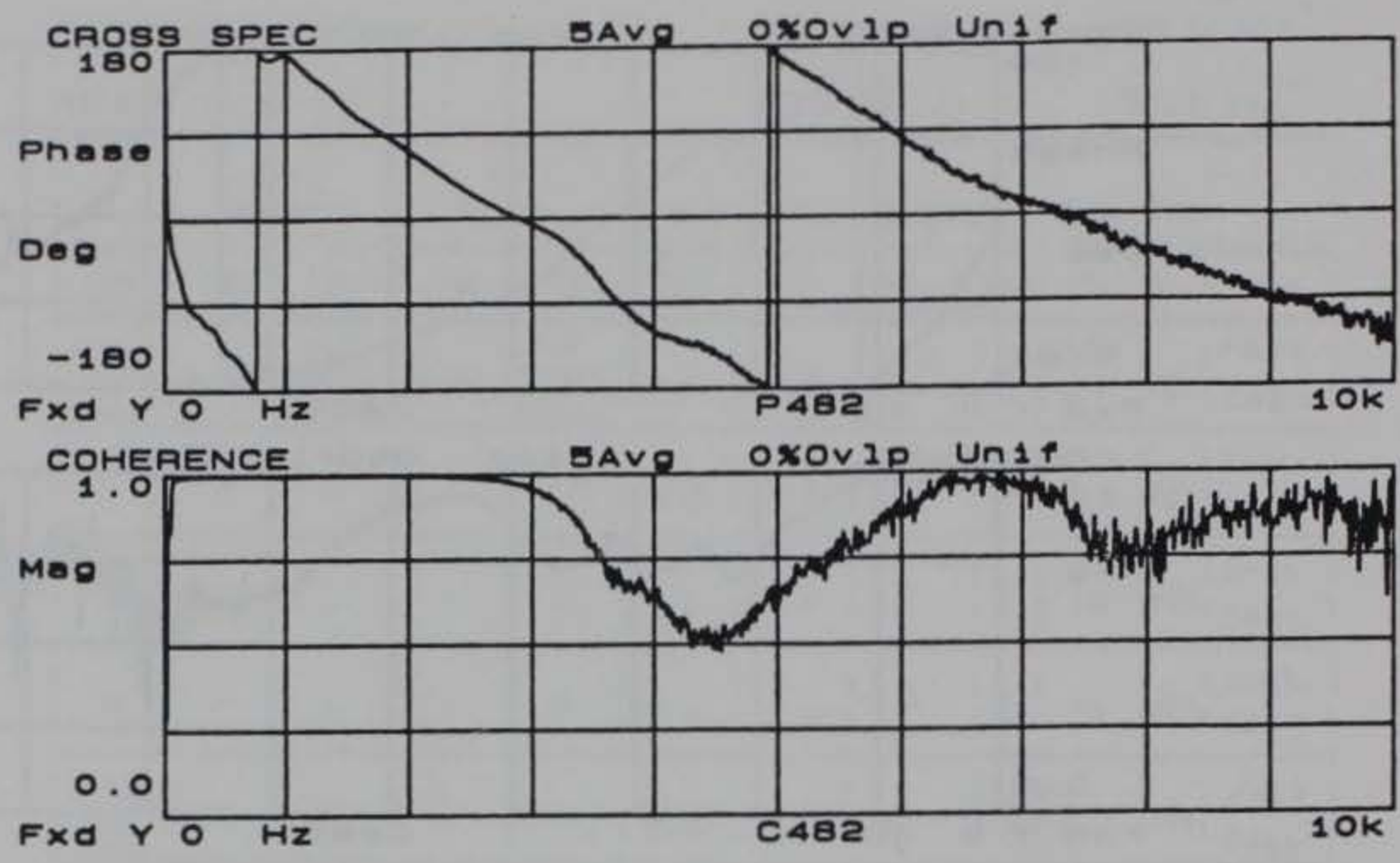

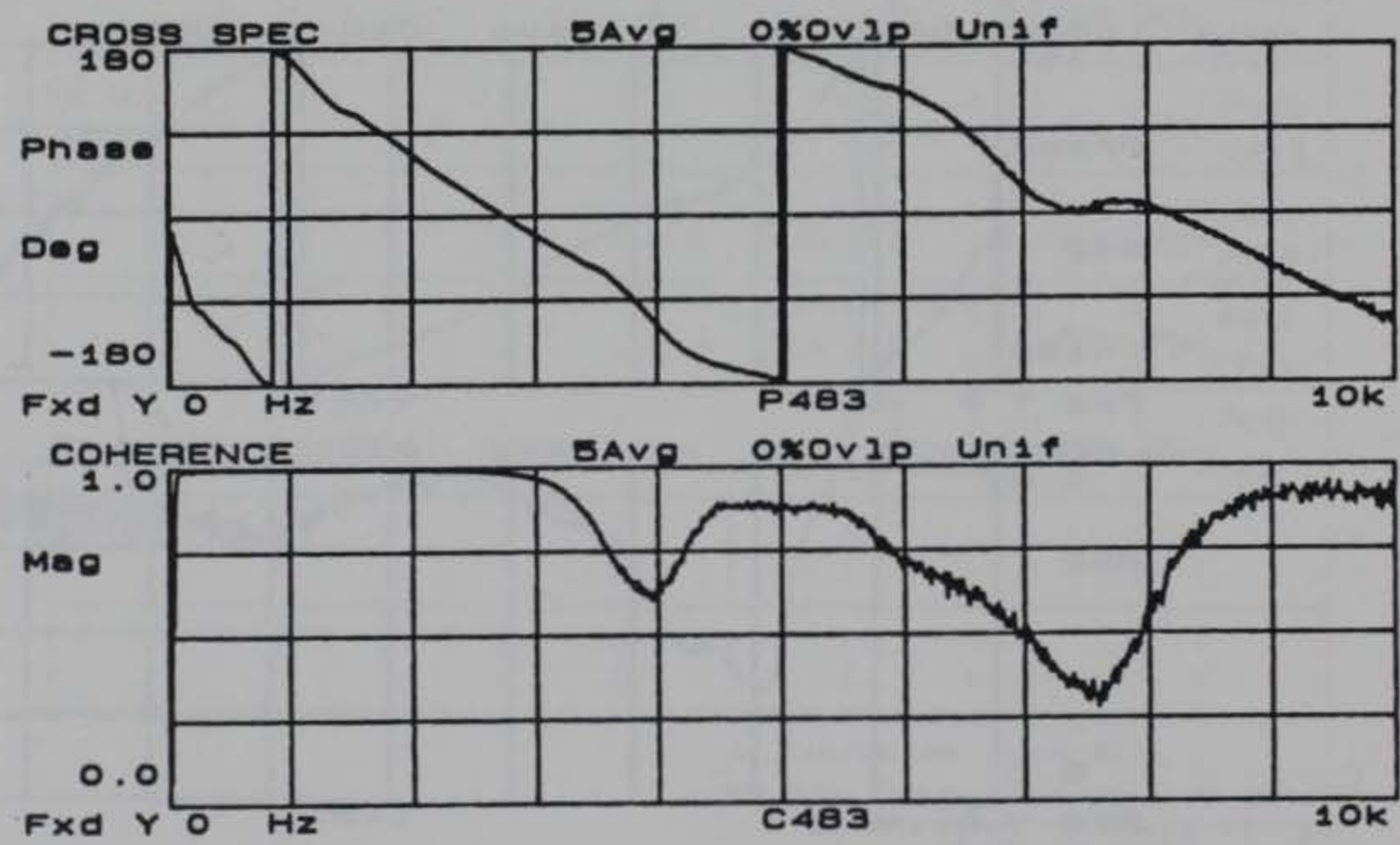

Figure F3. Phase and coherence records for 1.0 ft. receiver spacing at Site 12

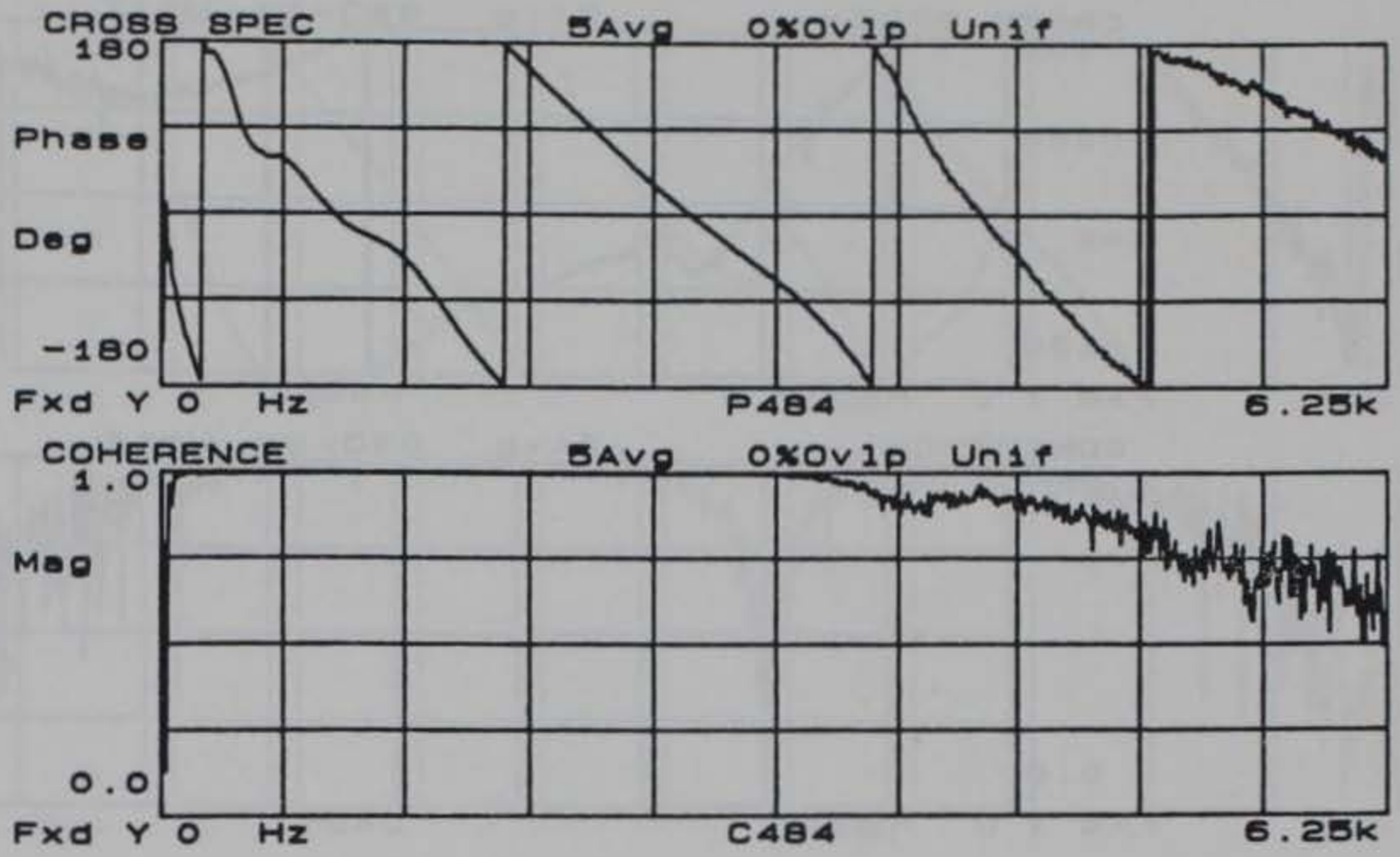

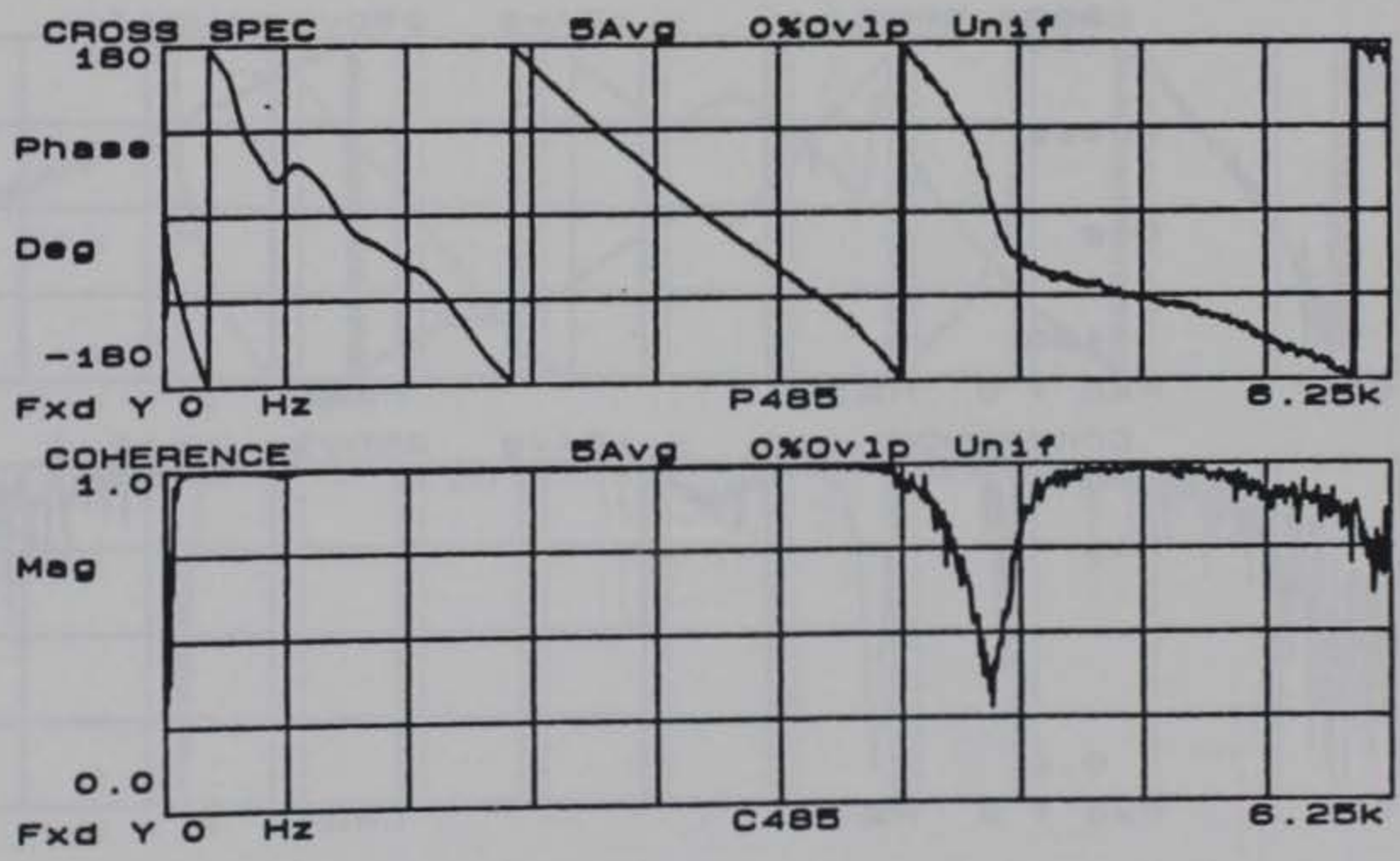

Figure F4. Phase and coherence records for 2.0 ft. receiver spacing at Site 12

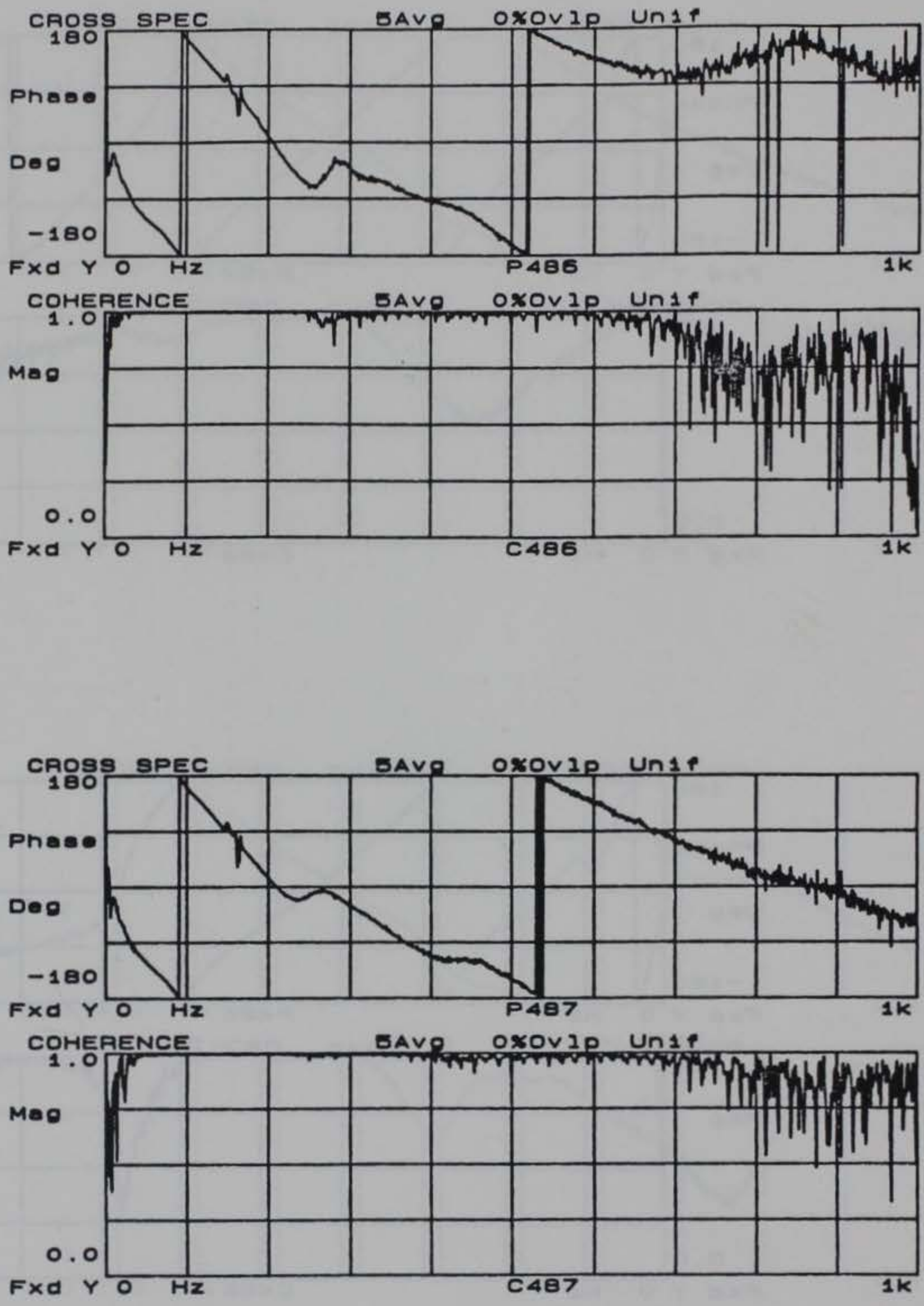

Figure F5. Phase and coherence records for 4.0 ft. receiver spacing at Site 12

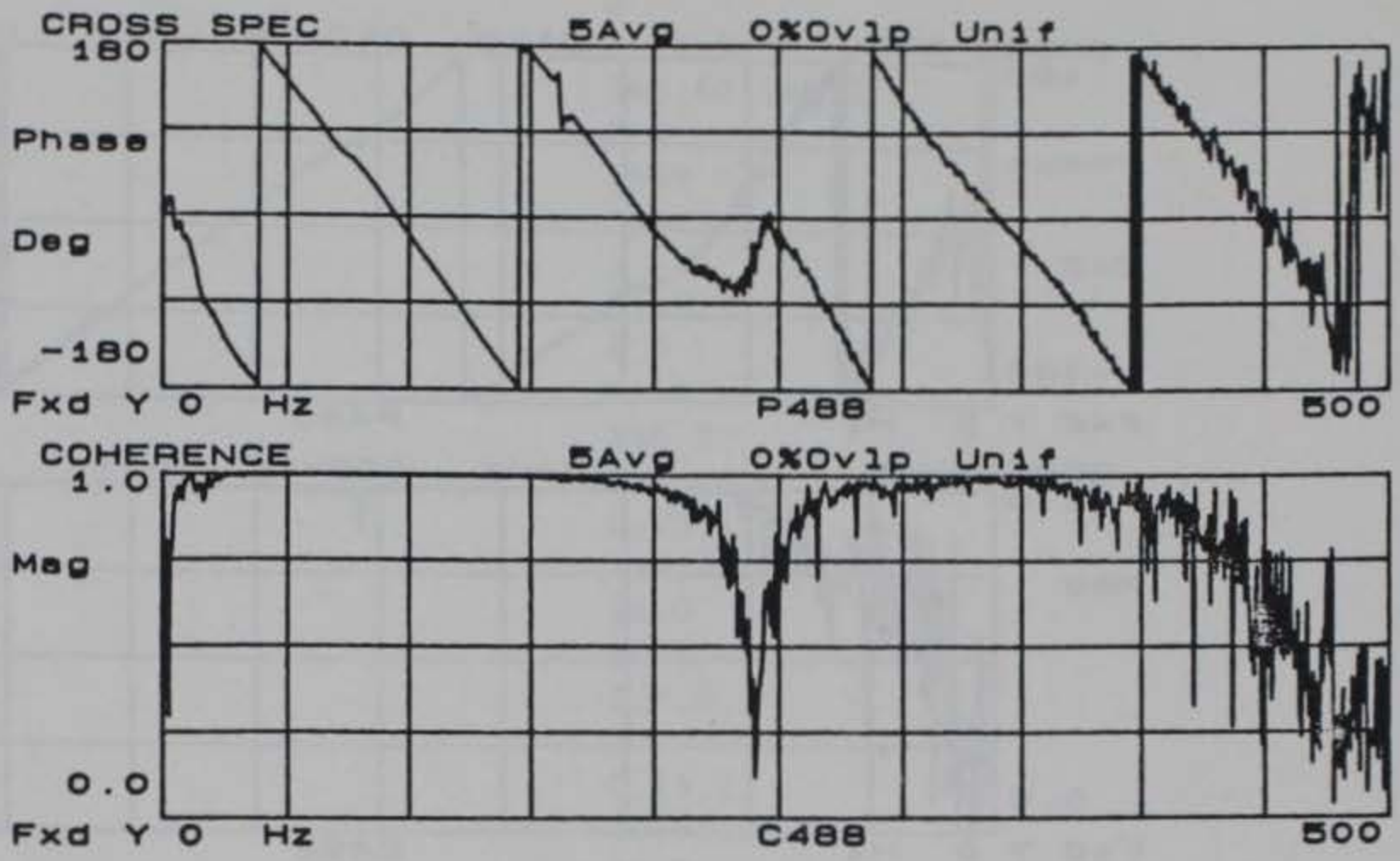

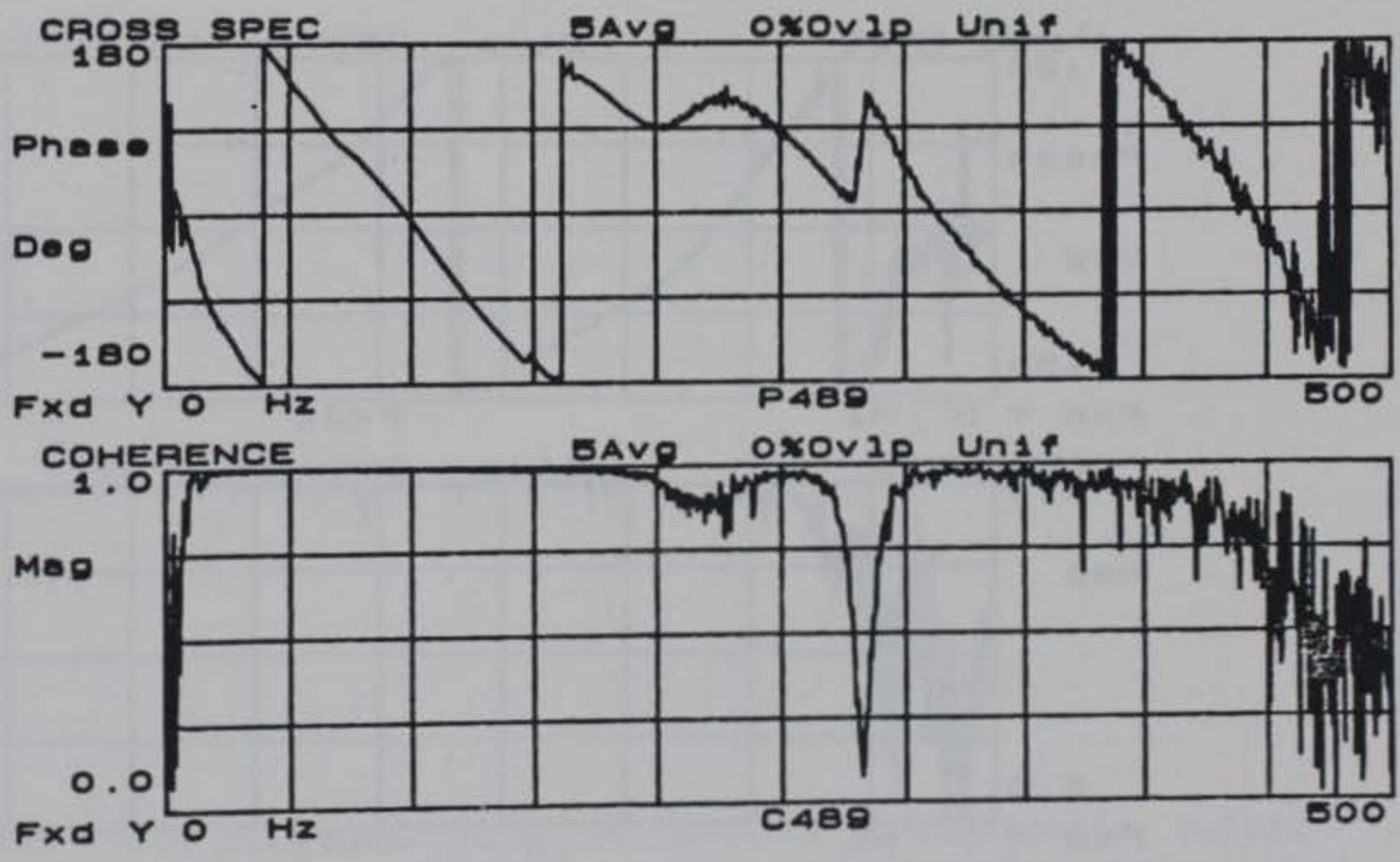

Figure F6. Phase and coherence records for 8.0 ft. receiver spacing at Site 12

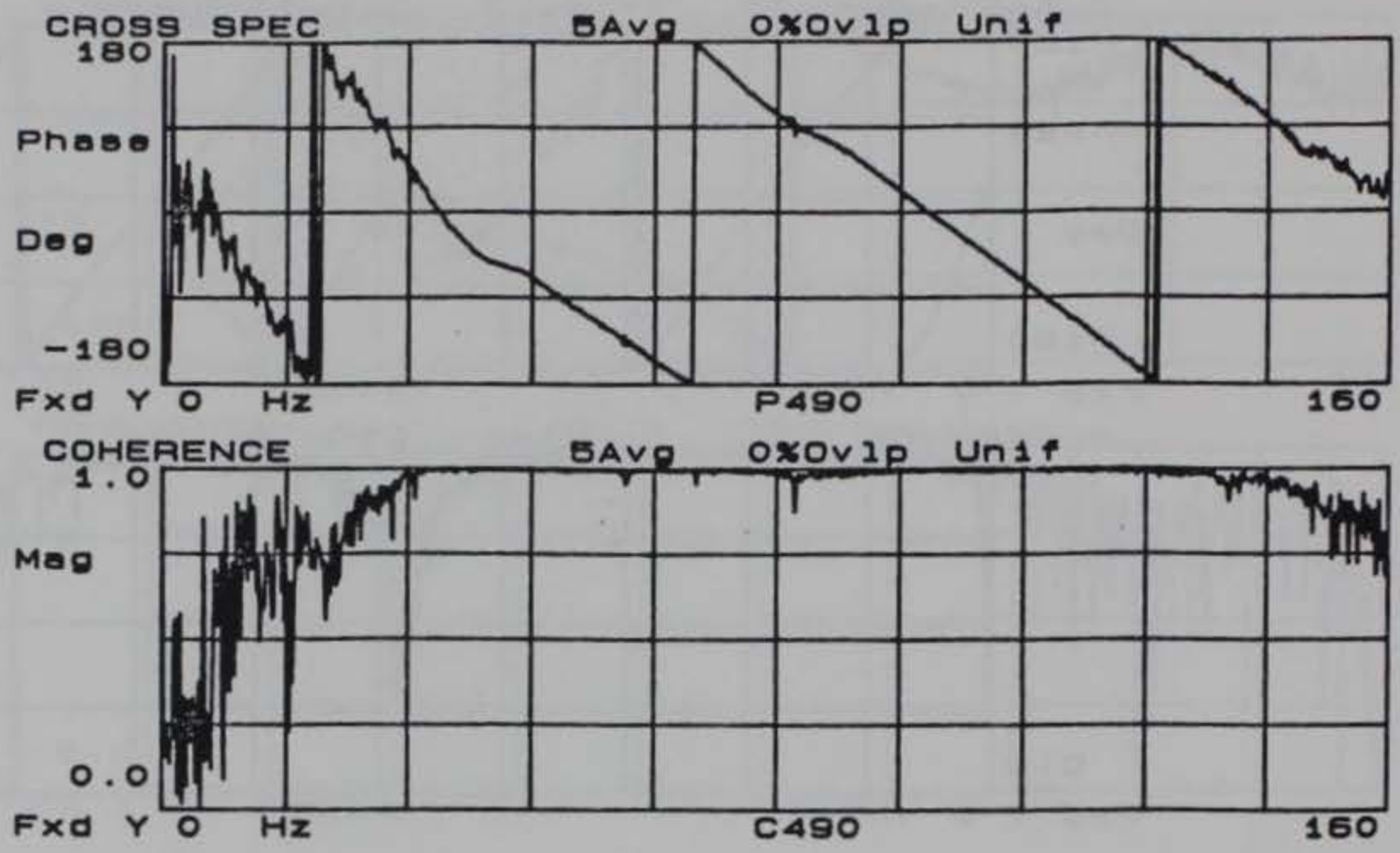

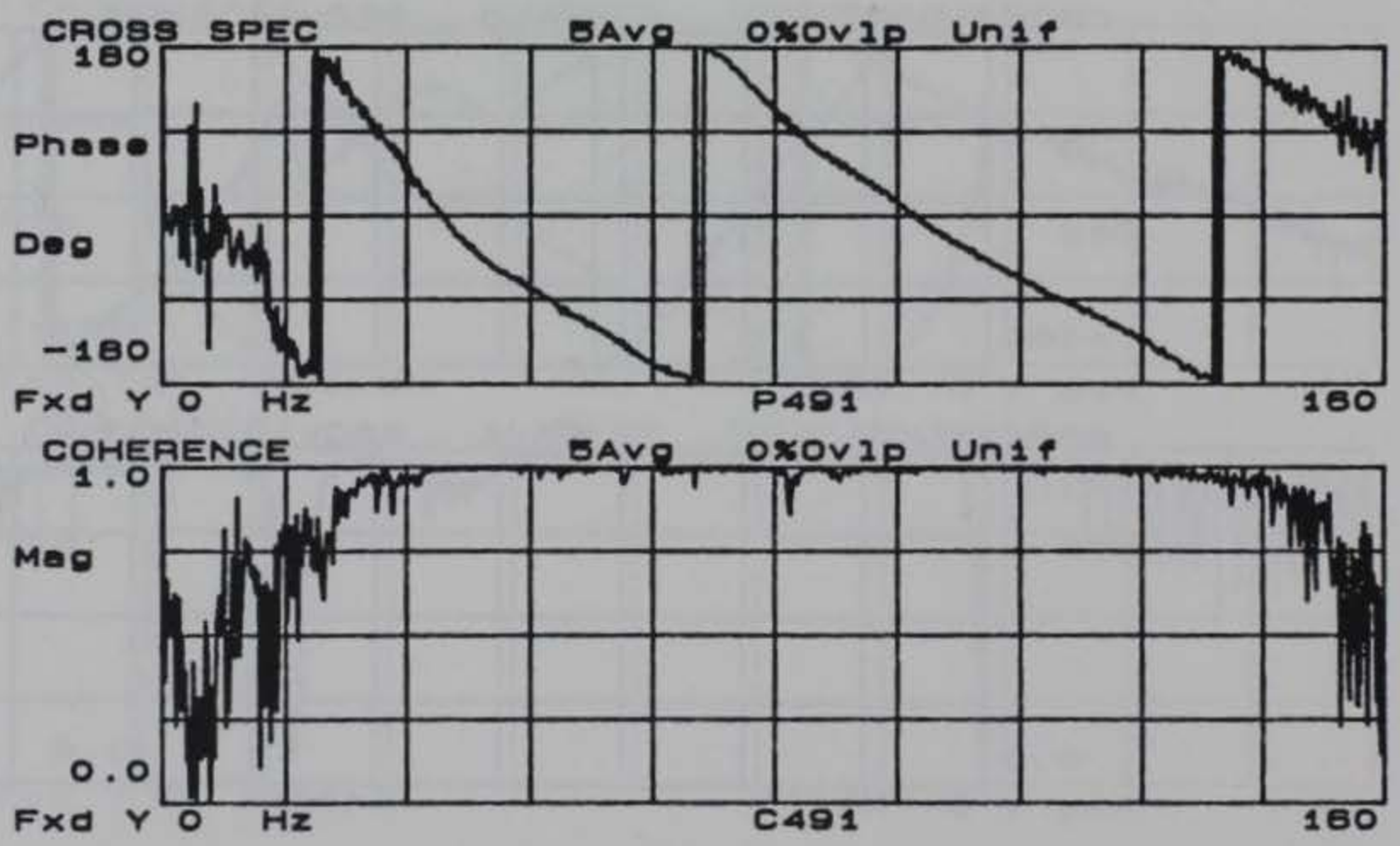

Figure F7. Phase and coherence records for 16.0 ft. receiver spacing at Site 12

```
P480
7500
1
0,1500,0
0.5
P481
11000
1
0,1500,0
0.5
P482
6950
1
0,187,0
1.0
P483
6000
1
0,200,0
1.0
P484
3164
1
0,125,0
2.0
P485
3477
2
0,125,0
335,735,1
2.0
P486
247.5
2
0,50,0
146,173,1
4.0
P487
225
2
0,50,0
142.5,173,1
4.0
P488
190
2
0,20,0
145.62,168.12,2
8.0
P489
145
1
0,20,0
8.0
P490
136.2
2
0,25,1
129,130,3
16.0
P491
129.6
2
0,25,1
69,71,2
16.0
```

Figure F8. Data file containing the names of phase records, cutoff frequencies, poor data ranges, and receiver spacings used by the computer program SASW in constructing the dispersion curve for Site 12